The Next Generation Virgo Cluster Survey. XXXIV. Ultracompact Dwarf Galaxies in the Virgo Cluster

Chengze Liu, Patrick Côté, Eric W Peng, Joel Roediger, Hongxin Zhang, Laura Ferrarese, Ruben Sánchez-Janssen, Puragra Guhathakurta, Xiaohu Yang, Yipeng Jing, et al.

Draft version July 31, 2020
Typeset using LaTeX **twocolumn** style in AASTeX63

The Next Generation Virgo Cluster Survey. XXXIV. Ultra-Compact Dwarf (UCD) Galaxies in the Virgo Cluster.

Chengze Liu,[1] Patrick Côté,[2] Eric W. Peng,[3,4] Joel Roediger,[2] Hongxin Zhang,[5,6] Laura Ferrarese,[2] Ruben Sánchez-Janssen,[7] Puragra Guhathakurta,[8] Xiaohu Yang,[1] Yipeng Jing,[1] Karla Alamo-Martínez,[9] John P. Blakeslee,[2] Alessandro Boselli,[10] Jean-Charles Cuilandre,[11] Pierre-Alain Duc,[12] Patrick Durrell,[13] Stephen Gwyn,[2] Andres Jordán,[14,15] Youkyung Ko,[3] Ariane Lançon,[12] Sungsoon Lim,[2,16] Alessia Longobardi,[10] Simona Mei,[17,18] J. Christopher Mihos,[19] Roberto Muñoz,[9] Mathieu Powalka,[12] Thomas Puzia,[9] Chelsea Spengler,[2] and Elisa Toloba[20]

[1] *Department of Astronomy, School of Physics and Astronomy, and Shanghai Key Laboratory for Particle Physics and Cosmology, Shanghai Jiao Tong University, Shanghai 200240, China*

[2] *Herzberg Astronomy and Astrophysics Research Centre, National Research Council of Canada, 5071 W. Saanich Road, Victoria, BC, V9E 2E7, Canada*

[3] *Department of Astronomy, Peking University, Beijing 100871, China*

[4] *Kavli Institute for Astronomy and Astrophysics, Peking University, Beijing 100871, China*

[5] *School of Astronomy and Space Science, University of Science and Technology of China, Hefei 230026, China*

[6] *CAS Key Laboratory for Research in Galaxies and Cosmology, Department of Astronomy, University of Science and Technology of China, Hefei, Anhui 230026, China*

[7] *STFC UK Astronomy Technology Centre, Royal Observatory, Blackford Hill, Edinburgh, EH9 3HJ, UK*

[8] *UCO/Lick Observatory, Department of Astronomy and Astrophysics, University of California Santa Cruz, 1156 High Street, Santa Cruz, CA 95064, USA*

[9] *Instituto de Astrofsica, Pontificia Universidad Católica de Chile, Av. Vicuña Mackenna 4860, 7820436 Macul, Santiago, Chile*

[10] *Aix-Marseille Univ, CNRS, CNES, LAM, Marseille, France*

[11] *AIM Paris Saclay, CNRS/INSU, CEA/Irfu, Université Paris Diderot, Orme des Merisiers, F-91191 Gif-sur-Yvette Cedex, France*

[12] *Université de Strasbourg, CNRS, Observatoire astronomique de Strasbourg, UMR 7550, F-67000 Strasbourg, France*

[13] *Department of Physics and Astronomy, Youngstown State University, Youngstown, OH 44555, USA*

[14] *Facultad de Ingeniería y Ciencias, Universidad Adolfo Ibáñez, Av. Diagonal las Torres 2640, Peñalolén, Santiago, Chile*

[15] *Millennium Institute for Astrophysics, Chile*

[16] *University of Tampa, 401 West Kennedy Boulevard, Tampa, FL 33606, USA*

[17] *Université de Paris, F-75013, Paris, France, LERMA, Observatoire de Paris, PSL Research University, CNRS, Sorbonne Université, F-75014 Paris, France*

[18] *Jet Propulsion Laboratory and Cahill Center for Astronomy & Astrophysics, California Institute of Technology, 4800 Oak Grove Drive, Pasadena, California 91011, USA*

[19] *Department of Astronomy, Case Western Reserve University, 10900 Euclid Ave, Cleveland, OH 44106, USA*

[20] *Department of Physics, University of the Pacific, 3601 Pacific Avenue, Stockton, CA 95211, USA*

Submitted to The Astrophysical Journal Supplement

ABSTRACT

We present a study of ultra compact dwarf (UCD) galaxies in the Virgo cluster based mainly on imaging from the Next Generation Virgo Cluster Survey (NGVS). Using ∼100 deg^2 of u^*giz imaging, we have identified more than 600 candidate UCDs, from the core of Virgo out to its virial radius. Candidates have been selected through a combination of magnitudes, ellipticities, colors, surface brightnesses, half-light radii and, when available, radial velocities. Candidates were also visually validated from deep NGVS images. Subsamples of varying completeness and purity have been defined to explore the properties of UCDs and compare to those of globular clusters and the nuclei of dwarf galaxies with the aim of delineating the nature and origins of UCDs. From a surface density map, we find the UCDs to be mostly concentrated within Virgo's main subclusters, around its brightest galaxies. We identify

Corresponding author: Chengze Liu
czliu@sjtu.edu.cn

several subsamples of UCDs — i.e., the brightest, largest, and those with the most pronounced and/or asymmetric envelopes — that could hold clues to the origin of UCDs and possible evolutionary links with dwarf nuclei. We find some evidence for such a connection from the existence of diffuse envelopes around some UCDs, and comparisons of radial distributions of UCDs and nucleated galaxies within the cluster.

Keywords: galaxies: clusters: individual (Virgo) — galaxies: evolution — galaxies: dwarf — galaxies: nuclei — galaxies: star clusters: general

1. INTRODUCTION

Roughly two decades ago, investigators reported the discovery of a potentially new class of stellar system in the Fornax cluster (Hilker et al. 1999; Drinkwater et al. 2000; Phillipps et al. 2001). These systems appeared to bridge the gap between normal globular clusters (GCs) and early-type galaxies (including the subset of compact elliptical galaxies), and so were named as ultra-compact dwarf galaxies (UCDs). Since then, such objects have been identified around field galaxies (e.g., Norris & Kannappan 2011; Jennings et al. 2014) as well as in galaxy groups and clusters: i.e., Virgo (Haşegan et al. 2005; Jones et al. 2006), Abell 1689 (Mieske et al. 2005), Centaurus (Mieske et al. 2007a), Hydra (Wehner & Harris 2007), Abell S0740 (Blakeslee & Barber DeGraaff 2008), Coma (Madrid et al. 2010), the NGC 1023 group (Mieske et al. 2007b), the Dorado group (Evstigneeva et al. 2007a), the NGC 5044 group (Faifer et al. 2017), the NGC 3613 group (De Bórtoli et al. 2020) and the NGC 1132 fossil group (Madrid 2011). While UCDs have luminosities comparable to faint dwarf elliptical (dE) galaxies, their sizes (∼10 to 100 pc) are smaller than "normal" dEs and yet larger than typical GCs. Due to their compact sizes and high stellar densities, they pose significant challenges for standard models of dwarf galaxy formation (see, e.g., Strader et al. 2013).

UCD formation models, which remain mostly qualitative in nature, generally invoke one of two basic scenarios. The first posits that UCDs may simply be the most massive members of the GC population, associated with the high-luminosity tail of the GC luminosity function (e.g., Mieske et al. 2002) or possibly arising through mergers of massive star clusters (e.g., Fellhauer & Kroupa 2002). The second asserts that UCDs are the surviving nuclear star clusters of nucleated dwarf elliptical galaxies (dE,Ns) whose surrounding low surface brightness envelopes were removed via tidal stripping (e.g., Bekki et al. 2001). Of course, it is entirely possible that UCDs are not a monolithic population: i.e., that they are manifested through both scenarios (Haşegan et al. 2005; Hilker 2006; Mieske et al. 2006; Da Rocha et al. 2011).

In recent years, evidence has mounted in favor of a tidal stripping origin for at least some of these objects. Arguably the strongest evidence comes from studies of the internal kinematics of UCDs: analyses of their integrated light show that UCDs can have high dynamical-to-stellar mass ratios (Forbes et al. 2014; Janz et al. 2015), while adaptive optics (AO) assisted integral-field unit (IFU) spectroscopy has enabled the discovery of supermassive black holes (SMBHs) in several systems (Seth et al. 2014; Ahn et al. 2017, 2018; Afanasiev et al. 2018). Concurrently, a kinematic study of the UCD population around M87 has shown that they follow radially-biased orbits (Zhang et al. 2015). Meanwhile, photometric studies have revealed the presence of UCDs with asymmetric/tidal features (e.g., Jennings et al. 2015; Mihos et al. 2015; Voggel et al. 2016; Schweizer et al. 2018), UCDs with diffuse envelopes, which populate an apparent sequence in strength from dE,N to UCD (e.g., Drinkwater et al. 2003; Haşegan et al. 2005; Penny et al. 2014; Liu et al. 2015a), and clustering of GCs around UCDs (Voggel et al. 2016). With regards to stellar contents, investigators have found color-magnitude and mass-metallicity relations (e.g., Côté et al. 2006; Brodie et al. 2011; Zhang et al. 2018), the absence of color gradients (Liu et al. 2015a), and similarities in stellar populations to nuclei (e.g., Paudel et al. 2010; Janz et al. 2016). Additionally, N-body simulations and semi-analytic models have demonstrated the viability of tidal stripping (within a cosmological framework) to transform dE,Ns to UCDs (e.g., Bekki et al. 2003; Pfeffer & Baumgardt 2013; Pfeffer et al. 2014, 2016, Mayes et al. 2020, in prep.). From this it seems clear that at least some portion of the population (e.g., massive UCDs) represent the stripped remnants of nucleated dwarf galaxies.

A prerequisite for the development and testing of any quantitative UCD formation model is reliable data on the physical properties of these objects, drawn from surveys with well-understood selection functions. Such data has proved elusive, though, and existing UCD samples are usually built from heterogeneous programs. Although they have been across a wide range of environments, most UCDs are located in groups and clusters, or

associated with massive galaxies (e.g., Liu et al. 2015a). As the richest concentration of galaxies near the Milky Way (MW), the Virgo cluster is an ideal environment for a comprehensive UCD survey. A handful of systems were first discovered in Virgo by Haşegan et al. (2005) through a combination of Keck spectroscopy and HST imaging from the ACS Virgo Cluster Survey (Côté et al. 2004). Additional UCDs were later found in both imaging and/or spectroscopic programs (e.g., Jones et al. 2006; Chilingarian & Mamon 2008; Brodie et al. 2011; Strader et al. 2013; Liu et al. 2015a,b; Sandoval et al. 2015; Zhang et al. 2015; Ko et al. 2017). These studies have tended to focus on UCDs associated with M87 or a few other of the brightest galaxies in Virgo. Currently, the largest UCD sample in this cluster contains ∼150 objects, spread over the M87, M49 and M60 regions (Liu et al. 2015a).

Given its enormous extent on the sky, a wide-field imaging survey is essential for building a homogeneous and complete sample of Virgo UCDs. The Next Generation Virgo cluster Survey (NGVS; Ferrarese et al. 2012) is a deep, multi-band (u^*griz) imaging campaign of the Virgo cluster carried out with the MegaCam instrument on the Canada France Hawaii Telescope (CFHT). The survey covers an area of 104 deg^2 and is typified by excellent image quality, with a median FWHM of 0.54″ in the i-band (see their Figure 8). In principle, we can use these NGVS images to measure half-light radii for all compact Virgo objects brighter than $g \sim 21.5$ mag and larger than $r_h \sim 10$ pc (see Liu et al. 2015a), potentially producing the largest and the most complete sample of UCDs in any environment. The analysis presented here builds on previous NGVS papers that have focused on the photometric and kinematic properties of UCDs (e.g., Liu et al. 2015a,b; Zhang et al. 2015). It also complements other papers in the NGVS series dealing with other stellar systems in Virgo, including globular clusters (i.e., Durrell et al. 2014; Powalka et al. 2016a; Longobardi et al. 2018), galaxies (Guérou et al. 2015; Sánchez-Janssen et al. 2016; Ferrarese et al. 2016; Roediger et al. 2017; Ferrarese et al. 2020), and their nuclei (i.e., Spengler et al. 2017; Sánchez-Janssen et al. 2019).

This paper is structured as follows. In §2 we provide an overview of the NGVS and the data products used in our analysis, while §3 describes the methodology we have used to identify UCD candidates. In §4 we present our results, including a new catalog of UCD candidates, and draw attention to a number of particularly interesting sub-samples therein. We discuss these findings in §5, and in §6, summarize our conclusions and outline directions for future work. Throughout this study, we adopt a common distance to all UCDs (16.5 Mpc Mei et al. 2007; Blakeslee et al. 2009), corresponding to a distance modulus of $(m\text{-}M) = 31.09$ and physical scale of 80 pc arcsec^{-1}.

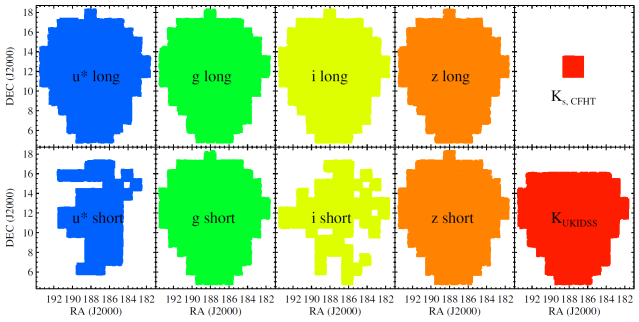

Figure 1. The areal coverage of our optical and near-infrared imaging, organized by exposure length (*top*: long, *bottom*: short). The NGVS achieved 100% completeness for the long exposures in the u^*giz bands and in the gz bands for the short exposures; short exposures in the u^*i bands were only partially completed. The NGVS-IR (K_s-band, Muñoz et al. 2014) imaging only covers the center of sub-cluster A, while the UKIDSS (K-band, Lawrence et al. 2007) data cover most of the NGVS footprint.

2. DATA

2.1. *Overview*

The primary source of data used in this study is the NGVS. The survey footprint covers the two main subclusters of Virgo (A and B, centered on M87 and M49, respectively) out to their virial radii (i.e., $R_{200} = 5.^\circ38$ for Virgo A and $3.^\circ33$ for Virgo B). As described in Muñoz et al. (2014) and Liu et al. (2015a), the NGVS is an ideal resource for the study of compact stellar systems, e.g., GCs, UCDs and dwarf nuclei. The NGVS imaging consists of short and long exposures, where the former can be used to find UCDs brighter than $g \sim 18.5$ mag. Such objects are interesting given that they define the extreme of UCD formation (and, in some cases, even host supermassive black holes; Seth et al. 2014, Ahn et al. 2018).

Figure 1 shows the final observing status of the NGVS, organized by exposure length. We have excluded the r-band since those observations had to be partially sacrificed due to CFHT's dome shutter failure in 2012A. For the long exposures, the survey is fully complete in the remaining bands, while only partial areal coverage was achieved for the short exposures in the u^* ($\sim 50\%$ completeness) and i ($\sim 57\%$ completeness) bands.

Near-infrared imaging has proved to be a powerful tool for UCD selection (Muñoz et al. 2014; Liu et al. 2015a). As shown in the upper right corner of Figure 1, we have deep K_s-band images in the central 4 deg^2 of sub-cluster A (NGVS-IR; Muñoz et al. 2014), which we

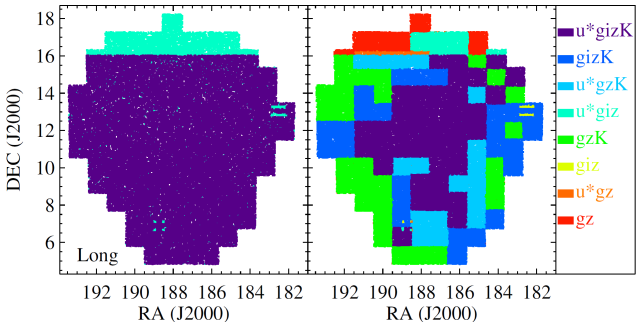

Figure 2. Summary of the spatial dependence of the multi-wavelength photometry used to select UCDs, divided by exposure length (*left*: long exposure catalog, *right*: short exposure catalog).

have previously used to select a high-purity UCD sample around M87 (Liu et al. 2015a). Alternatively, as shown in the bottom-right panel of Figure 1, K-band imaging from UKIDSS (Lawrence et al. 2007) covers a large fraction of the NGVS footprint. About $\sim$ 70% of the bright objects [$g_0 < 21.5$ mag, where g_0 is the aperture-corrected magnitude measured within a 16-pixel diameter ($\sim 3''$) and corrected for Galactic extinction] in the NGVS have counterparts in the UKIDSS K-band. Thus, although UKIDSS is much shallower than the NGVS-IR (5σ limiting magnitude $\sim$18.4 and $\sim$24.4 mag, respectively), it is nonetheless useful for separating UCDs from background galaxies among the bright objects.

We summarize the combinations of imaging data at hand, separated by exposure length, in Figure 2. For the case of the long exposures (left panel), the footprint is simply divided into two areas depending on the availability of UKIDSS K-band imaging. The short exposure map (right panel) is much more complicated owing to the incompleteness in the associated u^* and i band imaging.

Full details on the reduction of NGVS images can be found in Ferrarese et al. (2012). To generate a homogeneous catalog of compact objects, we run SExtractor (Bertin & Arnouts 1996) in double-image mode. We detect objects in the g-band and then measure a set of parameters, including aperture magnitudes, in the u^*giz bands. In this study, we measure the luminosity and color of all detected objects with aperture magnitudes. To minimize systematics, we apply aperture corrections that account for PSF variations within, and between, fields. Specifically, we use corrected $3.0''$-diameter aperture magnitudes to represent total magnitudes and corrected $1.5''$-diameter aperture magnitudes to estimate colors.

For the catalog generation and magnitude correction, we follow the method of Liu et al. (2015a), with one exception. Liu et al. (2015a) subtracted models of the diffuse light from nearby massive galaxies (M87, M49, and M60), whereas this is avoided in the current analysis to have a homogeneous catalog. We generate independent catalogs based on the short and long exposure images and then merge them into one afterwards. We adopt measurements from the short exposure catalog for those objects which are saturated in the long exposures; otherwise measurements are taken from the long exposure catalog.

In addition to the imaging that forms the basis of this study, there are many past spectroscopic programs targetting the Virgo cluster that we can draw upon. Ferrarese et al. (2012) summarized the relevant programs for Virgo compact stellar systems (i.e., GCs, UCDs and dE,Ns) as of 2012; these include radial velocity measurements from various MMT/Hectospec, Magellan/IMACS, VLT/VIMOS and AAT/AAOmega programs (see the paper for details). Since then, a number of NGVS-motivated spectroscopic programs have been undertaken (see, e.g., Zhang et al. 2015, 2018; Toloba et al. 2016; Spengler et al. 2017; Longobardi et al. 2018). We have collected radial velocities from these and other previous works (Binggeli et al. 1985; Hanes et al. 2001; Côté et al. 2003; Brinchmann et al. 2008; Strader et al. 2011, 2012; Pota et al. 2013; Blom et al. 2014; Norris et al. 2014; Li et al. 2015; Pota et al. 2015; Forbes et al. 2017; Ko et al. 2017; Toloba et al. 2018), as well as from the NASA/IPAC Extragalactic Database (NED)[1], the SIMBAD Astronomical Database[2] (Wenger et al. 2000) and the Sloan Digital Sky Survey (SDSS, Abolfathi et al. 2018). In all, we have a total of 31,346 velocity measurements for objects in the NGVS footprint brighter than $g_0 = 21.5$ mag. This database includes foreground stars, GCs, UCDs, galaxies in Virgo, and background galaxies. In what follows, we make use of this large velocity catalog to eliminate contaminants from our photometric UCD selection, as well as to recover UCDs that miss our cuts.

2.2. *Size Measurements*

Size is the defining parameter of UCDs[3]. As shown by Liu et al. (2015a), the excellent image quality of the NGVS allows us to measure reliable sizes for compact objects in Virgo (mainly GCs, UCDs, and galactic nuclei) larger than $\sim$10 pc (see their Section 2.3). We measure half-light radii using the KINGPHOT package

[1] https://ned.ipac.caltech.edu/

[2] http://simbad.u-strasbg.fr/simbad/

[3] Unless stated otherwise, we use the term "size" to refer to an object's half-light radius, r_h, exclusively.

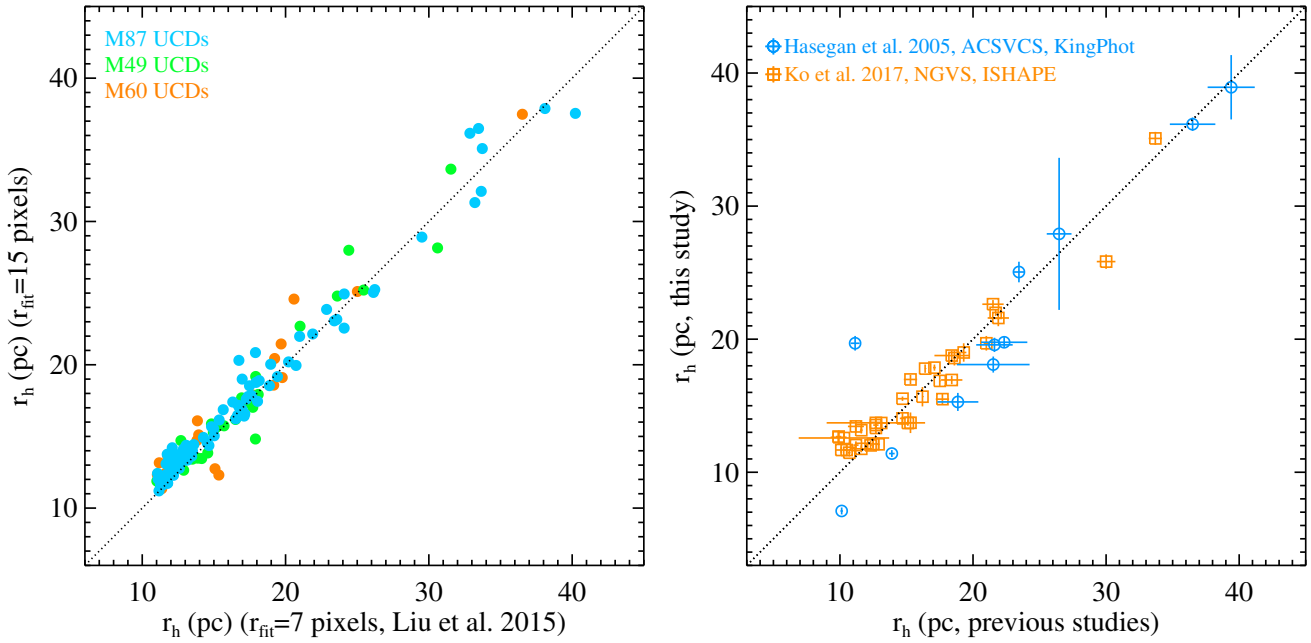

Figure 3. *Left panel:* Comparison of r_h measurements for UCDs based on different fitting radii, $r_{\rm fit}$ (7 vs 15 pixels), with data taken from Liu et al. (2015a). *Right panel:* Comparison of r_h measured using different data (blue circles, ACSVCS data, Haşegan et al. 2005) or different methods (orange squares, ISHAPE software, Ko et al. 2017).

(Jordán et al. 2005), focusing on the g and i bands because of the former's depth and the latter's exquisite seeing. Comparisons of the two sets of r_h measurements show that they are consistent with each other (see Figure 3 in Liu et al. 2015a). Jordán et al. (2005) show that KINGPHOT r_h measurements are biased to larger values when $r_h \gtrsim r_{\rm fit}/2$ (where $r_{\rm fit}$ is fitting radius within which we adopt KINGPHOT), which is ∼50 pc for an $r_{\rm fit} = 7$ pixels (used in Liu et al. 2015a) at the distance of Virgo. This choice of $r_{\rm fit}$ is reasonable since previous works shows that most UCDs are smaller than 40 pc (Brodie et al. 2011; Chiboucas et al. 2011; Strader et al. 2011; Penny et al. 2012). However, in the interests of determining whether there are larger UCDs in Virgo, we run KINGPHOT with $r_{\rm fit} = 15$ pixels in this study. Thus, our KINGPHOT measurements would be biased for objects with $r_h \gtrsim 110$ pc.

The left panel of Figure 3 compares our UCD r_h measurements from Liu et al. (2015a) for the two values of $r_{\rm fit}$ above. We note that the larger $r_{\rm fit}$ yields slightly larger sizes when $r_h \lesssim 16$ pc. Otherwise, the two sets of r_h measurements are statistically equivalent, so we therefore adopt the KINGPHOT measurements made with $r_{\rm fit} = 15$ pixels. The right panel of this figure shows a comparison between the r_h measurements from this work and those from previous studies. The blue circles are taken from Haşegan et al. (2005), who measured r_h using KINGPHOT and HST data (ACSVCS, Côté et al. 2004). The orange squares denote the r_h measurements from Ko et al. (2017), who used ISHAPE software and NGVS data. From this figure, we can see that our r_h measurements are consistent with the measurements from previous studies, even though they used different methodologies and/or data sets.

3. UCD SELECTION

We select UCD candidates within the multi-dimensional parameter space of magnitude, ellipticity ($e \equiv 1 - b/a$), color, surface brightness, and half-light radius, which we now describe and justify[4]. We begin by adopting simple magnitude cuts of $14.0 < g_0 < 21.5$ mag, where the lower bound corresponds to the saturation limit of our g-band short exposures and the upper bound to the limit of accurate measurements of half-light radii (see §2 in Liu et al. 2015a for details). We also apply a simple cut on ellipticity, adhering to the empirical result that most spectroscopically-confirmed UCDs in Virgo (i.e., $v_r < 3500$ km/s) have $e < 0.3$ (see, e.g., Zhang et al. 2015).

As we have previously shown (Muñoz et al. 2014; Liu et al. 2015a; Powalka et al. 2016a,b), the combination of $u^* g i K_s$ photometry proves to be a highly effective tool for discriminating extragalactic GCs and UCDs from background galaxies and foreground stars. Un-

[4] It is worth bearing in mind that UCD selection criteria are often driven as much by observational details, such as limiting magnitudes and angular resolution, as by considerations of formation physics.

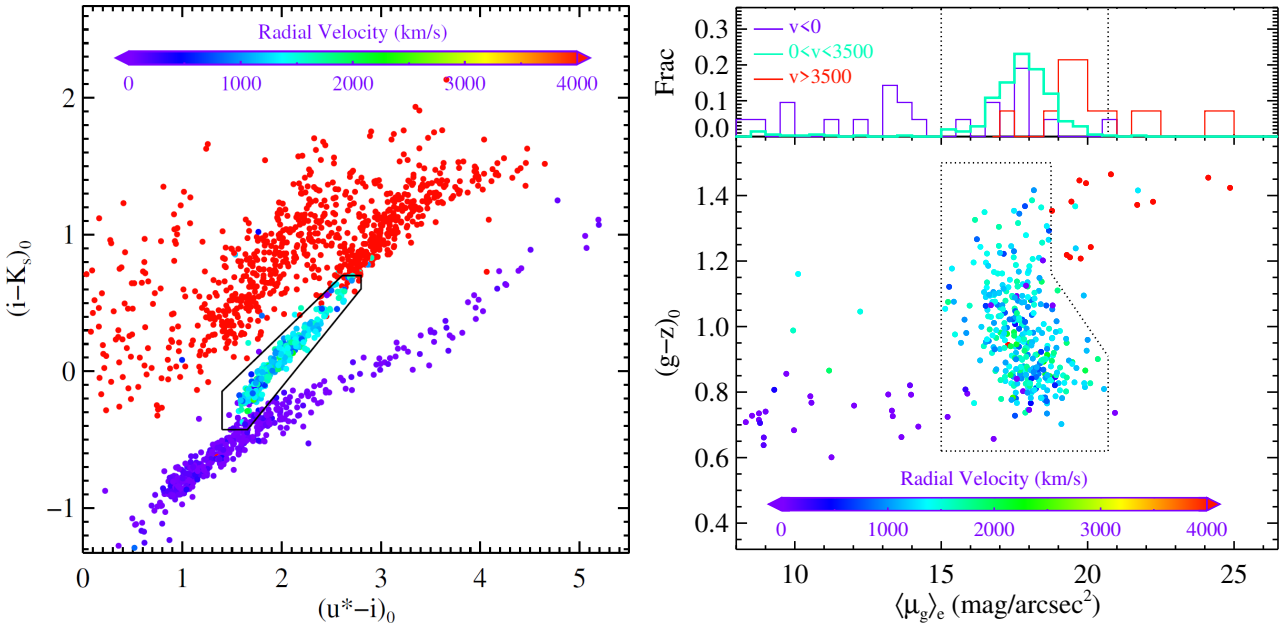

Figure 4. *Left panel:* The u^*iK_s color-color diagram. The solid polygon represents our GC+UCD selection box in this plane. The points are colored by their associated radial velocity measurements, reflected in the color bar at top. *Right panel:* The distribution of mean surface brightness, $\langle\mu_g\rangle_e$, (in broad bins of radial velocity; top) and $(g-z)_0$ color as a function of $\langle\mu_g\rangle_e$ for the objects lying within our selection region on the left. The dotted polygon shows the next layer of our selection, based on surface brightness, and the points are colored by their associated radial velocities.

fortunately, Figure 1 shows that we only have K_s-band imaging for the central 4 deg^2 of sub-cluster A from the NGVS-IR (see Muñoz et al. 2014 for details). Moreover, in the u^* and i bands, only partial coverage is available in the short exposure category. In an attempt to balance homogeneity and accuracy, we base the color portion of our UCD selection on our u^*, g, i, z and UKIDSS K-band photometry. The UKIDSS data, although shallower than that from NGVS-IR, is sufficient for our purpose, i.e. to select UCD candidates with $g_0 < 21.5$ mag. We will describe our u^*giK_s- and u^*gizK-based selections and compare their results in the following two subsections.

3.1. *u^*giK_s-Based Selection*

In the left panel of Figure 4, we show the cuts employed as part of our u^*giK_s-based selection. There, we plot in the (u^*-i) vs. $(i-K_s)$ plane, the ∼2000 objects from our spectroscopic catalog that satisfy our magnitude and ellipticity cuts. The points have been colored by their measured radial velocities and can be divided into three main groups: background galaxies (red dots; $v \gtrsim 3500$ km/s), Virgo members (green and cyan dots; $0 \lesssim v \lesssim 3500$ km/s), and foreground stars (blue and purple dots; $v \lesssim 0$ km/s)[5]. It is clear that Virgo members can be readily distinguished from background galaxies and foreground stars in the u^*iK_s color-color diagram. To isolate Virgo members, we therefore adopt the following color cuts:

$$\begin{cases} 1.400 \leq (u^*-i)_0 \leq 2.800; \\ -0.427 \leq (i-K_s)_0 \leq 0.700; \\ (i-K_s)_0 \leq -1.127 + 0.700 \times (u^*-i)_0; \\ (i-K_s)_0 \geq -1.917 + 0.900 \times (u^*-i)_0. \end{cases} \quad (1)$$

which are indicated by the irregular polygon in the figure.

The right-hand panel of Figure 4 shows the $(g-z)_0$ color as a function of mean effective surface brightness, $\langle\mu_g\rangle_e$, which is the average surface brightness measured within the half-light radius. The points show those objects that passed our color cuts in the u^*iK_s diagram and, again, are colored according to their radial velocities. It is clear from the distribution that we can use surface brightness to further improve the purity of our Virgo sample by removing background galaxies and some foreground stars. The dotted polygon shows the

[5] Note that this very basic redshift classification is not strictly correct; some Virgo members do indeed have negative radial velocities, such as objects belonging to the M86 group (see, e.g., Boselli et al. 2018; Park et al. 2012) and many stars have positive radial velocities (Katz et al. 2019).

exact cuts in surface brightness that we adopt, which are described by the following functions:

$$\begin{cases} 0.620 \leq (g-z)_0 \leq 1.500; \\ \langle\mu_g\rangle_e \geq 15.000 \text{ mag/arcsec}^2; \\ \langle\mu_g\rangle_e \leq 18.750 \text{ mag/arcsec}^2, \\ \qquad \text{when } 1.163 \leq (g-z)_0 \leq 1.500; \\ \langle\mu_g\rangle_e \leq 27.692 - 7.692 \times (g-z)_0, \\ \qquad \text{when } 0.909 \leq (g-z)_0 \leq 1.163; \\ \langle\mu_g\rangle_e \leq 20.700 \text{ mag/arcsec}^2, \\ \qquad \text{when } 0.620 \leq (g-z)_0 \leq 0.909. \end{cases} \tag{2}$$

The combination of the cuts applied to this point leaves us with a broad sample of Virgo members that includes compact elliptical galaxies, galactic nuclei (in low-mass galaxies), UCDs, and GCs. To isolate the UCDs within this sample, we apply one final set of cuts based on our measured half-light radii, which are:

$$\begin{cases} 11 < \langle r_h \rangle < 100 \text{ pc}; \\ \dfrac{|r_{h,g} - r_{h,i}|}{\langle r_h \rangle} \leq 0.5; \\ \dfrac{r_{h,g,\text{error}}}{r_{h,g}} \leq 15\%; \\ \dfrac{r_{h,i,\text{error}}}{r_{h,i}} \leq 15\%. \end{cases} \tag{3}$$

where $\langle r_h \rangle$ represents the weighted mean of the half-light radii measured in the g and i bands. These cuts mimic ones often used in previous studies to separate UCDs and GCs (e.g., Brodie et al. 2011; Strader et al. 2011; Penny et al. 2012). Though arbitrary, this is not an unreasonable choice since the typical size of either MW or extragalactic GCs is ∼3 pc and most GCs are smaller than ∼ 10 pc (e.g., van den Bergh et al. 1991; Jordán et al. 2005). Furthermore, Liu et al. (2015a) have shown that r_h measurements based on NGVS imaging are reliable for bright objects ($g_0 < 21.5$ mag) larger than $r_h \sim 10$ pc (see §2.3 of their paper). The lower limit on $\langle r_h \rangle$ used in this study roughly matches the limiting resolution of NGVS imaging.

3.2. *u^*giz- and u^*gizK-Based Selection*

Given the lack of deep K_s-band imaging over most of the NGVS footprint, we have developed an alternative strategy for selecting UCDs based on the u^*, g, i, z and (where available) K bands. As seen in Figure 1, the NGVS imaging is not fully complete in the u^* and i bands for the short exposures. As argued in Muñoz et al. (2014), the u^* band is essential when selecting UCDs due to its sensitivity to young/hot stellar populations, which allows for the removal of background star-forming galaixes. The left panel of Figure 5 shows the u^*gz color-color diagram for the same spectroscopic sample (following the same color-coding) as in Figure 4. In this case, we can see that the spaces occupied by background galaxies, Virgo members, and foreground stars more heavily overlap with each other. Nevertheless, the Virgo members still form a relatively tight sequence in this plane, such that we can select a sample of these objects with high completeness, albeit with more contamination. We adopt a color selection (represented by the polygon) within this diagram of the form:

$$\begin{cases} 0.850 \leq (u^*-g)_0 \leq 1.790; \\ 0.620 \leq (g-z)_0 \leq 1.500; \\ (g-z)_0 \leq 0.190 + 0.770 \times (u^*-g)_0; \\ (g-z)_0 \geq -0.300 + 0.930 \times (u^*-g)_0. \end{cases} \tag{4}$$

The objects that satisfy these cuts are plotted in the plane of color versus surface brightness in the right-hand panel of Figure 5. Although many contaminants pass our color-color cuts, it is possible to eliminate most of these following the same cuts on surface brightness that we applied to our u^*giK_s sample (Equation 2; dotted polygon in this panel). These cuts are not as effective as before, however, and leave behind a number of background galaxies (red dots). Fortunately, we can remove most of these residual contaminants wherever we have K-band data. Figure 6 shows the gzK color-color diagram for those objects from our spectroscopic catalog that satisfy our u^*gz and surface brightness cuts. For a given $(g-z)_0$ color, background galaxies tend to be redder in $(z-K)_0$ than Virgo members, and we use the following relationship to isolate the latter:

$$(z-K)_0 \leq 1.480 + 0.780 \times (g-z)_0. \tag{5}$$

After this, we apply the same size cuts as before (Equation 3) to arrive at our sample of UCD candidates.

3.3. *Comparing our Selection Methods*

In this section, we compare the UCD catalogs derived from the two selection methods described above. For this comparison, the best region within the NGVS footprint is the center of sub-cluster A, where we have u^*, g, i, z, K_s (NGVS-IR), and K (UKIDSS) band fluxes and radial velocities for ∼2000 objects. Among this sample, 71 are spectroscopically-confirmed UCDs that were already known from previous work (mainly Strader et al. 2011 and Zhang et al. 2015).

As described in §3.1, we divide these objects into three groups according to their radial velocities: background galaxies ($v > 3500$ km/s), Virgo members ($0 < v < 3500$ km/s) and foreground stars ($v < 0$ km/s). Within

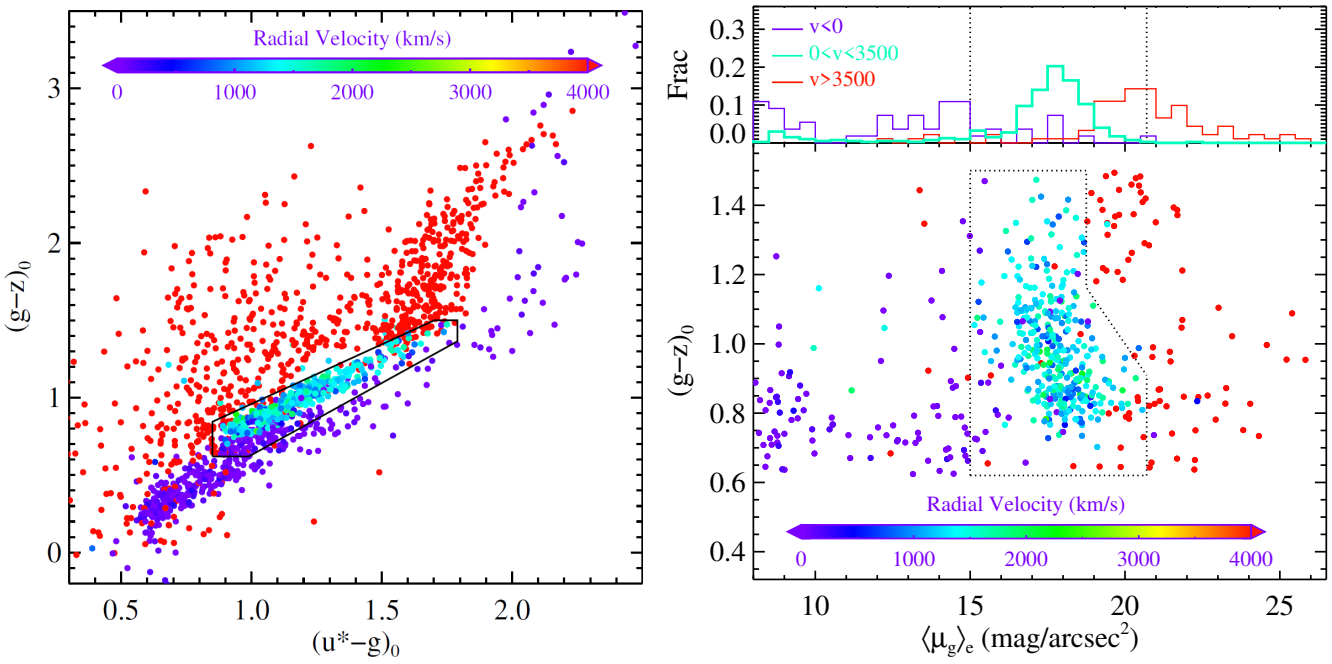

Figure 5. As in Figure 4 but based on the u^*gz color-color diagram instead.

Table 1. Application of our Photometric UCD Selection Methods (u^*giK_s, u^*giz, u^*gizK) to a Spectroscopic Training Set.

	u^*giK_s				u^*giz				u^*gizK			
velocity	$v < 0$	$0 < v < 3500$		$v > 3500$	$v < 0$	$0 < v < 3500$		$v > 3500$	$v < 0$	$0 < v < 3500$		$v > 3500$
Obj. Type	Stars	UCDs	dE,Ns	BGs	Stars	UCDs	dE,Ns	BGs	Stars	UCDs	dE,Ns	BGs
$g_0 < 21.5$ & $e < 0.3$	183	71	17	841	183	71	17	841	183	71	17	841
Color-Color Diagram	21	71	9	14	55	69	10	91	55	69	10	91
$\langle\mu_g\rangle_e$	8	69	6	1	10	68	7	17	10	68	7	17
$\langle r_h\rangle$	2	67	4	0	2	66	5	14	2	66	5	14
gzK	...	...	...	...	...	...	...	...	2^a	66^b	5^c	1

[a] These two "stars" lie in the NGVS-1+1 field, where many Virgo members have negative radial velocities. We consider these two objects as UCDs, in which case all three of our selection methods successfully cull the stars from our training set.

[b] Two of these objects are included in our final UCD catalog, while the remaining three have half-light radii of 0.0, 10.1 and 10.8 pc.

[c] These 5 objects are included in the Virgo Cluster Catalogue (VCC; Binggeli et al. 1985).

the "Virgo" group, we only consider two sub-classes of objects: UCDs and galaxies classified in previous or contemporaneous studies as nucleated dwarf elliptical galaxies, which have identifiable point sources at their centers (Binggeli et al. 1985; Sánchez-Janssen et al. 2019; Ferrarese et al. 2020). Diffuse, non-nucleated dwarfs are explicitly excluded in our selection pipeline.

As listed in Table 1, we have 183 stars, 71 UCDs, 17 dE,Ns, and 841 background galaxies (BGs) which satisfy our magnitude and ellipticity criteria (i.e., $14.0 < g_0 < 21.5$ mag and $e < 0.3$). Following this, we successively apply our color, surface brightness, and size cuts, with the choice of colors being the only variable. Table 1 presents the number of objects from each group that survive each step of our selection functions.

For the u^*giK_s-based selection, the color and surface brightness cuts are quite effective at eliminating most of the contaminants. In the end, we find 2 stars ($\sim 1\%$), 67 UCDs ($\sim 94\%$), 4 dE,Ns ($\sim 24\%$) and zero BGs satisfying all of the criteria[6]. For comparison, we find that 2 stars ($\sim 1\%$), 66 UCDs ($\sim 93\%$), 5 dE,N's ($\sim 29\%$)

[6] These percentages represent the fraction of objects, within each group, with $g_0 < 21.5$ mag and $e < 0.3$ that survive all of the selection criteria.

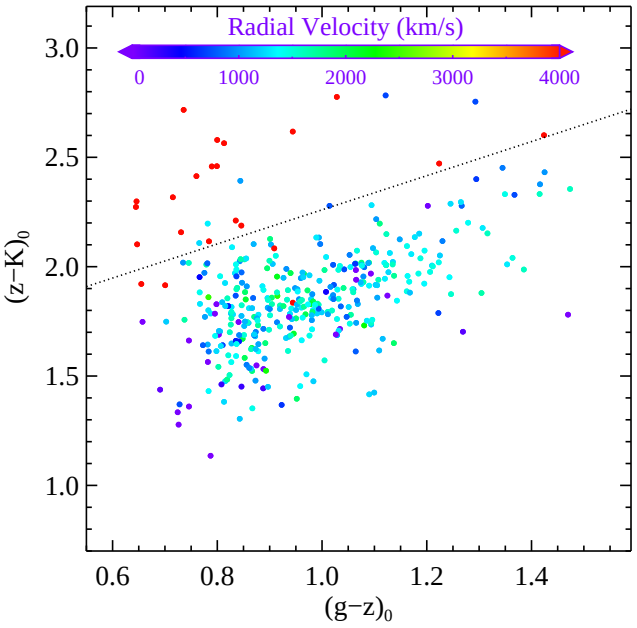

Figure 6. gzK color-color diagram for u^*gz-selected UCD candidates. Different colors indicate different radial velocities as given by color bar. The black dotted line is used to separate background galaxies and UCD candidates.

and 14 BGs ($\sim 2\%$) pass the cuts in our u^*giz-based selection. Thus, both methods achieve a completeness of $> 90\%$ with respect to UCD selection. Conversely, the former method is much better than the latter in culling BGs from the sample. With the addition of K-band data though, we can reduce the number of BGs that pass our u^*giK-based selection from 14 to 1, which compares very favourably with the results of our u^*giK_s-based selection.

As for the other contaminants, we note that all three of our selection methods pass two objects from our training set that are labelled as foreground stars. In fact, these two objects are really UCDs that have negative radial velocities through their association with the M86 subgroup. This shows that the combination of optical and near-infrared photometry removes most foreground and background objects. Where this photometric combination falls short is in rejecting dE,Ns, but we can easily accomplish this through visual inspection since nuclei are surrounded by obvious envelopes.

To summarize, our tests in the central 4 deg^2 of sub-cluster A show that a u^*gizK-based selection of UCDs can be a reliable alternative to that based on u^*giK_s. Hereafter, we mainly rely on our u^*gizK selection method to detect UCD candidates wherever K-band data is available, and u^*giz otherwise.

3.4. *Data Inputs for the Full Catalog*

Based on the material presented to this point, the selection of UCDs would ideally rely on data in the u^*gzK bands for color and surface brightness cuts, and in the g- and i-bands for size cuts. However, as shown in Figure 2, we do not possess imaging in the u^*, i and K bands over the full NGVS footprint. In Table 2, we list the available combinations of photometric data and the corresponding selection method applied in each case. Approximately 90% of bright objects ($g_0 < 21.5$ mag) detected in the NGVS have data in either the u^*gizK or u^*giz bands; all other objects are covered by some subsample of the five available bands.

Table 2 also shows the number ($N_{\rm UCDs}$) and the fraction ($f_{\rm UCDs}$) of UCDs selected by each method. Most of our UCD candidates ($\sim$91%) are selected through either the u^*gizK- or u^*giz-based methods, which were discussed in previous sections. It is noteworthy that only $\sim$37% (286) of these candidates are selected from $\sim$60% of our catalog that has u^*gizK data. Proportionally, we expect to find $\sim$145 UCD candidates from $\sim$30% of the catalog. However, 465 candidates ($\sim$60%) are selected from the $\sim$30% of the catalog that do not have K band data. As described above, K band data is efficient to eliminate BGs. This suggests that the portion of our UCD sample selected via the u^*giz-based method is inflated through contamination by BGs. Note that the other selection methods we have employed contribute just 28 objects to our UCD sample (or $\sim$3%). In all, we have identified 779 UCD candidates based on photometry alone.

Finally we note that if only g- and z-band data are available, we select UCD candidates using the following color cut:

$$0.620 \leq (g-z)_0 \leq 1.500. \quad (6)$$

Also, if i-band half-light radii are not available, we apply the following cuts to the corresponding g-band value:

$$\begin{cases} 11 < r_{h,g} < 100 \text{ pc}; \\ \dfrac{r_{h,g,\rm error}}{r_{h,g}} \leq 15\%. \end{cases} \quad (7)$$

3.5. *Spectroscopically-Selected Virgo Members*

In Figures 5 and 6, we see that a few confirmed Virgo members fall outside our color selection windows. Some of these objects lie close to the window boundaries though and therefore could be UCD candidates. The purpose of our color selection criteria are, first and foremost, to reduce or eliminate contamination from background galaxies. For these few cases, if we know from their radial velocities that they are not background objects, then we do not require color criteria. We assume that the Virgo members are UCDs if they satisfy our

Table 2. Summary of Multi-Band Datasets Over the NGVS Footprint and the Corresponding UCD Selection Methods.

Bands	$f_{\rm Objs}$	Selection Method	$N_{\rm UCDs}$	$f_{\rm UCDs}$	$N_{\rm UCDs,class=1}$	$f_{\rm UCDs,class=1}$
(1)	(2)	(3)	(4)	(5)	(6)	(7)
u^*gizK	59.0%	$u^*gzK + \langle\mu_g\rangle_e + \langle r_h\rangle$	286	34.5%	235	38.4%
u^*giz	29.3%	$u^*gz + \langle\mu_g\rangle_e + \langle r_h\rangle$	465	56.2%	363	59.3%
u^*gzK	2.4%	$u^*gzK + \langle\mu_g\rangle_e + r_{h,g}$	4	0.5%	0	0.0%
u^*gz	0.2%	$u^*gz + \langle\mu_g\rangle_e + r_{h,g}$	1	0.1%	0	0.0%
$gizK$	3.8%	$gzK + \langle\mu_g\rangle_e + \langle r_h\rangle$	1	0.1%	0	0.0%
giz	0.1%	$gz + \langle\mu_g\rangle_e + \langle r_h\rangle$	0	0.0%	0	0.0%
gzK	4.3%	$gzK + \langle\mu_g\rangle_e + r_{h,g}$	9	1.1%	0	0.0%
gz	0.9%	$gz + \langle\mu_g\rangle_e + r_{h,g}$	13	1.6%	0	0.0%
gi+spec	···	$(v_r < 3500$ km/s$) + \langle r_h\rangle$	49	5.9%	14	2.3%
Total	100%	···	828	100%	612	100%

NOTE– (1) the available filter combinations; (2) the fraction of the parent sample covered by each filter combination; (3) the UCD selection method employed; (4) the number of UCD candidates selected; (5) the fraction of all UCD candidates selected; (6) the number of UCDs which survive visual inspection; (7) the fraction of all classified UCDs.

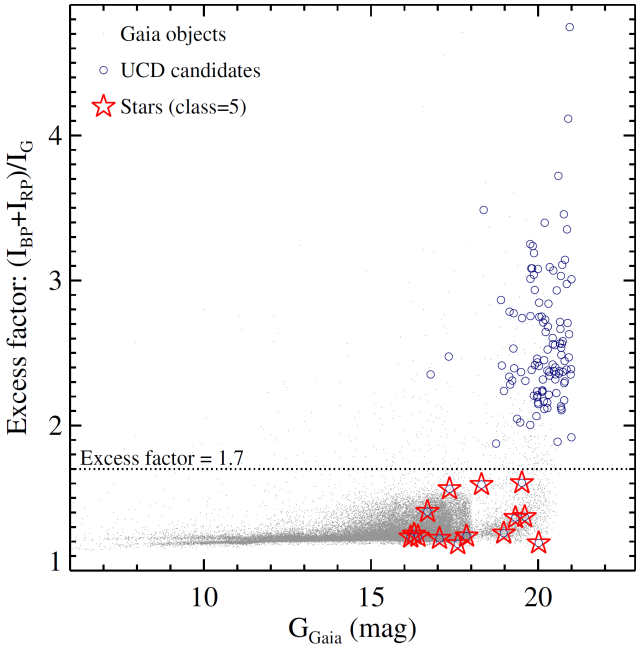

Figure 7. Gaia BP/RP flux excess factor – $(I_{BP} + I_{RP})/I_G$ – as a function of G-band magnitude. Gray dots are Gaia sources in the NGVS footprint. Blue circles are UCD candidates which have a Gaia counterpart. Red stars are objects classified as stars (`class = 5`) in this study. The black dotted line shows an excess factor of 1.7, a division that is found to separate stellar and extended sources.

size cuts (Equation 3, or 7 if i-band data are not available). This assumption is reasonable as most objects in the literature in this size range are UCDs. There are ∼8000 Virgo objects with $v < 3500$ km/s and do not satisfy our color or/and surface brightness cuts. Among these objects, we find an additional 49 UCD candidates through this "perturbation" method and henceforth refer to them as "spectroscopically-selected UCD".

In Table 1, we recover 66 of the 71 known UCDs using either our u^*giz- or u^*gizK-based methods (the remaining five do not meet all of our selection criteria). In reality, two of these five "missing" UCDs are included in the spectroscopically-selected UCD sample. The three remaining UCDs have $\langle r_h\rangle = 0.0$ (due to the bad image quality in this region), 10.1 and 10.8 pc individually: i.e., two of the three are slightly smaller than our size criterion.

3.6. *Visual Inspection*

As explained above, we have objectively selected 828 UCD candidates: 779 and 49 based on photometric and spectroscopic information, respectively. As a final hedge against contamination, we execute one last step — visual inspection of the NGVS images, whereby we classify each candidate as either a: (1) = `probable UCD`; (2) = `dwarf nucleus`; (3) = `background galaxy`; (4) = `blended object`; (5) = `star`; (6) = `star-forming region`.

Some contaminants can be difficult to identify from visual inspection alone and, in such cases, we classify objects using additional information. For example, a nucleated dwarf galaxy (`class = 2`) usually contains a

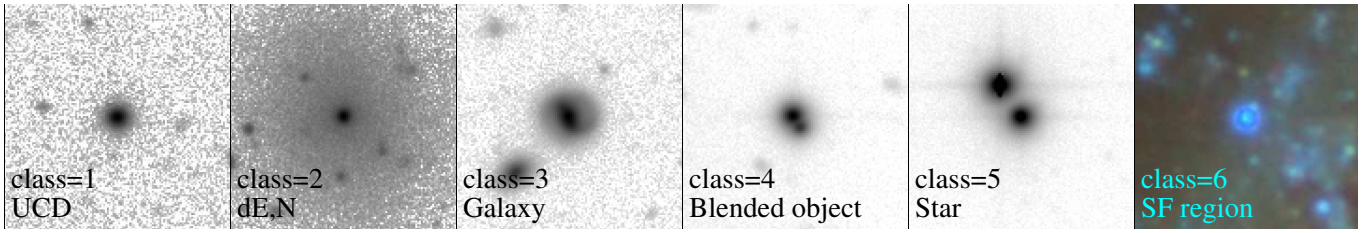

Figure 8. UCD candidates are divided into six classes by visual inspection. From left to right: UCD – class = 1; nucleated dwarf elliptical galaxy (dE,N) – class = 2; background galaxy – class = 3; blended object – class = 4; star – class = 5; star-forming region – class = 6. The image size in each panel is 120 × 120 pixels, where 120 pixels $\sim 22.32''$ $\sim$ 1.8 kpc at Virgo distance.

nucleus at its photocenter (although some are slightly off-centered) and a stellar halo component surrounding it. Some UCDs are also embedded in low-surface brightness envelopes (e.g., Haşegan et al. 2005) making it difficult to distinguish dE,Ns from UCDs with envelopes. We therefore classify objects as dE,Ns only when they appear in either the VCC (Binggeli et al. 1985) or NGVS galaxy catalogs (Ferrarese et al. 2020). Background galaxies are identified with the help of redshift measurements, and all objects with $v_r > 3500$ km/s are immediately classified as such (`class = 3`). Blended objects (`class = 4`) are relatively easy to identify, although they may not be separable in NGVS images if they are too close. We make use of Gaia DR2 data (Riello et al. 2018) to help further separate UCDs and stars (`class = 5`), in that stars can have significant proper motions (i.e., 3σ significance) and UCDs can be resolved in Gaia imaging (see Voggel et al. 2020). Figure 7 shows the BP/RP flux excess factor, which is defined as flux ratio $(I_{BP} + I_{RP})/I_G$, as a function of Gaia G band magnitude. Briefly, the fluxes in BP and RP bands (I_{BP} and I_{RP}) are measured in a window of 3.5×2.1 arcsec^2 while the flux in G band (I_G) is derived from PSF fitting. For point sources, the flux excess factor should be $\gtrsim$1 (the BP and RP filters overlap at around 6500Å and are broader than the G band, especially at the red side, see Evans et al. 2018). As shown in Figure 7, most of Gaia targets have small flux excess factors while the excess factor of extended objects can be much larger: e.g., most of our UCD candidates (blue circles) in Figure 7 have excess factors of 2–4. We draw a line at an excess factor of 1.7 and classify sources below this level as stars. Finally, the star-forming regions (`class = 6`) are also easy to identify due to their blue colors.

In summary, among our 828 UCD candidates, we find 612 probable UCDs (598 identified on the basis of photometry alone), 41 nucleated dwarf galaxies, 132 background galaxies, 12 blended objects, 14 stars and 17 star-forming regions. Representative images for these six types of objects are shown in Figure 8. As can be seen in the final two columns of Table 2, 235 of the photometrically identified UCDs are u^*gizK-selected while the remaining 363 are u^*giz-selected. The UCD candidates initially selected based on other methods (i.e., u^*gzK, u^*gz, $gizK$, giz, gzK, and gz) are classified as contaminants after visual inspection — one of the reasons that we only test the u^*giz- and u^*gizK- selection methods in §3.3.

3.7. *Catalog of UCD Candidates*

Tables 3 and 4 present observed and derived parameters for all of our UCD candidates[7]. Since visual inspection is inevitably subjective, we list all 828 objectively-selected candidates in these tables. We plan to measure radial velocities in future spectroscopic campaigns and assess their Virgo membership directly. Indeed, some of these "contaminants" (such as apparent star-forming regions with UCD-like sizes) are interesting in their own right and will be investigated in future papers.

3.8. *Summary of UCD Selection Function*

Given the complexity of our methodology, Figure 9 summarizes our UCD selection function in the form of a flowchart. An inspection of this figure shows that our selection process involves two main channels: one based on photometry (right) and the other on spectroscopy (left), which we now describe.

We begin with the photometric algorithm. There are 346,948 objects in the NGVS that satisfy our magnitude ($14.0 < g_0 < 21.5$ mag) and ellipticity ($e < 0.3$) cuts. All of these objects have g- and z-band data, while u^*-, i- and K-data are more limited. Note that only objects detected in our short exposures lack u^*- and i-band data (see Figure 2), and so are drawn from the bright end of the UCD luminosity function. We then apply successive cuts based on each object's color (or colors), surface brightness (Equation 2), position in the gzK diagram (Equation 5; if K-band data available), and half-light radius (Equation 3 if i-band data available; otherwise Equation 7). Our color cuts are based

[7] See https://gax.sjtu.edu.cn/data/UCDs.html

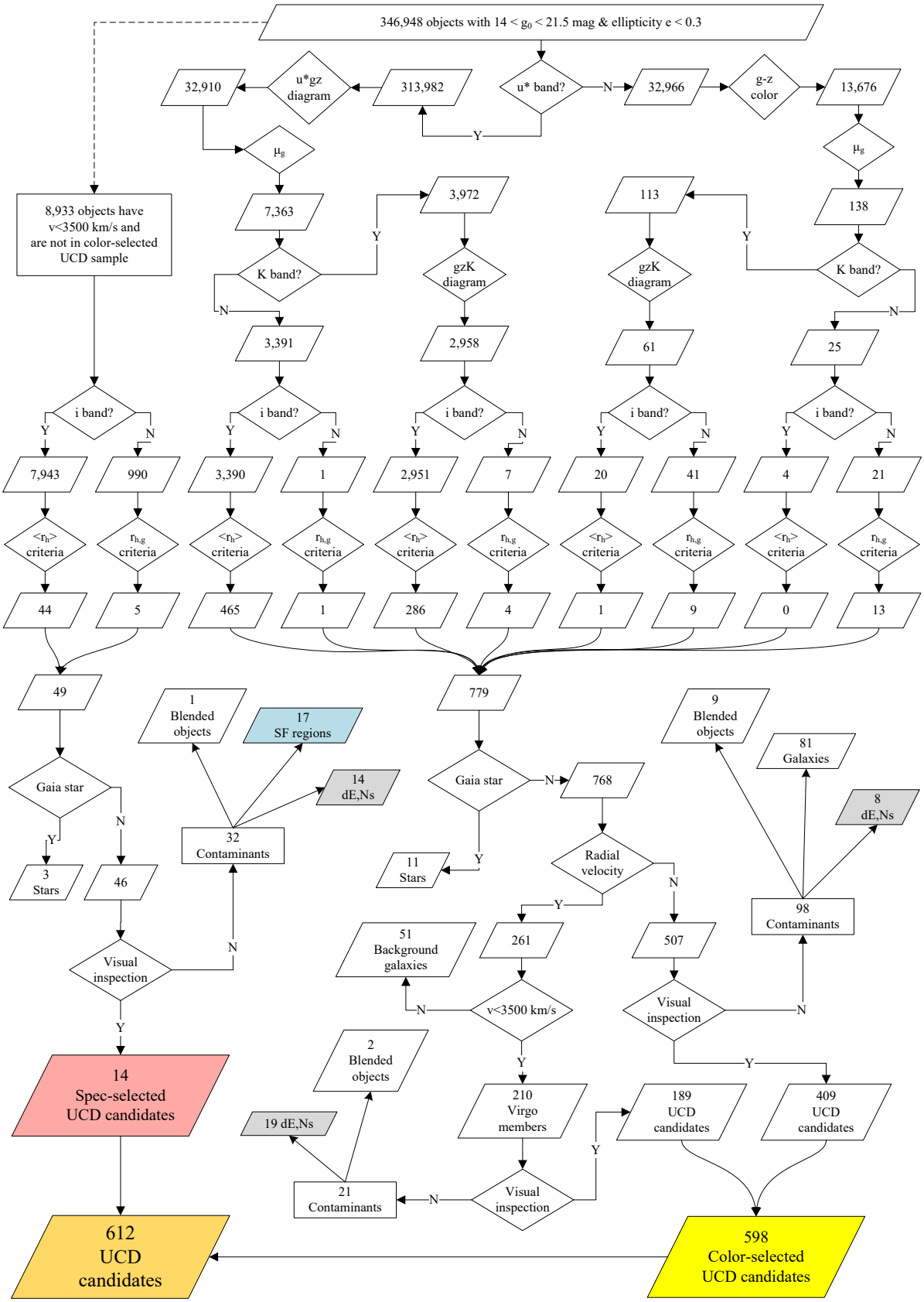

Figure 9. The "Pachinko Machine" plot illustrating the UCD selection methods used in this study. Our UCD selection is based on the combination of magnitude ($14.0 < g_0 < 21.5$ mag), ellipticity ($e \equiv (1 - b/a) < 0.3$), color-color diagram, surface brightness and half-light radius cuts and visual inspection. In total, a sample of 612 UCDs were identified in NGVS imaging.

on the u^*gz diagram (Equation 4) for those objects having u^*-band data; otherwise, we consider the $(g-z)$ color alone (Equation 6).

These selection criteria dramatically reduce our original photometric sample from 346,948 objects to 779 candidate UCDs. With the assist of Gaia (see Figure 7), 11 of these candidates are re-classified as stars. To further reduce the number of contaminants, we place a cut on radial velocities (when available) and visually inspect the candidates (see Figure 8). Another fifty-one candidates are removed for having a radial velocity in excess of $v = 3500$ km/s and 119 more are removed following visual inspection. The latter group is comprised of 27 dE,Ns, 81 background galaxies and 11 blended objects. Our final photometric UCD sample contains 598 UCD candidates.

We now describe the spectroscopic selection function depicted in Figure 9. As stated earlier, this path is intended to select UCD candidates that fall outside our color and/or surface brightness selection windows. Using this approach, we find 49 more candidates which meet our radius cuts, while visual inspection shows that they are comprised of 14 probable UCDs, 17 star-forming regions, 14 dE,Ns, 3 stars and 1 blended object.

Overall, we have identified 612 UCD candidates, the majority of which (598) come from our photometric selection function. This constitutes the largest sample of UCD candidates identified to date. While we would prefer a simple and homogeneous selection, the lack of data in the u^*, i, and K bands over the full NGVS footprint necessitates certain compromises. That said, the great majority ($598/612 \simeq 97.7\%$) of these UCD candidates have been selected based on their u^*giz or u^*gizK colors.

We refer to the full group of candidates as the "`all UCD sample`". Within this group, 235 candidates have been selected on the basis of their u^*gizK data, so we refer to this as the "u^*gizK `UCD sample`". We also have a "`spec-UCD sample`", which contains the 203 candidates that have been spectroscopically confirmed as members of the Virgo cluster. The "`all UCD sample`" has the highest completeness but the largest number of contaminants. Conversely, the "`spec-UCD sample`" has the fewest contaminants but is inevitably biased by the choice of spectroscopic targets. Finally, the "u^*gizK `UCD sample`" strikes the greatest balance between completeness, contamination, and homogeneity (see Table 1).

3.9. *UCDs from Previous Studies*

As nearest rich cluster of galaxies, many previous investigations have studied UCDs in virgo (e.g., Haşegan et al. 2005; Jones et al. 2006; Evstigneeva et al. 2007b; Strader et al. 2011; Liu et al. 2015a; Zhang et al. 2015; Ko et al. 2017). Our sample contains 186 UCDs that have already been reported, while 29 systems from previous work are excluded. We list the properties of each member of the latter group in Table 5, including name, right ascension, declination, ellipticity, magnitude, half-light radius, radial velocity, the sources of velocity measurements, and the primary reason why it is not included in our sample. Among these 29 UCDs, six are fainter than $g_0 = 21.5$ mag, three have high ellipticity ($e > 0.3$), 12 do not satisfy the radius criteria, four are located just outside the selection window in $(g-z)_0$ vs. μ_g diagram, two are classified as background galaxies by gzK diagram, and two escaped detection in the NGVS images because they are projected close to saturated stars. We also note that 9 of these 29 UCDs lack radial velocity measurements.

4. RESULTS

To understand the nature and origin of UCDs — and the extent to which they differ from other compact stellar systems — it is important to first understand how their properties compare to those of GCs and nuclei, where evolutionary links to UCDs may exist. To this end, we now describe various samples of each class of compact stellar system in Virgo available to us.

Globular Clusters:

- `ACSVCS GCs`: The sample of GCs from the HST ACS Virgo Cluster Survey. The objects with $p_{gc} > 0.95$ are included in this sample, where p_{gc} represents the probability that an object is a GC (Peng et al. 2006a; Jordán et al. 2009).
- `Bright GCs`: A magnitude-limited ($g_0 < 21.5$ mag) sample of NGVS objects that satisfy our UCD selection criteria but have $\langle r_h \rangle < 11$ pc. This sample includes GC candidates without velocity measurements and GCs with $v_r < 3500$ km/s. Background galaxies with $v_r > 3500$ km/s are removed from the sample.
- `Spec GCs`: The subset of `bright GCs` with radial velocities $v_r < 3500$ km/s.

Ultra Compact Dwarfs:

- `All UCDs`: Our full sample of 612 UCD candidates, which satisfy all of our selection criteria and pass our visual inspection. Amongst this sample, 203 ($\sim$1/3) have $v_r < 3500$ km/s; all others lack radial velocity information.

Table 5. The properties of UCDs which are in previous studies but not included in this study.

Name	α_{J2000} (deg)	δ_{J2000} (deg)	e	g_0 (mag))	$\langle r_h \rangle$ (pc))	v_r (km/s)	v_{source}	Note
(1)	(2)	(3)	(4)	(5)	(6)	(7)	(8)	(9)
S1508	187.6308727	12.4235661	0.07	22.018	···	2419	S11	$g_0 > 21.5$ mag
S825	187.7126346	12.3554004	0.16	21.613	···	1142	S11	$g_0 > 21.5$ mag
S723	187.7239811	12.3393933	0.07	21.737	···	1398	NED,S11	$g_0 > 21.5$ mag
H44905	187.7378222	12.3944049	0.20	21.921	···	1564	NED,S11	$g_0 > 21.5$ mag
H30401	187.8279366	12.2624564	0.18	21.593	···	1323	NED,S11	$g_0 > 21.5$ mag
T15886	188.1520299	12.3491986	0.23	22.974	···	1349	NED,S11	$g_0 > 21.5$ mag
S991	187.6937514	12.3382605	0.34	20.701	16.67	1004	S11	$e > 0.3$
S672	187.7280306	12.3606434	0.31	20.739	15.50	735	S11	$e > 0.3$
NGVS-J124002.08+105517.2	190.0086686	10.9214418	0.50	21.338	3.48	···	···	$e > 0.3$
NGVS-J122926.23+081658.8	187.3593098	8.2829991	0.05	21.373	9.06	465	MMT14	$\langle r_h \rangle < 11$ pc
NGVS-J123009.17+074127.5	187.5381980	7.6909633	0.08	19.449	10.76	···	···	$\langle r_h \rangle < 11$ pc
NGVS-J123015.56+083445.0	187.5648407	8.5791729	0.07	20.822	10.33	-129	MMT14	$\langle r_h \rangle < 11$ pc
H20718	187.5818069	12.1568298	0.03	20.989	10.76	876	MMT09,S11	$\langle r_h \rangle < 11$ pc
M87UCD-31	187.7305441	12.4110907	0.02	20.860	10.09	1301	MMT09	$\langle r_h \rangle < 11$ pc
M87UCD-14	187.7681413	13.1784860	0.12	20.200	10.83	1345	MMT09,AAT12	$\langle r_h \rangle < 11$ pc
NGVS-J122849.25+075919.4	187.2051905	7.9887156	0.03	21.179	13.37	···	···	$\lvert r_{h,g} - r_{h,i} \rvert > (r_{h,g} + r_{h,i})/2$
NGVS-J123004.35+073932.2	187.5181421	7.6589449	0.09	21.437	11.19	1043	MMT14	$\lvert r_{h,g} - r_{h,i} \rvert > (r_{h,g} + r_{h,i})/2$
S8005	187.6925322	12.4064233	0.02	20.444	27.91	1883	S11	$\lvert r_{h,g} - r_{h,i} \rvert > (r_{h,g} + r_{h,i})/2$
S9053	187.7013369	12.4946708	0.16	21.313	30.25	829	S11,IMACS16	$\lvert r_{h,g} - r_{h,i} \rvert > (r_{h,g} + r_{h,i})/2$
S686	187.7242079	12.4718872	0.05	20.499	16.31	817	S11	$\lvert r_{h,g} - r_{h,i} \rvert > (r_{h,g} + r_{h,i})/2$
S6003	187.7922587	12.2744282	0.08	21.277	14.19	1818	S11	$\lvert r_{h,g} - r_{h,i} \rvert > (r_{h,g} + r_{h,i})/2$
NGVS-J122806.14+065909.0	187.0255686	6.9858243	0.19	20.200	27.66	···	···	$(g-z)_0$ VS. μ_g diagram
NGVS-J123949.21+110135.3	189.9550398	11.0264758	0.03	21.080	12.73	···	···	$(g-z)_0$ VS. μ_g diagram
NGVS-J124216.65+114428.6	190.5693756	11.7412681	0.06	21.273	12.44	···	···	$(g-z)_0$ VS. μ_g diagram
NGVS-J124244.72+111240.5	190.6863239	11.2112384	0.12	20.491	32.90	···	···	$(g-z)_0$ VS. μ_g diagram
NGVS-J122708.94+074228.3	186.7872607	7.7078639	0.08	19.340	47.81	···	···	$(g-z)_0$ VS. $(z-K_{UKIDSS})_0$ diagram
NGVS-J122828.60+070228.2	187.1191854	7.0411563	0.11	20.646	28.26	···	···	$(g-z)_0$ VS. $(z-K_{UKIDSS})_0$ diagram
S887	187.7038900	12.3654400	···	21.190	···	1811	S11	Fail to detect
H30772	187.7419100	12.2672800	···	20.750	···	1225	NED,S11	Fail to detect

NOTE– (1) UCD name; (2) RA; (3) Dec; (4) Ellipticity; (5) g band magnitude; (6) Half-light radius; (7) Radial velocity; (8)The source of velocity measurement; (9) The reason why this UCD is not included in this study.

- u^*gizK `UCDs`: The subset of 235 UCDs selected from u^*gizK data, a fraction of which have velocity measurements.
- `Spec UCDs`: The subset of 203 UCDs with $v_r < 3500$ km/s.

Stellar Nuclei:

- `All nuclei`: The entire sample of 551 nuclei from the NGVS galaxy catalog (Sánchez-Janssen et al. 2019; Ferrarese et al. 2020).
- `Bright nuclei`: The subset of 339 bright ($g_0 < 21.5$ mag) nuclei from the NGVS galaxy catalog.
- u^*gizK `nuclei`: The sample of 41 nuclei that satisfy our UCD selection criteria and are classified as dE,Ns by visual inspection (i.e., `class=2`).

In the analysis that follows, we mainly focus on the `bright GCs`, u^*gizK `UCDs` and `bright nuclei` samples. This means that, for the first time, we are using homogeneous samples of GCs, UCDs and nuclei *selected from the same data set using consistent selection criteria*. We also use the `ACSVCS GCs`, `all UCDs` and `all nuclei` samples when we require higher completeness, while the `spec GCs` and `spec UCDs` samples are drawn on when cleaner samples are required.

A complementary approach is to study individual UCDs with special properties that can shed light on their origins. For example, Seth et al. (2014) found a supermassive black hole (SMBH) in M60-UCD1, which comprises 15% of the system's total mass. This single piece of evidence strongly suggests that the progenitor of M60-UCD1 was a nucleated dwarf galaxy.

In this section, we will summarize the basic statistical properties of our UCD samples, compare to those of GCs and nuclei, and examine interesting sub-samples of UCDs found in the NGVS (e.g., Liu et al. 2015b).

4.1. *Spatial Distribution*

The upper two panels of Figure 10 show number density maps for our `all UCDs` sample in Virgo. Durrell et al. (2014) found that the spatial distribution of Virgo GCs is similar to that of its X-ray-emitting gas, so we compare the distribution of UCDs (color-coded number density map) and X-ray gas (contours) in panel (a) of Figure 10. Consistent with Durrell et al. (2014), we find the densest concentrations of UCDs (i.e., the brightest regions in the map) are located in the regions that have the greatest amount of X-ray gas. This finding is also

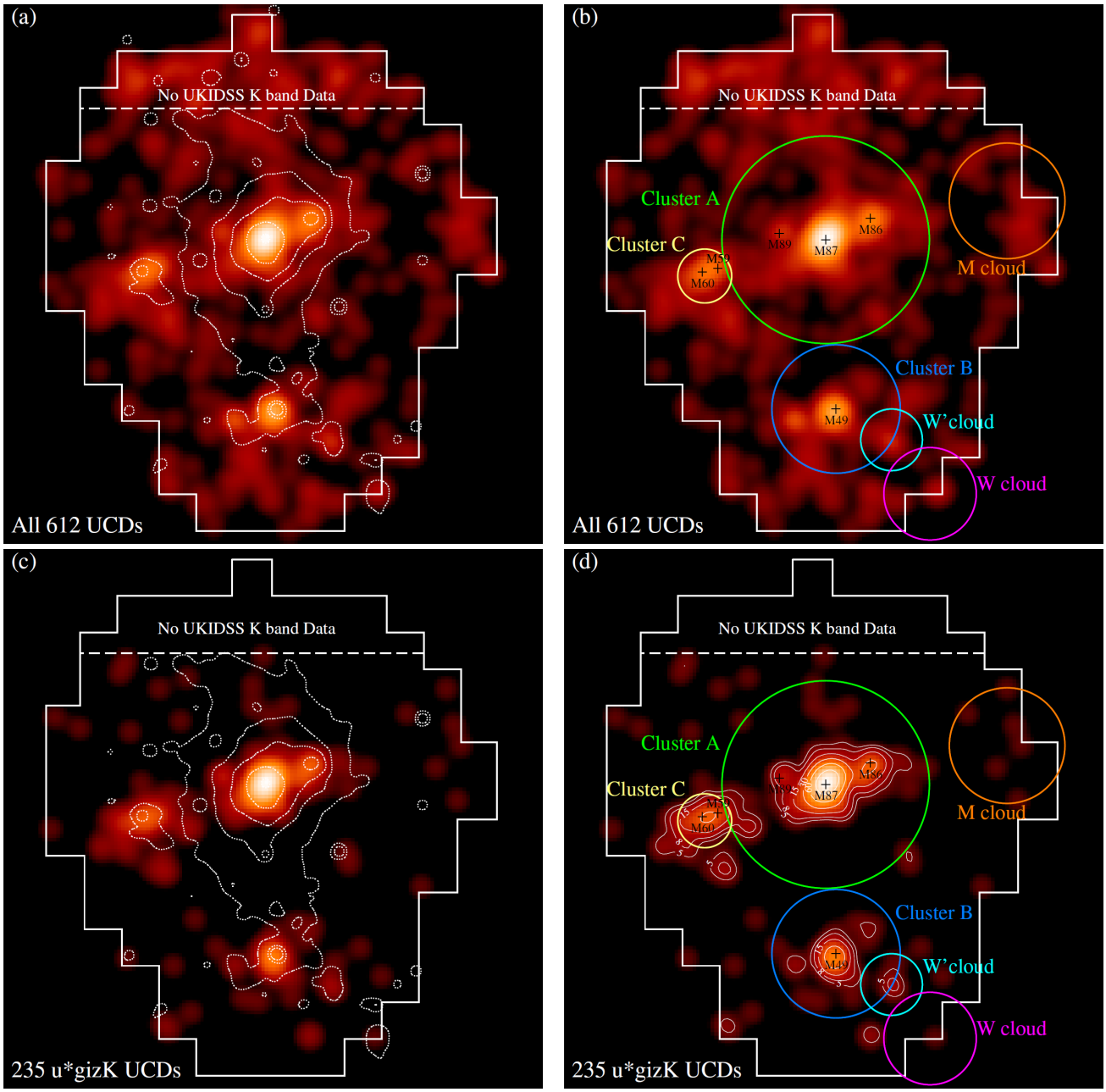

Figure 10. The number density map of 612 `all UCDs` (upper panels) and 235 u^*gizK `UCDs` (lower panels) identified in the NGVS. The maps have been smoothed with a Gaussian kernel with fixed FWHM $\approx 12'$. The white solid polygon in each panel denotes the NGVS survey region. We have no UKIDSS K-band data above the white dashed line in each panel. The contours in left panels show the distribution of X-rays from the Rosat all sky survey in the 0.4-2.4 keV energy range (Böhringer et al. 1994). In the right panels, we show the locations of a few bright galaxies (black crosses) and known galaxy sub-structures (color circles). The contours in panel (d) show the number density contours of $\Sigma_{\rm UCD} = 5, 8, 15, 30$ and 60 deg^{-2}.

consistent with the observed correlation between number of UCDs and the X-ray gas mass of their host ($N_{\rm UCD}$ vs. $M_{\rm gas}$; see Figure 17 in Liu et al. 2015a).

The number density map shown in the panel (b) is the same as in the panel (a), but overlaid with known substructures in the cluster (i.e., the colored circles). The locations and radii of the substructures are taken from Boselli et al. (2014). Most of the UCDs are concentrated in sub-cluster A (green), sub-cluster B (blue) and sub-cluster C (yellow) (see also Liu et al. 2015a). There are far fewer UCDs in the other three substructures: the W' (cyan), W (purple) and M clouds (red). This may be due, in part, to the fact that these three substructures are located farther away from us (Mei et al. 2007;

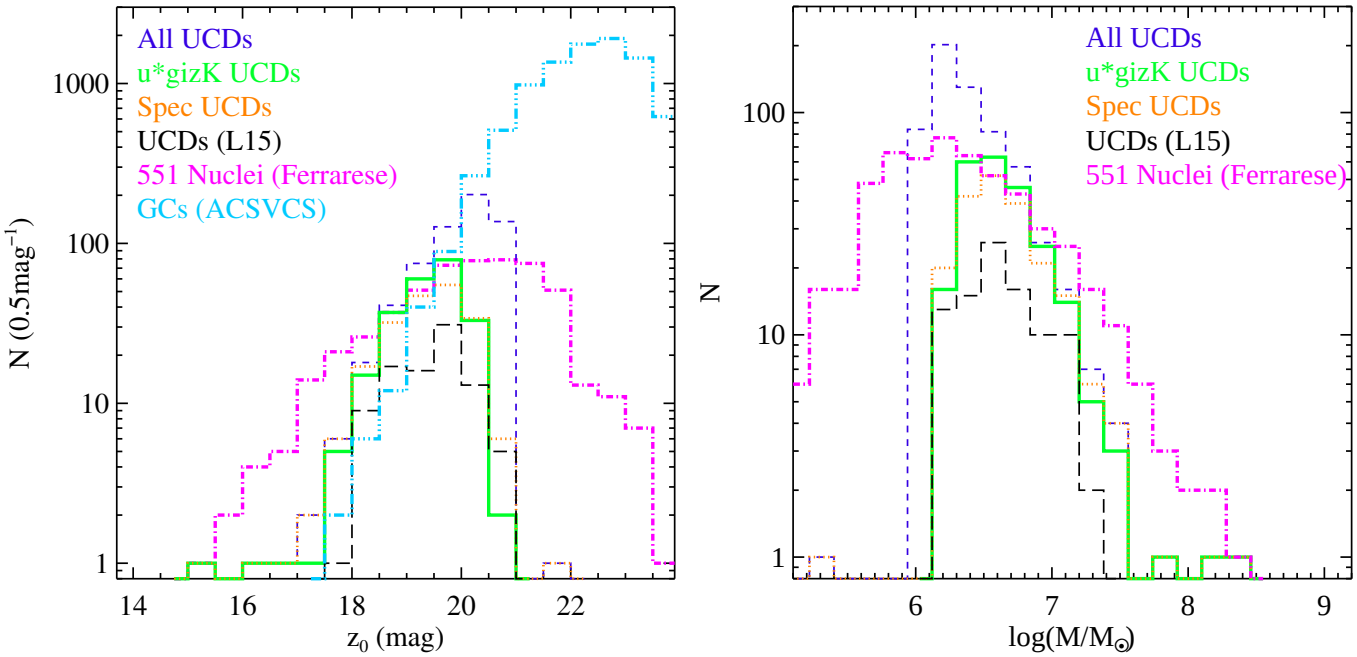

Figure 11. The distribution of z-band magnitudes (*left panel*) and stellar masses (*right panel*) for compact stellar systems in Virgo. Blue short-dashed line: `all UCDs` sample (612 candidates); green solid line: u^*gizK `UCDs` sample (235 candidates); orange dotted line: `spec UCDs` sample (203 candidates); black long-dashed line: 92 UCDs from Liu et al. (2015a); cyan line: `ACSVCS GCs` sample (Jordán et al. 2009); magenta line: `all nuclei` sample (Ferrarese et al. 2020).

Cantiello et al. 2018), making it more difficult to identify UCDs (by size). At the same time, the reduced gas mass (see the contours in panel a) in these substructures are also likely to be a factor. This is especially true for the M cloud, which shows no significant amount of X-ray gas. Based on the $N_{\rm UCD}$-$M_{\rm gas}$ scaling relation (Liu et al. 2015a) then, the absence of UCDs in this region would not be surprising. In addition, the edges of the NGVS footprint cut through the M and W clouds. This may be another reason why we do not detect many UCDs in these regions.

The lower two panels of Figure 10 show number density maps for our u^*gizK `UCDs` sample. As noted above, and as can be seen in the plots, this sample is noticeably cleaner. We also point out that the number densities from the `all UCDs` sample are higher in the regions without UKIDSS K-band data (above the white dashed lines in panels (a) and (b)), indicating elevated contamination in this region. The u^*gizK `UCDs` are mainly concentrated around a handful of luminous galaxies: e.g., M87, M49, M60, M59, M86 and M89 (black crosses). The galaxies with low densities of UCDs cannot be seen in this map as we smooth the distribution using a large kernel (∼12' ∼ 60 kpc).

Table 8 of Liu et al. (2015a) presents estimates of the number density of contaminants in the NGVS based on four control fields. The mean density for our u^*giz-selection method is 2.25 deg^{-2}. As demonstrated in §3.3, our u^*gizK-selection method should be much cleaner by comparison. Indeed, Liu et al. (2015a) estimated the contaminant number density using their $u^*giK_{\rm VISTA}$ selection method to be just 0.9 deg^{-2} (the last row of their Table 8). The contours in panel (d) represent number densities of $\Sigma_{\rm UCD} = 5, 8, 15, 30$ and 60 deg^{-2}. We note that there are a few regions with $\Sigma_{\rm UCD} > 5$ deg^{-2} that fall outside of any known substructures. They may be intracluster UCDs or UCDs associated with low- or intermediate-mass galaxies (e.g., Fahrion et al. 2019). We intend to focus on these regions in future papers.

4.2. *Luminosity and Stellar Mass Distribution*

Our homogeneous sample provides us with an opportunity to carry out a study of the UCD luminosity function (UCDLF). The left panel of Figure 11 shows histograms of z-band magnitudes for a variety of UCD samples, which are identified in the upper-left corner. The distribution for the `all UCDs` sample (blue, short-dashed histogram) has a higher peak value than all other UCD samples, which we suspect is due to contamination (especially at the faint end). Note that the truncation at $z_0 \sim 21.0$ mag is the result of our magnitude cut at $g_0 = 21.5$ mag and is therefore artificial.

For the other, smaller samples of UCDS, we find a peak at roughly $z_0 \sim 19.75$ mag. Note that the `spec UCDs` sample (orange dotted line) may be biased be-

cause brighter UCDs are more amenable to spectroscopic follow-up. The u^*gizK `UCDs` sample (green solid line) has higher completeness than the `spec UCDs` sample but is limited by the shallow UKIDSS K-band imaging, which may cause us to miss some objects at the faint end. The UCD sample from Liu et al. (2015a) (black long dashed line) is the best available based strictly on the u^*giK_s selection method, where the K_s-band data reach to $\sim$ 24 mag. For comparison, we also show in Figure 11 the GC luminosity function (GCLF) from the ACSVCS (cyan line), which exhibits the well-known turnover for this population (e.g., Jordán et al. 2007; Villegas et al. 2010). Despite the fact that three of our UCDLFs also exhibit turnovers, we cannot ensure that these features are authentic. It is quite probable that, depending on where we place our (subjective) size cut (set at $r_h = 11$ pc), the prominence and location of this peak would change.

The right panel of Figure 11 shows distributions of stellar mass for UCDs and nuclei. Stellar masses have been determined using the relationships between stellar mass-to-light ratios and colors from Bell et al. (2003). We calculate four sets of stellar masses, based on the relations for $(u-g)$, $(u-i)$, $(u-z)$ and $(g-z)$ colors (see their Table 7), and use the mean value for each object in the figure. Other than the `all UCDs` sample, there appears to be a peak in the UCD stellar mass function at $M_* \sim 10^{6.6}$ M$_\odot$, roughly equivalent to that seen in the UCDLF. Again though, because of our selection criteria, we cannot be sure whether this is a genuine characteristic of the UCD population.

The magenta lines in both panels of Figure 11 show the luminosity and mass functions for the `all nuclei` sample that consists of 551 dE,N nuclei. The nuclei LF shows a clear turnover around $z_0 \sim 20.5$ mag and $M_* \sim 10^{6.2}$ M$_\odot$ and covers a larger stellar mass range ($10^{5.0} \lesssim M_* \lesssim 10^{8.5}$ M$_\odot$) than UCDs. Sánchez-Janssen et al. (2019) studied the mass function of nuclei in the Virgo core region and found a peak at $M_* \sim 10^{6.08}$ M$_\odot$, which is consistent with the result in this study.

4.3. *Color Distribution*

It is well established that bimodal color distributions are a common feature of GC systems in massive elliptical galaxies (e.g., Gebhardt & Kissler-Patig 1999; Kundu & Whitmore 2001; Peng et al. 2006a). Interestingly, a bimodal color distribution has also been observed for the UCDs surrounding M87 (Liu et al. 2015a), making it the only galaxy in the Virgo cluster that shows significant UCD color bimodality.[8] With our new UCD sample, we can examine for the first time the color distribution for UCDs distributed over the entire Virgo cluster.

Figure 12 shows the color distribution for the `ACSVCS GCs` (the first row, magenta histogram), `bright GCs` (the second row, cyan histograms), u^*gizK `UCDs` (the third row, green histograms) and `bright nuclei` (the forth row, purple histogram). All objects are brighter than $g_0 = 21.5$ mag. Because we have only g and z data for the `ACSVCS GCs`, the first row shows only a $(g-z)_0$ distribution. By contrast, a total of six color indices – $(u^*-g)_0$, $(u^*-i)_0$, $(u^*-z)_0$, $(g-i)_0$, $(g-z)_0$ and $(i-z)_0$ – are shown (from left to right) in the second, third and forth rows. The distributions of GCs, UCDs and nuclei have red tails for all indices except $(i-z)_0$ for the nuclei. To quantify the bimodality of color distributions, we use Gaussian Mixture Modeling (GMM; Muratov & Gnedin 2010) and assume a homoscedastic distribution: i.e., two sub-populations having the same dispersions. As described by Muratov & Gnedin (2010), a dimensionless peak separation ratio D (see Equation A3 in their paper) should be larger than 2 for a bimodal distribution. We measure D for the color distribution in each panel of Figure 12. The D parameters for GCs and UCDs are larger than 2 while those for nuclei are smaller than 2. In addition, the unimodal distribution is rejected at a level better than 1% for `bright GCs` and better than 0.1% for `ACSVCS GCs` and u^*gizK `UCDs`.

The best-fit GMM models are shown in Figure 12 as well. For those distributions found to be bimodal, blue and red curves are used to represent the individual components (with vertical dashed lines marking their respective means), while the black curves represent their sums. Conversely, where unimodal distributions are favored, we show the best-fit Gaussians (black curves) and the corresponding means (vertical dashed lines).

In the case of a bimodal color distribution, GMM also yields the probability that a given object belongs to the blue or red component. We therefore calculate the fraction of objects belonging to the blue sub-population, $f_{\rm blue}$. The $f_{\rm blue}$, based on the $(g-z)_0$ color index, is 77% (±4%), 84% (±1%) and 89% (±3%) for `ACSVCS GCs`, `bright GCs` and UCDs. Based on ACSVCS data, Peng et al. (2006a) concluded that the blue GC fraction for individual galaxies ranges from 85% to 40%, and decreases with increasing host galaxy luminosity.

There are two main reasons why the blue fractions are different between `ACSVCS` and `bright GCs`. First,

[8] The bimodal UCD color distribution for M49 reported in Liu et al. (2015a) has low statistical significance.

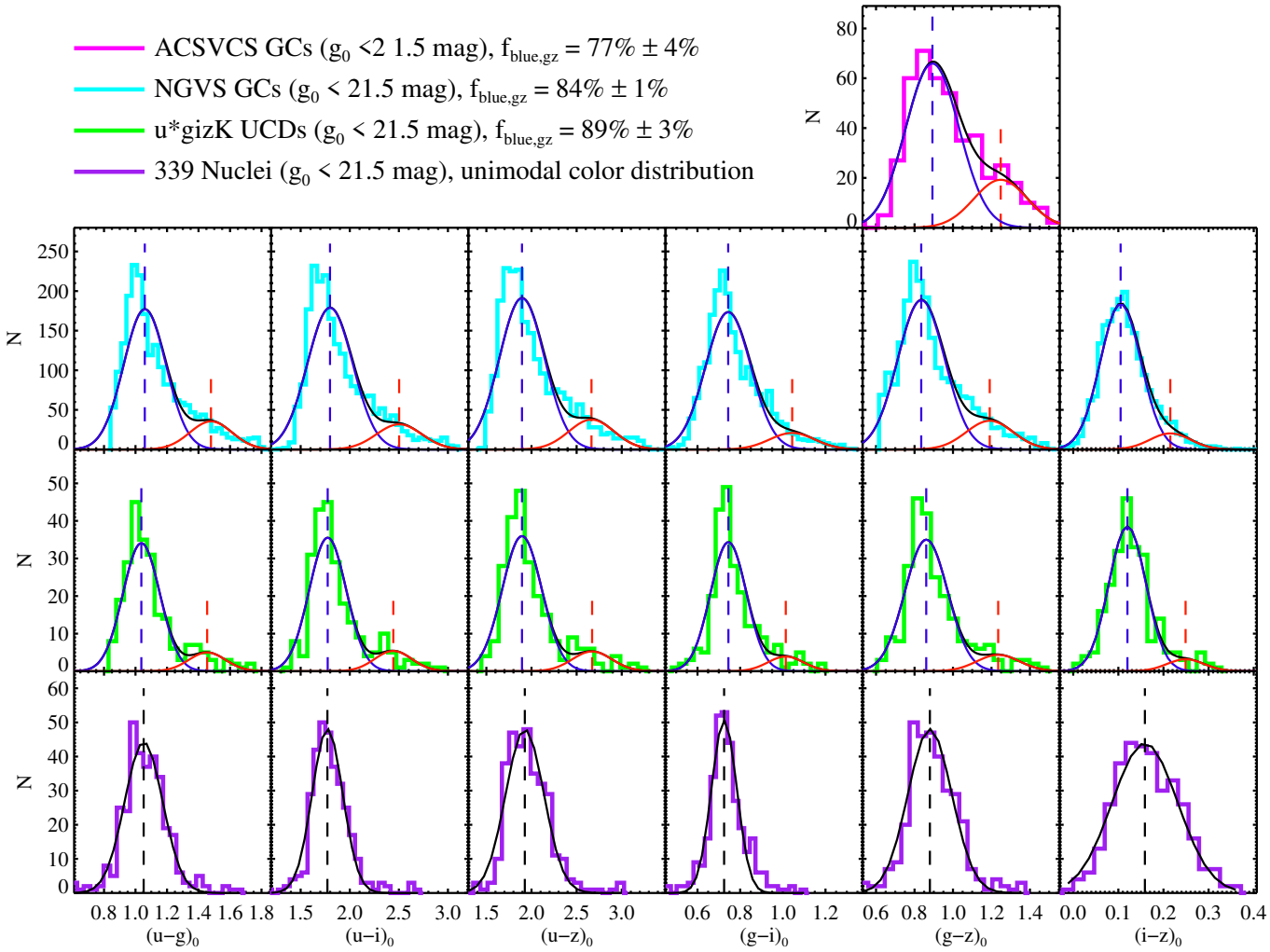

Figure 12. The color histograms for `ACSVCS GCs` (the first row, magenta histogram), `bright GCs` (the second row, cyan histograms), u^*gizK `UCDs` (the third row, green histograms) and `bright nuclei` (the forth row, purple histogram). All objects are brighter than $g_0 = 21.5$ mag. Colors plotted, from left to right, are: $(u-g)_0$, $(u-i)_0$, $(u-z)_0$, $(g-i)_0$, $(g-z)_0$ and $(i-z)_0$. For the bimodal color distributions, we show blue and red Gaussian components (blue and red curves) and their sums (black curves). For the unimodal color distributions, we plot the best fit single Gaussians using black curves. The vertical dashed line(s) shows the mean(s) of the associated color distribution(s).

the blue fraction of `bright GCs` is calculated over the entire cluster which contains many more dwarf galaxies (which have higher $f_{\rm blue}$) than the ACSVCS galaxy sample. Second, as described in Jordán et al. (2005), almost all the GCs in the Virgo cluster can be resolved in ACSVCS imaging, which enables a very clean GC selection (see Peng et al. 2006a; Jordán et al. 2009), while our `bright GC` sample is contaminated by many background galaxies when the K-band data is not available (see Table 1). Therefore, our `bright GC` sample contains more dwarf galaxies and is less pure than the `ACSVCS GC` sample, causing it to have a higher blue fraction. For nuclei, we can see from the last row of Figure 12 that the vast majority are blue with just a few having red colors. Since a unimodal distribution is preferred for this group, we are unable to calculate a blue fraction on the basis of GMM alone. However, considering that the blue and red components for GCs and UCDs cross at $(g-z)_0 \sim 1.1$, we can split the nuclei distribution at this color to calculate their blue fraction. In so doing, we find an $f_{\rm blue} \sim 95\%$.

To summarize, for objects brighter than $g_0 = 21.5$, GMM fitting shows that GCs and UCDs exhibit bimodal color distributions while the nuclei follow a unimodal distribution with a small tail to red colors. Ordering these groups of compact stellar systems by $f_{\rm blue}$, from low to high, yields: `ACSVCS GCs` < `bright GCs` $\lesssim$ UCDs < `bright nuclei`.

4.4. *Size Distribution*

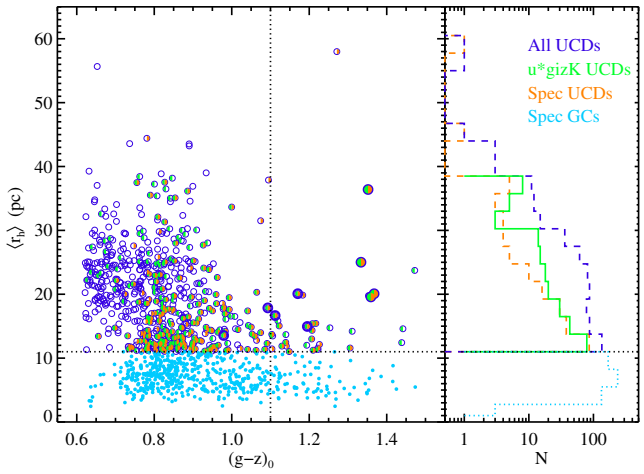

Figure 13. *Left panel:* Mean half-light radius vs. $(g-z)_0$ color for `spec GCs` (cyan filled circles) and UCDs (`all UCDs`: blue open circles; u^*gizK `UCDs`: green filled semi-circles; `spec UCDs`: orange filled semi-circles). The four larger circles are those UCDs that are known to host SMBHs: i.e., M60-UCD1 (Seth et al. 2014), M59-UCD3 (Ahn et al. 2018), M59cO (Ahn et al. 2017) and VUCD3 (Ahn et al. 2017). The five thicker blue circles denote the five bright UCDS in Figure 14 that have not yet been studied for SMBHs. The vertical black dotted line shows the $(g-z)_0$ color, which is used to divide the GCs and UCDs into red and blue sub-populations. *Right panel*: r_h distribution for `all UCDs` (blue long-dashed line), u^*gizK `UCDs` (green solid line), `spec UCDs` (orange short-dashed line), and `spec GCs` (cyan dotted line). The horizontal black dotted line in both panels shows a half-light radius of 11 pc, which is used to separate UCDs from GCs.

In order to select UCDs, we have measured half-light radii for all bright objects ($g_0 < 21.5$) in the NGVS footprint using KINGPHOT. The left panel of Figure 13 plots $\langle r_h \rangle$ versus $(g-z)_0$ for our `all` (blue open circles), u^*gizK (green filled semi-circles), and `spec UCDs` samples (orange filled semi-circles), and `spec GCs` sample (cyan dots). It is worth noting that the majority of UCDs with very blue colors, $(g-z)_0 \lesssim 0.7$, lack radial velocity measurements, a situation we aim to improve upon through dedicated spectroscopic follow-up. The right panel shows the distribution of half-light radii for both UCDs and GCs. The dotted horizontal line marks $\langle r_h \rangle = 11$ pc, the size used to separate GCs from UCDs, while the dotted vertical line indicates the color, $(g-z)_0 = 1.1$, used to divide the UCDs into blue and red sub-populations (see §4.3).

The mean r_h of UCDs is $\overline{r_h} = 19.8$ pc with a standard deviation of $\sigma_{r_h} = 6.8$ pc. For sub-populations, the mean r_h and standard deviations are $\overline{r_h} = 20.0$ pc and $\sigma_{r_h} = 6.8$ pc for the blue UCDs, and $\overline{r_h} = 14.6$ pc and $\sigma_{r_h} = 3.8$ pc for the red UCDs. The blue UCDs are larger and cover a wider range in half-light radius than red ones.

As discussed in Liu et al. (2015a), when comparing to HST-based values, we find that we overestimate the half-light radii of smaller objects ($r_h \lesssim 11$ pc). Thus, we suspect that many diffuse GCs are included in our UCD sample. This may explain why we see such a high degree of similarity between the color distributions of our NGVS-based samples of GCs and UCDs.

At the time of writing, SMBHs have been detected in four Virgo UCDs. These objects (all of which were objectively identified by our selection function) are indicated by the large circles in the left panel of Figure 13). These are M60-UCD1 (Seth et al. 2014), M59cO (Ahn et al. 2017), VUCD3 (Ahn et al. 2017) and M59-UCD3 (Ahn et al. 2018). Interestingly, all four objects are quite red, with colors of $(g-z)_0 \sim 1.35$. Based on the color-magnitude relation for UCDs, we know that the redder systems tend to be brighter. To date, no blue UCD is known to contain a SMBH, although we have many promising bright, blue UCD candidates in our sample. These are obvious targets for future spectroscopic searches for SMBHs.

4.5. *Sub-samples of Unique UCDs*

As noted above, we find no significant color differences between our UCD and GC samples. However, some UCDs, by virtue of their extreme or unusual properties, have a special significance for understanding the origin of these systems and their relationship to "normal" GCs. In this section, we pause to consider these unique UCDs.

4.5.1. *The Brightest UCDs*

We begin with the subset of UCDs that are known to contain a SMBH. The first such detection was made in M60-UCD1, where Seth et al. (2014) found a SMBH of mass $\sim 2.1 \times 10^7$ $M_\odot$. The inferred mass fraction (15%) suggests that the progenitor of M60-UCD1 was a dwarf galaxy. Soon afterwards, an even more massive system in Virgo, M59-UCD3, was co-reported by Liu et al. (2015b) and Sandoval et al. (2015). Later, Ahn et al. (2018) showed that this UCD also contains a SMBH of mass 4.2×10^6 $M_\odot$. SMBHs have also been found in two more Virgo UCDs, M59cO and VUCD3 (Ahn et al. 2017). The discovery that UCDs can harbor SMBHs is crucial evidence of a dE,N origin for at least some UCDs.

One property that unifies the four UCDs with known SMBHs is their luminosity: they are all very bright. Based on this, we have carried out a search for bright UCDs using the NGVS short-exposures. Figure 14

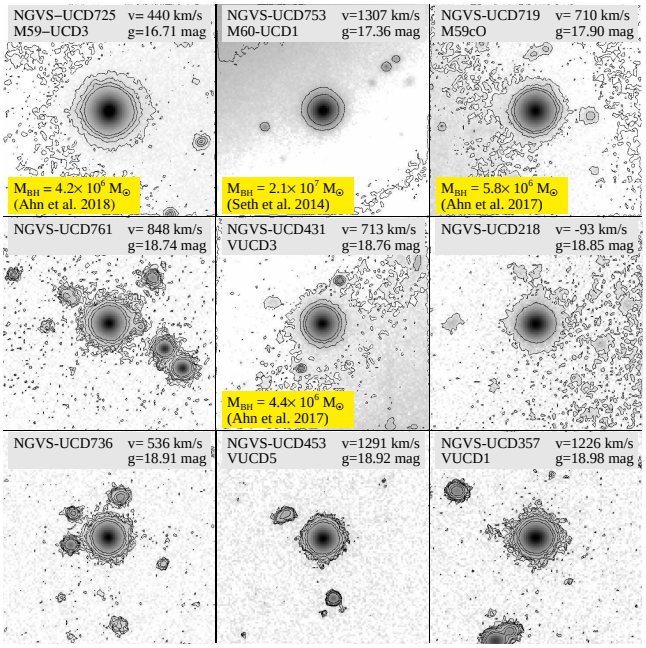

Figure 14. NGVS g-band images for the brightest nine UCDs in Virgo cluster. Radial velocities used to confirm cluster membership are available for each of these objects. Four of these UCDs are known to host SMBHs, the masses of which are reported in the panels. The image size in each panel is 120 × 120 pixels, where 120 pixels $\sim 22.32''$ ~ 1.8 kpc at Virgo distance.

presents g-band cutouts for the nine brightest UCD candidates in our sample, which shows that M59-UCD3, M60-UCD1 and M59cO are the brightest three UCDs in all of Virgo, and the only three brighter than $g_0 = 18$ mag. The next brightest UCD, NGVS-UCD761, with $g_0 = 18.74$ and $(g-z)_0 = 1.11$, represents a new detection and is a tantalizing target for future SMBH searches.

Figure 15 shows the locations of the 23 UCDs in Virgo that are brighter than $g_0 = 19.5$ mag. The red stars represent the three brightest systems. We note that the third- (M59cO) and fourth-brightest UCDs (NGVS-UCD761) are separated by a significant magnitude gap ($\Delta g_0 = 0.84$ mag). The fourth ($g_0 = 18.74$ mag) to ninth-ranked ($g_0 = 18.98$ mag) UCDs are shown as black squares in Figure 15, while blue triangles represent UCDs in the range of $19.0 < g_0 < 19.5$ mag.

Interestingly, all 23 UCDs with $g_0 < 19.5$ mag are located in Virgo's three main sub-clusters (black dotted circles). About half of these objects are in Cluster A (centred on M87) — 4 with $18.5 < g_0 < 19.0$ and 11 $19.0 < g_0 < 19.5$. Curiously, the brightest three UCDs are all located in Cluster C, a much smaller sub-cluster centred on M60. On the contrary, only one bright UCD (20th-ranked; $g_0 = 19.39$) is found in Cluster B (centred

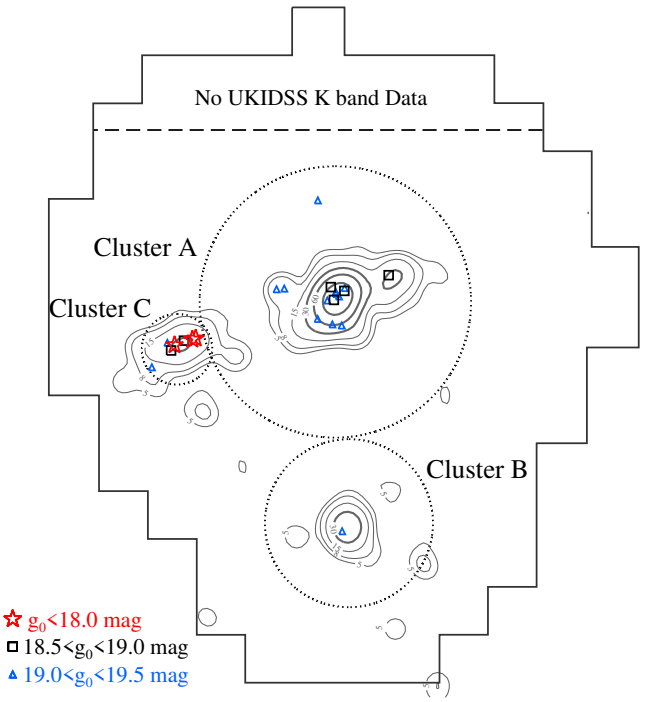

Figure 15. The spatial distribution of bright u^*gizK UCDs with $g_0 < 19.5$ mag. Red stars show the three UCDs with $g_0 < 18.0$ mag. Black squares show the six UCDs with $18.5 < g_0 < 19.0$ mag (note that there are no UCDs are in the magnitude range $18.0 < g_0 < 18.5$ mag). Blue triangles show the fourteen UCDs with $19.0 < g_0 < 19.5$ mag. Contours show the surface density distributions for the sample of 235 u^*gizK UCDs (see Figure 10). The large dotted circles show Virgo's three main sub-clusters: i.e., clusters A, B and C, which are centred on M87, M49 and M60, respectively.

on M49). It is puzzling why Cluster C is so special in this regard. Perhaps the fact that this substructure contains two massive galaxies in close proximity to one another makes it a conducive environment to forming bright UCDs (e.g. through tidal stripping).

4.5.2. *The Largest UCDs*

Figure 16 shows g-band cutouts for the nine largest UCDs in our sample. The largest, NGVS-UCD769 ($\langle r_h \rangle = 58$ pc[9].), also happens to be the brightest ($g_0 = 19.11$ mag) and reddest one ($(g-z)_0 = 1.27$) of this sub-sample; the remaining eight all have $(g-z)_0 \lesssim 1.1$. There is, interestingly, no overlap between the nine brightest and nine largest UCDs in our sample. Only two of the largest UCDs currently have measured radial velocities.

We note that three UCDs in Figure 16 (NGVS-UCD549, 506 and 757) have bright neighbors. Recall

[9] Note that the largest nucleus in Virgo has $r_h \sim 60$ pc (Côté et al. 2006)

that when we measure the half-light radius of an object, KINGPHOT fits the image using PSF-convolved King models within a fitting radius, $r_{\rm fit}$ (15 pixels here). In Figure 3, we compare r_h measurements based on different fitting radii, $r_{\rm fit} = 7$ or 15 pixels. The measurements are fully consistent even for the UCDs surrounding the three most luminous galaxies in the Virgo cluster (M87, M49 and M60). We conclude then that light from neighboring galaxies does not seriously affect our r_h measurements. In addition, we test our measurement procedure by injecting artificial UCDs across a range of environments covered by the NGVS footprint. We find that the KINGPHOT measurements are quite robust unless the UCD falls very close to a bright point source, like the blended objects shown in Figure 8.

Using the ACSVCS data, Jordán et al. (2005) found the vast majority of GCs in the Virgo cluster are smaller than $r_h = 10$ pc, with their average size being $\langle r_h \rangle = 2.70 \pm 0.35$ pc. In addition, they found no correlation between half-light radius and luminosity for `bright GCs` ($z \leq 22.9$ mag). Meanwhile, using ACSVCS data as well, Côté et al. (2006) found that nuclei follow a size-magnitude relation, with more luminous nuclei having larger half-light radii. A similar result has been found for UCDs, although not as tight (i.e., more luminous UCDs are usually larger; Côté et al. 2006; Penny et al. 2014). Dabringhausen et al. (2012) have also reported that UCDs follow a size-magnitude relation, while GCs do not.

It is worth pointing out that, several GCs in our MW are also larger than $r_h = 10$ pc (van den Bergh & Mackey 2004). Such extended star clusters (ESCs) have also been found around other nearby galaxies, e.g., M31 (Huxor et al. 2005, 2014), Scl-dE1 (Da Costa et al. 2009), M51 (Hwang & Lee 2008) and NGC 6822 (Hwang et al. 2011). These ESCs mainly populate the faint end of the GCLF (Peng et al. 2006b; Liu et al. 2016), with those around the MW and M31 being fainter than $M_V = -7$ (van den Bergh & Mackey 2004; Hwang et al. 2011). Conversely, the typical UCD is brighter than ESCs by two magnitudes or more ($-13 < M_V < -9$ mag; Willman & Strader 2012), and more still for the largest UCDs. Therefore, it is quite likely that the largest UCDs in Virgo originate under different circumstances than "normal" GCs.

4.5.3. *UCDs with Asymmetric/Tidal Features*

If tidal stripping of dE,Ns produce UCDs, then we should be able to find some objects undergoing such a transformation (i.e., UCDs that exhibit asymmetries and/or tidal features). Of course, this exercise may be complicated by short transformation timescales and/or

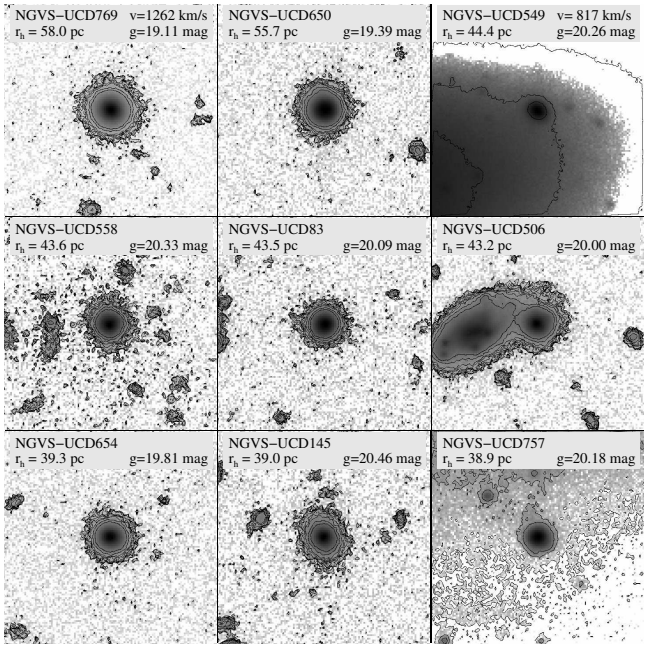

Figure 16. NGVS g-band images for the largest nine UCDs in Virgo cluster. The image size in each panel is 120×120 pixels, where 120 pixels $\sim 22.32''$ ~ 1.8 kpc at the distance of Virgo.

potentially low surface brightnesses of any stripped material (Pfeffer & Baumgardt 2013). Nonetheless, a few UCDs with asymmetric or tidal features have indeed been found in recent years through deep surveys (e.g., Jennings et al. 2015; Mihos et al. 2015; Voggel et al. 2016; Schweizer et al. 2018). Another potential complication surrounds the interpretation of such features – for instance, several GCs around the MW are known to possess prominent tidal structures, such as NGC 6715 (Ibata et al. 1994; Bellazzini et al. 2008), Palomar 5 (Odenkirchen et al. 2001), and ω Cen (Ibata et al. 2019). However, most of these objects have been flagged by other studies as unusual members of the MW GC system (Johnson et al. 2015; Milone et al. 2017; Gratton et al. 2019), such that they are commonly held as remnants of nucleated satellites that were disrupted by the MW's tidal field (e.g., Bekki & Freeman 2003; Majewski et al. 2003; Küpper et al. 2015).

The high sensitivity of the NGVS images ($\mu_g \lesssim 29$ mag arcsec^{-2}; Ferrarese et al. 2012) allows us to search for such features within our UCD sample. Our search indeed results in a handful of UCDs with apparent asymmetries. If confirmed as being tidal in origin, these features would offer direct evidence that at least some UCDs are the descendants of nucleated galaxies.

Figure 17 shows one candidate tidal structure associated with NGVS-UCD330. This UCD ($v_r = 1628$ km/s) is a satellite of VCC 1250 ($v_r = 1963$ km/s).

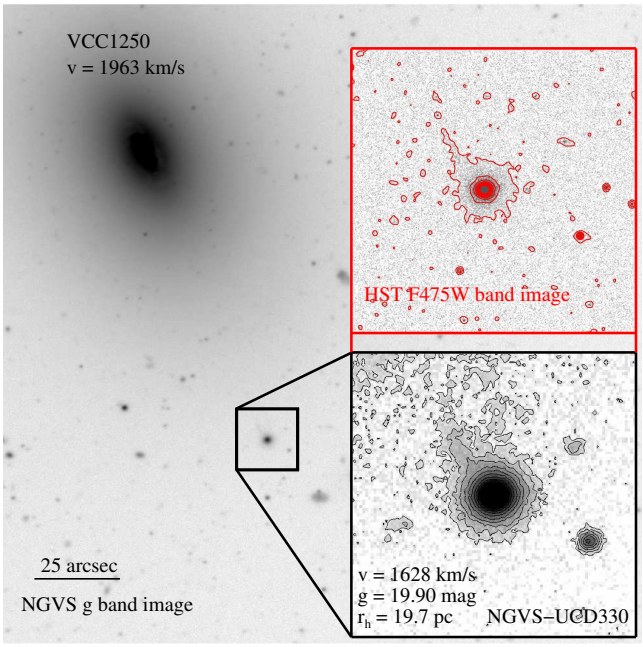

Figure 17. NGVS g-band image for galaxy VCC 1250. The small panels shows the NGVS and HST images of NGVS-UCD330, a UCD that shows signs of an extra-tidal structure. The inset image with red contours is taken from the HST ACS Virgo Cluster Survey.

It was previously identified as VCC1250_1 by Haşegan et al. (2005), who also noted that it appeared to be embedded in a diffuse envelope. Both the NGVS and HST images in Figure 17 reveal an asymmetric structure emanating from this object and pointing towards VCC 1250. Thus, NGVS-UCD330 may be an example of a UCD caught in the act of losing what remains of its diffuse envelope. The putative tidal stream associated with this UCD is unusual in that we only detect one arm. However, we cannot rule out the second arm as being hidden by projection or surface brightness effects. Follow-up spectroscopy of this object would help us determine its origins.

4.5.4. *UCDs with Envelopes*

Using HST imaging, Haşegan et al. (2005) found three UCDs in Virgo that are embedded within shallow envelopes — evidence that they may be related to the nuclei of dE,Ns with extremely low surface brightness and/or compact stellar halos. There are 22 UCD candidates in our sample that also have HST imaging from the ACSVCS (Côté et al. 2004). We have checked these HST images to look for envelopes. Some systems, like NGVS-UCD298 (top panel of Figure 18), show no evidence of envelopes in either the ACSVCS or NGVS images. Others, like NGVS-UCD414 (middle panel of Figure 18), have small envelopes that are visible only in the

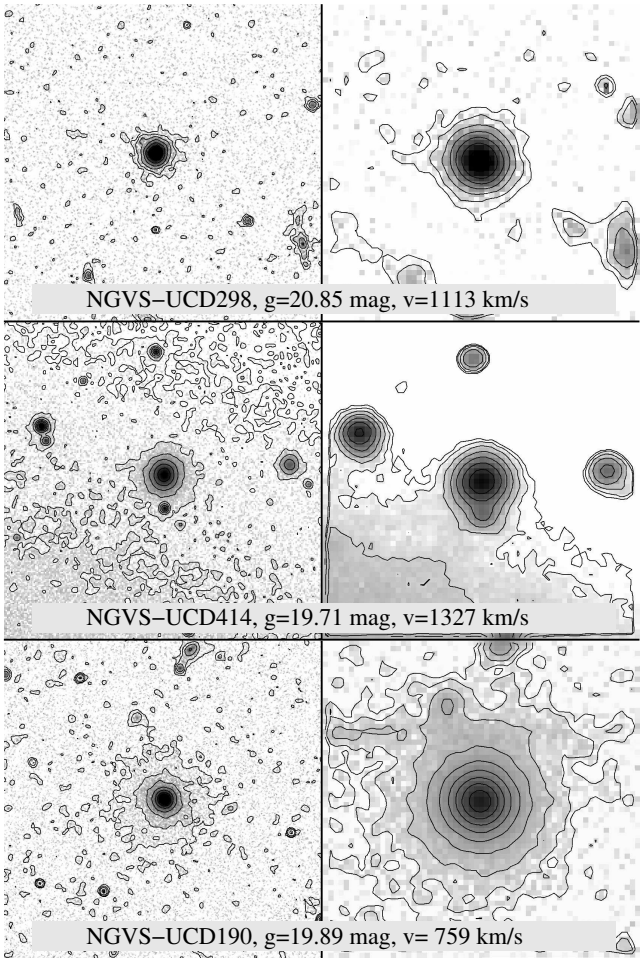

Figure 18. HST F475W ($\sim$ SDSS g-band) images (left panels) and NGVS g-band images (right panels) for 3 UCD candidates, NGVS-UCD298, 414 and 190 (from top to bottom panel). Each of these objects are confirmed radial velocity members of the Virgo cluster (i.e., $v_r < 3500$ km/s). The image size in each panel is ~ 0.9 kpc $\times 0.9$ kpc.

ACSVCS images thanks to its exceptional image quality. The remainder, like NGVS-UCD190 (bottom panel of Figure 18), have large (yet still diffuse) envelopes that can be seen in both ACSVCS and NGVS images. In all, we find about half of the 22 UCD candidates with HST imaging are embedded in diffuse envelopes that are visible in the space-based images.

The above comparison demonstrates that we can detect envelopes around UCDs in the NGVS imaging, provided they are large enough. Our search reveals 41 instances of such features, and these cases have been accordingly flagged in Table 4. Most of these UCDs are found around M87 and M60/M59, with just a couple located sub-cluster B. Note that, in this section, we have focused on UCDs with envelopes that are obvious based on visual inspection — which is admittedly subjective.

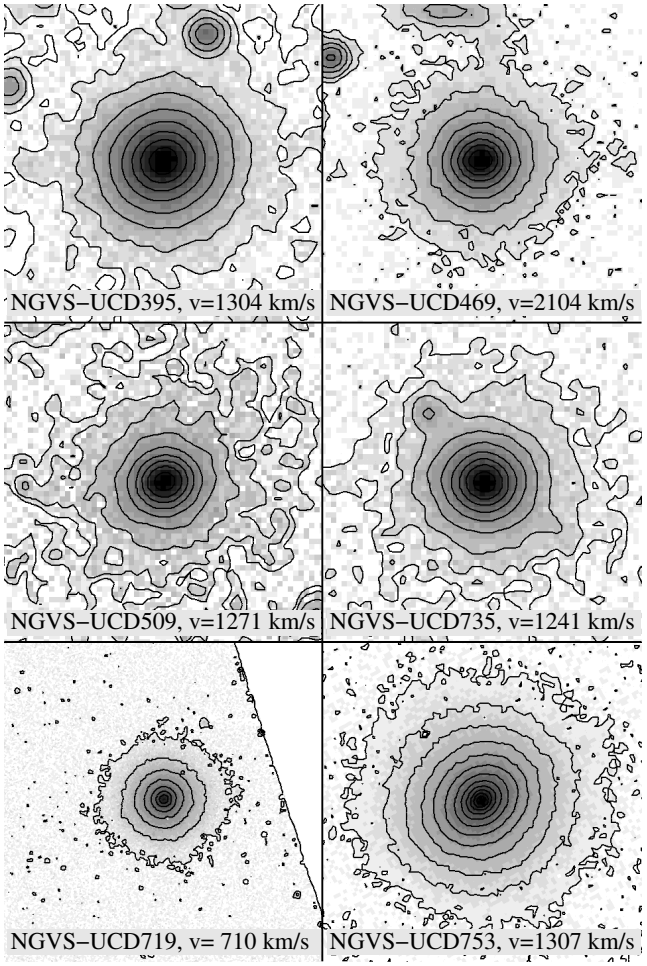

Figure 19. NGVS g-band images for 4 UCDs (upper four panels) and HST F475W ($\sim$ SDSS g band) images for 2 UCDs (lower two panels) having visible envelopes. Each of these objects are confirmed radial velocity members of the Virgo cluster (i.e., $v_r < 3500$ km/s). The image size in each panel is the same with Figure 18.

Because this sample is not suitable for statistical analysis, we will postpone the detailed investigation of the properties of UCD envelopes to future work (Wang et al., in prep.). In the next section though we will introduce a parameter, $\Delta_{\rm env}$, to examine basic properties of the envelope.

Figure 19 presents NGVS g-band images for four UCDs (upper four panels) and HST F475W ($\sim$SDSS g-band) images for two UCDs (lower two panels) that are confirmed radial velocity members of the Virgo cluster and possess clear stellar envelopes. We see in both sets of imaging that these envelopes have near-zero ellipticity. From a morphological perspective, UCDs with diffuse envelopes look quite similar to dE,Ns, adding weight to the argument of an evolutionary connection between the two classes. Moreover, NGVS-UCD719 (lower-left panel of Figure 19, also known as M59cO; Chilingarian & Mamon 2008) and NGVS-UCD753 (lower-right panel of Figure 19, also known as M60-UCD1; Strader et al. 2013) are two of the four UCDs known to possess central SMBHs (Seth et al. 2014; Ahn et al. 2017). We do not, however, observe any tidal features around them (e.g., Küpper et al. 2010; Jennings et al. 2015; Schweizer et al. 2018).

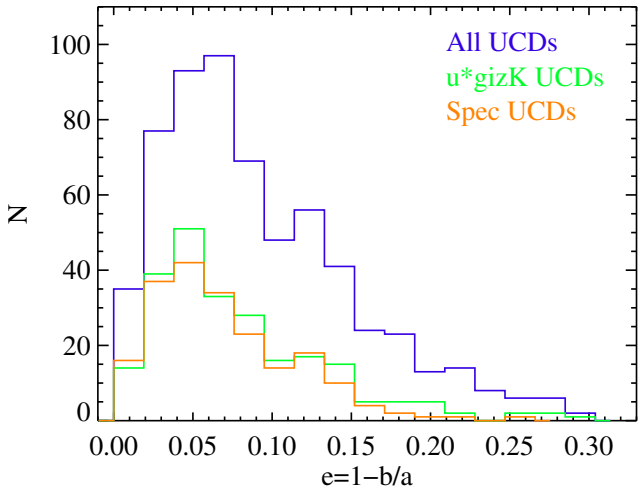

Figure 20. The ellipticity distributions of `all UCDs` (blue histogram), u^*gizK-`UCDs` (green histogram) and `spec-UCDs` sample (orange histogram).

As with tidal features, the interpretation of envelopes around Virgo UCDs is also potentially complicated by the fact that similar structures have recently been detected around the MW GCs NGC 7089 (Kuzma et al. 2016) and NGC 1851 (Kuzma et al. 2018). Once again though, these GCs are unusual in their chemistries (e.g., possessing broad dispersions in their abundances of iron and neutron-capture elements; Johnson et al. 2015; Milone et al. 2017), suggesting that they are actually the remnant nuclei of disrupted nucleated galaxies.

5. DISCUSSION

We have selected candidate Virgo UCDs from a combination of ellipticity, magnitude, colors, surface brightness, half-light radii, visual inspection and, when available, radial velocity. At the outset, we imposed a requirement that ellipticity $e < 0.3$ since most spectroscopically-confirmed UCDs are quite round (Zhang et al. 2015). We show the ellipticity distributions of our UCD samples in Figure 20 to gauge the impact this has on our selection function. As can be seen, the ellipticity distributions peak at $\sim$0.05-0.07, and decrease to roughly zero by $e \approx 0.3$. We conclude then that the criterion $e < 0.3$ does not significantly bias our selection of UCDs.

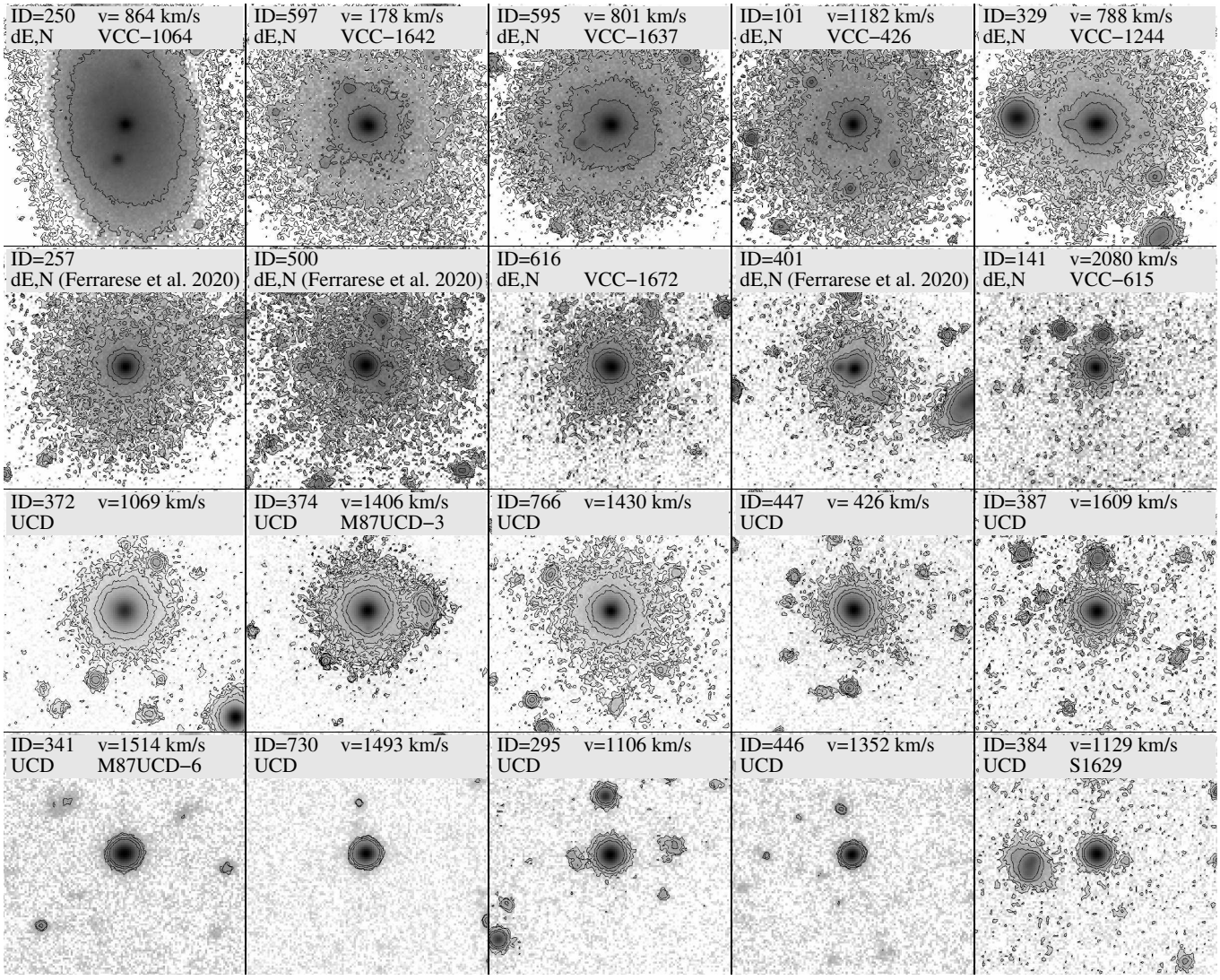

Figure 21. Mosaic of g-band images for 20 objectively selected UCD candidates from the NGVS. The image size is 120×120 pixels (where 120 pixels = $22.32''$ ~ 1.8 kpc in Virgo cluster). The upper row shows five nucleated dwarf galaxies (dE,N) from the VCC catalog (Binggeli et al. 1985). All of them are confirmed spectroscopic members of the Virgo cluster (i.e., $v_r < 3500$ km/s). Another five dE,Ns shown in the second row include two VCC galaxies (ID=613 and 141) and three newly discovered galaxies from the NGVS (ID=257, 497 and 401; Ferrarese et al. 2020). Four of these five dE,Ns do not have radial velocity measurements, but they are likely cluster members given their extended, low surface brightness envelopes. The rightmost galaxy in this row (ID=141) is an ultra-diffuse galaxy (UDG) that has a large extent (larger than the figure size) and very diffuse structure (e.g., Toloba et al. 2018). The third row shows five UCDs with apparent envelopes while the bottom row shows another five UCDs that have no discernible envelope. All these ten UCDs are radial velocity members of the cluster ($v_r < 3500$ km/s). The contours in each of the first 15 panels show the isophotes with constant surface brightness level. The innermost isophote is 25 mag/arcsec^2 and each interval between successive isophotes is 0.5 mag/arcsec^2. The 10 dE,Ns (the top two rows) have been sorted by the size of the stellar halo while the UCDs (the bottom two rows) by the envelope parameter, $\Delta_{\rm env}$.

Our selection yields a catalog of more than 600 candidates within the $\sim$100 deg^2 footprint of the NGVS, making it the largest and most homogeneous UCD catalog for any environment to date. Moreover, our selection algorithm also produces samples of `bright GCs` and galactic nuclei, such that we can compare directly the properties of these different populations.

Our large and complete sample also makes it possible to identify groups of UCDs with extreme or interesting properties, which may shed light on UCD origins in general. In this section, we examine our results using both approaches and discuss the implications for models of UCD formation.

We begin by noting that the nuclei of dwarf galaxies are embedded in stellar envelopes that can vary widely in

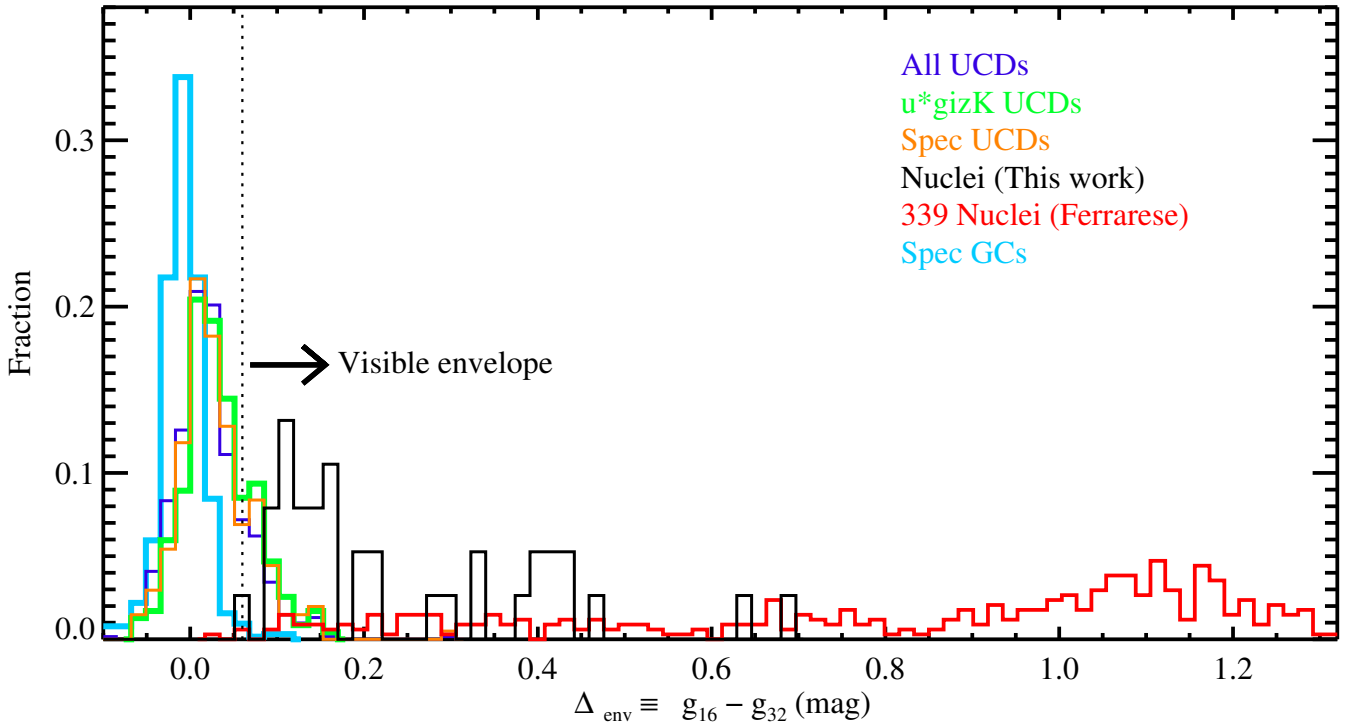

Figure 22. The envelope parameter, $\Delta_{\rm env}$, distribution for the `spec GCs` (cyan), `all UCDs` (blue), u^*gizK `UCDs` (green), `spec UCDs` (orange), u^*gizK `nuclei` (black) and `bright nuclei` (red). We have divided the UCDs into two subgroups at $\Delta_{\rm env} = 0.06$, shown by the dotted vertical line.

surface brightness (see, e.g., Ferrarese et al. 2006; Spengler et al. 2017; Toloba et al. 2018). In other words, when we visually classify our UCD candidates, it can be difficult to distinguish UCDs with faint envelopes from nuclei in low-mass galaxies. To solve this, we remove from our samples any objects that have been classified as galaxies in either the VCC (Binggeli et al. 1985) or the NGVS galaxy catalogs (Ferrarese et al. 2016, 2020).

Figure 21 shows a mosaic of NGVS g-band images for representative sub-samples of ten dE,Ns and ten UCDs. Most of these objects are confirmed radial velocity members of Virgo. Note that this mosaic is an updated version of Figure 32 in Liu et al. (2015a), which was based on just $\sim$ 100 UCD candidates near M87, and that the dE,Ns have been sorted by the prominence of their stellar envelopes. We can see that the envelopes of the first few dwarfs are significant, making it easy to identify these systems as galaxies. However, as the envelopes become progressively smaller and fainter, the distinction between dE,Ns and UCDs becomes blurred. For instance, it is difficult to distinguish the dE,Ns in the second row of Figure 21 from the UCDs in the third row, based on morphology alone. Note that the systems in the second row are classified as galaxies in either the VCC (ID = 613 and 141, Binggeli et al. 1985) or NGVS galaxy catalogs[10] (Ferrarese et al. 2016; Sánchez-Janssen et al. 2019; Ferrarese et al. 2020). Finally, as the bottom row of Figure 21 illustrates, most of our UCD candidates do not have visible envelopes, or they are too diffuse to detect with NGVS imaging.

Figure 21 prompts an obvious question: might there be an evolutionary sequence that links dE,N galaxies to UCDs, with the latter representing the end-state of severe and continuous tidal stripping? Such a link was suggested by Liu et al. (2015a) who examined the distribution of dwarf galaxies and UCDs in the cores of the Virgo A and B sub-clusters. Armed with a cluster-wide sample of UCDs and galaxies, we can now revisit this claim. Bekki & Yong (2012) found from their numerical simulations a morphological sequence similar to that shown in Figure 21 (see the lower panel of their Figure 2). During the transformation from a dwarf galaxy to a bare nucleus, they showed that the stellar halo is stripped efficiently and decreases in size steadily over time. In other words, the physical extent of a given UCD envelope may indicate which stage the system falls along the evolutionary sequence from dE,N to UCD.

[10] Of course, in both of these catalogs, galaxy classifications were based on several properties, not just morphology.

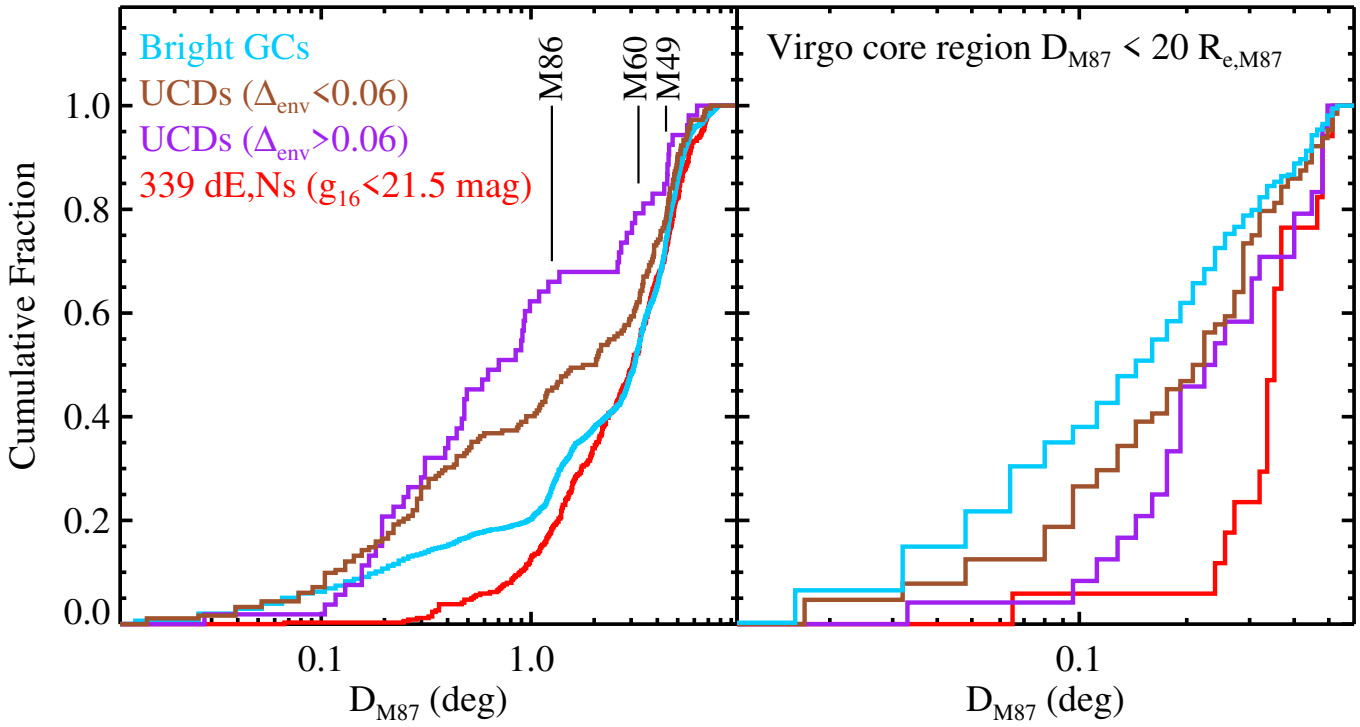

Figure 23. Cumulative distributions for the projected distance from M87 (D_{M87}) for the `bright GCs` (cyan lines), UCDs with $\Delta_{env} < 0.06$ (brown lines), UCDs with $\Delta_{env} > 0.06$ (purple lines) and `bright nuclei` (red lines). *Left panel:* the distribution for the entire NGVS survey area; *Right panel:* the distribution for the Virgo core region (within 20 $R_{e,M87}$). The three black vertical lines in the left panel show the location of M86, M60 and M49.

To further explore such a connection, Liu et al. (2015a) introduced a parameter to describe the strength of a UCD's envelope. This parameter is defined as $\Delta_{env} \equiv g_{16} - g_{32}$, where g_{16} and g_{32} are g-band magnitudes measured within apertures of 16 ($\sim$3.0″) and 32 pixels ($\sim$6.0″) diameter, respectively. Based on this definition, point-like sources should have $\Delta_{env} \simeq 0$ while extended sources will tend to have $\Delta_{env} > 0$.

Figure 22 shows the distribution of envelope parameters for compact objects in the NGVS. The GCs are closely distributed around $\Delta_{env} \sim 0$, with a small tail to $\Delta_{env} > 0.06$ (marked by the dotted vertical line). The low envelope strengths of GCs are to be expected given the vast majority of them are unresolved in NGVS imaging. Meanwhile, the dE,Ns show much larger envelope strengths ($\Delta_{env} > 0.06$). For UCDs, the envelope strengths typically fall between those of GCs and dE,Ns. Following Liu et al. (2015a), we subdivide the UCDs into two groups at $\Delta_{env} = 0.06$. UCDs with $\Delta_{env} > 0.06$, whose envelopes are clearly evident, more closely resemble nuclei and are thus distinct from GCs.

Previous studies have found dramatic differences in the cumulative radial distributions of UCDs and dE,Ns in galaxy clusters (e.g., Drinkwater et al. 2002, 2004; Mieske et al. 2004b; Jones et al. 2006; Mieske et al. 2007a; Liu et al. 2015a; Pfeffer et al. 2016), but the situation between UCDs and GCs is less clear (e.g. Mieske et al. 2004a, 2012). Generally, GCs are highly concentrated towards cluster centers, while dE,Ns are less concentrated, and UCDs lie intermediate between the two. If the majority of UCDs are nothing more than the high luminosity tail of the GC population, then we might reasonably expect the radial distributions of GCs and UCDs to resemble each other. On the other hand, if most UCDs form through tidal stripping of dE,Ns, then we should expect the UCD radial profile to have a high central concentration: i.e., stripped galaxies would tend to lie deeper in the gravitational wells of their hosts. As noted in §4, our UCD sample most certainly contains some number of GCs because bright, extended GCs (although rare) do exist and we systematically overestimate the sizes of GCs. We can, however, invoke Δ_{env} to produce a UCD sample that is more heavily weighted to objects born of tidal stripping.

The right panel of Figure 23 shows the cumulative radial distribution of UCDs, `bright GCs` (cyan lines), and `bright nuclei` (red lines) in the core of sub-cluster A ($D_{M87} < 20R_{e,M87}$). Here, we separate the UCDs into two groups: those without envelopes ($\Delta_{env} \leq 0.06$; brown line) and those with ($\Delta_{env} > 0.06$; purple line). Consistent with previous studies, the ordered sequence of systems from high to low concentration in this re-

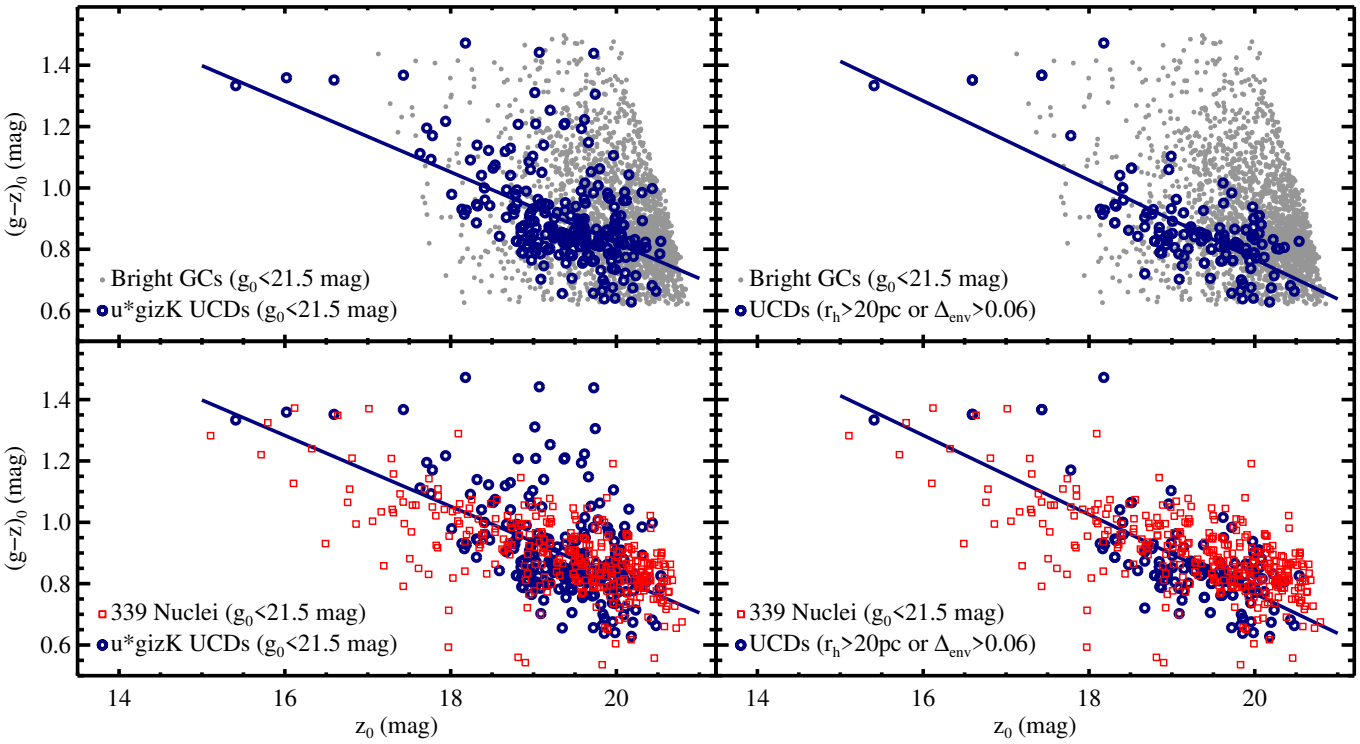

Figure 24. Color-magnitude diagram (CMD) for `bright GCs` (gray points), UCDs (blue open circles) and `bright nuclei` (red open squares). *Upper-left panel:* CMDs for `bright GCs` and u^*gizK `UCDs`; *Lower-left panel:* CMDs for `bright nuclei` and u^*gizK `UCDs`; *Upper-right panel:* CMDs for `bright GCs` and UCDs with $r_h < 20$ pc or $\Delta_{\rm env} > 0.06$; *Lower-right panel:* CMDs for `bright nuclei` and UCDs with $r_h < 20$ pc or $\Delta_{\rm env} > 0.06$. The blue solid lines in the left two panels are the best linear fit for u^*gizK `UCDs`. The blue solid lines in the right two panels are the best linear fit for UCDs with $r_h < 20$ pc or $\Delta_{\rm env} > 0.06$.

gion goes: GCs, UCDs without envelopes, UCDs with envelopes, and dE,Ns. As expected, the UCDs with envelopes are less centrally concentrated than those without. The difference in radial distributions between GCs and UCDs with $\Delta_{\rm env} > 0.06$ is clear.

In the left panel of Figure 23, we show, for the first time, the radial distribution of UCDs, GCs, and nuclei over the entire Virgo cluster. In the outer regions, the distributions of `bright GCs` and dE,Ns grow at similar rates. This makes sense since, at large clustercentric distances, GCs will be found around the individual galaxy members. On the other hand, there is a clear difference in how bright GCs and UCDs with envelopes are distributed in the outskirts of the cluster. Most notably, the distribution of UCDs with envelopes exhibits clear bumps that coincide with the locations of the three luminous galaxies, M86, M60 and M49 (marked by the black vertical lines). This indicates that the UCDs with envelopes are mainly associated with giant galaxies, where the gravitational potential is deep enough to strip the diffuse components of dE,Ns.

Another way we can attempt to isolate those UCDs formed via tidal stripping is by increasing the value of our size cut to $r_h > 20$ pc. In the right-hand panels of Figure 24, we examine the color-magnitude relation of UCDs with $\Delta_{\rm env} > 0.06$ or $r_h > 20$ pc and compare to those for the `bright GCs` (upper-right panel) and `bright nuclei` (lower-right panel). Meanwhile, the left-hand panels show a similar comparison, but using our u^*gizK `UCDs` sample instead. Placing more restrictive cuts on r_h and $\Delta_{\rm env}$ has the effect of removing many red UCDs at faint luminosities ($z_0 \gtrsim 18.5$ mag). The color-magnitude relation for the u^*gizK `UCDs` sample is

$$(g-z)_0 = -0.12(\pm0.01)z_0 + 3.13(\pm0.05), \quad (8)$$

while that for our more restricted UCD sample is,

$$(g-z)_0 = -0.13(\pm0.01)z_0 + 3.35(\pm0.04), \quad (9)$$

which are shown as blue solid lines in Figure 24.

At face value, it looks like the distributions of UCDs and nuclei overlap well in the color-magnitude plane. This compares well with previous work (e.g., Côté et al. 2006; Brodie et al. 2011) which found general agreement between the color-magnitude relations of nuclei and UCDs, in the sense that brighter UCDs and nuclei tend to be redder. However, as seen in lower-right panel of Figure 24, there is a lack of blue UCDs at bright magnitudes ($z_0 \lesssim 18.0$) and that UCDs are bluer

than nuclei at faint magnitudes ($z_0 \gtrsim 18.0$). To evaluate the significance of these differences, we have run a 2D Kolmogorov-Smirnov Test (Peacock 1983; Fasano & Franceschini 1987) on the distributions for UCDs and nuclei. The resulting p-values are quite small, implying that the distributions do not share a common parent. Also, in agreement with previous work (e.g., Brodie et al. 2011), we find that UCDs occupy a narrower range of color than GCs, especially at faint magnitudes. The color-magnitude relations of UCDs, nuclei and GCs are thought to be the result of an underlying mass-metallicity relation for each population, with more massive systems tending to have higher metallicities, and GCs tending to have higher metallicities than UCDs and nuclei at a given mass (especially at low masses; Zhang et al. 2018).

As described in the introduction, recent studies are finding more support for the galactic nuclei origin for UCDs. For UCDs formed this way, one would expect to find some transition objects: e.g., UCDs with tidal streams. However, only a small number of UCDs have been found to show such tidal structures (e.g., Figure 17, Jennings et al. 2015; Mihos et al. 2015; Voggel et al. 2016; Schweizer et al. 2018). On the other hand, many more UCDs were found to show diffuse, but circular, envelopes as shown in Figure 19, Figure 21 and also previous studies (e.g., Drinkwater et al. 2003; Haşegan et al. 2005). Bekki & Yong (2012) have established that diffuse and circular envelopes can indeed be found around nuclei when the stellar halos of dwarf galaxies have been mostly stripped by tidal forces. Pfeffer & Baumgardt (2013) have also demonstrated that while the stellar halos of dwarf galaxies are reduced during the tidal stripping, they can still be visible at later stages, especially for the more massive and extended UCDs. By contrast, tidal streams are often much fainter and only can be observable for those UCDs that are still experiencing significant stripping.

Two decades have passed since the discovery of UCDs, and yet, we still lack an understanding of what fraction of them originate through the formation of GC systems versus tidal stripping. One of the chief reasons for this is the difficulty of identifying a given compact stellar system as a bare nuclear star cluster based on its integrated light. More locally though, following years of study using high-resolution spectroscopy and resolved photometry, we now know that the GC system of the MW includes several unusual objects. These anomalous GCs tend to have very high surface mass densities, large intrinsic metallicity dispersions, spreads in the abundances of s-process elements, complex sub-giant branches, kinematic subpopulations, and tidal streams (see the review of Gratton et al. 2019, and references therein). Many of these (massive) GCs are thought to be remnants of nucleated dwarf galaxies (e.g., M54 (Ibata et al. 1994), ω Cen (Bekki & Freeman 2003)), and thus can be considered local examples of UCDs.

Beyond the Local Group, however, there is no consensus definition for what is a UCD. Investigators typically base their selection on arbitrary size ($10 \lesssim r_h \lesssim 100$) and luminosity/mass cuts ($10^6 \lesssim M_* \lesssim 10^8$ M$_\odot$), or simply observational limits (e.g., $r_h > 11$ pc in this study). As a result, it is very challenging to isolate within current UCD samples those that are GC-like from those that are nuclei-like, as discussed by Hilker (2011). Nevertheless, recent work makes it clear that many UCDs (e.g., massive UCDs, UCDs with tidal structures or diffuse envelopes) are indeed the nuclei of stripped dwarfs. Moreover, based on the Guo et al. (2011) semi-analytic model, Pfeffer et al. (2014) have demonstrated that both massive GCs ($M_* \gtrsim 10^5$ M$_\odot$) and UCDs can form via tidal disruption of dwarf galaxies. Also, Mayes et al. (in prep.) use the EAGLE simulation suite (Crain et al. 2015) to show that there is an overlap between stripped nuclei and "normal" GCs in the stellar mass range $M_* \lesssim 2 \times 10^6$ M$_\odot$.

To date, there are $\sim 10^3$ known UCDs in the local universe, more than half of which were found on the basis of photometric data alone. Obtaining spectroscopic observations for larger samples of UCDs (to measure radial velocities, velocity dispersions, and stellar populations) will be essential for understanding their nature. Fortunately, the next generation of ground- and space-based observatories promise to ameliorate this current deficit.

6. SUMMARY AND CONCLUSIONS

Using deep, wide-field u^*, g, i, z imaging from the Next Generation Virgo Cluster Survey (NGVS) and K band data from the UKIDSS, we have carried out a systematic search for UCDs across the entire Virgo cluster (~ 104 deg^2). We describe our search methodology — which is based on a combination of photometric (magnitude and color) information, half-light radius and surface brightness measurements, and radial velocity measurements, when available — and present a sample of 612 UCD candidates. Among this UCD sample are 235 candidates selected on the basis of deep u^*gizK data (our highest purity subsample) and 203 UCDs that are confirmed radial velocity members of the cluster (i.e., $v_r < 3500$ km/s). This is the largest and most homogeneous sample of UCDs presented to date for any cluster environment, and the first of its kind for the Virgo cluster. Our principal findings can be summarized as follows:

1. We construct the first number density map for UCDs in the Virgo Cluster, and show that UCDs are highly concentrated towards the largest and brightest galaxies: e.g., M87, M49, M60-M59 and M86 (see also Liu et al. 2015a).

2. The UCDs, as a population, have bimodal color distributions. The fraction of UCDs belonging to the blue population is 89% ± 3%. This is slightly higher than that of `bright GCs` (84%±1% for NGVS GCs and 77% ± 4% for `ACSVCS GCs`) and slightly smaller than that of `bright nuclei` (95%).

3. We measure the mean half-light radius for UCDs to be 19.8±6.8 pc. The blue UCDs (20.0±6.8 pc) are systematically larger than their red counterparts (14.6 ± 3.8 pc). The largest UCD candidate in our sample is NGVS-UCD769 with $r_h = 58.0$ pc.

4. Based on our analysis (i.e., number density maps and color distributions), we find no dramatic differences between UCDs and the brightest GCs (i.e., those objects with $g_0 < 21.5$ mag). However, when we rely on the cleanest possible UCD sample (with reduced contamination from GCs), some differences begin to appear (i.e., in their cumulative radial distributions and color magnitude relations).

5. We identify a number of UCDs having properties that point to a connection with the nuclei of dwarf galaxies. This includes the most luminous and largest UCDs, UCDs with obvious stellar envelopes, and UCDs embedded in diffuse asymmetric structures.

6. There are tight color-magnitude relations for UCDs and dwarf nuclei, with brighter objects being redder. At the faint end, UCDs and nuclei are bluer and have a narrower color range than GCs.

Some obvious extensions of this work present themselves, most of which involve spectroscopic observations, e.g., the property of envelopes of UCDs, searching for SMBHs in massive UCDs, the specific frequencies for the UCDs around massive galaxies. Our radial velocity survey for UCD candidates brighter than $g_0 \sim 19.5$ mag is complete, allowing membership to be established for candidates brighter than $M_g \sim -12$, which corresponds to a stellar mass of $\sim 10^{6.9}$ $M_\odot$ (Bell et al. 2003). It will be valuable to extend this work to the limit of our photometric catalog ($g \sim 21.5$ mag) and thus obtain a complete sample of UCDs down to a stellar mass of $\sim 10^{6.1}$ $M_\odot$. AO-assisted IFU spectroscopy for select UCDs (i.e., the brightest and largest objects, or those objects embedded in stellar envelopes) will allow the detection of SMBHs in these objects and provide a first glimpse into the SMBH occupation fraction in a magnitude-limited UCD sample. Finally, while the NGVS has made it possible to identify UCDs larger than $r_h \sim 11$ pc throughout the Virgo cluster, space-quality imaging will be needed to extend this work to the smaller radii and fainter magnitudes typical of GCs; in the future, high-resolution imaging from the Euclid or Roman space telescopes will allow the GC/UCD size-magnitude relation(s) to be mapped roughly to the level of the GCLF turnover using spatially complete samples and unbiased structural measurements.

ACKNOWLEDGMENTS

The NGVS team owes a debt of gratitude to the director and the staff of the Canada France Hawaii Telescope who helped make the survey a reality. This work is based on observations obtained with MegaPrime/MegaCam, a joint project of CFHT and CEA/DAPNIA, at the Canada France Hawaii Telescope (CFHT) which is operated by the National Research Council (NRC) of Canada, the Institut National des Sciences de Univers of the Centre National de la Recherche Scientifique (CNRS) of France, and the University of Hawaii. This work is based in part on data products produced at Terapix available at the Canadian Astronomy Data Centre as part of the Canada-France-Hawaii Telescope Legacy Survey, a collaborative project of NRC and CNRS.

C.L. acknowledges support from the National Natural Science Foundation of China (NSFC, Grant No. 11673017, 11833005, 11933003, 11621303, 11973033 and 11203017). C.L. is supported by Key Laboratory for Particle Physics,Astrophysics and Cosmology, Ministry of Education, and Shanghai Key Laboratory for Particle Physics and Cosmology(SKLPPC). This work is supported by 111 project No. B20019. EWP acknowledges support from the National Natural Science Foundation of China through Grant No. 11573002. HXZ acknowledges a support from the CAS Pioneer Hundred Talents Program and the National Natural Science Foundation of China (NSFC, Grant No. 11421303, 11973039). AL acknowledges support from the French Centre National d'Etudes Spatiales (CNES). EWP thanks Karina Voggel for discussions in which she suggested the use of Gaia data in UCD selection.

This work was supported in part by the Sino-French LIA-Origins joint exchange program, by the French Agence Nationale de la Recherche (ANR) Grant

Programme Blanc VIRAGE (ANR10-BLANC-0506-01), and by the Canadian Advanced Network for Astronomical Research (CANFAR) which has been made possible by funding from CANARIE under the Network-Enabled Platforms program. This research used the facilities of the Canadian Astronomy Data Centre operated by the National Research Council of Canada with the support of the Canadian Space Agency. This research has made use of the NASA/IPAC Extragalactic Database (NED), which is funded by the National Aeronautics and Space Administration and operated by the California Institute of Technology. This research has made use of the SIMBAD database, operated at CDS, Strasbourg, France. This publication has made use of data products from the Sloan Digital Sky Survey (SDSS). Funding for SDSS and SDSS-II has been provided by the Alfred P. Sloan Foundation, the Participating Institutions, the National Science Foundation, the U.S. Department of Energy, the National Aeronautics and Space Administration, the Japanese Monbukagakusho, the Max Planck Society, and the Higher Education Funding Council for England. This work is based in part on data obtained as part of the UKIRT Infrared Deep Sky Survey.

This research uses data obtained through the Telescope Access Program (TAP), which has been funded by the National Astronomical Observatories, Chinese Academy of Sciences, and the Special Fund for Astronomy from the Ministry of Finance. Observations reported here were obtained at the MMT Observatory, a joint facility of the University of Arizona and the Smithsonian Institution.

Facility: CFHT - Canada-France-Hawaii Telescope.

APPENDIX

As described in §3, we use strict half-light radius criteria to select UCD candidates, including: (1) a radius cut ($11 < \langle r_h \rangle < 100$ pc); (2) a requirement that the half-light radii measured in the g and i bands are in rough agreement ($|r_{h,g} - r_{h,i}|/\langle r_h \rangle \leq 0.5$); and (3) a condition that the fraction radius errors are smaller than 15% in both bands ($r_{h,g,\mathrm{error}}/r_{h,g} \leq 15\%$ and $r_{h,i,\mathrm{error}}/r_{h,i} \leq 15\%$). In this section, we take a closer look at objects that do not satisfy our radius criteria (but satisfy all other selection criteria). We divide such objects into three groups: objects with larger errors; objects with larger differences between two bands and; objects with smaller radius measurements.

Objects with larger errors (i.e. $r_{h,g,\mathrm{error}}/r_{h,g} > 15\%$ or/and $r_{h,i,\mathrm{error}}/r_{h,i} > 15\%$): We visually inspected the imaging for objects with larger errors for their radius measurements. Most of these objects are blends or have poor image quality (i.e., sources located close to chips gaps or near saturated objects). We can not classify these objects as bonafide UCDs using the NGVS images alone.

Objects with larger differences (i.e. $|r_{h,g} - r_{h,i}|/\langle r_h \rangle > 0.5$): The differences in image quality (PSF) is the primary reason for large differences in radius measurements. If an object is larger than 11 pc in both the g and i bands, then we believe it be may indeed be a UCD candidate although the radius difference between two bands is large. We list nine such objects in Table 6.

Objects with smaller radius measurements (i.e. $\langle r_h \rangle < 11$ pc): Most objects with smaller measured radii are likely to be GCs. However, if they have visible envelopes, then they are viable UCD candidates. We find eight objects that have half-light radii slightly below our $r_h = 11$ pc limit but appear to show diffuse envelopes. These are listed in Table 6.

To ensure our samples are as homogeneous as possible, we have not used these 17 UCD candidates in our analysis but they are included here for completeness.

REFERENCES

Abolfathi, B., Aguado, D. S., Aguilar, G., et al. 2018, ApJS, 235, 42, doi: 10.3847/1538-4365/aa9e8a

Afanasiev, A. V., Chilingarian, I. V., Mieske, S., et al. 2018, MNRAS, 477, 4856, doi: 10.1093/mnras/sty913

Ahn, C. P., Seth, A. C., den Brok, M., et al. 2017, ApJ, 839, 72, doi: 10.3847/1538-4357/aa6972

Ahn, C. P., Seth, A. C., Cappellari, M., et al. 2018, ApJ, 858, 102, doi: 10.3847/1538-4357/aabc57

Bekki, K., Couch, W. J., & Drinkwater, M. J. 2001, ApJL, 552, L105, doi: 10.1086/320339

Bekki, K., Couch, W. J., Drinkwater, M. J., & Shioya, Y. 2003, MNRAS, 344, 399, doi: 10.1046/j.1365-8711.2003.06916.x

Bekki, K., & Freeman, K. C. 2003, MNRAS, 346, L11, doi: 10.1046/j.1365-2966.2003.07275.x

Bekki, K., & Yong, D. 2012, MNRAS, 419, 2063, doi: 10.1111/j.1365-2966.2011.19856.x

Table 6. The probable UCD candidates not included in the main sample.

	ID	α_{J2000} (deg)	δ_{J2000} (deg)	g_0 (mag)	$r_{h,g}$ (pc)	$r_{h,i}$ (pc)	v_r (km/s)	v_{source}
	(1)	(2)	(3)	(4)	(5)	(6)	(7)	(8)
$r_h > 11$ pc in both g and i bands but large difference between the two	1	186.5656471	16.0492075	19.857±0.001	17.75±1.37	35.32±1.70	···	···
	2	185.1411400	15.8494361	21.548±0.005	15.95±2.05	28.76±1.21	···	···
	3	188.7565072	17.0687625	21.094±0.003	15.13±1.37	28.27±0.89	···	···
	4	188.2201250	16.0768933	21.431±0.006	13.32±1.06	28.21±1.73	···	···
	5	190.6792998	16.5254659	21.468±0.005	11.78±0.70	25.20±0.76	···	···
	6	186.1282677	16.7516812	21.528±0.004	16.96±0.55	28.31±1.00	···	···
	7	188.3270896	16.7757418	21.418±0.004	11.26±0.70	22.63±0.60	···	···
	8	187.8761745	17.1490799	20.986±0.003	20.89±0.58	12.22±0.83	···	···
	9	188.7443865	17.1551750	20.584±0.002	11.69±0.54	24.27±1.09	···	···
Candidates with visible envelopes	1	187.2897173	12.6860435	19.596±0.001	33.40±0.95	0.61±0.00	1159	MMT09
	2	188.8007729	9.3776914	19.531±0.001	2.84±1.59	13.63±1.10	1406	AAT12
	3	187.7426763	11.9746280	20.694±0.002	10.76±0.40	10.09±0.49	1230	MMT09
	4	187.1924549	13.7198340	19.743±0.001	11.69±1.04	9.75±0.65	1022	AAT12
	5	188.3663498	10.6465580	20.490±0.002	9.95±0.24	11.13±0.45	···	···
	6	187.6404154	10.3641505	19.421±0.001	10.45±0.31	7.80±0.43	143	MMT09,AAT12
	7	187.1115755	13.0907153	19.996±0.001	10.06±0.31	8.54±0.33	1040	MMT09,AAT12
	8	187.4479438	9.8971556	20.915±0.002	10.16±0.55	8.44±0.40	···	···

NOTE– (1) Object ID number; (2) R.A.; (3) Decl.; (4) Aperture-corrected g magnitude within a 3-arcsec diameter aperture; (5) Half-light radius in g band; (6) Half-light radius in i band; (7) Radial velocity; (8) The source of velocity measurement: AAT12: Anglo-Australian Telescope (AAT) 2012 program; MMT09: Multiple Mirror Telescope (MMT) 2009 program (Ferrarese et al. 2012).

Bell, E. F., McIntosh, D. H., Katz, N., & Weinberg, M. D. 2003, ApJS, 149, 289, doi: 10.1086/378847

Bellazzini, M., Ibata, R. A., Chapman, S. C., et al. 2008, AJ, 136, 1147, doi: 10.1088/0004-6256/136/3/1147

Bertin, E., & Arnouts, S. 1996, A+AS, 117, 393

Binggeli, B., Sandage, A., & Tammann, G. A. 1985, AJ, 90, 1681, doi: 10.1086/113874

Blakeslee, J. P., & Barber DeGraaff, R. 2008, AJ, 136, 2295, doi: 10.1088/0004-6256/136/6/2295

Blakeslee, J. P., Jordán, A., Mei, S., et al. 2009, ApJ, 694, 556, doi: 10.1088/0004-637X/694/1/556

Blom, C., Forbes, D. A., Foster, C., Romanowsky, A. J., & Brodie, J. P. 2014, MNRAS, 439, 2420, doi: 10.1093/mnras/stu095

Böhringer, H., Briel, U. G., Schwarz, R. A., et al. 1994, Natur, 368, 828, doi: 10.1038/368828a0

Boselli, A., Voyer, E., Boissier, S., et al. 2014, A+A, 570, A69, doi: 10.1051/0004-6361/201424419

Boselli, A., Fossati, M., Ferrarese, L., et al. 2018, A+A, 614, A56, doi: 10.1051/0004-6361/201732407

Brinchmann, J., Kunth, D., & Durret, F. 2008, A+A, 485, 657, doi: 10.1051/0004-6361:200809783

Brodie, J. P., Romanowsky, A. J., Strader, J., & Forbes, D. A. 2011, AJ, 142, 199, doi: 10.1088/0004-6256/142/6/199

Cantiello, M., Blakeslee, J. P., Ferrarese, L., et al. 2018, ApJ, 856, 126, doi: 10.3847/1538-4357/aab043

Chiboucas, K., Tully, R. B., Marzke, R. O., et al. 2011, ApJ, 737, 86, doi: 10.1088/0004-637X/737/2/86

Chilingarian, I. V., & Mamon, G. A. 2008, MNRAS, 385, L83, doi: 10.1111/j.1745-3933.2008.00438.x

Côté, P., McLaughlin, D. E., Cohen, J. G., & Blakeslee, J. P. 2003, ApJ, 591, 850, doi: 10.1086/375488

Côté, P., Blakeslee, J. P., Ferrarese, L., et al. 2004, ApJS, 153, 223, doi: 10.1086/421490

Côté, P., Piatek, S., Ferrarese, L., et al. 2006, ApJS, 165, 57, doi: 10.1086/504042

Crain, R. A., Schaye, J., Bower, R. G., et al. 2015, MNRAS, 450, 1937, doi: 10.1093/mnras/stv725

Da Costa, G. S., Grebel, E. K., Jerjen, H., Rejkuba, M., & Sharina, M. E. 2009, AJ, 137, 4361, doi: 10.1088/0004-6256/137/5/4361
Da Rocha, C., Mieske, S., Georgiev, I. Y., et al. 2011, A+A, 525, A86+, doi: 10.1051/0004-6361/201015353
Dabringhausen, J., Kroupa, P., Pflamm-Altenburg, J., & Mieske, S. 2012, ApJ, 747, 72, doi: 10.1088/0004-637X/747/1/72
De Bórtoli, B. J., Bassino, L. P., Caso, J. P., & Ennis, A. I. 2020, MNRAS, 87, doi: 10.1093/mnras/staa086
Drinkwater, M., Bekki, K., Couch, W., et al. 2002, in IAU Symposium, Vol. 207, Extragalactic Star Clusters, ed. D. P. Geisler, E. K. Grebel, & D. Minniti, 287
Drinkwater, M. J., Gregg, M. D., Couch, W. J., et al. 2004, PASA, 21, 375, doi: 10.1071/AS04048
Drinkwater, M. J., Gregg, M. D., Hilker, M., et al. 2003, Natur, 423, 519
Drinkwater, M. J., Jones, J. B., Gregg, M. D., & Phillipps, S. 2000, PASA, 17, 227, doi: 10.1071/AS00227
Durrell, P. R., Côté, P., Peng, E. W., et al. 2014, ApJ, 794, 103, doi: 10.1088/0004-637X/794/2/103
Evans, D. W., Riello, M., De Angeli, F., et al. 2018, A+A, 616, A4, doi: 10.1051/0004-6361/201832756
Evstigneeva, E. A., Drinkwater, M. J., Jurek, R., et al. 2007a, MNRAS, 378, 1036, doi: 10.1111/j.1365-2966.2007.11856.x
Evstigneeva, E. A., Gregg, M. D., Drinkwater, M. J., & Hilker, M. 2007b, AJ, 133, 1722, doi: 10.1086/511958
Fahrion, K., Georgiev, I., Hilker, M., et al. 2019, A+A, 625, A50, doi: 10.1051/0004-6361/201834941
Faifer, F. R., Escudero, C. G., Scalia, M. C., et al. 2017, A+A, 599, L8, doi: 10.1051/0004-6361/201730493
Fasano, G., & Franceschini, A. 1987, MNRAS, 225, 155, doi: 10.1093/mnras/225.1.155
Fellhauer, M., & Kroupa, P. 2002, MNRAS, 330, 642, doi: 10.1046/j.1365-8711.2002.05087.x
Ferrarese, L., Côté, P., Jordán, A., et al. 2006, ApJS, 164, 334, doi: 10.1086/501350
Ferrarese, L., Côté, P., Cuillandre, J.-C., et al. 2012, ApJS, 200, 4, doi: 10.1088/0067-0049/200/1/4
Ferrarese, L., Côté, P., Sánchez-Janssen, R., et al. 2016, ApJ, 824, 10, doi: 10.3847/0004-637X/824/1/10
Ferrarese, L., Côté, P., MacArthur, L. A., et al. 2020, ApJ, 890, 128, doi: 10.3847/1538-4357/ab339f
Forbes, D. A., Norris, M. A., Strader, J., et al. 2014, MNRAS, 444, 2993, doi: 10.1093/mnras/stu1631
Forbes, D. A., Alabi, A., Brodie, J. P., et al. 2017, AJ, 153, 114, doi: 10.3847/1538-3881/153/3/114
Gebhardt, K., & Kissler-Patig, M. 1999, AJ, 118, 1526, doi: 10.1086/301059
Gratton, R., Bragaglia, A., Carretta, E., et al. 2019, A+ARv, 27, 8, doi: 10.1007/s00159-019-0119-3
Guérou, A., Emsellem, E., McDermid, R. M., et al. 2015, ApJ, 804, 70, doi: 10.1088/0004-637X/804/1/70
Guo, Q., White, S., Boylan-Kolchin, M., et al. 2011, MNRAS, 413, 101, doi: 10.1111/j.1365-2966.2010.18114.x
Haşegan, M., Jordán, A., Côté, P., et al. 2005, ApJ, 627, 203, doi: 10.1086/430342
Hanes, D. A., Côté, P., Bridges, T. J., et al. 2001, ApJ, 559, 812, doi: 10.1086/322346
Hilker, M. 2006, ArXiv Astrophysics e-prints
Hilker, M. 2011, in EAS Publications Series, Vol. 48, EAS Publications Series, ed. M. Koleva, P. Prugniel, & I. Vauglin, 219–224, doi: 10.1051/eas/1148050
Hilker, M., Infante, L., Vieira, G., Kissler-Patig, M., & Richtler, T. 1999, A+AS, 134, 75, doi: 10.1051/aas:1999434
Huxor, A. P., Tanvir, N. R., Irwin, M. J., et al. 2005, MNRAS, 360, 1007, doi: 10.1111/j.1365-2966.2005.09086.x
Huxor, A. P., Mackey, A. D., Ferguson, A. M. N., et al. 2014, MNRAS, 442, 2165, doi: 10.1093/mnras/stu771
Hwang, N., & Lee, M. G. 2008, AJ, 135, 1567, doi: 10.1088/0004-6256/135/4/1567
Hwang, N., Lee, M. G., Lee, J. C., et al. 2011, ApJ, 738, 58, doi: 10.1088/0004-637X/738/1/58
Ibata, R. A., Bellazzini, M., Malhan, K., Martin, N., & Bianchini, P. 2019, NatAs, 3, 667, doi: 10.1038/s41550-019-0751-x
Ibata, R. A., Gilmore, G., & Irwin, M. J. 1994, Natur, 370, 194, doi: 10.1038/370194a0
Janz, J., Forbes, D. A., Norris, M. A., et al. 2015, MNRAS, 449, 1716, doi: 10.1093/mnras/stv389
Janz, J., Norris, M. A., Forbes, D. A., et al. 2016, MNRAS, 456, 617, doi: 10.1093/mnras/stv2636
Jennings, Z. G., Strader, J., Romanowsky, A. J., et al. 2014, AJ, 148, 32, doi: 10.1088/0004-6256/148/2/32
Jennings, Z. G., Romanowsky, A. J., Brodie, J. P., et al. 2015, ApJL, 812, L10, doi: 10.1088/2041-8205/812/1/L10
Johnson, C. I., Rich, R. M., Pilachowski, C. A., et al. 2015, AJ, 150, 63, doi: 10.1088/0004-6256/150/2/63
Jones, J. B., Drinkwater, M. J., Jurek, R., et al. 2006, AJ, 131, 312, doi: 10.1086/497960
Jordán, A., Côté, P., Blakeslee, J. P., et al. 2005, ApJ, 634, 1002, doi: 10.1086/497092
Jordán, A., McLaughlin, D. E., Côté, P., et al. 2007, ApJS, 171, 101, doi: 10.1086/516840
Jordán, A., Peng, E. W., Blakeslee, J. P., et al. 2009, ApJS, 180, 54, doi: 10.1088/0067-0049/180/1/54

Katz, D., Sartoretti, P., Cropper, M., et al. 2019, A+A, 622, A205, doi: 10.1051/0004-6361/201833273
Ko, Y., Hwang, H. S., Lee, M. G., et al. 2017, ApJ, 835, 212, doi: 10.3847/1538-4357/835/2/212
Kundu, A., & Whitmore, B. C. 2001, AJ, 121, 2950, doi: 10.1086/321073
Küpper, A. H. W., Balbinot, E., Bonaca, A., et al. 2015, ApJ, 803, 80, doi: 10.1088/0004-637X/803/2/80
Küpper, A. H. W., Kroupa, P., Baumgardt, H., & Heggie, D. C. 2010, MNRAS, 401, 105, doi: 10.1111/j.1365-2966.2009.15690.x
Kuzma, P. B., Da Costa, G. S., & Mackey, A. D. 2018, MNRAS, 473, 2881, doi: 10.1093/mnras/stx2353
Kuzma, P. B., Da Costa, G. S., Mackey, A. D., & Roderick, T. A. 2016, MNRAS, 461, 3639, doi: 10.1093/mnras/stw1561
Lawrence, A., Warren, S. J., Almaini, O., et al. 2007, MNRAS, 379, 1599, doi: 10.1111/j.1365-2966.2007.12040.x
Li, B., Peng, E. W., Zhang, H.-x., et al. 2015, ApJ, 806, 133, doi: 10.1088/0004-637X/806/1/133
Liu, C., Peng, E. W., Côté, P., et al. 2015a, ApJ, 812, 34, doi: 10.1088/0004-637X/812/1/34
Liu, C., Peng, E. W., Toloba, E., et al. 2015b, ApJL, 812, L2, doi: 10.1088/2041-8205/812/1/L2
Liu, Y., Peng, E. W., Lim, S., et al. 2016, ApJ, 830, 99, doi: 10.3847/0004-637X/830/2/99
Longobardi, A., Peng, E. W., Côté, P., et al. 2018, ApJ, 864, 36, doi: 10.3847/1538-4357/aad3d2
Madrid, J. P. 2011, ApJ, 737, L13, doi: 10.1088/2041-8205/737/1/L13
Madrid, J. P., Graham, A. W., Harris, W. E., et al. 2010, ApJ, 722, 1707, doi: 10.1088/0004-637X/722/2/1707
Majewski, S. R., Skrutskie, M. F., Weinberg, M. D., & Ostheimer, J. C. 2003, ApJ, 599, 1082, doi: 10.1086/379504
Mei, S., Blakeslee, J. P., Côté, P., et al. 2007, ApJ, 655, 144, doi: 10.1086/509598
Mieske, S., Hilker, M., & Infante, L. 2002, A+A, 383, 823, doi: 10.1051/0004-6361:20011833
—. 2004a, A+A, 418, 445, doi: 10.1051/0004-6361:20035723
Mieske, S., Hilker, M., Infante, L., & Jordán, A. 2006, AJ, 131, 2442, doi: 10.1086/500583
Mieske, S., Hilker, M., Jordán, A., Infante, L., & Kissler-Patig, M. 2007a, A+A, 472, 111, doi: 10.1051/0004-6361:20077631
Mieske, S., Hilker, M., & Misgeld, I. 2012, A+A, 537, A3, doi: 10.1051/0004-6361/201117634
Mieske, S., Infante, L., Hilker, M., et al. 2005, A+A, 430, L25, doi: 10.1051/0004-6361:200400119
Mieske, S., West, M. J., & de Oliveira, C. M. 2007b, in Groups of Galaxies in the Nearby Universe, ed. I. Saviane, V. D. Ivanov, & J. Borissova, 103, doi: 10.1007/978-3-540-71173-5_16
Mieske, S., Infante, L., Benítez, N., et al. 2004b, AJ, 128, 1529, doi: 10.1086/423701
Mihos, J. C., Durrell, P. R., Ferrarese, L., et al. 2015, ApJL, 809, L21, doi: 10.1088/2041-8205/809/2/L21
Milone, A. P., Piotto, G., Renzini, A., et al. 2017, MNRAS, 464, 3636, doi: 10.1093/mnras/stw2531
Muñoz, R. P., Puzia, T. H., Lançon, A., et al. 2014, ApJS, 210, 4, doi: 10.1088/0067-0049/210/1/4
Muratov, A. L., & Gnedin, O. Y. 2010, ApJ, 718, 1266, doi: 10.1088/0004-637X/718/2/1266
Norris, M. A., & Kannappan, S. J. 2011, MNRAS, 414, 739, doi: 10.1111/j.1365-2966.2011.18440.x
Norris, M. A., Kannappan, S. J., Forbes, D. A., et al. 2014, MNRAS, 443, 1151, doi: 10.1093/mnras/stu1186
Odenkirchen, M., Grebel, E. K., Rockosi, C. M., et al. 2001, ApJL, 548, L165, doi: 10.1086/319095
Park, H. S., Lee, M. G., & Hwang, H. S. 2012, ApJ, 757, 184, doi: 10.1088/0004-637X/757/2/184
Paudel, S., Lisker, T., & Janz, J. 2010, ApJ, 724, L64, doi: 10.1088/2041-8205/724/1/L64
Peacock, J. A. 1983, MNRAS, 202, 615, doi: 10.1093/mnras/202.3.615
Peng, E. W., Jordán, A., Côté, P., et al. 2006a, ApJ, 639, 95, doi: 10.1086/498210
Peng, E. W., Côté, P., Jordán, A., et al. 2006b, ApJ, 639, 838, doi: 10.1086/499485
Penny, S. J., Forbes, D. A., & Conselice, C. J. 2012, MNRAS, 422, 885, doi: 10.1111/j.1365-2966.2012.20669.x
Penny, S. J., Forbes, D. A., Strader, J., et al. 2014, MNRAS, 439, 3808, doi: 10.1093/mnras/stu232
Pfeffer, J., & Baumgardt, H. 2013, MNRAS, 433, 1997, doi: 10.1093/mnras/stt867
Pfeffer, J., Griffen, B. F., Baumgardt, H., & Hilker, M. 2014, MNRAS, 444, 3670, doi: 10.1093/mnras/stu1705
Pfeffer, J., Hilker, M., Baumgardt, H., & Griffen, B. F. 2016, MNRAS, 458, 2492, doi: 10.1093/mnras/stw498
Phillipps, S., Drinkwater, M. J., Gregg, M. D., & Jones, J. B. 2001, ApJ, 560, 201, doi: 10.1086/322517
Pota, V., Forbes, D. A., Romanowsky, A. J., et al. 2013, MNRAS, 428, 389, doi: 10.1093/mnras/sts029
Pota, V., Brodie, J. P., Bridges, T., et al. 2015, MNRAS, 450, 1962, doi: 10.1093/mnras/stv677
Powalka, M., Lançon, A., Puzia, T. H., et al. 2016a, ApJS, 227, 12, doi: 10.3847/0067-0049/227/1/12
Powalka, M., Puzia, T. H., Lançon, A., et al. 2016b, ApJL, 829, L5, doi: 10.3847/2041-8205/829/1/L5

Riello, M., De Angeli, F., Evans, D. W., et al. 2018, A+A, 616, A3, doi: 10.1051/0004-6361/201832712

Roediger, J. C., Ferrarese, L., Côté, P., et al. 2017, ApJ, 836, 120, doi: 10.3847/1538-4357/836/1/120

Sánchez-Janssen, R., Ferrarese, L., MacArthur, L. A., et al. 2016, ApJ, 820, 69, doi: 10.3847/0004-637X/820/1/69

Sánchez-Janssen, R., Côté, P., Ferrarese, L., et al. 2019, ApJ, 878, 18, doi: 10.3847/1538-4357/aaf4fd

Sandoval, M. A., Vo, R. P., Romanowsky, A. J., et al. 2015, ApJL, 808, L32, doi: 10.1088/2041-8205/808/1/L32

Schlegel, D. J., Finkbeiner, D. P., & Davis, M. 1998, ApJ, 500, 525, doi: 10.1086/305772

Schweizer, F., Seitzer, P., Whitmore, B. C., Kelson, D. D., & Villanueva, E. V. 2018, ApJ, 853, 54, doi: 10.3847/1538-4357/aaa424

Seth, A. C., van den Bosch, R., Mieske, S., et al. 2014, Natur, 513, 398, doi: 10.1038/nature13762

Spengler, C., Côté, P., Roediger, J., et al. 2017, ApJ, 849, 55, doi: 10.3847/1538-4357/aa8a78

Strader, J., Romanowsky, A. J., Brodie, J. P., et al. 2011, ApJS, 197, 33, doi: 10.1088/0067-0049/197/2/33

Strader, J., Fabbiano, G., Luo, B., et al. 2012, ApJ, 760, 87, doi: 10.1088/0004-637X/760/1/87

Strader, J., Seth, A. C., Forbes, D. A., et al. 2013, ApJL, 775, L6, doi: 10.1088/2041-8205/775/1/L6

Toloba, E., Li, B., Guhathakurta, P., et al. 2016, ApJ, 822, 51, doi: 10.3847/0004-637X/822/1/51

Toloba, E., Lim, S., Peng, E., et al. 2018, ApJL, 856, L31, doi: 10.3847/2041-8213/aab603

van den Bergh, S., & Mackey, A. D. 2004, MNRAS, 354, 713, doi: 10.1111/j.1365-2966.2004.08228.x

van den Bergh, S., Morbey, C., & Pazder, J. 1991, ApJ, 375, 594, doi: 10.1086/170220

Villegas, D., Jordán, A., Peng, E. W., et al. 2010, ApJ, 717, 603, doi: 10.1088/0004-637X/717/2/603

Voggel, K., Hilker, M., & Richtler, T. 2016, A+A, 586, A102, doi: 10.1051/0004-6361/201527070

Voggel, K. T., Seth, A. C., Sand, D. J., et al. 2020, arXiv e-prints, arXiv:2001.02243. https://arxiv.org/abs/2001.02243

Wehner, E. M. H., & Harris, W. E. 2007, ApJ, 668, L35, doi: 10.1086/522305

Wenger, M., Ochsenbein, F., Egret, D., et al. 2000, A+AS, 143, 9, doi: 10.1051/aas:2000332

Willman, B., & Strader, J. 2012, AJ, 144, 76, doi: 10.1088/0004-6256/144/3/76

Zhang, H.-X., Peng, E. W., Côté, P., et al. 2015, ApJ, 802, 30, doi: 10.1088/0004-637X/802/1/30

Zhang, H.-X., Puzia, T. H., Peng, E. W., et al. 2018, ApJ, 858, 37, doi: 10.3847/1538-4357/aab88a

Table 3. Photometric Properties of UCD Candidates

ID	Name	NGVSID	$t_{\rm obs}$	$\alpha_{\rm J2000}$	$\delta_{\rm J2000}$	$E(B-V)$	g_0	K	$(u^*-g)_0$	$(g-i)_0$	$(g-z)_0$	$\Delta_{\rm env}$	UCD
				(deg)	(deg)	(mag)	(mag)	(mag)	(mag)	(mag)	(mag)	(mag)	
(1)	(2)	(3)	(4)	(5)	(6)	(7)	(8)	(9)	(10)	(11)	(12)	(13)	(14)
1	NGVS-UCD1	NGVS-J120652.65+113246.5	l	181.7193703	11.5462618	0.028	19.212±0.002	···	0.554±0.004	-0.034±0.004	-0.034±0.006	0.018	0
2	NGVS-UCD2	NGVS-J120717.93+113846.7	l	181.8247260	11.6463089	0.032	21.074±0.003	···	0.984±0.011	0.650±0.007	0.822±0.010	0.105	1
3	NGVS-UCD3	NGVS-J120734.18+113626.0	l	181.8924309	11.6072260	0.028	21.492±0.004	···	1.062±0.011	0.600±0.007	0.709±0.012	0.032	1
4	NGVS-UCD4	NGVS-J120755.71+113921.2	l	181.9821228	11.6558897	0.030	21.057±0.003	···	0.892±0.008	0.633±0.006	0.725±0.010	0.079	1
5	NGVS-UCD5	NGVS-J120757.12+121954.2	l	181.9879964	12.3317198	0.027	21.444±0.004	···	1.089±0.011	0.648±0.007	0.723±0.012	0.005	0
6	NGVS-UCD6	NGVS-J120811.52+131327.6	l	182.0480094	13.2243239	0.030	21.408±0.004	···	0.910±0.012	0.525±0.009	0.673±0.019	0.015	1
7	NGVS-UCD7	NGVS-J120827.25+132407.4	l	182.1135389	13.4020547	0.032	21.373±0.004	···	0.920±0.010	0.656±0.007	0.724±0.013	0.009	1
8	NGVS-UCD8	NGVS-J120846.23+121935.8	l	182.1926310	12.3266129	0.026	21.338±0.003	···	0.970±0.010	0.770±0.007	0.852±0.012	0.032	1
9	NGVS-UCD9	NGVS-J120855.90+121833.2	l	182.2329343	12.3092174	0.027	21.415±0.004	···	1.032±0.011	0.796±0.007	0.892±0.011	0.060	1
10	NGVS-UCD10	NGVS-J120925.56+132007.7	l	182.3565013	13.3354611	0.034	19.007±0.001	···	0.877±0.003	0.588±0.002	0.711±0.003	0.197	0
11	NGVS-UCD11	NGVS-J120940.57+124434.6	l	182.4190392	12.7429512	0.029	19.783±0.001	···	0.921±0.004	0.721±0.003	0.851±0.004	0.039	1
12	NGVS-UCD12	NGVS-J120941.08+125503.0	l	182.4211738	12.9175066	0.032	19.930±0.001	···	1.600±0.005	1.046±0.002	1.225±0.003	0.020	0
13	NGVS-UCD13	NGVS-J120941.22+124807.1	l	182.4217388	12.8019625	0.029	21.059±0.003	···	0.878±0.008	0.593±0.006	0.640±0.010	-0.004	1
14	NGVS-UCD14	NGVS-J120943.81+125626.8	l	182.4325431	12.9407664	0.032	21.088±0.003	···	1.000±0.009	0.838±0.005	0.913±0.009	-0.111	0
15	NGVS-UCD15	NGVS-J121006.36+132053.9	l	182.5265164	13.3483006	0.035	21.332±0.004	···	1.225±0.011	0.819±0.006	0.930±0.010	0.011	1
16	NGVS-UCD16	NGVS-J121006.57+125615.4	l	182.5273734	12.9376208	0.033	20.193±0.002	···	0.855±0.005	0.612±0.004	0.653±0.006	0.102	1
17	NGVS-UCD17	NGVS-J121031.59+142329.4	l	182.6316283	14.3915054	0.036	20.212±0.002	17.297±0.099	1.553±0.009	1.143±0.003	1.353±0.004	-0.012	0
18	NGVS-UCD18	NGVS-J121032.19+132321.6	l	182.6341059	13.3893423	0.038	20.486±0.002	16.907±0.056	1.426±0.006	1.076±0.003	1.253±0.004	0.000	1
19	NGVS-UCD19	NGVS-J121047.40+144707.6	l	182.6974975	14.7854454	0.038	21.497±0.004	···	0.911±0.013	0.546±0.008	0.634±0.014	0.002	1
20	NGVS-UCD20	NGVS-J121048.93+121218.4	l	182.7038954	12.2051059	0.028	21.399±0.004	···	1.005±0.011	0.712±0.007	0.805±0.012	0.053	1
21	NGVS-UCD21	NGVS-J121051.39+115414.9	s	182.7141302	11.9041342	0.028	16.829±0.002	14.117±0.006	···	···	1.095±0.004	-0.020	0
22	NGVS-UCD22	NGVS-J121051.82+131916.5	l	182.7159328	13.3212427	0.038	20.605±0.002	···	0.981±0.006	0.675±0.004	0.761±0.007	0.040	0
23	NGVS-UCD23	NGVS-J121052.87+141130.9	l	182.7202974	14.1919277	0.042	19.580±0.001	15.962±0.023	1.726±0.005	1.058±0.002	1.370±0.002	0.057	0
24	NGVS-UCD24	NGVS-J121055.70+115839.6	l	182.7321029	11.9776564	0.027	19.786±0.001	16.473±0.042	1.491±0.004	0.930±0.002	1.119±0.003	0.019	1
25	NGVS-UCD25	NGVS-J121103.28+124013.6	l	182.7636873	12.6704570	0.026	21.070±0.003	···	0.852±0.008	0.647±0.006	0.718±0.009	0.013	1
26	NGVS-UCD26	NGVS-J121103.98+134328.1	l	182.7665718	13.7244767	0.033	21.385±0.004	···	1.098±0.010	0.710±0.007	0.876±0.013	0.018	1
27	NGVS-UCD27	NGVS-J121106.57+135959.8	l	182.7773917	13.9999439	0.047	20.669±0.002	18.242±0.194	0.874±0.007	0.552±0.005	0.676±0.008	0.030	1
28	NGVS-UCD28	NGVS-J121109.06+123935.7	l	182.7877655	12.6599274	0.026	21.477±0.004	···	1.088±0.012	0.645±0.008	0.713±0.014	0.040	1
29	NGVS-UCD29	NGVS-J121127.84+104254.1	l	182.8659962	10.7150366	0.026	21.231±0.003	···	0.975±0.009	0.600±0.007	0.665±0.011	0.018	1
30	NGVS-UCD30	NGVS-J121150.69+144020.0	l	182.9611992	14.6722180	0.034	20.069±0.001	17.580±0.118	0.856±0.007	0.627±0.004	0.750±0.005	0.007	0
31	NGVS-UCD31	NGVS-J121203.36+145646.5	l	183.0140015	14.9462408	0.032	20.924±0.002	18.025±0.183	0.993±0.010	0.802±0.005	0.938±0.008	0.016	1
32	NGVS-UCD32	NGVS-J121236.91+144649.8	l	183.1537725	14.7805109	0.033	21.338±0.003	···	0.852±0.011	0.608±0.007	0.706±0.012	0.023	1
33	NGVS-UCD33	NGVS-J121252.91+124121.4	l	183.2204675	12.6892760	0.030	21.086±0.004	···	1.001±0.011	0.649±0.007	0.680±0.012	0.055	0
34	NGVS-UCD34	NGVS-J121305.54+125312.0	l	183.2730893	12.8866545	0.033	20.426±0.002	18.115±0.173	0.853±0.006	0.669±0.004	0.762±0.006	0.083	1
35	NGVS-UCD35	NGVS-J121310.81+111925.2	l	183.2950532	11.3236761	0.032	21.498±0.004	···	0.899±0.014	0.654±0.009	0.663±0.022	0.062	1
36	NGVS-UCD36	NGVS-J121315.42+100737.1	l	183.3142622	10.1269729	0.022	21.316±0.004	···	0.973±0.012	0.657±0.008	0.688±0.011	0.023	1
37	NGVS-UCD37	NGVS-J121330.29+104301.9	l	183.3762015	10.7172051	0.027	20.927±0.003	···	0.885±0.009	0.608±0.007	0.681±0.011	0.039	1
38	NGVS-UCD38	NGVS-J121343.77+130338.6	l	183.4323907	13.0607096	0.030	21.451±0.004	···	0.904±0.010	0.789±0.007	0.855±0.011	0.038	0
39	NGVS-UCD39	NGVS-J121350.12+113906.9	l	183.4588402	11.6519070	0.028	20.877±0.002	···	0.879±0.006	0.636±0.005	0.683±0.008	0.014	1
40	NGVS-UCD40	NGVS-J121350.50+104136.6	l	183.4604291	10.6935073	0.027	21.160±0.003	···	0.956±0.009	0.569±0.007	0.660±0.011	0.088	0
41	NGVS-UCD41	NGVS-J121356.25+134035.2	s	183.4843746	13.6764551	0.030	17.952±0.004	14.486±0.007	···	···	1.381±0.010	0.222	0
42	NGVS-UCD42	NGVS-J121431.28+094514.4	l	183.6303525	9.7540128	0.017	20.279±0.002	17.659±0.107	0.983±0.005	0.688±0.004	0.847±0.004	0.042	1
43	NGVS-UCD43	NGVS-J121435.75+160829.8	l	183.6489700	16.1416151	0.033	18.775±0.001	···	0.926±0.002	0.732±0.002	0.891±0.002	0.224	0
44	NGVS-UCD44	NGVS-J121441.47+135441.2	l	183.6727962	13.9114378	0.029	21.480±0.004	···	0.927±0.011	0.647±0.008	0.727±0.014	-0.005	1
45	NGVS-UCD45	NGVS-J121452.31+160446.7	l	183.7179418	16.0796349	0.032	21.135±0.003	···	0.908±0.011	0.763±0.006	0.820±0.012	-0.011	0
46	NGVS-UCD46	NGVS-J121501.26+144034.0	l	183.7552498	14.6760998	0.034	20.971±0.002	···	1.120±0.009	0.739±0.005	0.829±0.009	0.051	1

Table 3 *continued*

Table 3 *(continued)*

ID	Name	NGVSID	$t_{\rm obs}$	$\alpha_{\rm J2000}$	$\delta_{\rm J2000}$	$E(B-V)$	g_0	K	$(u^*-g)_0$	$(g-i)_0$	$(g-z)_0$	$\Delta_{\rm env}$	UCD
				(deg)	(deg)	(mag)	(mag)	(mag)	(mag)	(mag)	(mag)	(mag)	
(1)	(2)	(3)	(4)	(5)	(6)	(7)	(8)	(9)	(10)	(11)	(12)	(13)	(14)
47	NGVS-UCD47	NGVS-J121504.62+064925.6	l	183.7692606	6.8237857	0.018	20.722±0.002	18.196±0.197	1.085±0.007	0.840±0.004	0.902±0.005	-0.023	0
48	NGVS-UCD48	NGVS-J121507.37+143317.2	l	183.7806964	14.5547768	0.034	20.962±0.002	···	0.897±0.008	0.654±0.005	0.736±0.009	0.008	1
49	NGVS-UCD49	NGVS-J121514.93+083530.2	l	183.8122140	8.5917108	0.017	21.336±0.004	···	1.146±0.012	0.784±0.007	0.825±0.010	-0.027	1
50	NGVS-UCD50	NGVS-J121516.14+132830.5	l	183.8172668	13.4751404	0.031	19.957±0.002	16.605±0.042	0.765±0.005	0.564±0.003	0.623±0.004	-0.213	0
51	NGVS-UCD51	NGVS-J121520.46+114351.2	l	183.8352681	11.7308932	0.025	21.221±0.003	···	0.920±0.011	0.679±0.008	0.730±0.009	0.021	1
52	NGVS-UCD52	NGVS-J121531.90+161654.9	l	183.8829061	16.2819090	0.035	21.353±0.004	···	0.882±0.011	0.797±0.006	0.852±0.012	0.018	1
53	NGVS-UCD53	NGVS-J121533.95+065102.2	l	183.8914576	6.8506000	0.018	21.480±0.004	···	1.037±0.013	0.821±0.007	0.901±0.009	0.002	1
54	NGVS-UCD54	NGVS-J121542.84+065024.4	l	183.9285083	6.8401028	0.019	21.298±0.003	···	1.031±0.011	0.705±0.007	0.776±0.008	0.007	1
55	NGVS-UCD55	NGVS-J121543.62+080052.7	l	183.9317469	8.0146495	0.021	21.350±0.005	···	0.868±0.013	0.732±0.010	0.768±0.014	-0.035	1
56	NGVS-UCD56	NGVS-J121559.52+161819.4	l	183.9980129	16.3053961	0.033	21.034±0.003	···	1.006±0.013	0.827±0.007	0.943±0.011	0.023	1
57	NGVS-UCD57	NGVS-J121600.62+141633.5	l	184.0025831	14.2759618	0.038	20.492±0.002	17.742±0.147	0.905±0.006	0.718±0.004	0.870±0.006	0.032	1
58	NGVS-UCD58	NGVS-J121603.72+150416.1	l	184.0155151	15.0711362	0.037	21.122±0.003	···	0.996±0.015	0.591±0.007	0.700±0.013	0.102	0
59	NGVS-UCD59	NGVS-J121617.56+105015.8	l	184.0731796	10.8377225	0.032	21.352±0.004	···	0.884±0.013	0.642±0.008	0.659±0.014	0.011	0
60	NGVS-UCD60	NGVS-J121631.68+155124.7	l	184.1320087	15.8568706	0.026	20.799±0.002	···	0.895±0.008	0.623±0.005	0.722±0.009	0.074	1
61	NGVS-UCD61	NGVS-J121632.60+092309.1	s	184.1358270	9.3858577	0.017	17.983±0.004	14.399±0.007	···	···	1.483±0.011	0.230	0
62	NGVS-UCD62	NGVS-J121648.99+133505.8	l	184.2041330	13.5849386	0.033	20.990±0.003	···	1.004±0.010	0.689±0.006	0.794±0.010	0.033	0
63	NGVS-UCD63	NGVS-J121649.78+133014.7	l	184.2074070	13.5040889	0.033	20.604±0.002	18.140±0.176	0.192±0.005	-0.712±0.009	-0.613±0.020	-0.825	0
64	NGVS-UCD64	NGVS-J121651.27+141360.0	l	184.2136410	14.2333229	0.035	21.375±0.004	···	0.953±0.012	0.559±0.008	0.626±0.014	0.026	1
65	NGVS-UCD65	NGVS-J121701.13+092427.1	s	184.2546935	9.4075253	0.018	18.840±0.014	15.864±0.022	···	···	0.824±0.044	0.206	0
66	NGVS-UCD66	NGVS-J121707.42+065754.7	l	184.2809048	6.9652057	0.019	21.476±0.004	···	1.047±0.015	0.639±0.008	0.725±0.011	0.003	1
67	NGVS-UCD67	NGVS-J121721.61+111348.9	l	184.3400357	11.2302383	0.032	21.433±0.005	···	1.050±0.015	0.790±0.009	0.886±0.013	0.020	1
68	NGVS-UCD68	NGVS-J121748.19+151824.0	l	184.4508107	15.3066755	0.028	21.453±0.004	···	0.859±0.010	0.629±0.007	0.625±0.012	-0.008	1
69	NGVS-UCD69	NGVS-J121751.17+155308.0	l	184.4632091	15.8855564	0.026	21.460±0.004	···	1.053±0.013	0.718±0.007	0.850±0.013	0.011	0
70	NGVS-UCD70	NGVS-J121757.63+161013.3	l	184.4901255	16.1703531	0.027	21.399±0.004	···	0.927±0.012	0.611±0.008	0.630±0.014	0.040	1
71	NGVS-UCD71	NGVS-J121811.33+065302.4	l	184.5472185	6.8840004	0.020	21.417±0.004	···	0.989±0.012	0.820±0.008	0.915±0.009	0.004	1
72	NGVS-UCD72	NGVS-J121816.97+163926.0	l	184.5707011	16.6572148	0.030	20.012±0.001	···	1.136±0.005	0.671±0.003	0.787±0.004	0.115	0
73	NGVS-UCD73	NGVS-J121825.04+171645.7	s	184.6043287	17.2793730	0.029	17.822±0.007	···	···	···	0.728±0.019	-0.062	0
74	NGVS-UCD74	NGVS-J121832.26+072733.7	l	184.6344124	7.4593505	0.021	21.106±0.003	18.568±0.236	0.916±0.009	0.730±0.006	0.832±0.007	0.031	1
75	NGVS-UCD75	NGVS-J121846.72+055638.8	l	184.6946699	5.9440973	0.020	21.342±0.004	···	1.116±0.014	0.695±0.007	0.818±0.012	0.035	1
76	NGVS-UCD76	NGVS-J121849.06+143912.1	l	184.7044002	14.6533714	0.038	21.282±0.005	···	0.925±0.014	0.716±0.009	0.826±0.014	-0.024	0
77	NGVS-UCD77	NGVS-J121851.36+090556.6	l	184.7140101	9.0990516	0.021	21.489±0.004	···	0.977±0.013	0.724±0.009	0.771±0.012	0.021	1
78	NGVS-UCD78	NGVS-J121852.73+142546.8	l	184.7197129	14.4296801	0.039	18.207±0.001	15.817±0.027	0.297±0.002	0.245±0.001	0.261±0.002	0.068	0
79	NGVS-UCD79	NGVS-J121858.75+120206.1	l	184.7447924	12.0350239	0.033	21.072±0.003	···	1.037±0.013	0.555±0.008	0.783±0.011	0.025	1
80	NGVS-UCD80	NGVS-J121900.19+090017.0	l	184.7507849	9.0047154	0.021	21.120±0.003	···	0.922±0.010	0.664±0.007	0.732±0.009	0.047	0
81	NGVS-UCD81	NGVS-J121900.41+055307.7	l	184.7516905	5.8854702	0.018	21.365±0.004	···	0.868±0.011	0.638±0.007	0.766±0.013	0.005	1
82	NGVS-UCD82	NGVS-J121906.50+130013.7	l	184.7770652	13.0038046	0.042	21.266±0.003	···	0.944±0.012	0.691±0.007	0.762±0.010	0.074	1
83	NGVS-UCD83	NGVS-J121912.82+162336.5	l	184.8033989	16.3934800	0.027	20.087±0.001	···	0.940±0.005	0.741±0.003	0.890±0.004	0.043	1
84	NGVS-UCD84	NGVS-J121913.64+054928.6	l	184.8068367	5.8245984	0.018	20.803±0.003	17.485±0.087	1.324±0.011	1.005±0.004	1.194±0.007	0.025	1
85	NGVS-UCD85	NGVS-J121916.77+171059.6	l	184.8198708	17.1832287	0.024	20.754±0.002	···	0.860±0.006	0.602±0.004	0.690±0.007	-0.025	1
86	NGVS-UCD86	NGVS-J121917.28+110032.9	l	184.8220084	11.0091500	0.035	21.179±0.003	···	1.058±0.010	0.826±0.006	0.957±0.007	0.033	0
87	NGVS-UCD87	NGVS-J121925.72+083039.5	l	184.8571689	8.5109851	0.020	21.452±0.004	···	1.019±0.013	0.745±0.008	0.848±0.011	-0.023	1
88	NGVS-UCD88	NGVS-J121927.58+170838.4	l	184.8648981	17.1439978	0.023	20.922±0.002	···	0.971±0.008	0.795±0.005	0.917±0.008	0.014	0
89	NGVS-UCD89	NGVS-J121927.67+055004.0	l	184.8652937	5.8344359	0.018	21.110±0.004	···	1.086±0.012	0.644±0.007	0.783±0.012	-0.005	1
90	NGVS-UCD90	NGVS-J121934.77+142526.4	l	184.8948948	14.4239915	0.037	20.736±0.002	···	0.862±0.007	0.583±0.005	0.677±0.008	0.019	1
91	NGVS-UCD91	NGVS-J121938.31+170043.9	l	184.9096101	17.0121823	0.024	19.776±0.002	···	0.883±0.005	0.756±0.004	0.824±0.005	0.081	0
92	NGVS-UCD92	NGVS-J121948.74+122435.8	l	184.9530954	12.4099381	0.037	18.774±0.001	15.378±0.015	1.638±0.003	1.119±0.001	1.400±0.001	0.092	0
93	NGVS-UCD93	NGVS-J121949.20+060053.7	s	184.9549885	6.0149214	0.020	15.330±0.001	11.995±0.001	···	1.032±0.002	1.307±0.002	0.413	0
94	NGVS-UCD94	NGVS-J121955.43+170921.2	l	184.9809395	17.1558898	0.025	20.607±0.002	···	1.037±0.007	0.812±0.004	0.953±0.006	0.018	1

Table 3 *continued*

Table 3 *(continued)*

ID	Name	NGVSID	t_{obs}	α_{J2000}	δ_{J2000}	$E(B-V)$	g_0	K	$(u^*-g)_0$	$(g-i)_0$	$(g-z)_0$	Δ_{env}	UCD
				(deg)	(deg)	(mag)	(mag)	(mag)	(mag)	(mag)	(mag)	(mag)	
(1)	(2)	(3)	(4)	(5)	(6)	(7)	(8)	(9)	(10)	(11)	(12)	(13)	(14)
95	NGVS-UCD95	NGVS-J122006.94+162041.0	l	185.0289350	16.3447223	0.027	20.639±0.002	···	0.944±0.007	0.784±0.004	0.869±0.006	0.023	1
96	NGVS-UCD96	NGVS-J122008.01+125100.5	l	185.0333669	12.8501506	0.050	20.314±0.002	16.898±0.051	1.463±0.008	1.105±0.003	1.311±0.003	0.059	1
97	NGVS-UCD97	NGVS-J122025.98+124853.3	l	185.1082438	12.8148176	0.049	21.382±0.004	···	0.995±0.013	0.593±0.008	0.646±0.012	-0.004	1
98	NGVS-UCD98	NGVS-J122031.85+100742.3	l	185.1327138	10.1284209	0.024	20.234±0.002	16.202±0.031	1.705±0.008	1.187±0.003	1.476±0.004	-0.180	0
99	NGVS-UCD99	NGVS-J122032.58+111705.4	l	185.1357588	11.2848272	0.033	20.775±0.002	···	0.855±0.009	0.653±0.006	0.763±0.008	0.119	1
100	NGVS-UCD100	NGVS-J122032.70+100703.7	l	185.1362421	10.1177017	0.024	18.600±0.001	14.988±0.011	1.727±0.003	1.136±0.001	1.404±0.002	0.085	0
101	NGVS-UCD101	NGVS-J122036.33+125305.1	l	185.1513543	12.8847388	0.047	21.166±0.003	···	1.006±0.012	0.721±0.007	0.814±0.009	0.154	0
102	NGVS-UCD102	NGVS-J122038.81+105854.7	l	185.1617080	10.9818520	0.035	21.447±0.004	18.893±0.308	1.009±0.014	0.697±0.008	0.760±0.011	0.062	0
103	NGVS-UCD103	NGVS-J122048.88+122333.5	l	185.2036578	12.3926498	0.036	21.026±0.003	···	0.952±0.010	0.603±0.007	0.759±0.008	0.023	1
104	NGVS-UCD104	NGVS-J122050.94+160724.7	l	185.2122552	16.1235140	0.028	20.918±0.003	···	1.033±0.009	0.720±0.005	0.808±0.009	0.018	1
105	NGVS-UCD105	NGVS-J122054.05+100044.4	l	185.2252274	10.0123427	0.022	21.367±0.004	···	0.893±0.012	0.589±0.009	0.668±0.013	0.005	1
106	NGVS-UCD106	NGVS-J122057.04+064320.5	l	185.2376787	6.7223666	0.018	20.929±0.003	···	0.966±0.010	0.626±0.006	0.660±0.012	0.024	1
107	NGVS-UCD107	NGVS-J122100.19+080838.5	l	185.2507862	8.1440259	0.020	20.551±0.002	18.301±0.193	0.947±0.007	0.590±0.005	0.664±0.007	0.017	1
108	NGVS-UCD108	NGVS-J122117.63+154412.4	l	185.3234564	15.7367774	0.022	21.412±0.004	···	1.068±0.013	0.786±0.007	0.928±0.012	0.052	1
109	NGVS-UCD109	NGVS-J122128.72+112210.2	l	185.3696523	11.3694955	0.036	21.347±0.004	···	0.966±0.011	0.800±0.007	0.870±0.009	0.059	0
110	NGVS-UCD110	NGVS-J122130.00+153841.7	l	185.3750201	15.6449242	0.022	21.096±0.003	···	0.888±0.010	0.627±0.007	0.713±0.014	-0.014	1
111	NGVS-UCD111	NGVS-J122130.31+134606.7	l	185.3762735	13.7685331	0.046	21.341±0.004	···	1.046±0.013	0.626±0.008	0.738±0.013	0.018	1
112	NGVS-UCD112	NGVS-J122130.45+135201.0	l	185.3768762	13.8669543	0.047	20.806±0.003	···	1.158±0.009	0.748±0.005	0.870±0.008	0.131	1
113	NGVS-UCD113	NGVS-J122130.68+082419.3	l	185.3778462	8.4053488	0.019	21.128±0.003	···	1.028±0.010	0.616±0.007	0.706±0.010	-0.029	1
114	NGVS-UCD114	NGVS-J122130.68+165212.1	l	185.3778490	16.8700392	0.027	21.076±0.003	···	1.037±0.010	0.689±0.006	0.809±0.010	0.010	1
115	NGVS-UCD115	NGVS-J122133.80+083052.3	l	185.3908515	8.5145406	0.019	21.407±0.004	···	0.880±0.011	0.799±0.008	0.866±0.010	-0.039	1
116	NGVS-UCD116	NGVS-J122138.78+154442.4	s	185.4115935	15.7450999	0.022	18.612±0.005	15.509±0.020	···	···	1.017±0.015	0.348	0
117	NGVS-UCD117	NGVS-J122140.43+113036.7	l	185.4184395	11.5102054	0.033	19.751±0.002	17.963±0.153	-0.042±0.005	-0.229±0.007	-0.233±0.010	0.319	0
118	NGVS-UCD118	NGVS-J122142.55+131644.2	l	185.4273021	13.2789532	0.054	21.074±0.003	···	0.922±0.010	0.593±0.007	0.648±0.009	0.023	1
119	NGVS-UCD119	NGVS-J122154.64+102242.9	l	185.4776538	10.3785814	0.027	20.843±0.003	17.901±0.148	1.007±0.009	0.756±0.006	0.882±0.009	-0.064	1
120	NGVS-UCD120	NGVS-J122157.93+125150.6	l	185.4913596	12.8640649	0.046	21.308±0.004	···	0.979±0.012	0.709±0.007	0.799±0.010	0.034	1
121	NGVS-UCD121	NGVS-J122203.29+114405.8	l	185.5136877	11.7349457	0.029	21.202±0.003	18.641±0.262	0.955±0.011	0.584±0.008	0.821±0.009	0.004	0
122	NGVS-UCD122	NGVS-J122204.09+075110.6	l	185.5170539	7.8529556	0.023	21.170±0.003	···	1.084±0.011	0.754±0.007	0.904±0.009	0.006	0
123	NGVS-UCD123	NGVS-J122209.22+121733.8	l	185.5384008	12.2927339	0.032	21.361±0.004	18.302±0.196	1.111±0.012	0.800±0.008	0.998±0.010	-0.027	1
124	NGVS-UCD124	NGVS-J122223.51+104243.8	l	185.5979422	10.7121663	0.039	21.177±0.003	18.499±0.251	0.856±0.009	0.731±0.006	0.802±0.009	0.087	1
125	NGVS-UCD125	NGVS-J122223.59+125302.5	l	185.5982830	12.8840360	0.042	21.224±0.003	18.360±0.195	0.957±0.011	0.810±0.006	0.893±0.009	0.018	1
126	NGVS-UCD126	NGVS-J122232.39+075258.3	l	185.6349460	7.8828713	0.023	21.327±0.004	···	0.880±0.012	0.594±0.009	0.694±0.012	0.016	1
127	NGVS-UCD127	NGVS-J122233.94+093452.9	l	185.6414199	9.5813501	0.023	21.065±0.003	···	0.889±0.009	0.533±0.007	0.647±0.010	0.054	1
128	NGVS-UCD128	NGVS-J122235.90+120929.1	l	185.6495859	12.1580775	0.028	19.423±0.001	···	0.392±0.003	-0.711±0.005	-0.739±0.007	-0.315	0
129	NGVS-UCD129	NGVS-J122236.43+054014.6	l	185.6517932	5.6707207	0.021	21.225±0.003	···	0.871±0.013	0.629±0.007	0.653±0.011	0.024	1
130	NGVS-UCD130	NGVS-J122236.72+135024.6	l	185.6530161	13.8401630	0.047	21.271±0.003	···	0.906±0.010	0.703±0.007	0.814±0.009	0.016	1
131	NGVS-UCD131	NGVS-J122238.45+104832.2	l	185.6602274	10.8089420	0.041	21.357±0.006	···	0.873±0.014	0.677±0.012	0.853±0.012	-0.044	0
132	NGVS-UCD132	NGVS-J122239.73+164241.2	l	185.6655317	16.7114454	0.024	21.373±0.005	···	0.995±0.014	0.834±0.008	0.868±0.014	0.015	1
133	NGVS-UCD133	NGVS-J122239.74+164245.8	l	185.6655818	16.7127148	0.024	21.294±0.004	···	0.929±0.013	0.693±0.008	0.706±0.014	-0.021	1
134	NGVS-UCD134	NGVS-J122241.18+094601.4	l	185.6715994	9.7670692	0.022	21.172±0.003	18.444±0.248	1.125±0.010	0.686±0.006	0.794±0.008	0.032	0
135	NGVS-UCD135	NGVS-J122241.45+045101.7	l	185.6727056	4.8504755	0.019	19.554±0.002	16.785±0.047	1.358±0.006	0.992±0.004	1.220±0.004	-0.001	0
136	NGVS-UCD136	NGVS-J122241.69+045040.9	l	185.6736913	4.8447005	0.019	20.510±0.004	17.761±0.114	1.273±0.011	0.901±0.007	1.121±0.008	-0.018	0
137	NGVS-UCD137	NGVS-J122253.83+155026.5	l	185.7242841	15.8406947	0.026	20.186±0.002	17.658±0.161	0.159±0.004	0.061±0.005	0.007±0.007	-0.927	0
138	NGVS-UCD138	NGVS-J122255.75+082106.5	l	185.7322722	8.3518064	0.024	21.122±0.003	···	1.005±0.011	0.562±0.008	0.646±0.012	0.073	1
139	NGVS-UCD139	NGVS-J122301.72+131023.9	l	185.7571618	13.1733051	0.053	20.461±0.002	17.664±0.118	1.160±0.006	0.829±0.004	0.940±0.004	0.004	1
140	NGVS-UCD140	NGVS-J122304.28+162649.1	l	185.7678140	16.4469710	0.025	21.063±0.003	···	0.915±0.010	0.712±0.006	0.765±0.009	0.059	1
141	NGVS-UCD141	NGVS-J122304.74+120056.4	l	185.7697328	12.0156623	0.027	21.401±0.004	···	1.199±0.012	0.797±0.009	0.892±0.010	0.087	0
142	NGVS-UCD142	NGVS-J122309.78+080934.9	l	185.7907680	8.1597032	0.022	21.364±0.004	···	0.905±0.011	0.669±0.007	0.718±0.012	0.045	1

Table 3 *continued*

Table 3 *(continued)*

ID	Name	NGVSID	$t_{\rm obs}$	$\alpha_{\rm J2000}$ (deg)	$\delta_{\rm J2000}$ (deg)	$E(B-V)$ (mag)	g_0 (mag)	K (mag)	$(u^*-g)_0$ (mag)	$(g-i)_0$ (mag)	$(g-z)_0$ (mag)	$\Delta_{\rm env}$ (mag)	UCD
(1)	(2)	(3)	(4)	(5)	(6)	(7)	(8)	(9)	(10)	(11)	(12)	(13)	(14)
143	NGVS-UCD143	NGVS-J122314.63+153418.2	l	185.8109770	15.5717173	0.027	21.190±0.003	···	0.988±0.012	0.625±0.008	0.771±0.013	-0.004	0
144	NGVS-UCD144	NGVS-J122316.20+092856.2	l	185.8174870	9.4822691	0.023	21.436±0.004	···	1.067±0.014	0.628±0.008	0.700±0.013	0.105	0
145	NGVS-UCD145	NGVS-J122319.26+162429.8	l	185.8302609	16.4082824	0.024	20.461±0.002	···	0.974±0.007	0.832±0.005	0.934±0.006	0.137	1
146	NGVS-UCD146	NGVS-J122321.78+155148.8	l	185.8407522	15.8635691	0.026	21.489±0.004	···	0.927±0.011	0.678±0.008	0.758±0.011	-0.052	0
147	NGVS-UCD147	NGVS-J122322.70+074845.6	l	185.8445888	7.8126600	0.022	19.699±0.001	15.832±0.024	1.732±0.006	1.188±0.002	1.472±0.002	0.052	1
148	NGVS-UCD148	NGVS-J122325.51+164122.2	l	185.8562741	16.6895074	0.026	20.457±0.002	···	0.912±0.007	0.773±0.004	0.876±0.005	0.031	1
149	NGVS-UCD149	NGVS-J122326.14+164734.1	l	185.8589213	16.7928003	0.026	21.219±0.003	···	1.005±0.012	0.628±0.007	0.704±0.011	0.057	0
150	NGVS-UCD150	NGVS-J122327.96+053326.7	l	185.8664995	5.5574151	0.021	21.212±0.003	···	0.855±0.011	0.678±0.007	0.734±0.009	-0.013	1
151	NGVS-UCD151	NGVS-J122334.06+131758.7	l	185.8919200	13.2996310	0.069	19.324±0.001	16.893±0.059	1.079±0.003	0.757±0.002	0.842±0.002	0.113	0
152	NGVS-UCD152	NGVS-J122334.39+070459.6	l	185.8932997	7.0832356	0.020	20.370±0.002	18.040±0.156	1.050±0.006	0.745±0.003	0.828±0.005	0.023	1
153	NGVS-UCD153	NGVS-J122337.43+131142.4	s	185.9059444	13.1951196	0.059	17.573±0.003	14.105±0.006	1.686±0.014	1.114±0.007	1.481±0.009	0.287	0
154	NGVS-UCD154	NGVS-J122337.86+144837.4	l	185.9077367	14.8103916	0.036	21.376±0.004	···	0.938±0.012	0.686±0.008	0.804±0.010	-0.025	1
155	NGVS-UCD155	NGVS-J122340.97+132539.7	l	185.9207231	13.4276881	0.052	21.307±0.004	···	0.980±0.010	0.569±0.009	0.631±0.010	0.015	1
156	NGVS-UCD156	NGVS-J122343.32+070629.0	l	185.9304975	7.1080530	0.021	21.450±0.004	···	0.988±0.013	0.691±0.007	0.791±0.013	0.088	1
157	NGVS-UCD157	NGVS-J122343.76+171354.2	l	185.9323262	17.2317242	0.025	21.053±0.003	···	0.868±0.009	0.778±0.005	0.810±0.008	0.005	1
158	NGVS-UCD158	NGVS-J122347.90+131036.7	l	185.9495936	13.1768626	0.053	21.072±0.003	···	1.096±0.011	0.650±0.007	0.732±0.009	0.053	0
159	NGVS-UCD159	NGVS-J122350.93+170553.3	l	185.9622174	17.0981407	0.027	21.467±0.004	···	0.906±0.013	0.718±0.008	0.712±0.013	-0.053	1
160	NGVS-UCD160	NGVS-J122352.64+135256.8	l	185.9693435	13.8824373	0.038	19.608±0.001	17.068±0.063	1.032±0.004	0.801±0.002	0.890±0.003	0.107	0
161	NGVS-UCD161	NGVS-J122352.70+071022.2	l	185.9695937	7.1728207	0.022	20.218±0.002	16.896±0.055	1.349±0.008	1.067±0.003	1.208±0.005	-0.025	1
162	NGVS-UCD162	NGVS-J122354.08+070457.0	l	185.9753180	7.0824915	0.022	21.185±0.003	···	1.182±0.012	0.838±0.006	0.948±0.009	-0.007	1
163	NGVS-UCD163	NGVS-J122359.08+164107.8	l	185.9961587	16.6854967	0.028	19.244±0.001	···	1.377±0.004	0.927±0.002	1.064±0.002	0.042	1
164	NGVS-UCD164	NGVS-J122406.15+160901.7	l	186.0256305	16.1504824	0.024	20.619±0.002	···	0.978±0.006	0.771±0.004	0.810±0.005	-0.032	1
165	NGVS-UCD165	NGVS-J122416.65+130029.0	l	186.0693841	13.0080615	0.042	21.339±0.003	···	0.897±0.010	0.706±0.007	0.755±0.010	0.039	1
166	NGVS-UCD166	NGVS-J122420.65+160602.5	l	186.0860279	16.1006945	0.024	21.011±0.003	···	1.034±0.008	0.775±0.005	0.888±0.007	0.030	1
167	NGVS-UCD167	NGVS-J122420.77+071841.7	l	186.0865524	7.3115896	0.021	20.048±0.002	16.938±0.061	1.392±0.006	0.938±0.003	1.085±0.004	-0.035	1
168	NGVS-UCD168	NGVS-J122424.28+071338.4	l	186.1011620	7.2273258	0.020	21.221±0.003	···	0.974±0.011	0.605±0.007	0.652±0.012	0.067	1
169	NGVS-UCD169	NGVS-J122437.09+134447.5	l	186.1545428	13.7465303	0.040	20.269±0.002	17.742±0.120	0.863±0.006	0.653±0.004	0.778±0.005	0.091	0
170	NGVS-UCD170	NGVS-J122443.34+111225.3	l	186.1805789	11.2070316	0.029	21.415±0.004	···	1.002±0.012	0.815±0.007	0.879±0.010	-0.041	1
171	NGVS-UCD171	NGVS-J122443.85+053746.7	l	186.1827187	5.6296297	0.021	19.097±0.001	15.513±0.015	1.390±0.004	1.348±0.002	1.661±0.002	-0.006	1
172	NGVS-UCD172	NGVS-J122444.30+123447.4	l	186.1846024	12.5798396	0.037	21.318±0.003	···	0.911±0.010	0.753±0.007	0.811±0.009	0.005	0
173	NGVS-UCD173	NGVS-J122444.75+150214.6	l	186.1864577	15.0373829	0.024	21.250±0.003	···	0.963±0.011	0.584±0.007	0.662±0.010	0.056	1
174	NGVS-UCD174	NGVS-J122445.71+162152.3	l	186.1904666	16.3645379	0.026	19.917±0.001	···	1.064±0.005	0.797±0.003	0.900±0.004	0.038	0
175	NGVS-UCD175	NGVS-J122446.23+122030.4	l	186.1926404	12.3417837	0.036	20.427±0.002	18.198±0.177	0.933±0.005	0.713±0.004	0.780±0.004	-0.034	1
176	NGVS-UCD176	NGVS-J122449.57+064534.5	s	186.2065257	6.7595961	0.027	18.714±0.005	15.727±0.019	···	0.745±0.012	0.913±0.013	0.395	0
177	NGVS-UCD177	NGVS-J122452.42+101200.0	l	186.2184031	10.2000073	0.026	21.368±0.004	···	0.942±0.011	0.582±0.008	0.665±0.011	0.014	1
178	NGVS-UCD178	NGVS-J122456.48+114309.6	l	186.2353418	11.7193458	0.036	21.070±0.003	···	0.931±0.009	0.680±0.007	0.671±0.009	0.064	0
179	NGVS-UCD179	NGVS-J122456.59+140008.4	l	186.2358097	14.0023324	0.042	21.318±0.003	···	0.913±0.010	0.725±0.007	0.824±0.009	0.015	1
180	NGVS-UCD180	NGVS-J122458.08+125342.2	l	186.2419985	12.8950443	0.041	20.885±0.003	18.262±0.223	1.207±0.010	0.861±0.005	0.983±0.007	-0.030	1
181	NGVS-UCD181	NGVS-J122459.42+104615.5	s	186.2475917	10.7709757	0.034	18.594±0.005	15.004±0.011	1.642±0.020	1.140±0.010	1.422±0.011	0.104	0
182	NGVS-UCD182	NGVS-J122503.27+092223.0	s	186.2636097	9.3730672	0.023	16.596±0.002	13.292±0.003	1.558±0.007	···	1.328±0.004	0.395	0
183	NGVS-UCD183	NGVS-J122516.37+073305.7	l	186.3182266	7.5515925	0.024	21.172±0.003	···	1.045±0.010	0.680±0.007	0.771±0.010	-0.014	1
184	NGVS-UCD184	NGVS-J122517.15+103000.8	l	186.3214418	10.5002175	0.031	21.238±0.003	···	0.947±0.009	0.673±0.007	0.716±0.009	0.019	1
185	NGVS-UCD185	NGVS-J122520.37+124244.9	l	186.3348603	12.7124795	0.037	21.038±0.004	···	0.869±0.011	0.712±0.008	0.809±0.009	0.034	1
186	NGVS-UCD186	NGVS-J122528.65+101828.3	l	186.3693718	10.3078580	0.030	21.481±0.004	···	0.986±0.012	0.642±0.009	0.732±0.011	-0.028	1
187	NGVS-UCD187	NGVS-J122529.17+171214.0	l	186.3715497	17.2038785	0.027	21.267±0.003	···	0.891±0.011	0.642±0.007	0.647±0.011	0.076	1
188	NGVS-UCD188	NGVS-J122531.18+130136.8	l	186.3799080	13.0268844	0.032	20.375±0.002	17.835±0.123	1.082±0.006	0.814±0.004	0.910±0.005	0.032	1
189	NGVS-UCD189	NGVS-J122532.82+113656.6	l	186.3867590	11.6157104	0.033	21.277±0.004	···	0.851±0.010	0.607±0.009	0.661±0.012	0.014	1
190	NGVS-UCD190	NGVS-J122537.48+124954.7	l	186.4061852	12.8318508	0.034	19.889±0.001	17.345±0.086	1.045±0.004	0.749±0.002	0.785±0.003	0.072	1

Table 3 *continued*

Table 3 *(continued)*

ID	Name	NGVSID	t_{obs}	α_{J2000}	δ_{J2000}	$E(B-V)$	g_0	K	$(u^*-g)_0$	$(g-i)_0$	$(g-z)_0$	Δ_{env}	UCD
				(deg)	(deg)	(mag)	(mag)	(mag)	(mag)	(mag)	(mag)	(mag)	
(1)	(2)	(3)	(4)	(5)	(6)	(7)	(8)	(9)	(10)	(11)	(12)	(13)	(14)
191	NGVS-UCD191	NGVS-J122538.30+125441.2	l	186.4095729	12.9114374	0.031	19.745±0.001	17.327±0.084	0.978±0.004	0.718±0.002	0.765±0.003	0.046	1
192	NGVS-UCD192	NGVS-J122544.05+124922.8	l	186.4335521	12.8229942	0.032	19.876±0.001	17.817±0.133	0.978±0.004	0.721±0.003	0.746±0.003	0.025	1
193	NGVS-UCD193	NGVS-J122544.68+130011.3	l	186.4361641	13.0031515	0.030	20.560±0.002	···	1.134±0.006	0.843±0.004	0.943±0.004	0.019	1
194	NGVS-UCD194	NGVS-J122549.94+084645.9	l	186.4580934	8.7794166	0.020	20.667±0.002	18.604±0.230	0.872±0.007	0.584±0.005	0.641±0.007	0.047	1
195	NGVS-UCD195	NGVS-J122554.23+054831.9	l	186.4759467	5.8088584	0.023	20.882±0.002	18.475±0.225	0.987±0.008	0.632±0.005	0.674±0.007	0.047	1
196	NGVS-UCD196	NGVS-J122554.43+103536.6	l	186.4767721	10.5934888	0.032	21.309±0.004	···	0.899±0.009	0.633±0.007	0.663±0.010	-0.034	1
197	NGVS-UCD197	NGVS-J122555.28+072329.9	l	186.4803246	7.3916381	0.025	21.264±0.003	···	1.038±0.012	0.770±0.006	0.910±0.010	-0.014	1
198	NGVS-UCD198	NGVS-J122556.22+131305.8	l	186.4842522	13.2182872	0.029	21.467±0.006	···	0.927±0.013	0.607±0.015	0.684±0.013	0.012	1
199	NGVS-UCD199	NGVS-J122556.47+130402.3	l	186.4852943	13.0672926	0.029	20.247±0.002	17.827±0.136	0.929±0.005	0.683±0.004	0.779±0.004	0.040	1
200	NGVS-UCD200	NGVS-J122557.92+100313.6	s	186.4913400	10.0537714	0.024	18.296±0.004	15.215±0.012	1.184±0.014	0.830±0.009	1.022±0.011	0.340	0
201	NGVS-UCD201	NGVS-J122600.38+054353.9	l	186.5015758	5.7316325	0.021	21.312±0.003	···	0.887±0.010	0.604±0.007	0.667±0.009	-0.001	1
202	NGVS-UCD202	NGVS-J122601.04+124915.4	l	186.5043390	12.8209509	0.030	21.388±0.004	···	0.992±0.011	0.698±0.007	0.785±0.009	-0.010	1
203	NGVS-UCD203	NGVS-J122603.82+151958.2	l	186.5159283	15.3328445	0.021	19.602±0.001	17.536±0.119	1.006±0.003	0.693±0.002	0.743±0.003	-0.037	0
204	NGVS-UCD204	NGVS-J122606.70+125139.3	l	186.5279324	12.8609296	0.029	19.306±0.001	16.609±0.042	1.095±0.004	0.794±0.002	0.927±0.003	0.293	0
205	NGVS-UCD205	NGVS-J122608.22+130121.4	l	186.5342596	13.0226076	0.029	20.360±0.002	18.138±0.180	0.944±0.004	0.720±0.003	0.755±0.004	-0.007	1
206	NGVS-UCD206	NGVS-J122610.07+125835.8	l	186.5419664	12.9766181	0.030	20.937±0.003	···	1.096±0.009	0.826±0.005	0.875±0.007	-0.054	1
207	NGVS-UCD207	NGVS-J122613.11+130643.2	l	186.5546323	13.1120099	0.029	20.106±0.001	···	0.887±0.004	0.693±0.003	0.747±0.004	0.300	1
208	NGVS-UCD208	NGVS-J122613.71+055421.7	l	186.5571068	5.9060183	0.020	20.524±0.002	18.159±0.163	0.879±0.006	0.540±0.004	0.638±0.007	0.041	1
209	NGVS-UCD209	NGVS-J122615.85+051127.0	l	186.5660400	5.1908274	0.018	21.144±0.003	···	0.908±0.010	0.654±0.006	0.763±0.008	0.029	1
210	NGVS-UCD210	NGVS-J122616.52+051747.7	l	186.5688168	5.2965786	0.018	21.206±0.003	···	1.018±0.011	0.690±0.006	0.837±0.008	0.031	1
211	NGVS-UCD211	NGVS-J122622.12+082429.6	l	186.5921473	8.4082311	0.022	21.099±0.003	18.398±0.209	0.905±0.009	0.701±0.006	0.802±0.009	-0.013	1
212	NGVS-UCD212	NGVS-J122624.79+141209.8	l	186.6032978	14.2027255	0.047	21.332±0.004	···	0.889±0.011	0.735±0.008	0.858±0.009	0.030	1
213	NGVS-UCD213	NGVS-J122624.94+103454.7	l	186.6039312	10.5818717	0.034	19.143±0.001	16.782±0.052	1.053±0.003	0.719±0.002	0.846±0.002	0.110	0
214	NGVS-UCD214	NGVS-J122628.28+171525.6	l	186.6178416	17.2571016	0.030	19.373±0.001	···	1.170±0.005	0.866±0.003	0.984±0.004	0.135	0
215	NGVS-UCD215	NGVS-J122628.69+125642.6	l	186.6195422	12.9451731	0.029	19.588±0.001	16.728±0.049	1.276±0.004	0.875±0.002	1.065±0.003	0.085	1
216	NGVS-UCD216	NGVS-J122630.57+121159.8	l	186.6273933	12.1999470	0.028	20.934±0.002	18.594±0.244	1.010±0.008	0.662±0.005	0.774±0.009	0.049	1
217	NGVS-UCD217	NGVS-J122633.05+123847.6	l	186.6377232	12.6465448	0.032	21.201±0.003	···	0.964±0.008	0.683±0.006	0.742±0.009	-0.001	1
218	NGVS-UCD218	NGVS-J122636.42+125512.9	l	186.6517649	12.9202432	0.028	18.846±0.001	15.939±0.023	1.318±0.002	0.900±0.001	1.093±0.002	0.008	1
219	NGVS-UCD219	NGVS-J122638.52+123702.7	l	186.6604828	12.6174078	0.032	20.452±0.002	18.338±0.194	1.008±0.005	0.697±0.004	0.760±0.005	0.018	1
220	NGVS-UCD220	NGVS-J122638.79+124545.8	l	186.6616379	12.7627091	0.030	20.409±0.002	17.986±0.142	0.996±0.005	0.700±0.004	0.818±0.005	0.023	1
221	NGVS-UCD221	NGVS-J122640.85+154555.0	l	186.6702257	15.7652708	0.026	20.131±0.002	16.356±0.046	1.644±0.006	1.152±0.003	1.399±0.003	0.054	0
222	NGVS-UCD222	NGVS-J122643.32+121743.9	l	186.6804830	12.2955235	0.027	20.654±0.002	18.229±0.167	0.933±0.007	0.692±0.004	0.855±0.007	0.092	0
223	NGVS-UCD223	NGVS-J122646.48+131732.2	l	186.6936702	13.2922909	0.027	21.295±0.003	···	0.903±0.008	0.683±0.006	0.732±0.009	0.009	0
224	NGVS-UCD224	NGVS-J122650.24+161618.3	s	186.7093386	16.2717391	0.025	16.631±0.002	···	1.424±0.007	0.895±0.004	1.205±0.005	0.339	0
225	NGVS-UCD225	NGVS-J122650.55+131914.1	l	186.7106063	13.3205733	0.026	21.350±0.003	···	0.981±0.009	0.711±0.007	0.793±0.010	0.011	1
226	NGVS-UCD226	NGVS-J122651.24+131058.5	l	186.7134865	13.1829051	0.028	19.873±0.001	···	0.078±0.004	-0.607±0.008	-0.568±0.014	0.185	0
227	NGVS-UCD227	NGVS-J122654.57+150309.6	l	186.7273593	15.0526728	0.033	20.029±0.002	···	0.102±0.004	-0.106±0.006	-0.144±0.009	-2.105	0
228	NGVS-UCD228	NGVS-J122654.62+170205.2	l	186.7275653	17.0347741	0.026	20.993±0.003	···	1.046±0.011	0.627±0.006	0.725±0.011	-0.028	1
229	NGVS-UCD229	NGVS-J122654.72+084129.9	l	186.7279848	8.6916361	0.019	21.288±0.003	···	0.927±0.012	0.596±0.008	0.691±0.011	0.008	1
230	NGVS-UCD230	NGVS-J122654.77+112431.2	l	186.7281979	11.4086551	0.037	21.321±0.004	···	1.003±0.011	0.737±0.007	0.856±0.008	-0.037	1
231	NGVS-UCD231	NGVS-J122656.56+123532.2	l	186.7356523	12.5922703	0.031	19.690±0.001	17.183±0.068	1.085±0.003	0.798±0.002	0.930±0.003	0.082	1
232	NGVS-UCD232	NGVS-J122703.08+123338.4	l	186.7628427	12.5606589	0.030	19.706±0.001	16.792±0.048	1.041±0.005	0.760±0.003	0.988±0.004	0.432	0
233	NGVS-UCD233	NGVS-J122705.40+151750.6	l	186.7724863	15.2973929	0.025	21.492±0.004	···	1.023±0.013	0.716±0.008	0.811±0.011	-0.016	1
234	NGVS-UCD234	NGVS-J122713.93+124021.2	l	186.8080543	12.6725514	0.030	20.227±0.002	17.639±0.101	0.992±0.005	0.678±0.004	0.830±0.005	0.093	1
235	NGVS-UCD235	NGVS-J122715.62+123207.1	l	186.8150697	12.5353191	0.028	20.440±0.002	18.155±0.164	0.871±0.005	0.502±0.004	0.657±0.006	0.057	1
236	NGVS-UCD236	NGVS-J122722.87+123259.1	l	186.8453030	12.5497623	0.028	20.558±0.002	17.786±0.117	1.151±0.006	0.815±0.004	0.964±0.005	0.030	1
237	NGVS-UCD237	NGVS-J122725.51+160949.2	l	186.8562983	16.1636647	0.024	20.469±0.002	···	0.855±0.005	0.590±0.004	0.674±0.005	0.121	1
238	NGVS-UCD238	NGVS-J122725.58+085002.1	l	186.8565918	8.8339101	0.024	20.511±0.002	16.847±0.054	1.640±0.009	1.127±0.003	1.442±0.004	0.018	1

Table 3 *continued*

Table 3 *(continued)*

ID	Name	NGVSID	$t_{\rm obs}$	$\alpha_{\rm J2000}$	$\delta_{\rm J2000}$	$E(B-V)$	g_0	K	$(u^*-g)_0$	$(g-i)_0$	$(g-z)_0$	$\Delta_{\rm env}$	UCD
				(deg)	(deg)	(mag)	(mag)	(mag)	(mag)	(mag)	(mag)	(mag)	
(1)	(2)	(3)	(4)	(5)	(6)	(7)	(8)	(9)	(10)	(11)	(12)	(13)	(14)
239	NGVS-UCD239	NGVS-J122725.97+155953.2	l	186.8582092	15.9981161	0.030	21.403±0.004	···	0.974±0.011	0.788±0.007	0.915±0.010	0.022	1
240	NGVS-UCD240	NGVS-J122727.19+125546.0	l	186.8632849	12.9294425	0.028	20.908±0.002	···	0.923±0.006	0.670±0.005	0.739±0.007	-0.014	1
241	NGVS-UCD241	NGVS-J122727.56+163929.6	l	186.8648136	16.6582171	0.022	20.667±0.002	···	0.879±0.007	0.768±0.004	0.837±0.007	0.024	0
242	NGVS-UCD242	NGVS-J122732.01+162232.8	l	186.8833828	16.3757873	0.023	21.383±0.004	···	0.998±0.015	0.711±0.009	0.805±0.013	-0.046	1
243	NGVS-UCD243	NGVS-J122737.62+162409.9	l	186.9067305	16.4027577	0.023	21.397±0.004	···	0.851±0.011	0.568±0.007	0.656±0.013	-0.015	1
244	NGVS-UCD244	NGVS-J122744.26+072542.5	l	186.9344272	7.4284640	0.022	20.565±0.002	18.211±0.184	0.948±0.006	0.648±0.004	0.732±0.006	-0.018	1
245	NGVS-UCD245	NGVS-J122745.56+124356.4	l	186.9398404	12.7323293	0.029	21.429±0.003	···	1.050±0.010	0.696±0.007	0.777±0.010	0.005	1
246	NGVS-UCD246	NGVS-J122749.26+152141.7	l	186.9552700	15.3615749	0.027	21.175±0.003	···	0.976±0.009	0.721±0.006	0.766±0.008	0.006	1
247	NGVS-UCD247	NGVS-J122802.11+101019.4	l	187.0088009	10.1720442	0.025	21.039±0.003	···	0.953±0.010	0.530±0.007	0.659±0.009	0.011	1
248	NGVS-UCD248	NGVS-J122802.90+132556.3	l	187.0120885	13.4323092	0.028	21.468±0.005	···	0.953±0.013	0.666±0.010	0.707±0.016	0.013	1
249	NGVS-UCD249	NGVS-J122803.46+065343.1	l	187.0144136	6.8953085	0.020	21.373±0.004	18.698±0.246	0.969±0.011	0.705±0.007	0.826±0.011	0.020	1
250	NGVS-UCD250	NGVS-J122804.95+133643.2	l	187.0206230	13.6120065	0.032	20.541±0.002	18.161±0.162	1.023±0.008	0.738±0.005	0.810±0.006	0.438	0
251	NGVS-UCD251	NGVS-J122804.99+133441.0	l	187.0208051	13.5780461	0.032	19.725±0.001	17.087±0.061	1.082±0.005	0.764±0.003	0.811±0.003	0.466	0
252	NGVS-UCD252	NGVS-J122806.62+122436.4	l	187.0275984	12.4101112	0.028	20.838±0.002	···	0.967±0.007	0.677±0.005	0.765±0.008	0.032	1
253	NGVS-UCD253	NGVS-J122807.59+110743.0	l	187.0316284	11.1286193	0.034	21.149±0.003	···	0.930±0.010	0.612±0.007	0.654±0.010	0.020	0
254	NGVS-UCD254	NGVS-J122810.61+094132.5	l	187.0442062	9.6923589	0.022	21.441±0.004	···	0.902±0.013	0.590±0.009	0.714±0.011	-0.074	0
255	NGVS-UCD255	NGVS-J122810.85+124333.7	l	187.0452024	12.7260184	0.024	21.334±0.004	···	0.981±0.010	0.680±0.007	0.755±0.012	0.002	0
256	NGVS-UCD256	NGVS-J122812.03+102155.1	l	187.0501411	10.3653090	0.028	20.533±0.002	18.287±0.183	0.965±0.008	0.717±0.005	0.786±0.006	0.087	0
257	NGVS-UCD257	NGVS-J122814.50+085950.3	l	187.0604065	8.9973068	0.019	21.031±0.003	···	0.850±0.009	0.627±0.006	0.769±0.009	0.151	0
258	NGVS-UCD258	NGVS-J122815.12+073316.3	l	187.0629968	7.5545279	0.025	21.208±0.003	···	1.018±0.010	0.573±0.008	0.656±0.011	-0.033	1
259	NGVS-UCD259	NGVS-J122818.74+112751.6	l	187.0780647	11.4643426	0.032	21.444±0.004	···	0.906±0.011	0.632±0.008	0.707±0.010	-0.016	1
260	NGVS-UCD260	NGVS-J122819.41+142454.4	l	187.0808949	14.4151140	0.033	21.001±0.003	18.502±0.223	0.937±0.009	0.650±0.006	0.714±0.008	0.043	1
261	NGVS-UCD261	NGVS-J122823.15+045312.0	l	187.0964715	4.8866652	0.016	21.380±0.003	···	0.986±0.012	0.657±0.007	0.670±0.010	-0.014	1
262	NGVS-UCD262	NGVS-J122823.88+110855.8	l	187.0995043	11.1488368	0.034	21.428±0.004	···	0.907±0.011	0.624±0.008	0.686±0.011	-0.017	1
263	NGVS-UCD263	NGVS-J122823.99+130725.6	l	187.0999431	13.1237853	0.023	20.351±0.002	17.968±0.144	1.050±0.005	0.715±0.004	0.809±0.005	0.048	1
264	NGVS-UCD264	NGVS-J122828.04+061828.9	l	187.1168536	6.3080382	0.016	21.218±0.003	···	0.886±0.011	0.724±0.006	0.762±0.012	0.029	1
265	NGVS-UCD265	NGVS-J122831.77+162814.6	l	187.1323807	16.4707183	0.027	20.495±0.002	···	0.856±0.007	0.772±0.004	0.820±0.006	0.002	0
266	NGVS-UCD266	NGVS-J122834.04+163419.1	l	187.1418225	16.5719590	0.027	20.965±0.003	···	0.993±0.009	0.781±0.005	0.853±0.009	-0.016	1
267	NGVS-UCD267	NGVS-J122835.88+080554.6	l	187.1494857	8.0985001	0.021	21.162±0.003	···	1.009±0.010	0.612±0.006	0.743±0.011	0.013	1
268	NGVS-UCD268	NGVS-J122837.21+122845.6	l	187.1550543	12.4793259	0.024	20.937±0.003	···	1.013±0.008	0.725±0.005	0.888±0.008	0.009	1
269	NGVS-UCD269	NGVS-J122844.78+072457.5	l	187.1865987	7.4159702	0.023	20.132±0.001	17.616±0.102	1.078±0.005	0.784±0.003	0.945±0.004	-0.022	1
270	NGVS-UCD270	NGVS-J122849.72+140927.2	l	187.2071836	14.1575645	0.046	21.385±0.005	···	0.971±0.015	0.743±0.010	0.875±0.012	0.149	0
271	NGVS-UCD271	NGVS-J122854.59+090149.2	l	187.2274546	9.0303355	0.019	21.332±0.003	···	0.873±0.010	0.621±0.007	0.662±0.012	-0.008	0
272	NGVS-UCD272	NGVS-J122855.03+132532.2	l	187.2293003	13.4256062	0.026	19.860±0.001	17.564±0.093	1.094±0.004	0.730±0.003	0.892±0.003	0.033	1
273	NGVS-UCD273	NGVS-J122856.78+113648.5	l	187.2365947	11.6134746	0.031	20.090±0.001	17.541±0.126	1.032±0.004	0.727±0.003	0.866±0.004	0.061	1
274	NGVS-UCD274	NGVS-J122856.90+130220.5	l	187.2370684	13.0390245	0.022	21.267±0.004	···	0.930±0.010	0.691±0.008	0.811±0.012	0.091	1
275	NGVS-UCD275	NGVS-J122857.39+155527.5	l	187.2391391	15.9242954	0.033	21.336±0.004	···	0.860±0.010	0.632±0.008	0.689±0.011	-0.029	1
276	NGVS-UCD276	NGVS-J122857.56+131430.9	s	187.2398539	13.2419121	0.023	15.353±0.001	12.124±0.002	1.487±0.005	1.012±0.002	1.295±0.003	0.341	0
277	NGVS-UCD277	NGVS-J122857.99+083513.8	l	187.2416238	8.5871653	0.021	18.735±0.001	15.307±0.013	1.460±0.003	1.039±0.001	1.280±0.001	0.130	0
278	NGVS-UCD278	NGVS-J122858.13+123942.2	s	187.2422263	12.6617226	0.021	17.498±0.003	14.203±0.006	1.509±0.016	1.066±0.008	1.367±0.011	0.414	0
279	NGVS-UCD279	NGVS-J122903.04+164145.1	l	187.2626545	16.6958478	0.026	19.989±0.001	···	0.944±0.005	0.738±0.003	0.842±0.004	0.019	1
280	NGVS-UCD280	NGVS-J122907.68+114746.9	l	187.2819939	11.7963574	0.028	19.885±0.001	17.482±0.082	0.987±0.004	0.713±0.002	0.870±0.003	0.033	1
281	NGVS-UCD281	NGVS-J122910.66+124304.1	l	187.2944300	12.7178096	0.022	20.805±0.002	18.337±0.206	1.100±0.008	0.782±0.004	0.860±0.008	0.011	1
282	NGVS-UCD282	NGVS-J122911.27+075749.5	l	187.2969534	7.9637561	0.023	20.878±0.003	18.286±0.200	1.025±0.009	0.687±0.005	0.699±0.009	-0.046	1
283	NGVS-UCD283	NGVS-J122912.09+123922.1	l	187.3003838	12.6561261	0.021	20.119±0.001	17.321±0.081	1.018±0.004	0.720±0.003	0.850±0.004	0.029	1
284	NGVS-UCD284	NGVS-J122913.39+094505.7	l	187.3057709	9.7515760	0.023	21.003±0.003	···	0.908±0.009	0.575±0.006	0.702±0.008	0.028	1
285	NGVS-UCD285	NGVS-J122914.87+115343.8	l	187.3119508	11.8955015	0.027	20.091±0.001	17.675±0.100	0.998±0.004	0.754±0.003	0.873±0.004	0.072	1
286	NGVS-UCD286	NGVS-J122915.84+170309.2	l	187.3159889	17.0525660	0.027	20.726±0.002	···	1.072±0.008	0.678±0.004	0.774±0.007	0.084	1

Table 3 *continued*

Table 3 *(continued)*

ID	Name	NGVSID	t_{obs}	α_{J2000}	δ_{J2000}	$E(B-V)$	g_0	K	$(u^*-g)_0$	$(g-i)_0$	$(g-z)_0$	Δ_{env}	UCD
				(deg)	(deg)	(mag)	(mag)	(mag)	(mag)	(mag)	(mag)	(mag)	
(1)	(2)	(3)	(4)	(5)	(6)	(7)	(8)	(9)	(10)	(11)	(12)	(13)	(14)
287	NGVS-UCD287	NGVS-J122917.81+115622.3	l	187.3242257	11.9395175	0.027	20.481±0.002	18.339±0.181	1.003±0.006	0.723±0.003	0.846±0.005	0.063	1
288	NGVS-UCD288	NGVS-J122918.59+163039.9	l	187.3274455	16.5110854	0.027	20.845±0.004	···	0.908±0.009	0.716±0.007	0.875±0.010	-0.040	1
289	NGVS-UCD289	NGVS-J122919.42+075557.6	l	187.3309103	7.9326532	0.023	21.420±0.004	···	1.135±0.015	0.856±0.007	0.978±0.012	0.046	1
290	NGVS-UCD290	NGVS-J122920.48+124338.0	l	187.3353139	12.7272334	0.022	19.759±0.001	16.915±0.056	1.209±0.004	0.887±0.002	1.041±0.003	-0.009	1
291	NGVS-UCD291	NGVS-J122920.83+133317.1	l	187.3367807	13.5547477	0.028	21.307±0.003	···	0.859±0.009	0.683±0.008	0.732±0.009	-0.027	1
292	NGVS-UCD292	NGVS-J122922.00+144143.1	l	187.3416875	14.6953053	0.036	21.130±0.003	···	1.025±0.012	0.637±0.008	0.719±0.010	0.106	1
293	NGVS-UCD293	NGVS-J122922.85+074901.2	l	187.3452098	7.8169941	0.025	20.720±0.002	18.199±0.183	0.999±0.007	0.722±0.004	0.789±0.006	0.034	1
294	NGVS-UCD294	NGVS-J122923.56+122702.2	l	187.3481595	12.4506217	0.023	19.939±0.001	16.844±0.053	1.113±0.009	0.654±0.006	0.835±0.008	0.640	0
295	NGVS-UCD295	NGVS-J122925.10+075407.0	l	187.3545827	7.9019461	0.024	20.144±0.001	17.654±0.110	1.008±0.005	0.724±0.003	0.791±0.004	-0.003	1
296	NGVS-UCD296	NGVS-J122928.21+075355.4	l	187.3675253	7.8987154	0.024	19.772±0.001	17.003±0.061	1.244±0.005	0.880±0.002	0.979±0.003	0.038	1
297	NGVS-UCD297	NGVS-J122928.53+160641.4	l	187.3688658	16.1115076	0.029	20.760±0.002	···	0.863±0.006	0.563±0.005	0.630±0.007	0.028	0
298	NGVS-UCD298	NGVS-J122928.62+075824.6	l	187.3692499	7.9734990	0.023	20.849±0.004	···	1.102±0.012	0.684±0.006	0.771±0.011	-0.021	1
299	NGVS-UCD299	NGVS-J122928.65+160037.4	l	187.3693834	16.0103846	0.029	20.877±0.002	···	0.869±0.007	0.656±0.005	0.695±0.007	0.028	1
300	NGVS-UCD300	NGVS-J122928.68+162938.8	l	187.3694835	16.4941166	0.028	19.246±0.001	···	1.102±0.004	0.810±0.002	1.014±0.003	0.217	0
301	NGVS-UCD301	NGVS-J122930.89+124119.6	l	187.3786961	12.6887865	0.021	20.572±0.002	17.487±0.091	1.496±0.007	0.901±0.004	1.206±0.005	0.000	1
302	NGVS-UCD302	NGVS-J122934.41+080540.9	l	187.3933684	8.0947073	0.022	20.413±0.002	18.247±0.202	0.957±0.006	0.691±0.004	0.758±0.006	0.037	0
303	NGVS-UCD303	NGVS-J122935.00+080328.8	s	187.3958189	8.0579927	0.022	16.900±0.002	13.533±0.004	1.736±0.011	0.921±0.006	1.239±0.006	0.333	0
304	NGVS-UCD304	NGVS-J122936.84+135618.1	l	187.4034859	13.9383641	0.039	21.304±0.003	···	0.963±0.010	0.694±0.007	0.779±0.009	0.020	1
305	NGVS-UCD305	NGVS-J122937.04+130620.9	l	187.4043352	13.1058186	0.022	20.917±0.002	18.490±0.264	0.916±0.006	0.620±0.005	0.700±0.008	0.024	0
306	NGVS-UCD306	NGVS-J122937.87+053357.6	l	187.4077737	5.5659973	0.019	21.461±0.004	···	0.993±0.012	0.656±0.007	0.768±0.010	0.013	1
307	NGVS-UCD307	NGVS-J122937.93+114058.1	l	187.4080249	11.6828049	0.035	21.071±0.003	···	0.948±0.008	0.666±0.005	0.858±0.008	0.012	1
308	NGVS-UCD308	NGVS-J122940.39+122728.1	l	187.4182889	12.4577948	0.023	19.872±0.001	17.296±0.072	1.064±0.004	0.739±0.002	0.805±0.003	0.029	1
309	NGVS-UCD309	NGVS-J122940.69+122930.4	l	187.4195474	12.4917716	0.023	20.834±0.002	17.644±0.099	1.434±0.007	0.939±0.004	1.148±0.006	-0.001	1
310	NGVS-UCD310	NGVS-J122940.95+130630.9	l	187.4206296	13.1085745	0.022	21.040±0.002	···	1.093±0.007	0.763±0.005	0.897±0.007	0.065	1
311	NGVS-UCD311	NGVS-J122941.32+123952.4	l	187.4221824	12.6645656	0.021	20.188±0.002	17.621±0.104	1.134±0.005	0.758±0.004	0.920±0.004	0.043	1
312	NGVS-UCD312	NGVS-J122941.56+124427.6	l	187.4231481	12.7410005	0.022	20.871±0.002	18.045±0.153	1.155±0.007	0.814±0.004	0.965±0.006	-0.016	1
313	NGVS-UCD313	NGVS-J122941.87+123020.6	l	187.4244746	12.5057218	0.023	20.878±0.002	18.161±0.172	1.050±0.006	0.707±0.005	0.844±0.007	0.027	1
314	NGVS-UCD314	NGVS-J122942.41+073444.8	l	187.4266909	7.5791066	0.020	20.232±0.001	17.881±0.124	1.032±0.005	0.734±0.003	0.852±0.004	-0.024	1
315	NGVS-UCD315	NGVS-J122943.11+080349.3	l	187.4296409	8.0636884	0.022	20.469±0.002	···	1.002±0.006	0.704±0.004	0.778±0.006	0.013	1
316	NGVS-UCD316	NGVS-J122943.46+105008.2	l	187.4310662	10.8356032	0.030	21.327±0.004	···	0.970±0.013	0.590±0.009	0.663±0.013	-0.012	1
317	NGVS-UCD317	NGVS-J122945.23+055512.8	l	187.4384408	5.9202303	0.021	20.377±0.002	17.868±0.124	1.021±0.006	0.751±0.003	0.871±0.005	0.154	0
318	NGVS-UCD318	NGVS-J122945.26+125100.9	l	187.4385743	12.8502556	0.020	20.436±0.002	17.987±0.143	1.067±0.005	0.738±0.003	0.851±0.005	0.018	1
319	NGVS-UCD319	NGVS-J122948.37+080042.0	l	187.4515565	8.0116645	0.022	20.658±0.004	···	1.064±0.010	0.773±0.006	0.882±0.009	0.051	1
320	NGVS-UCD320	NGVS-J122949.76+075542.5	l	187.4573302	7.9284789	0.022	20.392±0.002	17.555±0.105	1.011±0.006	0.797±0.004	0.899±0.005	0.009	1
321	NGVS-UCD321	NGVS-J122950.42+075420.7	l	187.4600911	7.9057410	0.023	20.706±0.002	···	1.148±0.007	0.840±0.004	0.957±0.006	0.019	1
322	NGVS-UCD322	NGVS-J122952.28+123737.8	l	187.4678275	12.6271618	0.021	20.727±0.002	17.742±0.116	1.245±0.008	0.841±0.004	1.053±0.006	0.017	1
323	NGVS-UCD323	NGVS-J122952.41+123504.1	l	187.4683729	12.5844673	0.022	19.666±0.001	17.597±0.102	1.027±0.004	0.659±0.003	0.854±0.003	0.082	1
324	NGVS-UCD324	NGVS-J122952.93+075559.5	l	187.4705543	7.9331882	0.022	20.458±0.002	18.049±0.165	0.869±0.007	0.824±0.004	0.976±0.007	0.024	1
325	NGVS-UCD325	NGVS-J122953.16+162615.1	l	187.4715000	16.4375371	0.029	21.437±0.004	···	0.977±0.013	0.765±0.007	0.902±0.012	-0.022	1
326	NGVS-UCD326	NGVS-J122954.60+163214.0	l	187.4775075	16.5372134	0.027	20.921±0.003	···	0.952±0.010	0.568±0.006	0.652±0.011	0.022	0
327	NGVS-UCD327	NGVS-J122954.98+123350.9	l	187.4790919	12.5641274	0.022	20.535±0.002	18.056±0.156	0.968±0.005	0.666±0.004	0.813±0.006	0.046	1
328	NGVS-UCD328	NGVS-J122955.91+075722.8	l	187.4829387	7.9563424	0.022	21.050±0.004	17.685±0.120	1.662±0.018	1.031±0.007	1.305±0.009	-0.025	1
329	NGVS-UCD329	NGVS-J122956.35+131312.1	l	187.4847729	13.2200175	0.024	19.933±0.001	17.739±0.127	0.984±0.004	0.725±0.003	0.773±0.005	0.124	0
330	NGVS-UCD330	NGVS-J122956.65+121931.4	l	187.4860324	12.3253775	0.027	19.899±0.001	17.213±0.067	1.064±0.004	0.787±0.002	0.852±0.003	0.068	1
331	NGVS-UCD331	NGVS-J122957.08+074820.0	l	187.4878332	7.8055582	0.024	19.649±0.001	16.986±0.062	1.013±0.004	0.813±0.002	0.934±0.003	0.009	1
332	NGVS-UCD332	NGVS-J122957.12+123602.9	l	187.4880101	12.6008164	0.022	20.185±0.001	17.882±0.132	0.970±0.004	0.684±0.003	0.821±0.004	-0.008	1
333	NGVS-UCD333	NGVS-J122957.60+075400.4	l	187.4899907	7.9001123	0.023	21.352±0.004	···	0.998±0.011	0.640±0.007	0.767±0.011	0.018	1
334	NGVS-UCD334	NGVS-J122957.80+083608.9	l	187.4908230	8.6024692	0.021	21.093±0.002	18.835±0.287	0.902±0.008	0.566±0.006	0.682±0.009	-0.013	1

Table 3 *continued*

Table 3 *(continued)*

ID	Name	NGVSID	t_{obs}	α_{J2000}	δ_{J2000}	$E(B-V)$	g_0	K	$(u^*-g)_0$	$(g-i)_0$	$(g-z)_0$	Δ_{env}	UCD
				(deg)	(deg)	(mag)	(mag)	(mag)	(mag)	(mag)	(mag)	(mag)	
(1)	(2)	(3)	(4)	(5)	(6)	(7)	(8)	(9)	(10)	(11)	(12)	(13)	(14)
335	NGVS-UCD335	NGVS-J122958.06+080409.2	l	187.4919199	8.0692203	0.022	19.673±0.001	16.843±0.056	1.177±0.004	0.860±0.002	0.994±0.003	-0.039	1
336	NGVS-UCD336	NGVS-J122958.95+075800.8	l	187.4956297	7.9668785	0.022	20.066±0.002	17.826±0.137	1.025±0.006	0.645±0.003	0.656±0.005	-0.009	1
337	NGVS-UCD337	NGVS-J122959.41+105122.5	l	187.4975414	10.8562452	0.028	21.494±0.004	···	0.911±0.013	0.637±0.009	0.676±0.012	0.199	0
338	NGVS-UCD338	NGVS-J122959.81+123812.5	l	187.4991997	12.6368191	0.021	20.613±0.002	17.862±0.129	1.123±0.006	0.814±0.004	1.016±0.005	0.080	1
339	NGVS-UCD339	NGVS-J123000.70+075523.4	l	187.5029155	7.9231588	0.022	20.188±0.001	17.667±0.117	1.075±0.006	0.717±0.003	0.855±0.005	0.117	1
340	NGVS-UCD340	NGVS-J123001.95+124226.9	l	187.5081245	12.7074632	0.022	19.792±0.001	17.559±0.098	0.907±0.005	0.680±0.003	0.702±0.004	0.036	1
341	NGVS-UCD341	NGVS-J123002.46+123633.8	l	187.5102303	12.6093774	0.022	20.127±0.001	17.583±0.101	1.097±0.004	0.754±0.003	0.901±0.004	0.005	1
342	NGVS-UCD342	NGVS-J123002.49+075846.7	l	187.5103664	7.9796416	0.022	20.902±0.003	···	0.984±0.010	0.703±0.006	0.786±0.010	0.009	1
343	NGVS-UCD343	NGVS-J123003.38+055843.4	l	187.5140830	5.9787256	0.020	20.944±0.003	···	1.003±0.009	0.684±0.005	0.794±0.008	-0.011	1
344	NGVS-UCD344	NGVS-J123003.57+140903.0	l	187.5148556	14.1508303	0.040	20.759±0.003	18.216±0.167	0.988±0.009	0.734±0.006	0.859±0.007	0.032	1
345	NGVS-UCD345	NGVS-J123004.05+120714.0	l	187.5168748	12.1205454	0.028	19.635±0.001	17.134±0.064	1.036±0.003	0.755±0.002	0.826±0.003	0.007	1
346	NGVS-UCD346	NGVS-J123004.71+144816.0	l	187.5196108	14.8044318	0.036	21.214±0.003	···	1.101±0.013	0.743±0.007	0.906±0.009	0.072	1
347	NGVS-UCD347	NGVS-J123005.08+080424.0	s	187.5211634	8.0733200	0.022	17.939±0.004	15.078±0.012	1.274±0.013	0.769±0.008	0.952±0.010	0.135	0
348	NGVS-UCD348	NGVS-J123005.27+123516.8	l	187.5219494	12.5880066	0.022	20.603±0.002	18.243±0.185	1.025±0.005	0.697±0.004	0.837±0.005	0.024	1
349	NGVS-UCD349	NGVS-J123005.39+074904.7	l	187.5224421	7.8179623	0.023	20.965±0.002	···	0.999±0.008	0.686±0.005	0.799±0.008	-0.002	1
350	NGVS-UCD350	NGVS-J123005.79+123223.0	l	187.5241083	12.5397227	0.023	19.755±0.001	17.239±0.075	1.051±0.003	0.744±0.002	0.877±0.003	0.021	1
351	NGVS-UCD351	NGVS-J123006.03+074901.2	l	187.5251438	7.8169882	0.023	21.172±0.003	···	0.982±0.009	0.702±0.006	0.831±0.009	0.001	1
352	NGVS-UCD352	NGVS-J123006.06+123954.0	l	187.5252472	12.6649911	0.021	19.402±0.001	16.843±0.052	1.141±0.003	0.758±0.002	0.942±0.002	-0.012	1
353	NGVS-UCD353	NGVS-J123006.13+122435.3	l	187.5255261	12.4098163	0.026	20.499±0.002	17.721±0.108	1.156±0.006	0.810±0.003	0.895±0.005	-0.013	1
354	NGVS-UCD354	NGVS-J123006.49+080844.4	l	187.5270465	8.1456620	0.022	20.033±0.001	17.265±0.074	1.145±0.004	0.839±0.002	0.949±0.003	0.010	1
355	NGVS-UCD355	NGVS-J123006.89+080509.5	l	187.5287169	8.0859729	0.022	20.373±0.002	17.886±0.144	0.979±0.005	0.734±0.003	0.808±0.005	0.015	1
356	NGVS-UCD356	NGVS-J123007.05+151838.1	s	187.5293779	15.3105829	0.032	18.153±0.003	15.482±0.019	···	1.012±0.007	1.208±0.009	-0.038	0
357	NGVS-UCD357	NGVS-J123007.57+123631.0	l	187.5315560	12.6086085	0.022	18.978±0.001	16.270±0.031	1.185±0.002	0.809±0.001	0.979±0.002	0.005	1
358	NGVS-UCD358	NGVS-J123008.39+082507.4	l	187.5349653	8.4187179	0.021	18.967±0.001	16.202±0.029	1.191±0.002	0.840±0.001	0.999±0.002	0.158	0
359	NGVS-UCD359	NGVS-J123009.31+171538.6	l	187.5387783	17.2607090	0.028	20.359±0.003	···	0.940±0.012	0.566±0.007	0.649±0.010	0.062	0
360	NGVS-UCD360	NGVS-J123009.82+123736.5	l	187.5409166	12.6267917	0.022	20.964±0.002	18.396±0.212	1.059±0.007	0.749±0.005	0.878±0.007	-0.022	1
361	NGVS-UCD361	NGVS-J123010.00+123604.7	l	187.5416813	12.6012960	0.022	21.421±0.003	···	1.031±0.010	0.711±0.007	0.855±0.010	-0.044	1
362	NGVS-UCD362	NGVS-J123010.61+073947.3	l	187.5441939	7.6631333	0.020	21.396±0.004	···	0.996±0.011	0.563±0.008	0.633±0.012	-0.011	1
363	NGVS-UCD363	NGVS-J123010.89+121143.7	l	187.5453676	12.1954817	0.025	20.931±0.002	18.428±0.210	0.981±0.008	0.691±0.005	0.737±0.009	0.288	0
364	NGVS-UCD364	NGVS-J123011.07+124721.7	l	187.5461360	12.7893579	0.022	20.502±0.002	17.708±0.114	1.099±0.005	0.755±0.004	0.900±0.005	0.021	1
365	NGVS-UCD365	NGVS-J123011.99+173400.2	l	187.5499548	17.5667257	0.025	21.205±0.003	···	1.107±0.011	0.683±0.007	0.824±0.010	0.006	1
366	NGVS-UCD366	NGVS-J123012.77+131520.1	l	187.5532048	13.2555711	0.025	20.938±0.002	···	1.009±0.006	0.714±0.005	0.813±0.007	0.031	1
367	NGVS-UCD367	NGVS-J123016.54+121556.8	l	187.5689245	12.2657856	0.023	19.957±0.001	17.631±0.103	0.963±0.005	0.700±0.003	0.848±0.004	0.087	1
368	NGVS-UCD368	NGVS-J123016.65+080454.4	l	187.5693858	8.0817884	0.022	20.779±0.002	···	1.015±0.007	0.766±0.004	0.844±0.006	0.019	1
369	NGVS-UCD369	NGVS-J123016.70+073938.9	l	187.5695943	7.6608132	0.020	20.985±0.002	18.187±0.181	0.966±0.007	0.714±0.005	0.826±0.007	-0.052	1
370	NGVS-UCD370	NGVS-J123017.32+180013.1	l	187.5721539	18.0036487	0.026	21.362±0.004	···	0.976±0.012	0.591±0.007	0.646±0.012	0.010	1
371	NGVS-UCD371	NGVS-J123017.55+135923.6	l	187.5731173	13.9898974	0.039	21.045±0.003	···	1.047±0.008	0.769±0.005	0.869±0.007	0.020	1
372	NGVS-UCD372	NGVS-J123018.06+075024.9	l	187.5752391	7.8402478	0.021	19.387±0.001	16.713±0.048	1.155±0.003	0.828±0.002	1.000±0.002	0.148	1
373	NGVS-UCD373	NGVS-J123018.39+122538.2	l	187.5766245	12.4272812	0.023	20.481±0.002	17.881±0.128	1.067±0.005	0.751±0.003	0.897±0.004	0.048	1
374	NGVS-UCD374	NGVS-J123020.05+115518.7	l	187.5835255	11.9218566	0.030	19.242±0.001	16.743±0.045	1.037±0.002	0.770±0.002	0.941±0.002	0.122	1
375	NGVS-UCD375	NGVS-J123020.60+121351.2	l	187.5858134	12.2308928	0.024	20.959±0.002	18.242±0.190	1.185±0.010	0.751±0.005	0.909±0.007	0.106	1
376	NGVS-UCD376	NGVS-J123020.63+123845.1	l	187.5859487	12.6458563	0.022	20.869±0.002	···	1.023±0.007	0.701±0.004	0.793±0.006	0.045	1
377	NGVS-UCD377	NGVS-J123021.34+145735.4	l	187.5889275	14.9598345	0.032	21.414±0.004	···	1.001±0.011	0.594±0.008	0.677±0.011	0.043	1
378	NGVS-UCD378	NGVS-J123021.71+172509.2	l	187.5904573	17.4192287	0.024	20.614±0.002	···	0.925±0.007	0.565±0.004	0.635±0.007	0.113	0
379	NGVS-UCD379	NGVS-J123021.83+122402.4	l	187.5909573	12.4006709	0.023	19.852±0.001	16.792±0.046	1.352±0.004	0.922±0.002	1.129±0.002	0.031	1
380	NGVS-UCD380	NGVS-J123022.88+170918.9	l	187.5953217	17.1552493	0.029	21.291±0.003	···	0.857±0.010	0.730±0.007	0.822±0.011	-0.001	1
381	NGVS-UCD381	NGVS-J123022.97+123148.7	l	187.5957142	12.5302030	0.022	19.683±0.001	17.234±0.074	1.033±0.004	0.737±0.002	0.821±0.003	0.093	1
382	NGVS-UCD382	NGVS-J123025.66+123541.6	l	187.6069255	12.5948970	0.021	20.090±0.001	17.820±0.123	1.009±0.004	0.704±0.002	0.782±0.004	0.013	1

Table 3 *continued*

Table 3 *(continued)*

ID	Name	NGVSID	$t_{\rm obs}$	$\alpha_{\rm J2000}$	$\delta_{\rm J2000}$	$E(B-V)$	g_0	K	$(u^*-g)_0$	$(g-i)_0$	$(g-z)_0$	$\Delta_{\rm env}$	UCD
				(deg)	(deg)	(mag)	(mag)	(mag)	(mag)	(mag)	(mag)	(mag)	
(1)	(2)	(3)	(4)	(5)	(6)	(7)	(8)	(9)	(10)	(11)	(12)	(13)	(14)
383	NGVS-UCD383	NGVS-J123025.75+122621.1	1	187.6073037	12.4391939	0.022	20.384±0.001	18.086±0.150	1.031±0.005	0.722±0.003	0.836±0.004	0.012	1
384	NGVS-UCD384	NGVS-J123026.56+122044.6	1	187.6106641	12.3457238	0.023	20.295±0.001	17.943±0.129	1.041±0.005	0.712±0.003	0.827±0.004	-0.009	1
385	NGVS-UCD385	NGVS-J123026.89+122331.1	1	187.6120606	12.3919727	0.022	19.856±0.001	17.171±0.065	1.107±0.004	0.766±0.002	0.888±0.003	-0.009	1
386	NGVS-UCD386	NGVS-J123027.21+122909.0	1	187.6133769	12.4858319	0.022	21.093±0.003	18.362±0.193	1.261±0.010	0.867±0.004	0.986±0.007	0.019	1
387	NGVS-UCD387	NGVS-J123027.37+074920.8	1	187.6140423	7.8224354	0.021	19.873±0.001	17.533±0.091	1.043±0.004	0.695±0.002	0.823±0.003	0.028	1
388	NGVS-UCD388	NGVS-J123027.56+123445.6	1	187.6148534	12.5793318	0.021	19.975±0.001	17.458±0.089	1.036±0.004	0.707±0.002	0.798±0.003	0.053	1
389	NGVS-UCD389	NGVS-J123029.91+123822.2	1	187.6246352	12.6394862	0.021	20.392±0.002	···	0.887±0.005	0.645±0.003	0.724±0.005	0.029	1
390	NGVS-UCD390	NGVS-J123029.94+074755.5	1	187.6247355	7.7987386	0.021	20.321±0.002	17.584±0.095	1.166±0.005	0.798±0.003	0.952±0.004	-0.009	1
391	NGVS-UCD391	NGVS-J123030.52+124015.8	1	187.6271488	12.6710593	0.022	19.990±0.001	17.248±0.073	1.174±0.005	0.832±0.003	0.963±0.003	0.047	1
392	NGVS-UCD392	NGVS-J123030.86+121841.7	1	187.6285848	12.3115702	0.023	19.663±0.001	17.073±0.059	1.077±0.003	0.760±0.002	0.915±0.002	0.072	1
393	NGVS-UCD393	NGVS-J123031.44+125156.6	1	187.6310140	12.8657139	0.021	20.070±0.001	17.089±0.065	1.307±0.005	0.922±0.002	1.103±0.003	0.089	1
394	NGVS-UCD394	NGVS-J123031.53+122602.6	1	187.6313771	12.4340543	0.022	20.222±0.001	17.935±0.130	0.939±0.004	0.682±0.003	0.783±0.004	0.006	1
395	NGVS-UCD395	NGVS-J123033.43+122954.3	1	187.6393011	12.4984263	0.021	19.170±0.001	16.691±0.043	1.081±0.003	0.761±0.002	0.886±0.002	0.141	1
396	NGVS-UCD396	NGVS-J123034.12+122246.5	1	187.6421762	12.3795701	0.022	21.258±0.003	···	0.999±0.009	0.702±0.006	0.811±0.008	-0.016	1
397	NGVS-UCD397	NGVS-J123034.15+160304.8	1	187.6422894	16.0513420	0.030	21.500±0.007	···	1.004±0.018	0.693±0.012	0.840±0.018	-0.027	1
398	NGVS-UCD398	NGVS-J123035.02+123452.7	1	187.6459088	12.5813043	0.021	20.428±0.002	18.161±0.168	0.996±0.006	0.720±0.004	0.830±0.005	0.154	1
399	NGVS-UCD399	NGVS-J123036.09+122201.6	1	187.6503598	12.3671024	0.023	20.661±0.002	18.141±0.156	0.880±0.008	0.651±0.004	0.762±0.006	0.002	0
400	NGVS-UCD400	NGVS-J123036.52+122152.8	1	187.6521568	12.3646754	0.023	20.468±0.002	18.166±0.159	1.031±0.007	0.724±0.004	0.875±0.005	0.009	1
401	NGVS-UCD401	NGVS-J123037.25+124609.2	1	187.6551921	12.7692272	0.023	20.356±0.002	18.215±0.181	0.987±0.006	0.714±0.004	0.811±0.005	0.131	0
402	NGVS-UCD402	NGVS-J123039.16+122132.5	1	187.6631534	12.3590141	0.023	20.637±0.002	18.369±0.192	0.965±0.007	0.759±0.004	0.935±0.005	0.041	1
403	NGVS-UCD403	NGVS-J123040.24+054128.8	1	187.6676738	5.6913198	0.021	21.477±0.004	···	0.883±0.012	0.609±0.009	0.660±0.012	0.002	1
404	NGVS-UCD404	NGVS-J123041.81+122341.2	1	187.6742276	12.3947905	0.023	21.122±0.004	···	0.956±0.009	0.718±0.006	0.806±0.008	-0.007	1
405	NGVS-UCD405	NGVS-J123043.25+122212.4	1	187.6802143	12.3701094	0.023	21.163±0.004	···	1.014±0.010	0.754±0.006	0.876±0.008	-0.020	1
406	NGVS-UCD406	NGVS-J123044.47+170150.8	1	187.6853052	17.0307800	0.029	21.475±0.004	···	1.060±0.016	0.653±0.009	0.719±0.017	0.019	0
407	NGVS-UCD407	NGVS-J123045.34+122033.5	1	187.6889032	12.3426296	0.024	20.595±0.002	18.289±0.180	0.971±0.007	0.734±0.004	0.866±0.006	0.031	1
408	NGVS-UCD408	NGVS-J123045.41+120710.0	1	187.6892099	12.1194456	0.027	21.452±0.003	···	1.208±0.013	0.804±0.006	1.010±0.009	0.032	1
409	NGVS-UCD409	NGVS-J123045.92+122501.6	1	187.6913132	12.4171095	0.022	20.228±0.002	17.824±0.128	0.987±0.005	0.743±0.003	0.851±0.004	-0.014	1
410	NGVS-UCD410	NGVS-J123045.95+113752.5	1	187.6914378	11.6312608	0.040	21.019±0.002	···	0.941±0.009	0.649±0.005	0.762±0.008	0.151	1
411	NGVS-UCD411	NGVS-J123046.65+122422.2	1	187.6943744	12.4061746	0.023	20.436±0.002	17.888±0.196	1.012±0.007	0.756±0.004	0.896±0.005	0.003	1
412	NGVS-UCD412	NGVS-J123047.40+123301.7	1	187.6974884	12.5504714	0.021	19.387±0.001	16.594±0.041	1.185±0.003	0.876±0.002	1.041±0.002	0.109	1
413	NGVS-UCD413	NGVS-J123047.66+120825.2	1	187.6985663	12.1403402	0.026	19.638±0.001	17.277±0.079	0.983±0.003	0.642±0.002	0.787±0.003	0.052	1
414	NGVS-UCD414	NGVS-J123047.70+122430.5	1	187.6987576	12.4084685	0.023	19.711±0.001	17.030±0.090	0.970±0.004	0.725±0.003	0.828±0.003	0.012	1
415	NGVS-UCD415	NGVS-J123047.97+121100.6	1	187.6998578	12.1835024	0.025	21.395±0.003	···	1.013±0.010	0.672±0.006	0.826±0.009	0.006	1
416	NGVS-UCD416	NGVS-J123048.20+123510.9	1	187.7008418	12.5863658	0.021	19.057±0.001	16.445±0.036	1.113±0.003	0.794±0.001	0.931±0.002	0.108	1
417	NGVS-UCD417	NGVS-J123049.28+123718.2	1	187.7053422	12.6217134	0.021	19.872±0.001	17.314±0.078	1.086±0.004	0.788±0.002	0.908±0.003	0.058	1
418	NGVS-UCD418	NGVS-J123049.49+121426.9	1	187.7062262	12.2408133	0.024	20.486±0.002	18.167±0.179	1.105±0.007	0.707±0.004	0.863±0.006	0.030	1
419	NGVS-UCD419	NGVS-J123049.61+121020.6	1	187.7067127	12.1723781	0.025	20.880±0.002	18.085±0.165	1.107±0.007	0.724±0.004	0.906±0.006	0.011	1
420	NGVS-UCD420	NGVS-J123050.05+122408.9	1	187.7085286	12.4024805	0.023	20.172±0.002	···	1.071±0.006	0.762±0.004	0.889±0.005	-0.124	1
421	NGVS-UCD421	NGVS-J123050.05+174524.9	1	187.7085556	17.7569297	0.024	21.364±0.004	···	0.855±0.011	0.700±0.007	0.762±0.011	-0.005	1
422	NGVS-UCD422	NGVS-J123050.65+174857.3	1	187.7110305	17.8159097	0.024	20.038±0.001	···	0.921±0.005	0.727±0.003	0.819±0.004	0.010	1
423	NGVS-UCD423	NGVS-J123051.07+122611.9	1	187.7127768	12.4366440	0.022	19.598±0.001	16.655±0.042	1.221±0.004	0.880±0.002	1.075±0.002	0.013	1
424	NGVS-UCD424	NGVS-J123051.65+121409.9	1	187.7152176	12.2360771	0.024	20.966±0.002	···	1.014±0.009	0.630±0.005	0.772±0.007	0.031	1
425	NGVS-UCD425	NGVS-J123051.75+122053.3	1	187.7156253	12.3481413	0.024	20.720±0.002	18.654±0.255	0.991±0.007	0.726±0.004	0.843±0.005	-0.017	1
426	NGVS-UCD426	NGVS-J123052.48+165141.0	1	187.7186850	16.8613964	0.028	20.478±0.002	···	1.052±0.007	0.749±0.004	0.900±0.006	0.123	0
427	NGVS-UCD427	NGVS-J123052.92+080125.6	1	187.7204963	8.0237682	0.022	21.401±0.003	···	1.004±0.010	0.737±0.006	0.821±0.010	0.021	1
428	NGVS-UCD428	NGVS-J123053.61+063632.5	1	187.7233550	6.6090319	0.017	20.339±0.002	18.172±0.161	0.916±0.006	0.697±0.004	0.791±0.006	0.145	0
429	NGVS-UCD429	NGVS-J123053.88+121712.4	1	187.7245098	12.2867887	0.024	21.021±0.003	18.253±0.176	1.115±0.011	0.817±0.005	0.959±0.008	0.017	1
430	NGVS-UCD430	NGVS-J123054.66+122022.6	1	187.7277339	12.3396026	0.024	21.214±0.003	···	0.872±0.009	0.668±0.006	0.768±0.009	0.005	1

Table 3 *continued*

Table 3 *(continued)*

ID	Name	NGVSID	$t_{\rm obs}$	$\alpha_{\rm J2000}$	$\delta_{\rm J2000}$	$E(B-V)$	g_0	K	$(u^*-g)_0$	$(g-i)_0$	$(g-z)_0$	$\Delta_{\rm env}$	UCD
				(deg)	(deg)	(mag)	(mag)	(mag)	(mag)	(mag)	(mag)	(mag)	
(1)	(2)	(3)	(4)	(5)	(6)	(7)	(8)	(9)	(10)	(11)	(12)	(13)	(14)
431	NGVS-UCD431	NGVS-J123057.38+122544.5	s	187.7391002	12.4290352	0.022	18.763±0.005	15.302±0.013	1.565±0.022	1.066±0.010	1.367±0.012	0.061	1
432	NGVS-UCD432	NGVS-J123058.58+112513.0	l	187.7440739	11.4202884	0.039	20.646±0.002	···	0.898±0.006	0.665±0.004	0.754±0.005	0.047	1
433	NGVS-UCD433	NGVS-J123059.90+121801.0	l	187.7495906	12.3002662	0.023	19.977±0.001	17.809±0.117	0.897±0.004	0.697±0.003	0.802±0.003	0.012	1
434	NGVS-UCD434	NGVS-J123101.03+154326.2	l	187.7542728	15.7239311	0.029	21.030±0.003	18.240±0.251	1.012±0.009	0.816±0.006	0.881±0.009	0.049	1
435	NGVS-UCD435	NGVS-J123101.16+074322.9	l	187.7548524	7.7230188	0.020	19.422±0.001	16.826±0.048	0.971±0.005	0.588±0.003	0.910±0.004	0.407	0
436	NGVS-UCD436	NGVS-J123101.47+121924.5	l	187.7561418	12.3234818	0.023	19.571±0.001	16.555±0.038	1.291±0.004	0.922±0.002	1.122±0.002	0.002	1
437	NGVS-UCD437	NGVS-J123102.14+122749.7	l	187.7589068	12.4638020	0.021	20.575±0.002	18.134±0.161	0.891±0.006	0.703±0.004	0.815±0.005	0.030	1
438	NGVS-UCD438	NGVS-J123102.59+123414.1	l	187.7607806	12.5705875	0.021	19.718±0.001	17.364±0.082	0.923±0.004	0.712±0.002	0.805±0.003	0.054	1
439	NGVS-UCD439	NGVS-J123103.00+052047.2	s	187.7624982	5.3464332	0.019	16.720±0.002	14.817±0.009	···	···	0.643±0.005	-0.030	0
440	NGVS-UCD440	NGVS-J123103.15+122501.3	l	187.7631068	12.4170373	0.023	21.137±0.003	···	0.934±0.010	0.683±0.006	0.798±0.008	-0.025	1
441	NGVS-UCD441	NGVS-J123103.69+123213.0	l	187.7653640	12.5369514	0.020	19.938±0.001	17.626±0.105	0.957±0.005	0.726±0.002	0.810±0.004	0.045	1
442	NGVS-UCD442	NGVS-J123103.86+153255.1	l	187.7660987	15.5486430	0.028	21.388±0.009	···	0.895±0.018	0.505±0.015	0.721±0.027	-0.007	1
443	NGVS-UCD443	NGVS-J123104.43+122321.2	l	187.7684432	12.3892322	0.023	20.589±0.002	18.212±0.173	0.927±0.007	0.686±0.005	0.809±0.007	0.050	1
444	NGVS-UCD444	NGVS-J123104.48+115636.4	l	187.7686568	11.9434521	0.028	19.050±0.001	16.602±0.041	1.086±0.002	0.765±0.002	0.914±0.002	0.080	1
445	NGVS-UCD445	NGVS-J123104.80+131436.6	l	187.7699863	13.2434961	0.026	20.554±0.002	18.363±0.201	1.015±0.007	0.680±0.004	0.823±0.007	0.107	1
446	NGVS-UCD446	NGVS-J123105.49+120054.3	l	187.7728918	12.0150887	0.028	20.724±0.002	18.598±0.248	0.903±0.007	0.665±0.004	0.783±0.006	-0.007	1
447	NGVS-UCD447	NGVS-J123109.91+080405.3	l	187.7912805	8.0681353	0.024	19.723±0.001	17.683±0.108	0.955±0.003	0.705±0.002	0.813±0.003	0.062	1
448	NGVS-UCD448	NGVS-J123110.22+121601.0	l	187.7925812	12.2669526	0.022	21.243±0.004	···	1.043±0.012	0.746±0.007	0.893±0.010	0.026	1
449	NGVS-UCD449	NGVS-J123111.31+123001.0	l	187.7971049	12.5002907	0.020	20.691±0.002	18.401±0.209	1.191±0.007	0.839±0.004	0.984±0.005	0.077	1
450	NGVS-UCD450	NGVS-J123111.37+152820.3	l	187.7973956	15.4723080	0.027	21.382±0.004	···	0.896±0.010	0.721±0.007	0.823±0.011	-0.050	1
451	NGVS-UCD451	NGVS-J123111.60+122030.1	l	187.7983424	12.3416929	0.023	20.182±0.001	17.972±0.149	0.957±0.004	0.708±0.002	0.819±0.003	0.003	1
452	NGVS-UCD452	NGVS-J123111.87+060631.0	l	187.7994391	6.1086126	0.019	21.473±0.004	···	1.003±0.013	0.548±0.008	0.635±0.015	0.003	1
453	NGVS-UCD453	NGVS-J123111.88+124101.1	l	187.7995036	12.6836354	0.025	18.916±0.001	15.882±0.023	1.360±0.003	0.972±0.002	1.170±0.002	0.052	1
454	NGVS-UCD454	NGVS-J123113.76+074811.9	l	187.8073500	7.8033039	0.020	21.220±0.003	···	0.974±0.009	0.713±0.006	0.801±0.009	-0.006	1
455	NGVS-UCD455	NGVS-J123113.81+121352.4	l	187.8075240	12.2312225	0.022	20.069±0.001	17.459±0.097	1.024±0.005	0.710±0.003	0.837±0.004	0.042	1
456	NGVS-UCD456	NGVS-J123115.63+095558.9	l	187.8151370	9.9330219	0.021	21.461±0.004	···	0.922±0.011	0.801±0.007	0.890±0.012	0.010	1
457	NGVS-UCD457	NGVS-J123115.73+121954.4	s	187.8155484	12.3317845	0.023	18.069±0.003	15.185±0.012	1.214±0.013	0.888±0.008	1.110±0.010	0.385	0
458	NGVS-UCD458	NGVS-J123116.32+121845.4	l	187.8180112	12.3126055	0.022	20.862±0.002	18.047±0.159	1.018±0.007	0.776±0.004	0.901±0.006	0.026	1
459	NGVS-UCD459	NGVS-J123119.09+121023.8	l	187.8295329	12.1732709	0.024	20.320±0.001	17.854±0.138	0.886±0.005	0.696±0.003	0.801±0.005	0.070	1
460	NGVS-UCD460	NGVS-J123119.27+122231.9	l	187.8303024	12.3755379	0.023	20.263±0.001	17.641±0.111	1.077±0.005	0.785±0.003	0.926±0.004	0.046	1
461	NGVS-UCD461	NGVS-J123120.00+121158.1	l	187.8333319	12.1994729	0.023	20.398±0.002	17.825±0.134	1.077±0.005	0.734±0.003	0.860±0.004	0.020	1
462	NGVS-UCD462	NGVS-J123120.78+064447.4	l	187.8365909	6.7465096	0.018	19.662±0.001	17.295±0.074	0.979±0.004	0.705±0.002	0.790±0.004	0.122	1
463	NGVS-UCD463	NGVS-J123123.06+061843.9	l	187.8460657	6.3121969	0.018	20.843±0.002	···	0.909±0.008	0.634±0.005	0.726±0.009	0.037	1
464	NGVS-UCD464	NGVS-J123124.75+122525.8	l	187.8531430	12.4238351	0.022	19.721±0.001	17.213±0.075	1.001±0.003	0.738±0.002	0.871±0.002	0.014	1
465	NGVS-UCD465	NGVS-J123125.07+161013.8	l	187.8544751	16.1704996	0.029	19.157±0.001	···	1.027±0.003	0.780±0.002	0.904±0.002	0.091	0
466	NGVS-UCD466	NGVS-J123125.25+121931.8	l	187.8551924	12.3254916	0.023	20.145±0.001	17.827±0.130	0.919±0.004	0.718±0.003	0.827±0.004	0.057	1
467	NGVS-UCD467	NGVS-J123127.09+180153.1	l	187.8628834	18.0314107	0.026	20.350±0.002	···	0.893±0.006	0.623±0.004	0.672±0.005	0.060	1
468	NGVS-UCD468	NGVS-J123127.35+123032.1	l	187.8639761	12.5089280	0.022	20.721±0.002	18.047±0.164	0.943±0.006	0.656±0.004	0.735±0.006	0.011	1
469	NGVS-UCD469	NGVS-J123128.36+122503.6	l	187.8681740	12.4176581	0.023	19.243±0.001	16.782±0.051	1.088±0.002	0.782±0.002	0.946±0.002	0.090	1
470	NGVS-UCD470	NGVS-J123131.70+113610.7	l	187.8820922	11.6029721	0.046	20.880±0.003	18.726±0.292	1.003±0.009	0.732±0.007	0.892±0.009	0.334	0
471	NGVS-UCD471	NGVS-J123131.70+124130.4	l	187.8820976	12.6917652	0.025	19.423±0.002	16.948±0.060	1.024±0.006	0.860±0.004	1.095±0.004	0.120	1
472	NGVS-UCD472	NGVS-J123133.30+073146.9	l	187.8887438	7.5296815	0.020	20.878±0.003	···	1.083±0.010	0.803±0.006	0.804±0.010	0.031	1
473	NGVS-UCD473	NGVS-J123135.13+123459.4	l	187.8963954	12.5831553	0.024	20.009±0.001	17.219±0.077	1.220±0.005	0.870±0.002	1.060±0.003	0.079	1
474	NGVS-UCD474	NGVS-J123135.18+151326.9	l	187.8965782	15.2241444	0.031	21.144±0.003	···	0.921±0.009	0.721±0.006	0.893±0.008	0.031	1
475	NGVS-UCD475	NGVS-J123135.54+115154.4	l	187.8980990	11.8651220	0.030	19.773±0.001	17.156±0.064	1.167±0.004	0.833±0.002	0.993±0.003	0.048	1
476	NGVS-UCD476	NGVS-J123136.39+173856.0	l	187.9016393	17.6488804	0.022	20.168±0.001	···	0.902±0.005	0.608±0.003	0.703±0.005	-0.004	1
477	NGVS-UCD477	NGVS-J123137.00+055024.0	l	187.9041521	5.8399950	0.016	19.784±0.001	16.242±0.032	1.537±0.005	1.063±0.002	1.271±0.003	0.043	0
478	NGVS-UCD478	NGVS-J123137.44+121740.7	l	187.9059964	12.2946458	0.023	20.522±0.002	···	0.930±0.005	0.693±0.004	0.800±0.005	0.008	1

Table 3 *continued*

Table 3 *(continued)*

ID	Name	NGVSID	$t_{\rm obs}$	$\alpha_{\rm J2000}$	$\delta_{\rm J2000}$	$E(B-V)$	g_0	K	$(u^*-g)_0$	$(g-i)_0$	$(g-z)_0$	$\Delta_{\rm env}$	UCD
				(deg)	(deg)	(mag)	(mag)	(mag)	(mag)	(mag)	(mag)	(mag)	
(1)	(2)	(3)	(4)	(5)	(6)	(7)	(8)	(9)	(10)	(11)	(12)	(13)	(14)
479	NGVS-UCD479	NGVS-J123137.51+174129.6	l	187.9062850	17.6915491	0.022	20.833±0.002	···	0.916±0.009	0.753±0.005	0.852±0.007	0.079	0
480	NGVS-UCD480	NGVS-J123138.53+115923.9	l	187.9105226	11.9899631	0.029	20.670±0.002	18.218±0.165	1.049±0.007	0.725±0.004	0.830±0.005	0.021	1
481	NGVS-UCD481	NGVS-J123140.23+165145.6	l	187.9176103	16.8626598	0.029	21.144±0.003	···	0.890±0.010	0.628±0.006	0.750±0.011	0.051	1
482	NGVS-UCD482	NGVS-J123143.93+164806.4	l	187.9330595	16.8017876	0.030	21.058±0.003	···	0.921±0.009	0.712±0.006	0.840±0.009	-0.006	1
483	NGVS-UCD483	NGVS-J123145.81+162007.3	l	187.9408579	16.3353599	0.025	20.986±0.003	···	1.028±0.009	0.660±0.005	0.779±0.009	0.005	1
484	NGVS-UCD484	NGVS-J123145.95+122721.1	l	187.9414772	12.4558589	0.025	21.260±0.003	···	0.899±0.008	0.661±0.005	0.776±0.008	0.036	1
485	NGVS-UCD485	NGVS-J123146.22+125104.8	l	187.9426023	12.8513433	0.023	20.759±0.002	···	0.950±0.007	0.712±0.004	0.798±0.006	0.094	1
486	NGVS-UCD486	NGVS-J123148.50+115032.4	l	187.9520863	11.8423353	0.031	20.570±0.002	17.488±0.089	1.417±0.008	0.973±0.003	1.210±0.004	-0.054	1
487	NGVS-UCD487	NGVS-J123149.49+173534.9	l	187.9562210	17.5930166	0.022	21.218±0.003	···	0.918±0.010	0.580±0.006	0.647±0.010	0.013	1
488	NGVS-UCD488	NGVS-J123152.90+121559.0	s	187.9704030	12.2663989	0.025	18.428±0.006	15.687±0.020	1.160±0.018	0.863±0.012	1.079±0.015	0.196	0
489	NGVS-UCD489	NGVS-J123152.92+150050.1	l	187.9705171	15.0139035	0.030	20.480±0.002	18.198±0.198	0.875±0.007	0.656±0.004	0.807±0.006	0.089	1
490	NGVS-UCD490	NGVS-J123152.99+122530.8	l	187.9707786	12.4252171	0.026	21.089±0.002	···	0.900±0.008	0.685±0.005	0.771±0.008	0.052	1
491	NGVS-UCD491	NGVS-J123153.99+172805.5	l	187.9749749	17.4681901	0.023	20.426±0.002	···	1.041±0.008	0.798±0.004	0.693±0.008	0.098	1
492	NGVS-UCD492	NGVS-J123155.11+164317.1	s	187.9796179	16.7214112	0.030	17.490±0.002	···	1.759±0.013	1.172±0.005	1.454±0.006	0.272	0
493	NGVS-UCD493	NGVS-J123155.53+175751.0	l	187.9813579	17.9641728	0.022	20.559±0.002	···	0.966±0.008	0.656±0.006	0.724±0.009	0.046	1
494	NGVS-UCD494	NGVS-J123156.77+072710.6	l	187.9865416	7.4529519	0.021	21.038±0.003	···	0.875±0.010	0.561±0.006	0.675±0.010	0.101	1
495	NGVS-UCD495	NGVS-J123157.60+124929.6	l	187.9900002	12.8248795	0.023	20.233±0.002	17.968±0.154	0.998±0.006	0.734±0.003	0.782±0.005	0.031	1
496	NGVS-UCD496	NGVS-J123157.99+131534.1	l	187.9916424	13.2594769	0.027	19.558±0.001	17.256±0.078	0.926±0.004	0.712±0.003	0.827±0.003	0.096	1
497	NGVS-UCD497	NGVS-J123201.72+121142.2	l	188.0071539	12.1950496	0.028	20.546±0.002	17.913±0.144	1.196±0.006	0.832±0.003	0.991±0.004	0.037	1
498	NGVS-UCD498	NGVS-J123204.35+122030.3	l	188.0181446	12.3417600	0.026	19.553±0.001	16.994±0.060	1.054±0.003	0.787±0.002	0.904±0.002	0.075	1
499	NGVS-UCD499	NGVS-J123206.47+070531.0	l	188.0269420	7.0919347	0.020	21.402±0.003	···	0.997±0.011	0.569±0.007	0.673±0.013	0.017	1
500	NGVS-UCD500	NGVS-J123212.41+133520.6	l	188.0517269	13.5890623	0.033	21.311±0.004	···	0.959±0.012	0.706±0.007	0.779±0.010	0.111	0
501	NGVS-UCD501	NGVS-J123212.59+074047.6	l	188.0524452	7.6798850	0.021	21.147±0.003	···	0.924±0.009	0.681±0.006	0.793±0.009	0.017	0
502	NGVS-UCD502	NGVS-J123213.66+142413.6	l	188.0569041	14.4037908	0.038	19.464±0.001	16.361±0.033	1.348±0.004	0.910±0.002	1.139±0.002	-0.012	1
503	NGVS-UCD503	NGVS-J123214.45+120159.0	l	188.0602078	12.0330677	0.029	20.550±0.002	18.047±0.149	1.106±0.006	0.818±0.003	0.950±0.005	0.078	1
504	NGVS-UCD504	NGVS-J123214.58+120305.3	l	188.0607413	12.0514861	0.029	19.343±0.001	16.805±0.049	1.158±0.003	0.835±0.002	0.961±0.002	0.088	1
505	NGVS-UCD505	NGVS-J123221.10+121613.4	l	188.0879285	12.2703979	0.027	20.677±0.002	18.097±0.175	0.931±0.008	0.749±0.005	0.863±0.007	0.065	1
506	NGVS-UCD506	NGVS-J123222.45+175605.2	l	188.0935249	17.9347836	0.021	19.997±0.001	···	0.934±0.006	0.771±0.003	0.890±0.005	0.089	1
507	NGVS-UCD507	NGVS-J123223.49+115755.0	l	188.0978948	11.9652686	0.032	20.080±0.001	17.355±0.080	1.104±0.005	0.812±0.003	0.949±0.004	0.012	1
508	NGVS-UCD508	NGVS-J123224.93+172218.5	l	188.1038823	17.3718167	0.026	21.473±0.004	···	0.974±0.015	0.628±0.009	0.728±0.014	0.041	0
509	NGVS-UCD509	NGVS-J123225.37+121956.8	l	188.1056893	12.3324460	0.027	20.424±0.002	17.989±0.159	0.979±0.006	0.704±0.004	0.783±0.005	0.078	1
510	NGVS-UCD510	NGVS-J123233.35+052104.3	l	188.1389637	5.3511951	0.023	21.114±0.003	···	0.876±0.010	0.627±0.007	0.650±0.010	0.027	0
511	NGVS-UCD511	NGVS-J123234.13+091703.8	l	188.1422142	9.2844023	0.020	20.718±0.002	···	0.882±0.007	0.601±0.005	0.670±0.007	0.027	0
512	NGVS-UCD512	NGVS-J123234.62+181123.1	l	188.1442695	18.1897487	0.025	20.755±0.002	···	0.864±0.008	0.727±0.005	0.791±0.007	0.018	0
513	NGVS-UCD513	NGVS-J123235.62+063516.0	l	188.1484232	6.5877906	0.019	21.283±0.004	···	0.862±0.011	0.627±0.007	0.703±0.014	0.001	1
514	NGVS-UCD514	NGVS-J123236.55+063528.9	l	188.1522983	6.5913656	0.019	21.414±0.004	···	0.929±0.013	0.686±0.008	0.691±0.015	0.069	1
515	NGVS-UCD515	NGVS-J123239.17+071541.8	l	188.1632128	7.2616000	0.019	21.332±0.003	···	1.041±0.010	0.689±0.006	0.804±0.010	0.018	1
516	NGVS-UCD516	NGVS-J123243.20+130858.9	l	188.1800144	13.1497065	0.030	21.362±0.003	···	0.906±0.011	0.606±0.007	0.640±0.011	0.049	0
517	NGVS-UCD517	NGVS-J123244.97+120411.6	l	188.1873819	12.0699021	0.035	21.424±0.003	···	0.957±0.011	0.700±0.006	0.785±0.010	0.053	1
518	NGVS-UCD518	NGVS-J123245.02+122039.9	l	188.1875839	12.3444244	0.028	21.025±0.002	···	1.006±0.007	0.726±0.004	0.810±0.007	0.066	1
519	NGVS-UCD519	NGVS-J123246.00+111447.9	l	188.1916702	11.2466459	0.051	21.292±0.004	···	0.982±0.012	0.658±0.007	0.761±0.011	0.036	0
520	NGVS-UCD520	NGVS-J123250.11+112440.7	s	188.2088009	11.4112973	0.056	17.930±0.004	14.654±0.008	1.512±0.014	1.026±0.009	1.277±0.009	0.098	0
521	NGVS-UCD521	NGVS-J123251.32+164659.1	l	188.2138432	16.7830971	0.028	21.464±0.005	···	0.864±0.013	0.655±0.008	0.779±0.014	-0.035	1
522	NGVS-UCD522	NGVS-J123254.89+172157.9	l	188.2286927	17.3660727	0.027	21.284±0.004	···	1.088±0.013	0.421±0.008	0.772±0.011	-0.016	1
523	NGVS-UCD523	NGVS-J123255.76+094417.9	l	188.2323294	9.7382970	0.021	21.258±0.003	···	0.981±0.010	0.714±0.007	0.861±0.010	-0.014	0
524	NGVS-UCD524	NGVS-J123256.67+115104.7	l	188.2361316	11.8512946	0.034	20.068±0.001	17.957±0.141	0.903±0.004	0.681±0.002	0.743±0.003	0.028	0
525	NGVS-UCD525	NGVS-J123259.96+110553.1	l	188.2498174	11.0980812	0.046	21.279±0.003	···	0.978±0.011	0.637±0.007	0.761±0.010	0.015	0
526	NGVS-UCD526	NGVS-J123302.86+065149.3	l	188.2619047	6.8637026	0.022	20.576±0.002	18.347±0.208	0.884±0.006	0.568±0.004	0.687±0.006	0.087	1

Table 3 *continued*

Table 3 *(continued)*

ID	Name	NGVSID	$t_{\rm obs}$	$\alpha_{\rm J2000}$ (deg)	$\delta_{\rm J2000}$ (deg)	$E(B-V)$ (mag)	g_0 (mag)	K (mag)	$(u^*-g)_0$ (mag)	$(g-i)_0$ (mag)	$(g-z)_0$ (mag)	$\Delta_{\rm env}$ (mag)	UCD
(1)	(2)	(3)	(4)	(5)	(6)	(7)	(8)	(9)	(10)	(11)	(12)	(13)	(14)
527	NGVS-UCD527	NGVS-J123308.79+061254.5	l	188.2866196	6.2151435	0.018	21.480±0.004	···	1.118±0.014	0.645±0.008	0.748±0.014	0.024	1
528	NGVS-UCD528	NGVS-J123311.25+070702.3	l	188.2968819	7.1172966	0.022	21.406±0.003	···	0.977±0.010	0.673±0.007	0.731±0.011	0.023	0
529	NGVS-UCD529	NGVS-J123319.22+050744.5	l	188.3300990	5.1290252	0.021	21.495±0.005	···	1.001±0.018	0.634±0.011	0.680±0.016	0.032	0
530	NGVS-UCD530	NGVS-J123321.82+152830.0	l	188.3409319	15.4750115	0.030	21.398±0.004	···	0.900±0.010	0.577±0.008	0.634±0.014	0.049	1
531	NGVS-UCD531	NGVS-J123323.69+162140.4	l	188.3487272	16.3612311	0.029	20.198±0.002	···	0.901±0.005	0.622±0.003	0.711±0.005	0.042	0
532	NGVS-UCD532	NGVS-J123324.31+175138.2	l	188.3513109	17.8606195	0.022	20.929±0.002	···	1.063±0.009	0.752±0.005	0.871±0.008	0.057	0
533	NGVS-UCD533	NGVS-J123329.47+121017.4	l	188.3727995	12.1715136	0.034	20.449±0.002	18.322±0.192	0.948±0.005	0.712±0.003	0.815±0.004	0.076	1
534	NGVS-UCD534	NGVS-J123330.72+112807.4	l	188.3780137	11.4687169	0.042	21.044±0.003	···	1.047±0.008	0.724±0.005	0.733±0.008	0.003	1
535	NGVS-UCD535	NGVS-J123333.26+113141.7	l	188.3885662	11.5282465	0.041	19.799±0.001	17.292±0.069	1.080±0.004	0.764±0.002	0.845±0.003	0.071	1
536	NGVS-UCD536	NGVS-J123336.21+151123.7	l	188.4008848	15.1899040	0.035	21.207±0.003	···	0.867±0.009	0.654±0.006	0.704±0.009	-0.095	1
537	NGVS-UCD537	NGVS-J123340.35+124413.0	l	188.4181250	12.7369318	0.029	19.931±0.001	17.377±0.084	0.741±0.007	0.791±0.004	1.109±0.006	0.412	0
538	NGVS-UCD538	NGVS-J123340.91+151738.1	l	188.4204560	15.2939037	0.036	21.174±0.003	···	0.993±0.010	0.690±0.006	0.812±0.008	0.013	1
539	NGVS-UCD539	NGVS-J123344.17+060925.6	l	188.4340211	6.1571001	0.020	21.337±0.004	···	0.951±0.014	0.522±0.009	0.683±0.017	0.018	1
540	NGVS-UCD540	NGVS-J123345.56+074201.1	l	188.4398352	7.7002945	0.022	20.752±0.002	18.374±0.219	1.172±0.008	0.858±0.004	1.008±0.006	0.055	1
541	NGVS-UCD541	NGVS-J123346.31+115702.3	l	188.4429573	11.9506384	0.036	20.868±0.003	17.829±0.124	1.257±0.009	0.905±0.005	1.063±0.006	0.008	1
542	NGVS-UCD542	NGVS-J123350.27+162515.0	l	188.4594394	16.4208336	0.029	21.473±0.004	···	0.871±0.011	0.658±0.008	0.771±0.012	-0.105	1
543	NGVS-UCD543	NGVS-J123353.66+074224.4	l	188.4735698	7.7067905	0.022	20.010±0.001	16.712±0.048	1.380±0.004	0.981±0.002	1.207±0.003	-0.018	1
544	NGVS-UCD544	NGVS-J123354.30+074158.1	l	188.4762489	7.6994591	0.022	21.180±0.003	18.104±0.171	1.363±0.010	0.935±0.005	1.141±0.007	-0.002	1
545	NGVS-UCD545	NGVS-J123356.84+052352.1	s	188.4868260	5.3978096	0.022	17.033±0.002	15.799±0.022	···	···	0.675±0.005	-0.037	0
546	NGVS-UCD546	NGVS-J123357.76+074129.6	l	188.4906660	7.6915521	0.022	21.068±0.003	···	1.118±0.008	0.816±0.005	0.932±0.007	-0.042	1
547	NGVS-UCD547	NGVS-J123359.05+104652.4	l	188.4960280	10.7812359	0.026	21.427±0.004	···	0.940±0.012	0.549±0.008	0.630±0.013	0.000	1
548	NGVS-UCD548	NGVS-J123359.09+074244.6	l	188.4962125	7.7124026	0.022	20.237±0.002	···	1.103±0.005	0.794±0.003	0.922±0.004	-0.060	1
549	NGVS-UCD549	NGVS-J123359.46+074225.8	l	188.4977556	7.7071554	0.022	20.263±0.002	16.082±0.028	0.901±0.006	0.613±0.005	0.781±0.006	-0.022	1
550	NGVS-UCD550	NGVS-J123359.60+114730.9	l	188.4983269	11.7919190	0.040	21.237±0.003	···	0.956±0.010	0.712±0.006	0.790±0.009	0.011	1
551	NGVS-UCD551	NGVS-J123402.20+064950.3	l	188.5091560	6.8306518	0.022	21.137±0.003	···	0.918±0.009	0.616±0.006	0.662±0.010	0.003	1
552	NGVS-UCD552	NGVS-J123402.45+060922.6	l	188.5102079	6.1562850	0.021	21.478±0.004	···	0.965±0.014	0.725±0.008	0.789±0.014	0.049	0
553	NGVS-UCD553	NGVS-J123403.34+053742.2	l	188.5139295	5.6283750	0.024	18.915±0.001	15.439±0.014	1.552±0.004	1.043±0.002	1.312±0.002	0.068	0
554	NGVS-UCD554	NGVS-J123403.90+154353.3	l	188.5162534	15.7314731	0.022	20.661±0.002	···	0.922±0.007	0.633±0.004	0.713±0.007	0.073	1
555	NGVS-UCD555	NGVS-J123406.46+162013.8	l	188.5269369	16.3371633	0.028	21.151±0.003	···	0.854±0.009	0.614±0.007	0.710±0.011	-0.042	0
556	NGVS-UCD556	NGVS-J123409.59+172636.0	l	188.5399759	17.4433429	0.027	21.429±0.005	···	1.053±0.016	0.764±0.010	0.864±0.013	0.050	1
557	NGVS-UCD557	NGVS-J123410.40+115929.3	l	188.5433527	11.9914691	0.041	20.461±0.002	18.345±0.205	0.975±0.006	0.743±0.004	0.842±0.005	0.079	1
558	NGVS-UCD558	NGVS-J123413.31+181004.7	l	188.5554576	18.1679625	0.023	20.330±0.002	···	0.908±0.006	0.580±0.004	0.737±0.007	0.082	1
559	NGVS-UCD559	NGVS-J123413.34+053949.6	l	188.5555889	5.6637896	0.023	21.492±0.004	···	1.000±0.014	0.683±0.008	0.819±0.011	0.088	1
560	NGVS-UCD560	NGVS-J123413.38+074107.0	l	188.5557528	7.6852884	0.022	19.206±0.001	···	1.117±0.003	0.868±0.002	1.022±0.002	-0.004	1
561	NGVS-UCD561	NGVS-J123416.42+081048.9	l	188.5684034	8.1802533	0.019	20.056±0.002	18.693±0.256	-0.006±0.004	-0.330±0.006	-0.472±0.011	-0.067	0
562	NGVS-UCD562	NGVS-J123418.18+130700.7	l	188.5757530	13.1168600	0.041	21.413±0.004	···	0.968±0.012	0.677±0.008	0.808±0.011	0.020	1
563	NGVS-UCD563	NGVS-J123418.30+081423.4	l	188.5762700	8.2398344	0.019	18.334±0.000	18.183±0.157	-0.155±0.001	-0.545±0.002	-0.704±0.003	0.210	0
564	NGVS-UCD564	NGVS-J123418.70+081144.5	l	188.5779066	8.1956951	0.019	20.020±0.002	···	-0.055±0.003	-0.488±0.005	-0.554±0.010	-0.363	0
565	NGVS-UCD565	NGVS-J123419.09+113615.1	l	188.5795441	11.6042074	0.045	20.244±0.002	17.828±0.113	1.007±0.005	0.692±0.003	0.820±0.004	0.027	1
566	NGVS-UCD566	NGVS-J123419.41+074025.8	l	188.5808827	7.6738359	0.022	21.111±0.003	···	0.880±0.009	0.720±0.006	0.780±0.009	0.012	1
567	NGVS-UCD567	NGVS-J123419.97+153536.6	l	188.5831997	15.5934963	0.028	20.632±0.002	···	0.977±0.007	0.615±0.005	0.625±0.008	0.047	1
568	NGVS-UCD568	NGVS-J123421.44+081425.7	l	188.5893159	8.2404761	0.019	18.715±0.001	17.099±0.059	-0.027±0.002	-0.224±0.002	-0.164±0.003	0.205	0
569	NGVS-UCD569	NGVS-J123422.71+081358.8	l	188.5946349	8.2330125	0.019	19.397±0.001	18.019±0.137	0.008±0.002	-0.361±0.003	-0.357±0.005	0.070	0
570	NGVS-UCD570	NGVS-J123425.34+081156.1	l	188.6055733	8.1989136	0.020	20.255±0.002	···	-0.122±0.003	-0.400±0.006	-0.561±0.012	0.113	0
571	NGVS-UCD571	NGVS-J123427.42+100534.2	l	188.6142469	10.0928380	0.023	21.128±0.004	···	1.050±0.010	0.771±0.006	0.853±0.009	-0.037	1
572	NGVS-UCD572	NGVS-J123428.47+144246.0	l	188.6186084	14.7127878	0.037	21.008±0.003	···	0.851±0.008	0.584±0.006	0.665±0.010	0.032	1
573	NGVS-UCD573	NGVS-J123429.27+124042.1	l	188.6219697	12.6783542	0.033	19.750±0.001	17.149±0.068	1.131±0.004	0.759±0.003	0.951±0.003	-0.022	1
574	NGVS-UCD574	NGVS-J123433.21+061047.7	l	188.6383554	6.1799130	0.019	21.325±0.004	···	0.884±0.011	0.590±0.007	0.744±0.013	0.078	1

Table 3 *continued*

Table 3 *(continued)*

ID	Name	NGVSID	t_{obs}	α_{J2000}	δ_{J2000}	$E(B-V)$	g_0	K	$(u^*-g)_0$	$(g-i)_0$	$(g-z)_0$	Δ_{env}	UCD
				(deg)	(deg)	(mag)	(mag)	(mag)	(mag)	(mag)	(mag)	(mag)	
(1)	(2)	(3)	(4)	(5)	(6)	(7)	(8)	(9)	(10)	(11)	(12)	(13)	(14)
575	NGVS-UCD575	NGVS-J123434.57+090628.8	l	188.6440267	9.1080057	0.022	21.113±0.003	···	0.969±0.009	0.617±0.006	0.748±0.009	0.027	1
576	NGVS-UCD576	NGVS-J123436.51+163152.4	s	188.6521113	16.5312172	0.030	18.073±0.004	···	···	···	0.701±0.011	0.215	0
577	NGVS-UCD577	NGVS-J123446.90+165239.7	s	188.6954364	16.8776856	0.029	17.790±0.003	···	···	···	0.738±0.009	0.177	0
578	NGVS-UCD578	NGVS-J123453.59+123915.7	l	188.7232921	12.6543712	0.034	19.172±0.001	15.912±0.023	1.449±0.003	0.993±0.002	1.217±0.002	0.016	1
579	NGVS-UCD579	NGVS-J123458.61+122052.0	l	188.7442107	12.3477740	0.036	21.396±0.004	···	0.954±0.013	0.679±0.010	0.811±0.011	0.006	1
580	NGVS-UCD580	NGVS-J123505.11+113730.4	l	188.7713004	11.6251084	0.045	19.292±0.001	15.699±0.018	1.680±0.004	1.179±0.002	1.447±0.002	-0.098	0
581	NGVS-UCD581	NGVS-J123509.57+135636.3	l	188.7898609	13.9434077	0.029	21.087±0.003	···	0.871±0.009	0.664±0.007	0.731±0.009	0.055	1
582	NGVS-UCD582	NGVS-J123514.70+121414.6	l	188.8112535	12.2373916	0.038	20.392±0.002	18.401±0.220	0.982±0.007	0.735±0.004	0.765±0.006	0.208	0
583	NGVS-UCD583	NGVS-J123515.60+171248.0	l	188.8150159	17.2133346	0.029	21.389±0.004	···	0.925±0.012	0.614±0.008	0.628±0.013	0.001	1
584	NGVS-UCD584	NGVS-J123515.91+113943.6	l	188.8162922	11.6621046	0.041	20.865±0.003	···	0.994±0.008	0.744±0.005	0.872±0.007	0.032	1
585	NGVS-UCD585	NGVS-J123519.41+161457.1	l	188.8308581	16.2491998	0.028	21.438±0.004	···	0.897±0.012	0.713±0.008	0.789±0.014	0.136	0
586	NGVS-UCD586	NGVS-J123521.64+123724.9	l	188.8401857	12.6235888	0.038	20.721±0.002	···	1.015±0.007	0.719±0.005	0.825±0.006	-0.041	1
587	NGVS-UCD587	NGVS-J123527.26+112939.2	l	188.8635753	11.4942176	0.040	20.692±0.002	···	0.995±0.007	0.736±0.004	0.851±0.006	0.070	0
588	NGVS-UCD588	NGVS-J123530.30+123824.3	l	188.8762704	12.6400855	0.040	19.133±0.001	16.550±0.041	1.146±0.003	0.822±0.002	0.928±0.002	0.006	1
589	NGVS-UCD589	NGVS-J123531.61+165200.2	l	188.8817025	16.8667122	0.029	20.274±0.002	···	0.984±0.006	0.611±0.004	0.702±0.006	0.051	0
590	NGVS-UCD590	NGVS-J123532.94+123151.4	l	188.8872576	12.5309508	0.040	20.094±0.002	17.514±0.098	1.188±0.005	0.775±0.003	0.919±0.004	0.005	1
591	NGVS-UCD591	NGVS-J123534.50+165610.7	l	188.8937691	16.9362971	0.030	19.752±0.001	···	0.897±0.005	0.606±0.003	0.698±0.004	0.180	0
592	NGVS-UCD592	NGVS-J123538.64+122428.1	l	188.9109818	12.4078104	0.039	21.480±0.004	···	0.879±0.013	0.679±0.009	0.796±0.012	0.029	0
593	NGVS-UCD593	NGVS-J123539.44+120056.7	l	188.9143227	12.0157471	0.053	20.908±0.003	18.198±0.168	1.021±0.009	0.746±0.005	0.863±0.007	0.006	1
594	NGVS-UCD594	NGVS-J123540.38+104159.0	l	188.9182489	10.6997324	0.024	20.235±0.001	18.128±0.156	0.903±0.005	0.595±0.003	0.659±0.005	0.085	0
595	NGVS-UCD595	NGVS-J123545.53+121053.1	l	188.9397110	12.1814137	0.043	20.398±0.002	18.245±0.201	0.978±0.007	0.682±0.004	0.774±0.005	0.162	0
596	NGVS-UCD596	NGVS-J123546.70+063956.1	l	188.9446027	6.6655908	0.020	21.422±0.004	···	0.989±0.014	0.677±0.008	0.769±0.016	0.082	0
597	NGVS-UCD597	NGVS-J123553.14+114054.8	l	188.9714233	11.6818993	0.038	20.620±0.002	···	0.949±0.007	0.686±0.005	0.787±0.006	0.113	0
598	NGVS-UCD598	NGVS-J123555.91+094039.7	l	188.9829637	9.6776872	0.021	20.493±0.002	···	0.898±0.006	0.556±0.004	0.646±0.006	-0.026	1
599	NGVS-UCD599	NGVS-J123557.34+081154.5	l	188.9889155	8.1984707	0.023	20.813±0.002	18.512±0.221	0.939±0.008	0.542±0.005	0.628±0.008	0.042	1
600	NGVS-UCD600	NGVS-J123605.25+114608.7	l	189.0218759	11.7690707	0.037	21.248±0.005	···	0.995±0.014	0.649±0.008	0.761±0.011	0.009	1
601	NGVS-UCD601	NGVS-J123608.04+111139.4	l	189.0335129	11.1942814	0.031	21.062±0.003	···	0.924±0.009	0.682±0.006	0.773±0.009	0.032	0
602	NGVS-UCD602	NGVS-J123611.76+170828.5	l	189.0489993	17.1412529	0.030	20.640±0.002	···	0.921±0.008	0.616±0.005	0.693±0.007	0.090	1
603	NGVS-UCD603	NGVS-J123612.00+165603.3	l	189.0500168	16.9342431	0.027	21.001±0.003	···	0.998±0.009	0.636±0.006	0.715±0.010	-0.027	1
604	NGVS-UCD604	NGVS-J123613.42+111443.2	l	189.0559242	11.2453250	0.032	21.428±0.004	···	1.024±0.012	0.754±0.007	0.892±0.011	0.030	1
605	NGVS-UCD605	NGVS-J123613.78+152348.4	l	189.0574186	15.3967897	0.032	21.255±0.003	···	0.924±0.010	0.615±0.007	0.674±0.012	-0.021	1
606	NGVS-UCD606	NGVS-J123614.74+110946.5	l	189.0614225	11.1629163	0.031	21.387±0.004	···	0.888±0.011	0.740±0.007	0.837±0.011	-0.002	1
607	NGVS-UCD607	NGVS-J123615.60+164317.5	l	189.0650112	16.7215310	0.027	19.931±0.001	···	0.950±0.005	0.733±0.003	0.840±0.004	0.170	0
608	NGVS-UCD608	NGVS-J123616.56+164023.8	l	189.0689995	16.6732657	0.028	21.299±0.004	···	1.106±0.014	0.744±0.007	0.847±0.012	-0.001	1
609	NGVS-UCD609	NGVS-J123617.61+045818.6	l	189.0733882	4.9718214	0.023	21.305±0.004	···	1.099±0.013	0.800±0.007	0.981±0.008	0.018	1
610	NGVS-UCD610	NGVS-J123621.51+163248.9	s	189.0896452	16.5469039	0.029	18.460±0.006	···	···	···	1.453±0.012	0.213	0
611	NGVS-UCD611	NGVS-J123627.34+053640.8	l	189.1139352	5.6113355	0.023	21.239±0.005	···	0.869±0.015	0.655±0.011	0.767±0.012	0.019	1
612	NGVS-UCD612	NGVS-J123628.33+164223.5	l	189.1180512	16.7065338	0.027	19.653±0.001	···	1.184±0.004	0.746±0.002	0.870±0.003	0.112	0
613	NGVS-UCD613	NGVS-J123628.88+144318.5	l	189.1203421	14.7217927	0.034	18.939±0.001	15.464±0.016	1.512±0.003	1.069±0.002	1.332±0.002	0.099	0
614	NGVS-UCD614	NGVS-J123630.31+161442.7	l	189.1263075	16.2452060	0.026	21.096±0.003	···	0.864±0.009	0.618±0.006	0.655±0.011	-0.018	1
615	NGVS-UCD615	NGVS-J123630.68+122912.0	l	189.1278371	12.4866764	0.045	21.255±0.004	···	1.075±0.012	0.778±0.007	0.884±0.009	-0.022	1
616	NGVS-UCD616	NGVS-J123632.59+123105.7	l	189.1358027	12.5182383	0.045	20.561±0.002	···	0.969±0.007	0.699±0.004	0.812±0.005	0.058	0
617	NGVS-UCD617	NGVS-J123635.04+161000.4	l	189.1460076	16.1667651	0.028	20.988±0.003	···	0.945±0.008	0.603±0.006	0.651±0.010	-0.028	1
618	NGVS-UCD618	NGVS-J123635.52+071801.5	l	189.1480029	7.3004169	0.022	21.425±0.003	···	0.952±0.012	0.736±0.007	0.861±0.012	0.038	1
619	NGVS-UCD619	NGVS-J123635.90+101832.4	l	189.1495893	10.3090055	0.020	21.090±0.003	···	0.964±0.009	0.514±0.007	0.678±0.010	0.002	1
620	NGVS-UCD620	NGVS-J123638.98+051732.7	l	189.1624324	5.2924298	0.022	21.241±0.004	···	0.922±0.013	0.686±0.008	0.727±0.012	0.019	0
621	NGVS-UCD621	NGVS-J123639.73+164131.4	l	189.1655554	16.6920536	0.027	20.640±0.002	···	1.054±0.008	0.752±0.004	0.808±0.007	0.018	1
622	NGVS-UCD622	NGVS-J123645.74+164132.0	s	189.1905715	16.6922328	0.027	18.728±0.007	···	···	···	1.385±0.014	0.251	0

Table 3 *continued*

Table 3 *(continued)*

ID	Name	NGVSID	$t_{\rm obs}$	$\alpha_{\rm J2000}$	$\delta_{\rm J2000}$	$E(B-V)$	g_0	K	$(u^*-g)_0$	$(g-i)_0$	$(g-z)_0$	$\Delta_{\rm env}$	UCD
				(deg)	(deg)	(mag)	(mag)	(mag)	(mag)	(mag)	(mag)	(mag)	
(1)	(2)	(3)	(4)	(5)	(6)	(7)	(8)	(9)	(10)	(11)	(12)	(13)	(14)
623	NGVS-UCD623	NGVS-J123648.39+073839.1	l	189.2016453	7.6441974	0.023	21.169±0.003	···	0.921±0.009	0.611±0.006	0.657±0.010	0.016	1
624	NGVS-UCD624	NGVS-J123653.27+100320.5	l	189.2219416	10.0557043	0.021	21.389±0.004	···	0.858±0.010	0.671±0.007	0.762±0.011	-0.029	1
625	NGVS-UCD625	NGVS-J123659.14+143816.6	l	189.2464299	14.6379545	0.031	20.665±0.002	···	0.906±0.007	0.568±0.005	0.695±0.008	0.031	1
626	NGVS-UCD626	NGVS-J123702.28+065531.2	s	189.2594838	6.9253217	0.023	16.547±0.002	···	···	-1.226±0.007	-1.180±0.011	0.137	0
627	NGVS-UCD627	NGVS-J123704.45+161639.1	l	189.2685218	16.2775386	0.027	19.279±0.001	···	0.958±0.003	0.661±0.002	0.744±0.003	0.239	0
628	NGVS-UCD628	NGVS-J123709.55+131131.0	l	189.2897924	13.1919454	0.047	21.296±0.005	···	0.986±0.014	0.683±0.010	0.750±0.013	-0.002	1
629	NGVS-UCD629	NGVS-J123714.20+171022.2	l	189.3091710	17.1728467	0.027	20.571±0.002	···	0.877±0.007	0.756±0.004	0.840±0.006	0.025	1
630	NGVS-UCD630	NGVS-J123716.00+094023.3	l	189.3166667	9.6731465	0.022	21.463±0.004	···	1.062±0.012	0.819±0.007	0.886±0.010	-0.051	1
631	NGVS-UCD631	NGVS-J123720.97+152220.0	s	189.3373698	15.3722309	0.039	18.689±0.005	15.511±0.020	1.757±0.022	···	1.373±0.013	0.154	0
632	NGVS-UCD632	NGVS-J123723.98+091245.2	l	189.3499033	9.2125633	0.024	20.872±0.002	···	0.967±0.008	0.709±0.005	0.800±0.007	0.045	1
633	NGVS-UCD633	NGVS-J123724.90+165029.4	l	189.3537366	16.8414902	0.027	19.318±0.001	···	1.129±0.003	0.827±0.002	0.977±0.002	0.152	0
634	NGVS-UCD634	NGVS-J123737.61+161353.4	l	189.4066902	16.2314879	0.032	21.311±0.004	···	0.983±0.010	0.784±0.007	0.865±0.011	0.003	1
635	NGVS-UCD635	NGVS-J123744.42+154126.2	l	189.4350733	15.6906006	0.035	20.841±0.003	···	0.933±0.009	0.696±0.007	0.832±0.009	0.065	1
636	NGVS-UCD636	NGVS-J123744.88+081405.7	l	189.4370188	8.2349203	0.024	21.108±0.003	···	0.935±0.009	0.570±0.006	0.644±0.010	0.007	1
637	NGVS-UCD637	NGVS-J123745.26+081839.5	l	189.4385813	8.3109678	0.025	21.415±0.003	···	0.939±0.011	0.591±0.007	0.718±0.011	0.036	0
638	NGVS-UCD638	NGVS-J123747.11+055126.0	l	189.4463033	5.8572117	0.020	21.159±0.003	···	0.979±0.010	0.635±0.006	0.761±0.011	0.029	1
639	NGVS-UCD639	NGVS-J123748.32+155705.0	l	189.4513362	15.9513920	0.042	21.284±0.004	···	0.918±0.012	0.705±0.007	0.808±0.013	-0.037	1
640	NGVS-UCD640	NGVS-J123749.09+052623.8	l	189.4545505	5.4399477	0.024	20.680±0.002	···	0.967±0.007	0.672±0.004	0.752±0.006	-0.007	1
641	NGVS-UCD641	NGVS-J123750.12+155745.5	l	189.4588265	15.9626429	0.042	21.333±0.004	···	0.987±0.012	0.650±0.008	0.765±0.013	-0.009	1
642	NGVS-UCD642	NGVS-J123752.21+112056.6	l	189.4675460	11.3490654	0.033	20.072±0.001	17.420±0.088	1.101±0.004	0.774±0.002	0.873±0.003	0.001	1
643	NGVS-UCD643	NGVS-J123752.90+141200.3	l	189.4704177	14.2000942	0.030	21.241±0.004	···	0.914±0.010	0.590±0.007	0.690±0.011	0.008	1
644	NGVS-UCD644	NGVS-J123759.11+115243.1	l	189.4962763	11.8786398	0.041	20.452±0.002	···	0.853±0.006	0.582±0.004	0.640±0.006	0.058	1
645	NGVS-UCD645	NGVS-J123800.35+144950.9	l	189.5014446	14.8307934	0.030	21.036±0.003	···	0.890±0.008	0.645±0.006	0.756±0.009	-0.002	1
646	NGVS-UCD646	NGVS-J123806.59+165412.8	l	189.5274448	16.9035669	0.026	21.420±0.004	···	1.072±0.013	0.816±0.007	0.941±0.011	0.035	1
647	NGVS-UCD647	NGVS-J123806.89+100956.0	l	189.5287213	10.1655536	0.020	17.864±0.000	17.253±0.067	0.700±0.001	-0.964±0.002	-0.825±0.002	0.161	0
648	NGVS-UCD648	NGVS-J123810.97+085318.0	l	189.5456965	8.8883441	0.023	20.984±0.003	18.374±0.221	1.000±0.010	0.716±0.007	0.816±0.008	0.024	1
649	NGVS-UCD649	NGVS-J123815.20+163142.8	l	189.5633365	16.5285616	0.025	19.344±0.001	···	1.418±0.004	1.001±0.002	1.123±0.003	0.094	0
650	NGVS-UCD650	NGVS-J123820.58+125034.0	l	189.5857605	12.8427729	0.046	19.395±0.001	···	0.947±0.004	0.609±0.002	0.653±0.003	0.081	1
651	NGVS-UCD651	NGVS-J123829.46+155942.1	l	189.6227410	15.9950375	0.040	21.119±0.004	···	0.880±0.011	0.595±0.009	0.676±0.014	0.013	1
652	NGVS-UCD652	NGVS-J123829.71+171621.6	l	189.6237883	17.2726546	0.024	20.901±0.005	···	0.885±0.016	0.700±0.011	0.820±0.018	-0.008	0
653	NGVS-UCD653	NGVS-J123831.11+092012.7	l	189.6296394	9.3368540	0.020	20.232±0.002	17.560±0.129	0.927±0.005	0.740±0.003	0.836±0.004	0.072	0
654	NGVS-UCD654	NGVS-J123833.20+165417.4	l	189.6383290	16.9048252	0.026	19.815±0.001	···	0.928±0.005	0.542±0.003	0.632±0.004	0.080	1
655	NGVS-UCD655	NGVS-J123833.88+063042.8	l	189.6411610	6.5118805	0.023	20.523±0.002	17.972±0.143	0.853±0.006	0.673±0.004	0.763±0.007	0.079	1
656	NGVS-UCD656	NGVS-J123844.99+151049.9	l	189.6874780	15.1805345	0.040	20.809±0.002	18.180±0.193	0.961±0.007	0.658±0.005	0.722±0.007	-0.026	1
657	NGVS-UCD657	NGVS-J123850.64+163357.0	l	189.7109956	16.5658212	0.025	21.096±0.003	···	0.853±0.008	0.569±0.006	0.681±0.010	-0.000	1
658	NGVS-UCD658	NGVS-J123851.17+171441.2	s	189.7132108	17.2447758	0.025	18.042±0.004	···	···	···	0.917±0.010	0.089	0
659	NGVS-UCD659	NGVS-J123851.96+155118.4	l	189.7164986	15.8551016	0.034	21.423±0.004	···	1.030±0.012	0.620±0.008	0.707±0.014	-0.020	1
660	NGVS-UCD660	NGVS-J123853.52+160511.9	l	189.7230003	16.0866458	0.034	21.490±0.005	···	0.915±0.014	0.769±0.008	0.869±0.014	0.017	1
661	NGVS-UCD661	NGVS-J123854.80+111015.1	l	189.7283288	11.1708549	0.028	20.324±0.002	17.854±0.121	1.029±0.005	0.747±0.003	0.862±0.004	0.001	1
662	NGVS-UCD662	NGVS-J123856.77+115949.5	l	189.7365607	11.9970937	0.039	20.819±0.002	18.192±0.177	1.018±0.008	0.762±0.005	0.840±0.007	0.050	1
663	NGVS-UCD663	NGVS-J123900.49+144342.3	s	189.7520365	14.7284293	0.028	17.498±0.003	15.213±0.016	···	···	0.787±0.007	-0.071	0
664	NGVS-UCD664	NGVS-J123909.32+112147.9	l	189.7888329	11.3633175	0.033	21.039±0.003	18.112±0.148	1.385±0.010	0.952±0.005	1.106±0.007	0.009	1
665	NGVS-UCD665	NGVS-J123912.84+142926.2	l	189.8034986	14.4906039	0.025	21.266±0.004	···	0.901±0.009	0.785±0.007	0.873±0.010	-0.035	1
666	NGVS-UCD666	NGVS-J123913.75+163341.2	l	189.8073094	16.5614463	0.024	19.457±0.001	···	0.858±0.003	0.606±0.002	0.628±0.003	0.023	0
667	NGVS-UCD667	NGVS-J123914.09+164334.7	l	189.8086893	16.7263143	0.023	21.420±0.004	···	0.983±0.012	0.648±0.008	0.760±0.013	0.012	1
668	NGVS-UCD668	NGVS-J123914.37+143325.9	l	189.8098604	14.5572037	0.025	21.474±0.004	···	0.996±0.011	0.560±0.009	0.662±0.014	0.048	1
669	NGVS-UCD669	NGVS-J123914.62+115754.3	l	189.8109028	11.9650757	0.039	21.407±0.004	···	0.925±0.011	0.668±0.007	0.758±0.011	-0.000	0
670	NGVS-UCD670	NGVS-J123923.52+170458.5	l	189.8479846	17.0829204	0.027	21.338±0.004	···	0.972±0.011	0.658±0.007	0.701±0.012	-0.029	1

Table 3 *continued*

Table 3 *(continued)*

ID	Name	NGVSID	t_{obs}	α_{J2000}	δ_{J2000}	$E(B-V)$	g_0	K	$(u^*-g)_0$	$(g-i)_0$	$(g-z)_0$	Δ_{env}	UCD
				(deg)	(deg)	(mag)	(mag)	(mag)	(mag)	(mag)	(mag)	(mag)	
(1)	(2)	(3)	(4)	(5)	(6)	(7)	(8)	(9)	(10)	(11)	(12)	(13)	(14)
671	NGVS-UCD671	NGVS-J123924.92+152142.2	s	189.8538188	15.3617096	0.038	18.479±0.005	14.866±0.010	1.648±0.023	···	1.408±0.011	0.148	0
672	NGVS-UCD672	NGVS-J123928.77+162929.9	s	189.8698615	16.4916417	0.025	17.707±0.005	···	···	···	1.410±0.010	0.195	0
673	NGVS-UCD673	NGVS-J123932.84+140623.7	l	189.8868368	14.1065914	0.031	21.153±0.003	18.779±0.292	0.861±0.011	0.606±0.007	0.664±0.011	0.033	1
674	NGVS-UCD674	NGVS-J123945.88+095248.5	l	189.9411546	9.8801380	0.017	21.216±0.004	···	1.005±0.013	0.711±0.008	0.815±0.012	0.015	1
675	NGVS-UCD675	NGVS-J123947.35+133210.7	l	189.9472726	13.5363073	0.031	18.942±0.001	15.518±0.017	1.483±0.004	1.100±0.002	1.277±0.002	-0.019	0
676	NGVS-UCD676	NGVS-J123948.51+162356.4	s	189.9521445	16.3989891	0.026	18.122±0.004	···	···	···	1.498±0.008	0.122	0
677	NGVS-UCD677	NGVS-J123950.58+095035.3	l	189.9607446	9.8431440	0.017	21.333±0.005	···	0.905±0.013	0.579±0.009	0.656±0.014	0.030	1
678	NGVS-UCD678	NGVS-J123952.57+095606.8	l	189.9690598	9.9352293	0.017	21.395±0.004	···	0.929±0.012	0.652±0.008	0.709±0.012	-0.021	0
679	NGVS-UCD679	NGVS-J123955.25+165757.0	l	189.9802123	16.9658366	0.022	20.566±0.002	···	0.935±0.008	0.747±0.005	0.874±0.007	0.026	1
680	NGVS-UCD680	NGVS-J124006.60+140100.0	l	190.0275117	14.0166799	0.038	20.922±0.003	···	0.878±0.008	0.664±0.005	0.718±0.009	-0.207	1
681	NGVS-UCD681	NGVS-J124010.88+103426.6	l	190.0453392	10.5740572	0.029	21.466±0.004	···	0.996±0.013	0.552±0.009	0.639±0.013	0.012	1
682	NGVS-UCD682	NGVS-J124011.25+095346.0	s	190.0468696	9.8961028	0.017	18.367±0.003	15.447±0.013	1.231±0.013	0.826±0.010	1.077±0.013	0.684	0
683	NGVS-UCD683	NGVS-J124013.49+101938.9	l	190.0562181	10.3274795	0.019	21.438±0.004	···	0.941±0.012	0.564±0.009	0.674±0.013	0.031	1
684	NGVS-UCD684	NGVS-J124017.00+074503.4	l	190.0708208	7.7509519	0.028	21.384±0.004	19.021±0.342	1.009±0.013	0.734±0.007	0.785±0.010	-0.027	1
685	NGVS-UCD685	NGVS-J124018.91+164629.9	s	190.0787760	16.7749779	0.022	16.291±0.001	···	···	···	0.913±0.004	0.229	0
686	NGVS-UCD686	NGVS-J124023.72+153719.3	s	190.0988130	15.6220173	0.037	17.303±0.002	14.834±0.009	1.484±0.008	···	1.087±0.006	-0.042	0
687	NGVS-UCD687	NGVS-J124030.56+060057.1	l	190.1273165	6.0158558	0.023	20.759±0.002	18.161±0.187	0.890±0.009	0.591±0.005	0.788±0.010	0.018	1
688	NGVS-UCD688	NGVS-J124031.80+112923.4	l	190.1325002	11.4898208	0.043	20.243±0.002	17.222±0.075	1.402±0.006	0.907±0.003	1.140±0.004	0.059	1
689	NGVS-UCD689	NGVS-J124033.75+055829.6	l	190.1406219	5.9748817	0.024	21.219±0.003	···	0.907±0.010	0.652±0.006	0.816±0.011	-0.008	1
690	NGVS-UCD690	NGVS-J124034.06+165939.4	l	190.1419150	16.9942703	0.023	21.124±0.004	···	1.010±0.013	0.759±0.007	0.906±0.012	0.017	1
691	NGVS-UCD691	NGVS-J124041.95+141546.4	l	190.1747751	14.2628896	0.039	20.807±0.003	···	0.910±0.010	0.645±0.007	0.688±0.009	0.088	0
692	NGVS-UCD692	NGVS-J124045.66+161546.6	s	190.1902401	16.2629552	0.021	17.644±0.003	···	1.737±0.015	···	1.406±0.007	0.247	0
693	NGVS-UCD693	NGVS-J124045.75+132350.7	l	190.1906157	13.3974226	0.027	21.318±0.004	···	1.023±0.012	0.596±0.007	0.670±0.010	0.025	1
694	NGVS-UCD694	NGVS-J124046.32+102433.4	l	190.1929844	10.4092665	0.023	21.346±0.004	···	0.886±0.010	0.725±0.007	0.752±0.010	0.009	1
695	NGVS-UCD695	NGVS-J124048.36+154122.8	l	190.2015042	15.6896652	0.037	21.419±0.004	···	0.899±0.012	0.702±0.008	0.797±0.014	0.014	1
696	NGVS-UCD696	NGVS-J124049.54+121138.1	l	190.2064072	12.1939068	0.039	21.202±0.003	18.342±0.196	1.183±0.011	0.918±0.005	1.043±0.008	0.041	1
697	NGVS-UCD697	NGVS-J124056.21+114940.2	l	190.2342181	11.8278312	0.029	20.908±0.002	18.630±0.266	0.931±0.008	0.719±0.005	0.852±0.007	0.106	1
698	NGVS-UCD698	NGVS-J124059.92+064806.8	l	190.2496846	6.8018810	0.022	21.169±0.003	···	0.962±0.010	0.761±0.006	0.881±0.008	-0.016	1
699	NGVS-UCD699	NGVS-J124100.98+163521.2	l	190.2540983	16.5892248	0.024	20.934±0.002	···	0.928±0.008	0.798±0.005	0.886±0.008	0.031	1
700	NGVS-UCD700	NGVS-J124103.48+091044.8	l	190.2645014	9.1791139	0.020	21.106±0.003	···	0.915±0.010	0.638±0.007	0.763±0.009	0.062	1
701	NGVS-UCD701	NGVS-J124105.98+164434.4	l	190.2749064	16.7428795	0.022	21.254±0.003	···	0.865±0.010	0.630±0.007	0.678±0.013	-0.056	1
702	NGVS-UCD702	NGVS-J124106.60+063341.9	l	190.2774805	6.5616338	0.021	21.021±0.004	···	1.004±0.013	0.639±0.009	0.767±0.013	0.054	1
703	NGVS-UCD703	NGVS-J124108.94+100732.3	l	190.2872529	10.1256346	0.018	20.790±0.002	18.254±0.155	0.931±0.008	0.668±0.005	0.772±0.008	0.001	1
704	NGVS-UCD704	NGVS-J124110.20+100748.9	l	190.2924889	10.1302417	0.018	21.215±0.004	18.608±0.215	1.027±0.012	0.713±0.008	0.806±0.010	0.044	1
705	NGVS-UCD705	NGVS-J124115.49+103811.9	l	190.3145415	10.6366475	0.024	21.260±0.003	18.209±0.149	1.097±0.011	0.826±0.006	0.985±0.009	0.021	1
706	NGVS-UCD706	NGVS-J124122.00+114658.8	l	190.3416759	11.7830032	0.029	21.224±0.003	···	0.983±0.012	0.634±0.007	0.785±0.014	0.016	1
707	NGVS-UCD707	NGVS-J124123.55+162856.4	s	190.3481308	16.4823372	0.021	17.858±0.004	···	···	···	1.481±0.008	0.252	0
708	NGVS-UCD708	NGVS-J124124.71+164806.7	l	190.3529510	16.8018714	0.021	20.252±0.002	···	1.114±0.006	0.737±0.003	0.893±0.005	0.108	1
709	NGVS-UCD709	NGVS-J124127.81+061321.8	l	190.3658805	6.2227092	0.023	20.555±0.002	18.027±0.141	1.020±0.007	0.588±0.004	0.701±0.007	0.028	1
710	NGVS-UCD710	NGVS-J124130.44+054710.4	s	190.3768414	5.7862313	0.024	18.332±0.009	15.943±0.023	···	···	1.040±0.020	-0.010	0
711	NGVS-UCD711	NGVS-J124134.58+145228.6	l	190.3940729	14.8746235	0.028	20.241±0.002	17.784±0.161	0.978±0.005	0.589±0.004	0.706±0.005	0.044	1
712	NGVS-UCD712	NGVS-J124136.28+162025.5	s	190.4011620	16.3404194	0.021	18.555±0.005	···	···	···	1.497±0.010	0.027	0
713	NGVS-UCD713	NGVS-J124136.68+132811.0	s	190.4028373	13.4697300	0.025	17.462±0.003	17.154±0.069	···	···	-0.409±0.011	-0.053	0
714	NGVS-UCD714	NGVS-J124137.65+134055.9	s	190.4068840	13.6821828	0.026	16.841±0.002	14.427±0.007	···	···	0.959±0.006	-0.044	0
715	NGVS-UCD715	NGVS-J124138.40+144540.1	l	190.4099883	14.7611252	0.030	21.409±0.005	···	0.855±0.012	0.710±0.011	0.811±0.014	0.009	0
716	NGVS-UCD716	NGVS-J124139.52+114011.6	l	190.4146865	11.6698947	0.033	20.833±0.002	17.973±0.141	1.395±0.009	0.976±0.004	1.223±0.005	0.007	1
717	NGVS-UCD717	NGVS-J124144.70+125609.8	l	190.4362389	12.9360516	0.031	21.098±0.003	···	1.070±0.012	0.782±0.006	0.881±0.008	0.027	1
718	NGVS-UCD718	NGVS-J124149.12+164309.1	l	190.4546582	16.7191929	0.021	21.495±0.004	···	0.969±0.012	0.589±0.008	0.647±0.014	-0.019	1

Table 3 *continued*

Table 3 *(continued)*

ID	Name	NGVSID	t_{obs}	α_{J2000}	δ_{J2000}	$E(B-V)$	g_0	K	$(u^*-g)_0$	$(g-i)_0$	$(g-z)_0$	Δ_{env}	UCD
				(deg)	(deg)	(mag)	(mag)	(mag)	(mag)	(mag)	(mag)	(mag)	
(1)	(2)	(3)	(4)	(5)	(6)	(7)	(8)	(9)	(10)	(11)	(12)	(13)	(14)
719	NGVS-UCD719	NGVS-J124155.34+114003.8	s	190.4805689	11.6677212	0.033	17.899±0.003	14.535±0.007	1.600±0.013	1.070±0.007	1.352±0.008	0.072	1
720	NGVS-UCD720	NGVS-J124205.30+103959.1	l	190.5220991	10.6664070	0.026	21.366±0.003	···	0.953±0.010	0.687±0.007	0.772±0.010	0.027	1
721	NGVS-UCD721	NGVS-J124206.57+162221.1	s	190.5273792	16.3725199	0.022	16.861±0.002	···	···	···	0.956±0.004	-0.036	0
722	NGVS-UCD722	NGVS-J124206.89+115144.7	l	190.5287016	11.8624190	0.028	20.862±0.002	···	1.086±0.007	0.782±0.004	0.902±0.006	0.017	1
723	NGVS-UCD723	NGVS-J124209.61+113654.7	l	190.5400246	11.6151888	0.030	20.830±0.002	18.485±0.215	1.023±0.007	0.735±0.004	0.817±0.006	0.015	1
724	NGVS-UCD724	NGVS-J124210.53+143348.5	l	190.5438883	14.5634640	0.025	21.387±0.004	···	1.022±0.011	0.616±0.008	0.677±0.013	-0.017	1
725	NGVS-UCD725	NGVS-J124211.05+113841.3	s	190.5460471	11.6447937	0.032	16.712±0.002	13.331±0.003	1.575±0.007	1.059±0.003	1.334±0.004	0.036	1
726	NGVS-UCD726	NGVS-J124211.75+161246.2	l	190.5489417	16.2128224	0.024	19.622±0.001	···	0.959±0.004	0.599±0.003	0.659±0.004	0.045	0
727	NGVS-UCD727	NGVS-J124217.54+105412.9	l	190.5730806	10.9035807	0.023	21.345±0.003	···	1.086±0.010	0.777±0.006	0.889±0.009	-0.010	1
728	NGVS-UCD728	NGVS-J124221.92+145928.1	l	190.5913533	14.9911501	0.022	21.157±0.003	···	0.983±0.009	0.545±0.007	0.630±0.012	0.078	1
729	NGVS-UCD729	NGVS-J124226.57+101623.3	l	190.6107179	10.2731396	0.018	20.727±0.002	18.276±0.153	0.918±0.008	0.678±0.004	0.737±0.007	0.023	1
730	NGVS-UCD730	NGVS-J124229.83+112029.7	l	190.6242758	11.3415871	0.027	19.875±0.001	17.279±0.079	1.143±0.004	0.787±0.002	0.919±0.003	0.002	1
731	NGVS-UCD731	NGVS-J124232.60+115702.6	l	190.6358256	11.9507163	0.028	21.063±0.003	···	0.986±0.008	0.735±0.005	0.836±0.008	-0.004	1
732	NGVS-UCD732	NGVS-J124235.74+114254.2	l	190.6489118	11.7150453	0.030	21.312±0.003	···	1.141±0.011	0.840±0.006	1.015±0.008	0.011	1
733	NGVS-UCD733	NGVS-J124238.75+115646.8	l	190.6614439	11.9463314	0.028	21.499±0.004	···	0.884±0.011	0.670±0.008	0.726±0.012	0.013	0
734	NGVS-UCD734	NGVS-J124246.72+145651.5	l	190.6946825	14.9476362	0.020	21.327±0.003	···	0.968±0.011	0.570±0.007	0.633±0.013	0.027	1
735	NGVS-UCD735	NGVS-J124248.01+115513.8	l	190.7000359	11.9204879	0.027	19.711±0.001	17.321±0.079	0.999±0.003	0.774±0.002	0.871±0.003	0.076	1
736	NGVS-UCD736	NGVS-J124251.12+113716.0	l	190.7130040	11.6211223	0.028	18.909±0.001	15.706±0.020	1.452±0.002	0.966±0.001	1.195±0.001	0.015	1
737	NGVS-UCD737	NGVS-J124259.12+074313.7	l	190.7463225	7.7204739	0.023	21.328±0.004	···	0.985±0.014	0.490±0.009	0.622±0.017	0.021	1
738	NGVS-UCD738	NGVS-J124300.05+101739.2	s	190.7502032	10.2942253	0.020	16.565±0.001	14.426±0.006	···	···	0.749±0.004	-0.037	0
739	NGVS-UCD739	NGVS-J124303.41+112718.6	l	190.7642081	11.4551632	0.025	20.960±0.002	18.247±0.188	1.036±0.007	0.708±0.004	0.777±0.007	-0.005	1
740	NGVS-UCD740	NGVS-J124304.03+170017.5	l	190.7668101	17.0048610	0.026	20.024±0.002	···	0.870±0.005	0.741±0.004	0.843±0.005	0.067	0
741	NGVS-UCD741	NGVS-J124307.70+114705.3	l	190.7820776	11.7848163	0.025	20.153±0.001	18.110±0.166	0.914±0.006	0.675±0.004	0.755±0.005	0.138	1
742	NGVS-UCD742	NGVS-J124311.06+080932.8	s	190.7960968	8.1591206	0.023	18.187±0.003	14.686±0.008	···	···	1.320±0.009	0.100	0
743	NGVS-UCD743	NGVS-J124312.34+170842.7	l	190.8014359	17.1452075	0.024	19.153±0.001	···	0.868±0.003	0.676±0.002	0.791±0.002	0.135	0
744	NGVS-UCD744	NGVS-J124312.47+111230.2	l	190.8019424	11.2083931	0.030	21.202±0.003	18.540±0.220	1.120±0.011	0.701±0.006	0.823±0.009	0.018	1
745	NGVS-UCD745	NGVS-J124312.75+092744.5	l	190.8031226	9.4623669	0.017	20.697±0.002	···	0.966±0.007	0.707±0.004	0.840±0.007	0.079	1
746	NGVS-UCD746	NGVS-J124315.49+113922.8	l	190.8145574	11.6563462	0.027	20.619±0.002	···	0.989±0.005	0.623±0.004	0.733±0.005	-0.006	1
747	NGVS-UCD747	NGVS-J124324.30+112343.2	l	190.8512567	11.3953461	0.024	20.693±0.002	18.196±0.167	0.964±0.006	0.694±0.004	0.763±0.006	0.040	1
748	NGVS-UCD748	NGVS-J124325.85+162350.6	l	190.8577084	16.3973796	0.026	20.783±0.003	···	1.078±0.009	0.686±0.005	0.820±0.008	0.017	1
749	NGVS-UCD749	NGVS-J124328.03+085314.8	l	190.8667867	8.8874400	0.020	21.344±0.004	···	0.964±0.013	0.753±0.008	0.857±0.013	0.139	1
750	NGVS-UCD750	NGVS-J124329.00+163811.3	l	190.8708218	16.6364660	0.023	21.484±0.004	···	0.969±0.013	0.702±0.008	0.817±0.013	0.002	1
751	NGVS-UCD751	NGVS-J124329.84+164041.0	l	190.8743188	16.6780616	0.023	20.968±0.003	···	0.928±0.009	0.656±0.005	0.788±0.009	-0.024	1
752	NGVS-UCD752	NGVS-J124330.18+123044.9	l	190.8757461	12.5124825	0.031	20.189±0.001	17.328±0.089	1.352±0.006	0.877±0.003	1.050±0.003	0.044	1
753	NGVS-UCD753	NGVS-J124335.97+113204.7	s	190.8998699	11.5346389	0.026	17.362±0.003	13.820±0.006	1.723±0.013	1.075±0.006	1.359±0.007	0.011	1
754	NGVS-UCD754	NGVS-J124338.51+113027.5	l	190.9104473	11.5076489	0.026	20.789±0.002	···	1.043±0.008	0.718±0.005	0.813±0.007	0.031	1
755	NGVS-UCD755	NGVS-J124338.94+114545.6	l	190.9122299	11.7626746	0.024	21.220±0.004	···	1.011±0.013	0.610±0.008	0.748±0.012	0.035	1
756	NGVS-UCD756	NGVS-J124338.94+131533.7	l	190.9122311	13.2593550	0.026	20.669±0.002	···	0.970±0.008	0.592±0.007	0.647±0.007	0.032	1
757	NGVS-UCD757	NGVS-J124339.44+162207.9	l	190.9143344	16.3688585	0.027	20.180±0.001	···	0.933±0.005	0.714±0.003	0.818±0.005	0.010	1
758	NGVS-UCD758	NGVS-J124343.16+102551.4	l	190.9298418	10.4309451	0.025	20.859±0.002	···	0.952±0.008	0.607±0.005	0.691±0.008	0.064	1
759	NGVS-UCD759	NGVS-J124345.03+111438.7	l	190.9376059	11.2440866	0.032	21.134±0.003	···	0.939±0.009	0.664±0.006	0.781±0.009	0.052	1
760	NGVS-UCD760	NGVS-J124348.51+143027.4	l	190.9521355	14.5076168	0.026	20.930±0.003	···	0.910±0.008	0.769±0.005	0.853±0.008	0.038	0
761	NGVS-UCD761	NGVS-J124352.42+112534.2	l	190.9684091	11.4261669	0.024	18.740±0.001	15.707±0.020	1.389±0.002	0.929±0.001	1.112±0.001	0.037	1
762	NGVS-UCD762	NGVS-J124352.48+112518.3	l	190.9686634	11.4217508	0.025	20.222±0.001	17.926±0.143	1.049±0.005	0.734±0.003	0.823±0.004	0.005	1
763	NGVS-UCD763	NGVS-J124359.12+092921.7	l	190.9963401	9.4893565	0.019	21.070±0.003	···	0.927±0.010	0.632±0.007	0.684±0.013	0.032	1
764	NGVS-UCD764	NGVS-J124407.29+160212.5	l	191.0303583	16.0368050	0.035	20.828±0.003	···	1.084±0.010	0.760±0.006	0.870±0.011	0.064	1
765	NGVS-UCD765	NGVS-J124408.54+161144.2	l	191.0355665	16.1956173	0.034	21.128±0.003	···	0.858±0.009	0.663±0.006	0.683±0.011	-0.400	0
766	NGVS-UCD766	NGVS-J124410.20+113443.2	l	191.0424886	11.5786578	0.030	19.425±0.001	16.981±0.062	1.106±0.003	0.750±0.002	0.842±0.002	0.073	1

Table 3 *continued*

Table 3 *(continued)*

ID	Name	NGVSID	$t_{\rm obs}$	$\alpha_{\rm J2000}$	$\delta_{\rm J2000}$	$E(B-V)$	g_0	K	$(u^*-g)_0$	$(g-i)_0$	$(g-z)_0$	$\Delta_{\rm env}$	UCD
				(deg)	(deg)	(mag)	(mag)	(mag)	(mag)	(mag)	(mag)	(mag)	
(1)	(2)	(3)	(4)	(5)	(6)	(7)	(8)	(9)	(10)	(11)	(12)	(13)	(14)
767	NGVS-UCD767	NGVS-J124415.46+162756.8	l	191.0644052	16.4657738	0.028	19.860±0.001	···	1.026±0.004	0.835±0.002	0.903±0.003	-0.028	1
768	NGVS-UCD768	NGVS-J124424.66+163755.1	l	191.1027439	16.6319708	0.026	20.891±0.002	···	1.152±0.009	0.828±0.005	1.021±0.007	-0.029	1
769	NGVS-UCD769	NGVS-J124426.53+111429.1	l	191.1105412	11.2414219	0.032	19.112±0.001	15.849±0.020	1.537±0.004	1.013±0.002	1.271±0.002	0.151	1
770	NGVS-UCD770	NGVS-J124435.24+170536.5	l	191.1468499	17.0934678	0.029	20.456±0.002	···	0.854±0.006	0.581±0.004	0.646±0.007	-0.016	1
771	NGVS-UCD771	NGVS-J124437.85+103801.1	l	191.1577272	10.6336481	0.026	19.914±0.001	17.185±0.066	1.085±0.004	0.816±0.002	0.932±0.003	0.042	1
772	NGVS-UCD772	NGVS-J124441.48+134556.5	l	191.1728164	13.7656955	0.025	20.088±0.001	17.519±0.103	1.057±0.005	0.773±0.003	0.864±0.004	0.043	1
773	NGVS-UCD773	NGVS-J124442.72+105518.8	l	191.1779999	10.9218846	0.027	21.388±0.003	···	0.888±0.011	0.691±0.007	0.723±0.011	0.006	1
774	NGVS-UCD774	NGVS-J124443.41+113428.4	l	191.1808612	11.5745425	0.028	21.116±0.003	18.216±0.170	1.087±0.008	0.833±0.005	0.959±0.007	-0.015	1
775	NGVS-UCD775	NGVS-J124453.66+161844.2	l	191.2235956	16.3122815	0.032	21.380±0.004	···	0.870±0.011	0.631±0.008	0.683±0.013	-0.051	1
776	NGVS-UCD776	NGVS-J124501.48+153820.6	l	191.2561512	15.6390669	0.031	20.886±0.002	18.197±0.184	1.060±0.009	0.723±0.005	0.872±0.009	0.050	1
777	NGVS-UCD777	NGVS-J124507.32+075531.0	l	191.2804803	7.9252887	0.025	20.813±0.003	18.220±0.193	1.117±0.009	0.741±0.005	0.785±0.008	0.016	1
778	NGVS-UCD778	NGVS-J124507.33+081059.9	l	191.2805406	8.1832996	0.024	20.912±0.003	···	0.907±0.009	0.624±0.005	0.624±0.010	0.015	1
779	NGVS-UCD779	NGVS-J124507.76+160014.8	l	191.2823129	16.0041102	0.035	21.288±0.004	···	0.918±0.010	0.699±0.007	0.765±0.013	-0.040	1
780	NGVS-UCD780	NGVS-J124508.16+163921.2	l	191.2840084	16.6558842	0.027	19.898±0.001	···	0.935±0.004	0.781±0.003	0.900±0.004	0.039	1
781	NGVS-UCD781	NGVS-J124524.02+110535.2	l	191.3500929	11.0930994	0.031	19.339±0.001	16.367±0.033	1.368±0.003	0.983±0.002	1.091±0.002	0.012	1
782	NGVS-UCD782	NGVS-J124530.83+165944.9	l	191.3784533	16.9957940	0.027	21.065±0.004	···	0.965±0.012	0.640±0.007	0.786±0.012	0.089	1
783	NGVS-UCD783	NGVS-J124531.21+112357.2	l	191.3800543	11.3992236	0.027	20.251±0.001	17.630±0.099	1.058±0.005	0.763±0.003	0.840±0.004	0.069	1
784	NGVS-UCD784	NGVS-J124539.33+104808.1	l	191.4138693	10.8022486	0.024	19.904±0.001	17.169±0.069	1.216±0.005	0.861±0.003	0.990±0.003	0.056	1
785	NGVS-UCD785	NGVS-J124541.65+165251.3	l	191.4235512	16.8809196	0.027	20.946±0.003	···	0.961±0.011	0.674±0.006	0.767±0.010	0.000	1
786	NGVS-UCD786	NGVS-J124544.65+112322.0	l	191.4360366	11.3894441	0.028	20.863±0.002	18.039±0.149	1.201±0.009	0.818±0.005	0.969±0.006	0.020	1
787	NGVS-UCD787	NGVS-J124547.81+165530.5	l	191.4492284	16.9251381	0.027	19.691±0.001	···	0.922±0.004	0.661±0.003	0.764±0.004	0.134	0
788	NGVS-UCD788	NGVS-J124549.18+151735.1	l	191.4549111	15.2930911	0.029	20.809±0.002	18.104±0.176	0.973±0.006	0.672±0.004	0.788±0.007	0.063	1
789	NGVS-UCD789	NGVS-J124558.10+113823.4	l	191.4920663	11.6398254	0.026	20.690±0.002	18.335±0.199	0.989±0.007	0.691±0.005	0.803±0.006	0.007	1
790	NGVS-UCD790	NGVS-J124600.72+162007.1	l	191.5030068	16.3353118	0.034	21.365±0.004	···	0.902±0.011	0.550±0.008	0.622±0.014	-0.029	1
791	NGVS-UCD791	NGVS-J124609.71+170816.8	s	191.5404543	17.1380007	0.028	17.373±0.005	···	···	···	0.775±0.014	-0.019	0
792	NGVS-UCD792	NGVS-J124611.03+130946.2	l	191.5459425	13.1628222	0.029	21.315±0.004	···	0.957±0.013	0.540±0.009	0.623±0.011	-0.011	1
793	NGVS-UCD793	NGVS-J124641.86+123033.9	l	191.6744104	12.5094257	0.025	21.475±0.005	···	0.866±0.013	0.745±0.009	0.819±0.011	-0.022	1
794	NGVS-UCD794	NGVS-J124647.46+161328.4	l	191.6977490	16.2245691	0.031	21.464±0.004	···	1.100±0.014	0.678±0.009	0.782±0.012	0.059	1
795	NGVS-UCD795	NGVS-J124648.98+103929.4	l	191.7040753	10.6581669	0.023	21.336±0.004	···	1.048±0.012	0.609±0.008	0.754±0.010	-0.008	1
796	NGVS-UCD796	NGVS-J124703.19+125831.1	l	191.7633059	12.9753170	0.025	20.575±0.002	···	0.985±0.007	0.671±0.004	0.764±0.006	0.035	1
797	NGVS-UCD797	NGVS-J124704.12+113150.8	l	191.7671809	11.5307833	0.026	21.066±0.005	18.343±0.248	0.920±0.011	0.679±0.009	0.810±0.013	-0.022	1
798	NGVS-UCD798	NGVS-J124734.17+104110.1	l	191.8923641	10.6861465	0.030	20.855±0.002	18.301±0.227	0.926±0.008	0.753±0.005	0.844±0.007	0.057	1
799	NGVS-UCD799	NGVS-J124739.73+095308.6	s	191.9155519	9.8857264	0.024	17.495±0.003	13.906±0.005	···	···	1.433±0.007	0.283	0
800	NGVS-UCD800	NGVS-J124749.30+145532.7	l	191.9553979	14.9257459	0.034	21.072±0.003	···	0.853±0.010	0.659±0.006	0.717±0.010	-0.001	1
801	NGVS-UCD801	NGVS-J124752.09+102509.7	l	191.9670282	10.4193705	0.024	21.199±0.004	···	0.903±0.012	0.624±0.008	0.726±0.012	-0.028	1
802	NGVS-UCD802	NGVS-J124754.47+111237.1	l	191.9769690	11.2103089	0.033	21.202±0.004	···	0.977±0.012	0.700±0.008	0.866±0.013	-0.008	1
803	NGVS-UCD803	NGVS-J124754.94+105200.9	l	191.9788998	10.8669236	0.051	20.191±0.002	17.541±0.108	0.941±0.007	0.733±0.004	0.842±0.007	0.144	1
804	NGVS-UCD804	NGVS-J124758.72+113736.1	l	191.9946806	11.6266888	0.028	21.477±0.004	···	0.938±0.016	0.782±0.009	0.881±0.012	0.002	1
805	NGVS-UCD805	NGVS-J124809.95+110006.5	l	192.0414730	11.0018167	0.039	21.019±0.003	···	1.190±0.010	0.710±0.006	0.847±0.008	-0.005	1
806	NGVS-UCD806	NGVS-J124814.49+090150.5	l	192.0603767	9.0306912	0.027	21.309±0.005	···	0.882±0.014	0.799±0.009	0.844±0.012	-0.049	1
807	NGVS-UCD807	NGVS-J124822.23+102004.8	l	192.0926170	10.3346662	0.025	20.873±0.003	···	0.928±0.009	0.729±0.006	0.831±0.008	0.006	1
808	NGVS-UCD808	NGVS-J124858.01+145103.7	l	192.2417282	14.8510293	0.029	20.829±0.002	···	1.016±0.009	0.570±0.006	0.702±0.008	-0.023	1
809	NGVS-UCD809	NGVS-J124929.62+160701.6	l	192.3734025	16.1171211	0.022	20.569±0.002	···	0.946±0.006	0.667±0.004	0.778±0.006	0.028	0
810	NGVS-UCD810	NGVS-J124937.36+144236.8	l	192.4056494	14.7102139	0.025	19.980±0.001	17.460±0.118	0.925±0.005	0.661±0.003	0.777±0.004	0.027	0
811	NGVS-UCD811	NGVS-J124949.05+135211.4	l	192.4543748	13.8698308	0.029	20.950±0.003	18.239±0.192	1.037±0.009	0.720±0.005	0.819±0.007	0.003	1
812	NGVS-UCD812	NGVS-J125006.01+112711.5	l	192.5250319	11.4531995	0.038	20.950±0.003	···	0.936±0.009	0.583±0.005	0.629±0.008	-0.009	1
813	NGVS-UCD813	NGVS-J125059.09+132028.8	l	192.7461992	13.3413362	0.030	19.296±0.001	15.792±0.024	1.645±0.004	1.063±0.002	1.335±0.002	0.064	0
814	NGVS-UCD814	NGVS-J125137.43+104622.4	l	192.9059442	10.7729003	0.022	21.486±0.005	···	0.943±0.014	0.722±0.008	0.747±0.013	-0.006	1

Table 3 *continued*

Table 3 *(continued)*

ID	Name	NGVSID	$t_{\rm obs}$	$\alpha_{\rm J2000}$	$\delta_{\rm J2000}$	$E(B-V)$	g_0	K	$(u^*-g)_0$	$(g-i)_0$	$(g-z)_0$	$\Delta_{\rm env}$	UCD
				(deg)	(deg)	(mag)	(mag)	(mag)	(mag)	(mag)	(mag)	(mag)	
(1)	(2)	(3)	(4)	(5)	(6)	(7)	(8)	(9)	(10)	(11)	(12)	(13)	(14)
815	NGVS-UCD815	NGVS-J125152.07+124102.0	l	192.9669586	12.6838826	0.027	20.873±0.003	···	0.853±0.009	0.632±0.005	0.624±0.008	-0.040	1
816	NGVS-UCD816	NGVS-J125215.24+121841.8	l	193.0635041	12.3116237	0.033	20.655±0.002	···	0.891±0.007	0.619±0.005	0.650±0.008	0.054	0
817	NGVS-UCD817	NGVS-J125234.27+141144.4	l	193.1428115	14.1956617	0.042	21.171±0.004	17.433±0.099	1.638±0.015	1.193±0.005	1.439±0.007	-0.009	1
818	NGVS-UCD818	NGVS-J125242.92+133745.5	l	193.1788394	13.6292929	0.035	21.258±0.004	···	0.928±0.013	0.633±0.007	0.699±0.010	-0.029	1
819	NGVS-UCD819	NGVS-J125250.00+111553.3	l	193.2083351	11.2648039	0.022	19.829±0.001	17.544±0.107	1.025±0.004	0.709±0.002	0.792±0.003	-0.016	1
820	NGVS-UCD820	NGVS-J125327.03+140122.8	l	193.3626044	14.0230120	0.031	21.472±0.004	···	0.991±0.012	0.661±0.008	0.732±0.012	0.057	1
821	NGVS-UCD821	NGVS-J122950.77+112235.0	l	187.4615359	11.3763935	0.036	21.363±0.004	···	0.076±0.008	-0.606±0.017	-0.573±0.025	0.035	1
822	NGVS-UCD822	NGVS-J123624.21+112633.1	l	189.1008577	11.4425184	0.034	21.317±0.004	17.890±0.134	1.333±0.013	0.875±0.006	1.104±0.008	-0.050	1
823	NGVS-UCD823	NGVS-J122950.49+132820.7	l	187.4603637	13.4724052	0.029	21.377±0.005	18.241±0.183	1.326±0.016	1.068±0.007	1.226±0.009	-0.053	1
824	NGVS-UCD824	NGVS-J122711.41+155347.0	l	186.7975472	15.8963901	0.031	20.773±0.002	17.871±0.181	0.823±0.011	0.538±0.008	0.659±0.011	0.674	0
825	NGVS-UCD825	NGVS-J122504.03+114158.0	l	186.2667939	11.6994346	0.035	21.171±0.003	17.816±0.114	1.466±0.014	1.086±0.007	1.353±0.007	0.045	1
826	NGVS-UCD826	NGVS-J122340.56+121242.6	l	185.9190022	12.2118292	0.029	21.385±0.003	18.157±0.160	1.416±0.013	0.995±0.007	1.222±0.007	0.016	1
827	NGVS-UCD827	NGVS-J122523.34+123532.5	l	186.3472705	12.5923520	0.035	20.402±0.002	17.499±0.094	1.346±0.006	0.977±0.003	1.183±0.004	0.058	1
828	NGVS-UCD828	NGVS-J122445.65+130259.8	l	186.1902227	13.0499427	0.035	20.658±0.002	17.846±0.132	1.254±0.009	0.901±0.004	1.075±0.006	0.082	1

NOTE– (1) Identification number; (2) UCD name; (3) Object name in NGVS catalog; (4) Exposure time: l = selected using long exposure data; s = selected using short exposure data; (5) Right ascension in decimal degrees; (6) Declination in decimal degrees; (7) Galactic extinction according to Schlegel et al. (1998); (8) Galactic extinction-corrected, aperture-corrected g-band magnitude found within a 16 pixels ($\sim$ 3-arcsec) diameter aperture. For details, see Liu et al. (2015a); (9) UKIDSS (Lawrence et al. 2007) K-band magnitude within a 3-arcsec diameter aperture; (10-12) Color index measured in an 8-pixel ($\sim$ 1.5-arcsec) diameter aperture, Galactic extinction corrected; (13) Envelop parameter: $\Delta_{\rm env} \equiv g_{16} - g_{32}$, where g_{16} and g_{32} are magnitudes in 16- and 32-pixel diameter apertures; (14) Object flag: 0=contaminant, 1=confirmed or possible UCD.

Table 4. Structural Properties and Other Information for UCD Candidates

Name	M_B	M_V	$\langle r_h \rangle$	$\log(M_*/M_{odot})$	v_r	$v_{\rm source}$	Class	Envelope	Method	OtherName
	(mag)	(mag)	(pc)		(km/s)					
(1)	(2)	(3)	(4)	(5)	(6)	(7)	(8)	(9)	(10)	(11)
NGVS-UCD1	-11.62	-11.38	14.03± 0.39	6.5	-38	SDSS	5	0	$(v_r < 3500\mathrm{km/s}) + \langle r_h \rangle$	···
NGVS-UCD2	-9.68	-9.21	29.86± 0.76	6.3	···	···	1	0	$u^*gz + \langle \mu_g \rangle_e + \langle r_h \rangle$	···
NGVS-UCD3	-9.27	-8.76	15.34± 0.38	6.1	···	···	1	0	$u^*gz + \langle \mu_g \rangle_e + \langle r_h \rangle$	···
NGVS-UCD4	-9.70	-9.27	29.48± 0.54	6.2	···	···	1	0	$u^*gz + \langle \mu_g \rangle_e + \langle r_h \rangle$	···
NGVS-UCD5	-9.33	-8.80	22.44± 0.28	6.1	···	···	3	0	$u^*gz + \langle \mu_g \rangle_e + \langle r_h \rangle$	···
NGVS-UCD6	-9.36	-8.93	24.29± 1.07	6.0	···	···	1	0	$u^*gz + \langle \mu_g \rangle_e + \langle r_h \rangle$	···
NGVS-UCD7	-9.40	-8.97	24.51± 0.37	6.1	···	···	1	0	$u^*gz + \langle \mu_g \rangle_e + \langle r_h \rangle$	···
NGVS-UCD8	-9.41	-8.95	23.33± 0.37	6.2	···	···	1	0	$u^*gz + \langle \mu_g \rangle_e + \langle r_h \rangle$	···
NGVS-UCD9	-9.30	-8.80	25.00± 0.68	6.2	···	···	1	0	$u^*gz + \langle \mu_g \rangle_e + \langle r_h \rangle$	···
NGVS-UCD10	-11.80	-11.39	65.92± 0.72	7.0	···	···	3	0	$u^*gz + \langle \mu_g \rangle_e + \langle r_h \rangle$	···
NGVS-UCD11	-11.00	-10.57	28.65± 0.68	6.8	···	···	1	0	$u^*gz + \langle \mu_g \rangle_e + \langle r_h \rangle$	···
NGVS-UCD12	-10.76	-9.97	11.48± 0.43	7.1	···	···	3	0	$u^*gz + \langle \mu_g \rangle_e + \langle r_h \rangle$	···
NGVS-UCD13	-9.74	-9.33	24.07± 0.44	6.2	···	···	1	0	$u^*gz + \langle \mu_g \rangle_e + \langle r_h \rangle$	···
NGVS-UCD14	-9.65	-9.18	20.57± 0.25	6.3	···	···	2	0	$u^*gz + \langle \mu_g \rangle_e + \langle r_h \rangle$	···
NGVS-UCD15	-9.41	-8.82	17.05± 0.64	6.3	···	···	1	0	$u^*gz + \langle \mu_g \rangle_e + \langle r_h \rangle$	···
NGVS-UCD16	-10.56	-10.16	37.04± 0.41	6.5	···	···	1	0	$u^*gz + \langle \mu_g \rangle_e + \langle r_h \rangle$	···
NGVS-UCD17	-10.34	-9.57	12.89± 0.52	7.0	···	···	5	0	$u^*gzK + \langle \mu_g \rangle_e + \langle r_h \rangle$	···
NGVS-UCD18	-10.21	-9.51	14.74± 0.36	6.8	···	···	1	0	$u^*gzK + \langle \mu_g \rangle_e + \langle r_h \rangle$	···
NGVS-UCD19	-9.26	-8.83	22.16± 0.50	6.0	···	···	1	0	$u^*gz + \langle \mu_g \rangle_e + \langle r_h \rangle$	···
NGVS-UCD20	-9.35	-8.87	24.18± 0.52	6.1	···	···	1	0	$u^*gz + \langle \mu_g \rangle_e + \langle r_h \rangle$	···
NGVS-UCD21	···	···	21.28± 0.12	7.7	···	···	5	0	$gzK + \langle \mu_g \rangle_e + r_{h,g}$	···
NGVS-UCD22	-10.19	-9.73	33.92± 1.32	6.4	···	···	3	0	$u^*gz + \langle \mu_g \rangle_e + \langle r_h \rangle$	···
NGVS-UCD23	-11.14	-10.28	17.83± 0.60	7.3	···	···	3	0	$u^*gzK + \langle \mu_g \rangle_e + \langle r_h \rangle$	···
NGVS-UCD24	-10.91	-10.17	15.83± 0.38	7.0	···	···	1	0	$u^*gzK + \langle \mu_g \rangle_e + \langle r_h \rangle$	···
NGVS-UCD25	-9.70	-9.30	27.89± 0.68	6.2	···	···	1	0	$u^*gz + \langle \mu_g \rangle_e + \langle r_h \rangle$	···
NGVS-UCD26	-9.38	-8.85	20.21± 0.46	6.2	···	···	1	0	$u^*gz + \langle \mu_g \rangle_e + \langle r_h \rangle$	···
NGVS-UCD27	-10.11	-9.69	26.68± 0.22	6.3	···	···	1	0	$u^*gzK + \langle \mu_g \rangle_e + \langle r_h \rangle$	···
NGVS-UCD28	-9.22	-8.70	21.83± 0.66	6.1	···	···	1	0	$u^*gz + \langle \mu_g \rangle_e + \langle r_h \rangle$	···
NGVS-UCD29	-9.49	-9.03	24.73± 0.35	6.1	···	···	1	0	$u^*gz + \langle \mu_g \rangle_e + \langle r_h \rangle$	···
NGVS-UCD30	-10.72	-10.31	37.03± 1.07	6.6	···	···	3	0	$u^*gzK + \langle \mu_g \rangle_e + \langle r_h \rangle$	···
NGVS-UCD31	-9.78	-9.30	28.03± 0.31	6.4	···	···	1	0	$u^*gzK + \langle \mu_g \rangle_e + \langle r_h \rangle$	···
NGVS-UCD32	-9.43	-9.03	14.31± 0.37	6.1	···	···	1	0	$u^*gz + \langle \mu_g \rangle_e + \langle r_h \rangle$	···
NGVS-UCD33	-9.66	-9.19	19.95± 0.72	6.2	···	···	3	0	$u^*gz + \langle \mu_g \rangle_e + \langle r_h \rangle$	···
NGVS-UCD34	-10.33	-9.93	38.42± 0.58	6.5	···	···	1	0	$u^*gzK + \langle \mu_g \rangle_e + \langle r_h \rangle$	···
NGVS-UCD35	-9.28	-8.86	20.88± 0.73	6.0	···	···	1	0	$u^*gz + \langle \mu_g \rangle_e + \langle r_h \rangle$	···
NGVS-UCD36	-9.42	-8.96	26.05± 0.59	6.1	···	···	1	0	$u^*gz + \langle \mu_g \rangle_e + \langle r_h \rangle$	···
NGVS-UCD37	-9.82	-9.40	27.70± 0.32	6.2	···	···	1	0	$u^*gz + \langle \mu_g \rangle_e + \langle r_h \rangle$	···
NGVS-UCD38	-9.30	-8.87	23.32± 0.69	6.1	···	···	3	0	$u^*gz + \langle \mu_g \rangle_e + \langle r_h \rangle$	···
NGVS-UCD39	-9.92	-9.51	14.56± 0.22	6.3	···	···	1	0	$u^*gz + \langle \mu_g \rangle_e + \langle r_h \rangle$	···
NGVS-UCD40	-9.55	-9.09	29.57± 1.14	6.2	···	···	3	0	$u^*gz + \langle \mu_g \rangle_e + \langle r_h \rangle$	···
NGVS-UCD41	···	···	40.07± 2.35	7.4	12656	SDSS,NED	3	0	$gzK + \langle \mu_g \rangle_e + r_{h,g}$	···
NGVS-UCD42	-10.48	-10.01	38.17± 0.79	6.6	···	···	1	0	$u^*gzK + \langle \mu_g \rangle_e + \langle r_h \rangle$	···
NGVS-UCD43	-11.95	-11.51	52.91± 1.22	7.2	···	···	3	0	$u^*gz + \langle \mu_g \rangle_e + \langle r_h \rangle$	···
NGVS-UCD44	-9.26	-8.82	17.31± 0.23	6.1	···	···	1	0	$u^*gz + \langle \mu_g \rangle_e + \langle r_h \rangle$	···
NGVS-UCD45	-9.61	-9.18	18.58± 0.76	6.2	···	···	3	0	$u^*gz + \langle \mu_g \rangle_e + \langle r_h \rangle$	···
NGVS-UCD46	-9.74	-9.20	26.94± 0.38	6.4	···	···	1	0	$u^*gz + \langle \mu_g \rangle_e + \langle r_h \rangle$	···

Table 4 *continued*

Table 4 *(continued)*

Name	M_B	M_V	$\langle r_h \rangle$	$\log(M_*/M_{odot})$	v_r	$v_{\rm source}$	Class	Envelope	Method	OtherName
	(mag)	(mag)	(pc)		(km/s)					
(1)	(2)	(3)	(4)	(5)	(6)	(7)	(8)	(9)	(10)	(11)
NGVS-UCD47	-10.00	-9.48	11.67± 0.83	6.5	···	···	4	0	$u^*gzK + \langle\mu_g\rangle_e + \langle r_h\rangle$	···
NGVS-UCD48	-9.83	-9.40	25.25± 0.64	6.3	···	···	1	0	$u^*gz + \langle\mu_g\rangle_e + \langle r_h\rangle$	···
NGVS-UCD49	-9.43	-8.87	20.52± 0.41	6.2	···	···	1	0	$u^*gz + \langle\mu_g\rangle_e + \langle r_h\rangle$	···
NGVS-UCD50	-10.90	-10.54	12.71± 0.34	6.6	394	SDSS	6	0	$(v_r < 3500\mathrm{km/s}) + \langle r_h\rangle$	···
NGVS-UCD51	-9.57	-9.13	18.56± 0.41	6.2	···	···	1	0	$u^*gz + \langle\mu_g\rangle_e + \langle r_h\rangle$	···
NGVS-UCD52	-9.41	-8.99	12.87± 0.44	6.2	···	···	1	0	$u^*gz + \langle\mu_g\rangle_e + \langle r_h\rangle$	···
NGVS-UCD53	-9.26	-8.76	23.58± 0.34	6.2	···	···	1	0	$u^*gz + \langle\mu_g\rangle_e + \langle r_h\rangle$	···
NGVS-UCD54	-9.47	-8.97	18.15± 0.28	6.2	···	···	1	0	$u^*gz + \langle\mu_g\rangle_e + \langle r_h\rangle$	···
NGVS-UCD55	-9.46	-9.05	26.95± 1.00	6.1	···	···	1	0	$u^*gz + \langle\mu_g\rangle_e + \langle r_h\rangle$	···
NGVS-UCD56	-9.67	-9.19	24.19± 0.34	6.3	···	···	1	0	$u^*gz + \langle\mu_g\rangle_e + \langle r_h\rangle$	···
NGVS-UCD57	-10.23	-9.80	28.40± 0.39	6.5	···	···	1	0	$u^*gzK + \langle\mu_g\rangle_e + \langle r_h\rangle$	···
NGVS-UCD58	-9.72	-9.24	26.69± 0.50	6.2	···	···	3	0	$u^*gz + \langle\mu_g\rangle_e + \langle r_h\rangle$	···
NGVS-UCD59	-9.37	-8.96	19.92± 0.55	6.1	···	···	3	0	$u^*gz + \langle\mu_g\rangle_e + \langle r_h\rangle$	···
NGVS-UCD60	-9.94	-9.51	29.59± 0.41	6.3	···	···	1	0	$u^*gz + \langle\mu_g\rangle_e + \langle r_h\rangle$	···
NGVS-UCD61	···	···	39.31± 0.82	7.4	20630	SDSS,NED	3	0	$gzK + \langle\mu_g\rangle_e + r_{h,g}$	···
NGVS-UCD62	-9.77	-9.29	27.95± 1.33	6.3	···	···	3	0	$u^*gz + \langle\mu_g\rangle_e + \langle r_h\rangle$	···
NGVS-UCD63	-10.37	-10.32	34.57± 2.60	5.6	-81	SDSS,NED	6	0	$(v_r < 3500\mathrm{km/s}) + \langle r_h\rangle$	···
NGVS-UCD64	-9.37	-8.92	22.20± 0.45	6.1	···	···	1	0	$u^*gz + \langle\mu_g\rangle_e + \langle r_h\rangle$	···
NGVS-UCD65	···	···	27.82± 1.37	6.8	1259	VCC,SDSS,NED	2	0	$(v_r < 3500\mathrm{km/s}) + \langle r_h\rangle$	VCC-216
NGVS-UCD66	-9.28	-8.77	19.63± 0.37	6.1	···	···	1	0	$u^*gz + \langle\mu_g\rangle_e + \langle r_h\rangle$	···
NGVS-UCD67	-9.29	-8.78	15.07± 0.44	6.2	···	···	1	0	$u^*gz + \langle\mu_g\rangle_e + \langle r_h\rangle$	···
NGVS-UCD68	-9.36	-8.95	11.32± 0.26	6.0	···	···	1	0	$u^*gz + \langle\mu_g\rangle_e + \langle r_h\rangle$	···
NGVS-UCD69	-9.21	-8.70	22.20± 1.11	6.1	···	···	3	0	$u^*gz + \langle\mu_g\rangle_e + \langle r_h\rangle$	···
NGVS-UCD70	-9.33	-8.89	21.40± 0.62	6.1	···	···	1	0	$u^*gz + \langle\mu_g\rangle_e + \langle r_h\rangle$	···
NGVS-UCD71	-9.40	-8.93	19.57± 0.51	6.2	···	···	1	0	$u^*gz + \langle\mu_g\rangle_e + \langle r_h\rangle$	···
NGVS-UCD72	-10.70	-10.15	34.32± 0.48	6.7	···	···	3	0	$u^*gz + \langle\mu_g\rangle_e + \langle r_h\rangle$	···
NGVS-UCD73	···	···	14.98± 0.71	7.2	7601	NTT17	3	0	$gz + \langle\mu_g\rangle_e + r_{h,g}$	···
NGVS-UCD74	-9.64	-9.21	22.79± 0.42	6.2	···	···	1	0	$u^*gzK + \langle\mu_g\rangle_e + \langle r_h\rangle$	···
NGVS-UCD75	-9.45	-8.91	23.34± 0.33	6.2	···	···	1	0	$u^*gz + \langle\mu_g\rangle_e + \langle r_h\rangle$	···
NGVS-UCD76	-9.52	-9.08	26.51± 1.08	6.2	···	···	3	0	$u^*gz + \langle\mu_g\rangle_e + \langle r_h\rangle$	···
NGVS-UCD77	-9.26	-8.79	18.85± 0.48	6.1	···	···	1	0	$u^*gz + \langle\mu_g\rangle_e + \langle r_h\rangle$	···
NGVS-UCD78	-12.73	-12.62	44.43± 1.42	7.0	2505	NED	6	0	$(v_r < 3500\mathrm{km/s}) + \langle r_h\rangle$	···
NGVS-UCD79	-9.71	-9.22	24.18± 0.64	6.2	···	···	1	0	$u^*gz + \langle\mu_g\rangle_e + \langle r_h\rangle$	···
NGVS-UCD80	-9.62	-9.18	26.61± 0.80	6.2	···	···	3	0	$u^*gz + \langle\mu_g\rangle_e + \langle r_h\rangle$	···
NGVS-UCD81	-9.44	-9.03	20.86± 0.39	6.1	···	···	1	0	$u^*gz + \langle\mu_g\rangle_e + \langle r_h\rangle$	···
NGVS-UCD82	-9.53	-9.08	23.87± 0.46	6.2	···	···	1	0	$u^*gz + \langle\mu_g\rangle_e + \langle r_h\rangle$	···
NGVS-UCD83	-10.64	-10.20	43.53± 0.66	6.7	···	···	1	0	$u^*gz + \langle\mu_g\rangle_e + \langle r_h\rangle$	···
NGVS-UCD84	-9.93	-9.28	12.01± 0.29	6.6	···	···	1	0	$u^*gzK + \langle\mu_g\rangle_e + \langle r_h\rangle$	···
NGVS-UCD85	-10.04	-9.63	16.97± 0.31	6.3	···	···	1	0	$u^*gz + \langle\mu_g\rangle_e + \langle r_h\rangle$	···
NGVS-UCD86	-9.56	-9.05	11.62± 0.70	6.3	···	···	3	0	$u^*gz + \langle\mu_g\rangle_e + \langle r_h\rangle$	···
NGVS-UCD87	-9.33	-8.84	18.37± 0.33	6.1	···	···	1	0	$u^*gz + \langle\mu_g\rangle_e + \langle r_h\rangle$	···
NGVS-UCD88	-9.83	-9.36	29.54± 0.83	6.4	···	···	3	0	$u^*gz + \langle\mu_g\rangle_e + \langle r_h\rangle$	···
NGVS-UCD89	-9.67	-9.15	28.14± 0.43	6.3	···	···	1	0	$u^*gz + \langle\mu_g\rangle_e + \langle r_h\rangle$	···
NGVS-UCD90	-10.05	-9.65	22.06± 0.31	6.3	···	···	1	0	$u^*gz + \langle\mu_g\rangle_e + \langle r_h\rangle$	···
NGVS-UCD91	-11.02	-10.60	31.96± 0.90	6.8	···	···	3	0	$u^*gz + \langle\mu_g\rangle_e + \langle r_h\rangle$	···
NGVS-UCD92	-11.89	-11.08	28.09± 0.67	7.6	17671	NTT17	3	0	$u^*gzK + \langle\mu_g\rangle_e + \langle r_h\rangle$	···
NGVS-UCD93	···	···	91.28± 6.85	8.9	2074	VCC,NED	2	0	$(v_r < 3500\mathrm{km/s}) + \langle r_h\rangle$	VCC-373
NGVS-UCD94	-10.12	-9.63	24.77± 0.70	6.5	···	···	1	0	$u^*gz + \langle\mu_g\rangle_e + \langle r_h\rangle$	···

Table 4 *continued*

Table 4 *(continued)*

Name	M_B	M_V	$\langle r_h \rangle$	$\log(M_*/M_{odot})$	v_r	$v_{\rm source}$	Class	Envelope	Method	OtherName
	(mag)	(mag)	(pc)		(km/s)					
(1)	(2)	(3)	(4)	(5)	(6)	(7)	(8)	(9)	(10)	(11)
NGVS-UCD95	-10.12	-9.67	23.33± 0.48	6.5	···	···	1	0	$u^*gz + \langle\mu_g\rangle_e + \langle r_h\rangle$	···
NGVS-UCD96	-10.37	-9.65	14.20± 0.29	6.9	···	···	1	1	$u^*gzK + \langle\mu_g\rangle_e + \langle r_h\rangle$	···
NGVS-UCD97	-9.36	-8.88	21.29± 0.54	6.1	···	···	1	0	$u^*gz + \langle\mu_g\rangle_e + \langle r_h\rangle$	···
NGVS-UCD98	-10.43	-9.59	12.24± 0.21	7.0	20296	AAT12	3	0	$u^*gzK + \langle\mu_g\rangle_e + \langle r_h\rangle$	···
NGVS-UCD99	-9.98	-9.58	33.54± 0.86	6.3	···	···	1	0	$u^*gz + \langle\mu_g\rangle_e + \langle r_h\rangle$	···
NGVS-UCD100	-12.08	-11.22	33.15± 0.31	7.7	20104	SDSS,NED	3	0	$u^*gzK + \langle\mu_g\rangle_e + \langle r_h\rangle$	···
NGVS-UCD101	-9.59	-9.11	13.06± 0.64	6.2	1182	VCC,NED	2	0	$u^*gz + \langle\mu_g\rangle_e + \langle r_h\rangle$	VCC-426
NGVS-UCD102	-9.29	-8.81	20.77± 0.53	6.1	···	···	3	0	$u^*gzK + \langle\mu_g\rangle_e + \langle r_h\rangle$	···
NGVS-UCD103	-9.65	-9.20	26.51± 0.43	6.2	···	···	1	0	$u^*gz + \langle\mu_g\rangle_e + \langle r_h\rangle$	···
NGVS-UCD104	-9.82	-9.32	31.63± 0.57	6.3	···	···	1	0	$u^*gz + \langle\mu_g\rangle_e + \langle r_h\rangle$	···
NGVS-UCD105	-9.38	-8.96	21.10± 0.60	6.1	···	···	1	0	$u^*gz + \langle\mu_g\rangle_e + \langle r_h\rangle$	···
NGVS-UCD106	-9.84	-9.38	27.73± 0.50	6.3	···	···	1	0	$u^*gz + \langle\mu_g\rangle_e + \langle r_h\rangle$	···
NGVS-UCD107	-10.23	-9.78	32.58± 0.65	6.4	···	···	1	0	$u^*gzK + \langle\mu_g\rangle_e + \langle r_h\rangle$	···
NGVS-UCD108	-9.33	-8.82	22.08± 0.53	6.2	···	···	1	0	$u^*gz + \langle\mu_g\rangle_e + \langle r_h\rangle$	···
NGVS-UCD109	-9.38	-8.92	23.68± 0.56	6.2	···	···	3	0	$u^*gz + \langle\mu_g\rangle_e + \langle r_h\rangle$	···
NGVS-UCD110	-9.60	-9.18	21.03± 0.55	6.2	···	···	1	0	$u^*gz + \langle\mu_g\rangle_e + \langle r_h\rangle$	···
NGVS-UCD111	-9.38	-8.88	24.60± 0.41	6.1	···	···	1	0	$u^*gz + \langle\mu_g\rangle_e + \langle r_h\rangle$	···
NGVS-UCD112	-9.91	-9.35	16.75± 0.54	6.4	···	···	1	1	$u^*gz + \langle\mu_g\rangle_e + \langle r_h\rangle$	···
NGVS-UCD113	-9.63	-9.14	20.35± 0.67	6.2	···	···	1	0	$u^*gz + \langle\mu_g\rangle_e + \langle r_h\rangle$	···
NGVS-UCD114	-9.67	-9.17	27.05± 0.64	6.3	···	···	1	0	$u^*gz + \langle\mu_g\rangle_e + \langle r_h\rangle$	···
NGVS-UCD115	-9.37	-8.95	15.79± 0.22	6.1	···	···	1	0	$u^*gz + \langle\mu_g\rangle_e + \langle r_h\rangle$	···
NGVS-UCD116	···	···	27.06± 2.51	7.0	1255	VCC,SDSS,NED	2	0	$(v_r < 3500\mathrm{km/s}) + \langle r_h\rangle$	VCC-490
NGVS-UCD117	-11.11	-11.17	93.67± 2.33	6.1	211	NED	6	0	$(v_r < 3500\mathrm{km/s}) + \langle r_h\rangle$	···
NGVS-UCD118	-9.68	-9.24	23.11± 0.42	6.2	···	···	1	0	$u^*gz + \langle\mu_g\rangle_e + \langle r_h\rangle$	···
NGVS-UCD119	-9.89	-9.41	13.87± 0.21	6.4	···	···	1	0	$u^*gzK + \langle\mu_g\rangle_e + \langle r_h\rangle$	···
NGVS-UCD120	-9.46	-8.99	16.18± 0.45	6.2	···	···	1	0	$u^*gz + \langle\mu_g\rangle_e + \langle r_h\rangle$	···
NGVS-UCD121	-9.58	-9.13	18.14± 0.53	6.2	···	···	3	0	$u^*gzK + \langle\mu_g\rangle_e + \langle r_h\rangle$	···
NGVS-UCD122	-9.64	-9.12	24.76± 1.01	6.3	···	···	3	0	$u^*gz + \langle\mu_g\rangle_e + \langle r_h\rangle$	···
NGVS-UCD123	-9.36	-8.83	16.58± 0.34	6.2	···	···	1	0	$u^*gzK + \langle\mu_g\rangle_e + \langle r_h\rangle$	···
NGVS-UCD124	-9.55	-9.14	21.12± 0.45	6.2	···	···	1	0	$u^*gzK + \langle\mu_g\rangle_e + \langle r_h\rangle$	···
NGVS-UCD125	-9.54	-9.08	18.17± 0.38	6.2	···	···	1	0	$u^*gzK + \langle\mu_g\rangle_e + \langle r_h\rangle$	···
NGVS-UCD126	-9.43	-9.02	21.61± 0.43	6.1	···	···	1	0	$u^*gz + \langle\mu_g\rangle_e + \langle r_h\rangle$	···
NGVS-UCD127	-9.67	-9.25	29.16± 0.38	6.2	···	···	1	0	$u^*gz + \langle\mu_g\rangle_e + \langle r_h\rangle$	···
NGVS-UCD128	-11.38	-11.22	36.18± 0.08	6.1	44	NED	6	0	$(v_r < 3500\mathrm{km/s}) + \langle r_h\rangle$	···
NGVS-UCD129	-9.55	-9.14	24.94± 0.63	6.1	···	···	1	0	$u^*gz + \langle\mu_g\rangle_e + \langle r_h\rangle$	···
NGVS-UCD130	-9.48	-9.05	20.76± 0.57	6.2	···	···	1	0	$u^*gz + \langle\mu_g\rangle_e + \langle r_h\rangle$	···
NGVS-UCD131	-9.54	-9.13	23.69± 1.00	6.1	···	···	3	0	$u^*gz + \langle\mu_g\rangle_e + \langle r_h\rangle$	···
NGVS-UCD132	-9.31	-8.84	20.72± 0.47	6.2	···	···	1	0	$u^*gz + \langle\mu_g\rangle_e + \langle r_h\rangle$	···
NGVS-UCD133	-9.43	-8.99	21.04± 0.66	6.1	···	···	1	0	$u^*gz + \langle\mu_g\rangle_e + \langle r_h\rangle$	···
NGVS-UCD134	-9.55	-9.00	19.55± 0.51	6.3	···	···	3	0	$u^*gzK + \langle\mu_g\rangle_e + \langle r_h\rangle$	···
NGVS-UCD135	-11.10	-10.44	13.55± 0.36	7.1	-103	NTT17	5	0	$u^*gzK + \langle\mu_g\rangle_e + \langle r_h\rangle$	···
NGVS-UCD136	-10.17	-9.55	13.16± 0.30	6.7	···	···	5	0	$u^*gzK + \langle\mu_g\rangle_e + \langle r_h\rangle$	···
NGVS-UCD137	-10.91	-10.87	23.06± 1.06	6.1	1478	NED	6	0	$(v_r < 3500\mathrm{km/s}) + \langle r_h\rangle$	···
NGVS-UCD138	-9.65	-9.17	34.78± 0.97	6.2	···	···	1	0	$u^*gz + \langle\mu_g\rangle_e + \langle r_h\rangle$	···
NGVS-UCD139	-10.30	-9.74	11.27± 0.29	6.6	878	MMT09	1	0	$u^*gzK + \langle\mu_g\rangle_e + \langle r_h\rangle$	···
NGVS-UCD140	-9.66	-9.22	24.92± 0.49	6.2	···	···	1	0	$u^*gz + \langle\mu_g\rangle_e + \langle r_h\rangle$	···
NGVS-UCD141	-9.34	-8.76	12.29± 0.58	6.2	2080	Toloba2018	2	0	$u^*gz + \langle\mu_g\rangle_e + \langle r_h\rangle$	VCC-615
NGVS-UCD142	-9.39	-8.97	19.34± 0.53	6.1	···	···	1	0	$u^*gz + \langle\mu_g\rangle_e + \langle r_h\rangle$	···

Table 4 *continued*

Table 4 *(continued)*

Name	M_B	M_V	$\langle r_h \rangle$	$\log(M_*/M_{odot})$	v_r	$v_{\rm source}$	Class	Envelope	Method	OtherName
	(mag)	(mag)	(pc)		(km/s)					
(1)	(2)	(3)	(4)	(5)	(6)	(7)	(8)	(9)	(10)	(11)
NGVS-UCD143	-9.64	-9.16	20.81± 1.15	6.2	···	···	3	0	$u^*gz + \langle\mu_g\rangle_e + \langle r_h\rangle$	···
NGVS-UCD144	-9.34	-8.82	23.37± 0.03	6.1	···	···	3	0	$u^*gz + \langle\mu_g\rangle_e + \langle r_h\rangle$	···
NGVS-UCD145	-10.24	-9.77	39.00± 0.68	6.6	···	···	1	1	$u^*gz + \langle\mu_g\rangle_e + \langle r_h\rangle$	···
NGVS-UCD146	-9.26	-8.82	15.11± 0.22	6.1	38777	SDSS	3	0	$u^*gz + \langle\mu_g\rangle_e + \langle r_h\rangle$	···
NGVS-UCD147	-11.02	-10.16	23.73± 0.53	7.3	···	···	1	1	$u^*gzK + \langle\mu_g\rangle_e + \langle r_h\rangle$	···
NGVS-UCD148	-10.29	-9.86	22.35± 0.35	6.5	···	···	1	0	$u^*gz + \langle\mu_g\rangle_e + \langle r_h\rangle$	···
NGVS-UCD149	-9.48	-8.99	25.85± 0.63	6.2	···	···	3	0	$u^*gz + \langle\mu_g\rangle_e + \langle r_h\rangle$	···
NGVS-UCD150	-9.56	-9.16	17.36± 0.38	6.2	···	···	1	0	$u^*gz + \langle\mu_g\rangle_e + \langle r_h\rangle$	···
NGVS-UCD151	-11.43	-10.91	21.80± 0.18	7.0	836	AAT12	2	0	$u^*gzK + \langle\mu_g\rangle_e + \langle r_h\rangle$	VCC-650
NGVS-UCD152	-10.41	-9.90	12.62± 0.34	6.6	1008	SIMBAD	1	0	$u^*gzK + \langle\mu_g\rangle_e + \langle r_h\rangle$	···
NGVS-UCD153	-13.06	-12.22	48.65± 0.61	8.1	12711	SDSS,NED	3	0	$u^*gzK + \langle\mu_g\rangle_e + \langle r_h\rangle$	···
NGVS-UCD154	-9.39	-8.94	11.42± 0.30	6.1	···	···	1	0	$u^*gz + \langle\mu_g\rangle_e + \langle r_h\rangle$	···
NGVS-UCD155	-9.42	-8.96	16.14± 0.47	6.1	···	···	1	0	$u^*gz + \langle\mu_g\rangle_e + \langle r_h\rangle$	···
NGVS-UCD156	-9.34	-8.87	12.49± 0.56	6.1	···	···	1	1	$u^*gz + \langle\mu_g\rangle_e + \langle r_h\rangle$	···
NGVS-UCD157	-9.67	-9.26	22.86± 0.56	6.3	···	···	1	0	$u^*gz + \langle\mu_g\rangle_e + \langle r_h\rangle$	···
NGVS-UCD158	-9.67	-9.14	21.31± 0.44	6.3	34473	MMT09	3	0	$u^*gz + \langle\mu_g\rangle_e + \langle r_h\rangle$	···
NGVS-UCD159	-9.27	-8.84	21.78± 0.51	6.1	···	···	1	0	$u^*gz + \langle\mu_g\rangle_e + \langle r_h\rangle$	···
NGVS-UCD160	-11.12	-10.63	11.88± 0.38	6.9	650	VCC,AAT12,SDSS,NED	2	0	$u^*gzK + \langle\mu_g\rangle_e + \langle r_h\rangle$	VCC-674
NGVS-UCD161	-10.44	-9.78	15.39± 0.26	6.9	1246	SDSS	1	0	$u^*gzK + \langle\mu_g\rangle_e + \langle r_h\rangle$	···
NGVS-UCD162	-9.57	-8.99	14.28± 0.35	6.3	795	SIMBAD	1	0	$u^*gz + \langle\mu_g\rangle_e + \langle r_h\rangle$	···
NGVS-UCD163	-11.45	-10.78	12.78± 0.17	7.2	1188	NTT17	1	0	$u^*gz + \langle\mu_g\rangle_e + \langle r_h\rangle$	NGC4350-AIMSS1
NGVS-UCD164	-10.14	-9.67	19.30± 0.33	6.5	···	···	1	0	$u^*gz + \langle\mu_g\rangle_e + \langle r_h\rangle$	···
NGVS-UCD165	-9.42	-9.00	12.63± 0.36	6.1	719	Ko2017	1	0	$u^*gz + \langle\mu_g\rangle_e + \langle r_h\rangle$	···
NGVS-UCD166	-9.73	-9.23	25.18± 0.36	6.3	···	···	1	0	$u^*gz + \langle\mu_g\rangle_e + \langle r_h\rangle$	···
NGVS-UCD167	-10.66	-9.98	11.36± 0.17	6.9	898	SIMBAD	1	0	$u^*gzK + \langle\mu_g\rangle_e + \langle r_h\rangle$	···
NGVS-UCD168	-9.53	-9.06	19.43± 0.36	6.1	···	···	1	0	$u^*gz + \langle\mu_g\rangle_e + \langle r_h\rangle$	···
NGVS-UCD169	-10.45	-10.05	32.30± 0.64	6.5	···	···	3	0	$u^*gzK + \langle\mu_g\rangle_e + \langle r_h\rangle$	···
NGVS-UCD170	-9.37	-8.89	19.40± 0.47	6.2	···	···	1	0	$u^*gz + \langle\mu_g\rangle_e + \langle r_h\rangle$	···
NGVS-UCD171	-11.58	-10.90	11.58± 0.48	7.5	-52	SDSS	1	0	$(v_r < 3500\mathrm{km/s}) + \langle r_h\rangle$	···
NGVS-UCD172	-9.45	-9.02	18.83± 0.34	6.2	52482	MMT09	3	0	$u^*gz + \langle\mu_g\rangle_e + \langle r_h\rangle$	···
NGVS-UCD173	-9.47	-9.01	23.34± 0.44	6.1	···	···	1	0	$u^*gz + \langle\mu_g\rangle_e + \langle r_h\rangle$	···
NGVS-UCD174	-10.78	-10.27	38.77± 1.27	6.8	···	···	3	0	$u^*gz + \langle\mu_g\rangle_e + \langle r_h\rangle$	···
NGVS-UCD175	-10.35	-9.90	11.47± 0.17	6.5	955	Ko2017	1	0	$u^*gzK + \langle\mu_g\rangle_e + \langle r_h\rangle$	···
NGVS-UCD176	···	···	33.63± 1.75	7.2	1065	VCC,SDSS,NED	2	0	$(v_r < 3500\mathrm{km/s}) + \langle r_h\rangle$	VCC-750
NGVS-UCD177	-9.39	-8.94	22.16± 0.32	6.1	···	···	1	0	$u^*gz + \langle\mu_g\rangle_e + \langle r_h\rangle$	···
NGVS-UCD178	-9.65	-9.20	22.78± 0.69	6.2	···	···	3	0	$u^*gz + \langle\mu_g\rangle_e + \langle r_h\rangle$	···
NGVS-UCD179	-9.42	-8.99	24.58± 0.56	6.2	···	···	1	0	$u^*gz + \langle\mu_g\rangle_e + \langle r_h\rangle$	···
NGVS-UCD180	-9.85	-9.26	16.93± 0.22	6.5	1219	Ko2017	1	0	$u^*gzK + \langle\mu_g\rangle_e + \langle r_h\rangle$	···
NGVS-UCD181	-12.08	-11.26	24.25± 0.45	7.7	20040	SDSS,NED	3	0	$u^*gzK + \langle\mu_g\rangle_e + \langle r_h\rangle$	···
NGVS-UCD182	-14.09	-13.32	70.79± 7.38	8.4	6840	SDSS,NED	3	0	$u^*gzK + \langle\mu_g\rangle_e + r_{h,g}$	···
NGVS-UCD183	-9.60	-9.10	19.97± 0.65	6.2	···	···	1	0	$u^*gz + \langle\mu_g\rangle_e + \langle r_h\rangle$	···
NGVS-UCD184	-9.53	-9.08	16.55± 0.44	6.2	···	···	1	0	$u^*gz + \langle\mu_g\rangle_e + \langle r_h\rangle$	···
NGVS-UCD185	-9.73	-9.32	25.83± 0.38	6.3	1079	MMT09	1	0	$u^*gz + \langle\mu_g\rangle_e + \langle r_h\rangle$	···
NGVS-UCD186	-9.27	-8.80	21.59± 0.42	6.1	···	···	1	0	$u^*gz + \langle\mu_g\rangle_e + \langle r_h\rangle$	···
NGVS-UCD187	-9.47	-9.04	23.52± 0.41	6.1	···	···	1	0	$u^*gz + \langle\mu_g\rangle_e + \langle r_h\rangle$	···
NGVS-UCD188	-10.39	-9.87	15.49± 0.22	6.6	1135	Ko2017	1	0	$u^*gzK + \langle\mu_g\rangle_e + \langle r_h\rangle$	···
NGVS-UCD189	-9.50	-9.10	19.01± 0.44	6.1	···	···	1	0	$u^*gz + \langle\mu_g\rangle_e + \langle r_h\rangle$	···
NGVS-UCD190	-10.87	-10.37	13.44± 0.33	6.8	759	Ko2017	1	1	$u^*gzK + \langle\mu_g\rangle_e + \langle r_h\rangle$	···

Table 4 *continued*

Table 4 *(continued)*

Name	M_B	M_V	$\langle r_h \rangle$	$\log(M_*/M_{odot})$	v_r	$v_{\rm source}$	Class	Envelope	Method	OtherName
	(mag)	(mag)	(pc)		(km/s)					
(1)	(2)	(3)	(4)	(5)	(6)	(7)	(8)	(9)	(10)	(11)
NGVS-UCD191	-11.04	-10.57	12.68± 0.23	6.8	-174	AAT12	1	0	$u^*gzK + \langle\mu_g\rangle_e + \langle r_h\rangle$	···
NGVS-UCD192	-10.89	-10.42	21.59± 0.27	6.7	-310	MMT09,AAT12	1	0	$u^*gzK + \langle\mu_g\rangle_e + \langle r_h\rangle$	···
NGVS-UCD193	-10.19	-9.64	12.02± 0.32	6.6	···	···	1	0	$u^*gz + \langle\mu_g\rangle_e + \langle r_h\rangle$	···
NGVS-UCD194	-10.10	-9.69	27.40± 0.38	6.3	···	···	1	0	$u^*gzK + \langle\mu_g\rangle_e + \langle r_h\rangle$	···
NGVS-UCD195	-9.83	-9.36	28.34± 0.54	6.3	···	···	1	0	$u^*gzK + \langle\mu_g\rangle_e + \langle r_h\rangle$	···
NGVS-UCD196	-9.48	-9.05	21.85± 0.31	6.1	···	···	1	0	$u^*gz + \langle\mu_g\rangle_e + \langle r_h\rangle$	···
NGVS-UCD197	-9.50	-9.00	21.67± 0.35	6.2	···	···	1	0	$u^*gz + \langle\mu_g\rangle_e + \langle r_h\rangle$	···
NGVS-UCD198	-9.27	-8.83	11.66± 0.26	6.0	···	···	1	0	$u^*gz + \langle\mu_g\rangle_e + \langle r_h\rangle$	···
NGVS-UCD199	-10.53	-10.09	18.58± 0.39	6.6	1134	Ko2017	1	0	$u^*gzK + \langle\mu_g\rangle_e + \langle r_h\rangle$	···
NGVS-UCD200	-12.39	-11.82	30.46± 1.25	7.5	1018	VCC,SDSS,NED	2	0	$(v_r < 3500\mathrm{km/s}) + \langle r_h\rangle$	VCC-856
NGVS-UCD201	-9.45	-9.03	19.28± 0.32	6.1	···	···	1	0	$u^*gz + \langle\mu_g\rangle_e + \langle r_h\rangle$	···
NGVS-UCD202	-9.39	-8.91	13.70± 0.18	6.1	-318	Ko2017	1	0	$u^*gz + \langle\mu_g\rangle_e + \langle r_h\rangle$	···
NGVS-UCD203	-11.10	-10.62	15.54± 0.70	6.8	···	···	5	0	$u^*gzK + \langle\mu_g\rangle_e + \langle r_h\rangle$	···
NGVS-UCD204	-11.42	-10.89	33.53± 0.80	7.0	1263	VCC,AAT12,SDSS,NED	2	0	$u^*gzK + \langle\mu_g\rangle_e + \langle r_h\rangle$	VCC-872
NGVS-UCD205	-10.43	-9.98	11.20± 0.19	6.5	···	···	1	0	$u^*gzK + \langle\mu_g\rangle_e + \langle r_h\rangle$	···
NGVS-UCD206	-9.84	-9.32	16.27± 0.24	6.4	···	···	1	0	$u^*gz + \langle\mu_g\rangle_e + \langle r_h\rangle$	···
NGVS-UCD207	-10.66	-10.24	27.57± 0.61	6.6	294	AAT12	1	0	$u^*gz + \langle\mu_g\rangle_e + \langle r_h\rangle$	···
NGVS-UCD208	-10.25	-9.84	23.46± 0.47	6.4	···	···	1	0	$u^*gzK + \langle\mu_g\rangle_e + \langle r_h\rangle$	···
NGVS-UCD209	-9.60	-9.17	23.82± 0.54	6.2	···	···	1	0	$u^*gz + \langle\mu_g\rangle_e + \langle r_h\rangle$	···
NGVS-UCD210	-9.55	-9.06	21.24± 0.42	6.2	···	···	1	0	$u^*gz + \langle\mu_g\rangle_e + \langle r_h\rangle$	···
NGVS-UCD211	-9.70	-9.27	20.92± 0.35	6.2	···	···	1	0	$u^*gzK + \langle\mu_g\rangle_e + \langle r_h\rangle$	···
NGVS-UCD212	-9.42	-9.00	24.82± 0.42	6.2	···	···	1	0	$u^*gz + \langle\mu_g\rangle_e + \langle r_h\rangle$	···
NGVS-UCD213	-11.62	-11.11	30.97± 1.52	7.1	1051	AAT12,SDSS,NED	2	0	$u^*gzK + \langle\mu_g\rangle_e + \langle r_h\rangle$	VCC-895
NGVS-UCD214	-11.31	-10.74	32.65± 0.40	7.1	13842	NTT17	3	0	$u^*gz + \langle\mu_g\rangle_e + \langle r_h\rangle$	···
NGVS-UCD215	-11.15	-10.52	20.31± 1.01	7.0	-186	AAT12	1	0	$u^*gzK + \langle\mu_g\rangle_e + \langle r_h\rangle$	···
NGVS-UCD216	-9.81	-9.32	28.83± 0.51	6.3	···	···	1	0	$u^*gzK + \langle\mu_g\rangle_e + \langle r_h\rangle$	···
NGVS-UCD217	-9.58	-9.12	11.55± 0.26	6.2	···	···	1	0	$u^*gz + \langle\mu_g\rangle_e + \langle r_h\rangle$	···
NGVS-UCD218	-11.88	-11.24	17.86± 0.12	7.3	-93	AAT12	1	0	$u^*gzK + \langle\mu_g\rangle_e + \langle r_h\rangle$	···
NGVS-UCD219	-10.33	-9.85	18.77± 0.26	6.5	69	Ko2017	1	0	$u^*gzK + \langle\mu_g\rangle_e + \langle r_h\rangle$	···
NGVS-UCD220	-10.37	-9.89	16.87± 0.24	6.5	-145	Ko2017	1	0	$u^*gzK + \langle\mu_g\rangle_e + \langle r_h\rangle$	···
NGVS-UCD221	-10.55	-9.74	13.55± 0.50	7.0	···	···	3	0	$u^*gzK + \langle\mu_g\rangle_e + \langle r_h\rangle$	···
NGVS-UCD222	-10.13	-9.68	12.58± 0.50	6.4	···	···	2	0	$u^*gzK + \langle\mu_g\rangle_e + \langle r_h\rangle$	···
NGVS-UCD223	-9.51	-9.08	13.79± 0.20	6.1	52184	MMT09	3	0	$u^*gz + \langle\mu_g\rangle_e + \langle r_h\rangle$	···
NGVS-UCD224	-14.05	-13.35	59.00± 1.16	8.3	13663	VCC,SDSS,NED	3	0	$u^*gz + \langle\mu_g\rangle_e + \langle r_h\rangle$	···
NGVS-UCD225	-9.46	-8.99	21.95± 0.37	6.2	···	···	1	0	$u^*gz + \langle\mu_g\rangle_e + \langle r_h\rangle$	···
NGVS-UCD226	-11.06	-11.06	54.75± 1.32	5.9	-3	SDSS	6	0	$(v_r < 3500\mathrm{km/s}) + \langle r_h\rangle$	···
NGVS-UCD227	-10.93	-10.92	29.11± 1.84	6.1	-61	SDSS	6	0	$(v_r < 3500\mathrm{km/s}) + \langle r_h\rangle$	···
NGVS-UCD228	-9.75	-9.25	19.99± 0.60	6.3	···	···	1	0	$u^*gz + \langle\mu_g\rangle_e + \langle r_h\rangle$	···
NGVS-UCD229	-9.49	-9.05	24.35± 0.87	6.1	···	···	1	0	$u^*gz + \langle\mu_g\rangle_e + \langle r_h\rangle$	···
NGVS-UCD230	-9.44	-8.96	11.03± 0.24	6.2	···	···	1	0	$u^*gz + \langle\mu_g\rangle_e + \langle r_h\rangle$	···
NGVS-UCD231	-11.07	-10.55	19.00± 0.49	6.9	610	Ko2017	1	1	$u^*gzK + \langle\mu_g\rangle_e + \langle r_h\rangle$	···
NGVS-UCD232	-11.08	-10.58	43.85± 3.98	6.9	849	VCC,SDSS,NED	2	0	$(v_r < 3500\mathrm{km/s}) + \langle r_h\rangle$	VCC-965
NGVS-UCD233	-9.24	-8.75	17.12± 0.32	6.1	···	···	1	0	$u^*gz + \langle\mu_g\rangle_e + \langle r_h\rangle$	···
NGVS-UCD234	-10.61	-10.13	14.35± 0.59	6.6	···	···	1	1	$u^*gzK + \langle\mu_g\rangle_e + \langle r_h\rangle$	···
NGVS-UCD235	-10.32	-9.91	22.90± 0.40	6.4	···	···	1	0	$u^*gzK + \langle\mu_g\rangle_e + \langle r_h\rangle$	···
NGVS-UCD236	-10.19	-9.64	14.05± 0.33	6.6	1219	MMT09	1	0	$u^*gzK + \langle\mu_g\rangle_e + \langle r_h\rangle$	···
NGVS-UCD237	-10.28	-9.88	25.05± 0.51	6.4	···	···	1	0	$u^*gz + \langle\mu_g\rangle_e + \langle r_h\rangle$	···
NGVS-UCD238	-10.15	-9.34	14.59± 0.32	6.9	···	···	1	0	$u^*gzK + \langle\mu_g\rangle_e + \langle r_h\rangle$	···

Table 4 *continued*

Table 4 *(continued)*

Name	M_B	M_V	$\langle r_h \rangle$	$\log(M_*/M_{odot})$	v_r	$v_{\rm source}$	Class	Envelope	Method	OtherName
	(mag)	(mag)	(pc)		(km/s)					
(1)	(2)	(3)	(4)	(5)	(6)	(7)	(8)	(9)	(10)	(11)
NGVS-UCD239	-9.31	-8.85	21.75± 0.44	6.2	···	···	1	0	$u^*gz + \langle\mu_g\rangle_e + \langle r_h\rangle$	···
NGVS-UCD240	-9.90	-9.46	11.76± 0.18	6.3	-275	Ko2017	1	0	$u^*gz + \langle\mu_g\rangle_e + \langle r_h\rangle$	···
NGVS-UCD241	-10.06	-9.65	27.60± 0.66	6.4	···	···	3	0	$u^*gz + \langle\mu_g\rangle_e + \langle r_h\rangle$	···
NGVS-UCD242	-9.32	-8.84	14.21± 0.44	6.1	···	···	1	0	$u^*gz + \langle\mu_g\rangle_e + \langle r_h\rangle$	···
NGVS-UCD243	-9.34	-8.94	19.63± 0.31	6.0	···	···	1	0	$u^*gz + \langle\mu_g\rangle_e + \langle r_h\rangle$	···
NGVS-UCD244	-10.24	-9.79	13.48± 0.31	6.4	1107	MMT14	1	0	$u^*gzK + \langle\mu_g\rangle_e + \langle r_h\rangle$	···
NGVS-UCD245	-9.35	-8.85	13.24± 0.23	6.1	···	···	1	0	$u^*gz + \langle\mu_g\rangle_e + \langle r_h\rangle$	···
NGVS-UCD246	-9.59	-9.12	22.03± 0.47	6.2	···	···	1	0	$u^*gz + \langle\mu_g\rangle_e + \langle r_h\rangle$	···
NGVS-UCD247	-9.67	-9.22	28.46± 0.67	6.2	···	···	1	0	$u^*gz + \langle\mu_g\rangle_e + \langle r_h\rangle$	···
NGVS-UCD248	-9.27	-8.82	20.86± 0.38	6.1	···	···	1	0	$u^*gz + \langle\mu_g\rangle_e + \langle r_h\rangle$	···
NGVS-UCD249	-9.41	-8.95	24.79± 0.95	6.1	···	···	1	0	$u^*gzK + \langle\mu_g\rangle_e + \langle r_h\rangle$	···
NGVS-UCD250	-10.17	-9.68	26.32± 0.04	6.5	865	VCC,NED	2	0	$u^*gzK + \langle\mu_g\rangle_e + \langle r_h\rangle$	VCC-1064
NGVS-UCD251	-11.00	-10.48	28.86± 2.10	6.8	113	VCC,AAT12,SDSS,NED	2	0	$(v_r < 3500\mathrm{km/s}) + \langle r_h\rangle$	VCC-1065
NGVS-UCD252	-9.94	-9.48	13.85± 0.44	6.3	599	MMT09	1	0	$u^*gz + \langle\mu_g\rangle_e + \langle r_h\rangle$	M87UCD-29
NGVS-UCD253	-9.58	-9.14	23.84± 0.95	6.2	···	···	3	0	$u^*gz + \langle\mu_g\rangle_e + \langle r_h\rangle$	···
NGVS-UCD254	-9.29	-8.87	20.59± 0.89	6.0	···	···	3	0	$u^*gz + \langle\mu_g\rangle_e + \langle r_h\rangle$	···
NGVS-UCD255	-9.43	-8.96	13.81± 0.83	6.1	-8	SIMBAD	4	0	$u^*gz + \langle\mu_g\rangle_e + \langle r_h\rangle$	···
NGVS-UCD256	-10.27	-9.81	11.16± 0.36	6.5	1340	VCC,KECK,NED	2	0	$u^*gzK + \langle\mu_g\rangle_e + \langle r_h\rangle$	VCC-1079
NGVS-UCD257	-9.75	-9.35	14.47± 0.49	6.2	157045	MMT14	2	0	$u^*gz + \langle\mu_g\rangle_e + \langle r_h\rangle$	···
NGVS-UCD258	-9.53	-9.05	21.06± 0.33	6.2	···	···	1	0	$u^*gz + \langle\mu_g\rangle_e + \langle r_h\rangle$	···
NGVS-UCD259	-9.32	-8.89	18.12± 0.26	6.1	···	···	1	0	$u^*gz + \langle\mu_g\rangle_e + \langle r_h\rangle$	···
NGVS-UCD260	-9.70	-9.25	25.71± 0.33	6.2	···	···	1	0	$u^*gzK + \langle\mu_g\rangle_e + \langle r_h\rangle$	···
NGVS-UCD261	-9.33	-8.86	15.77± 0.42	6.1	···	···	1	0	$u^*gz + \langle\mu_g\rangle_e + \langle r_h\rangle$	···
NGVS-UCD262	-9.32	-8.89	19.77± 0.39	6.1	···	···	1	0	$u^*gz + \langle\mu_g\rangle_e + \langle r_h\rangle$	···
NGVS-UCD263	-10.42	-9.92	22.77± 0.30	6.6	···	···	1	0	$u^*gzK + \langle\mu_g\rangle_e + \langle r_h\rangle$	···
NGVS-UCD264	-9.55	-9.13	25.72± 0.85	6.2	···	···	1	0	$u^*gz + \langle\mu_g\rangle_e + \langle r_h\rangle$	···
NGVS-UCD265	-10.22	-9.81	37.98± 1.22	6.5	···	···	3	0	$u^*gz + \langle\mu_g\rangle_e + \langle r_h\rangle$	···
NGVS-UCD266	-9.75	-9.27	17.17± 0.23	6.3	···	···	1	0	$u^*gz + \langle\mu_g\rangle_e + \langle r_h\rangle$	···
NGVS-UCD267	-9.58	-9.10	11.64± 0.26	6.2	713	MMT14	1	0	$u^*gz + \langle\mu_g\rangle_e + \langle r_h\rangle$	···
NGVS-UCD268	-9.83	-9.34	13.71± 0.24	6.3	1534	MMT09	1	0	$u^*gz + \langle\mu_g\rangle_e + \langle r_h\rangle$	M87UCD-30
NGVS-UCD269	-10.64	-10.12	11.37± 0.21	6.7	1393	MMT14	1	0	$u^*gzK + \langle\mu_g\rangle_e + \langle r_h\rangle$	···
NGVS-UCD270	-9.35	-8.89	15.16± 0.78	6.2	···	···	2	0	$u^*gz + \langle\mu_g\rangle_e + \langle r_h\rangle$	VCC-1137
NGVS-UCD271	-9.47	-9.05	19.26± 0.42	6.1	45498	MMT14	3	0	$u^*gz + \langle\mu_g\rangle_e + \langle r_h\rangle$	···
NGVS-UCD272	-10.91	-10.38	27.33± 0.32	6.8	···	···	1	0	$u^*gzK + \langle\mu_g\rangle_e + \langle r_h\rangle$	···
NGVS-UCD273	-10.67	-10.18	12.10± 0.29	6.7	1175	AAT12	1	1	$u^*gzK + \langle\mu_g\rangle_e + \langle r_h\rangle$	···
NGVS-UCD274	-9.54	-9.10	15.68± 0.48	6.2	1645	Ko2017	1	0	$u^*gz + \langle\mu_g\rangle_e + \langle r_h\rangle$	···
NGVS-UCD275	-9.42	-9.01	19.54± 0.29	6.1	···	···	1	0	$u^*gz + \langle\mu_g\rangle_e + \langle r_h\rangle$	···
NGVS-UCD276	-15.30	-14.57	62.09± 4.33	8.9	655	VCC,NED	2	0	$u^*gzK + \langle\mu_g\rangle_e + \langle r_h\rangle$	VCC-1146
NGVS-UCD277	-11.93	-11.22	31.53± 0.74	7.5	26777	NTT17	3	0	$u^*gzK + \langle\mu_g\rangle_e + \langle r_h\rangle$	···
NGVS-UCD278	-13.12	-12.38	80.46± 6.29	8.0	1416	VCC,SDSS,NED	2	0	$(v_r < 3500\mathrm{km/s}) + \langle r_h\rangle$	VCC-1148
NGVS-UCD279	-10.77	-10.32	34.48± 0.99	6.7	···	···	1	0	$u^*gz + \langle\mu_g\rangle_e + \langle r_h\rangle$	···
NGVS-UCD280	-10.89	-10.42	14.81± 0.27	6.8	731	AAT12	1	1	$u^*gzK + \langle\mu_g\rangle_e + \langle r_h\rangle$	···
NGVS-UCD281	-9.95	-9.42	13.33± 0.26	6.4	1224	MMT09	1	0	$u^*gzK + \langle\mu_g\rangle_e + \langle r_h\rangle$	M87UCD-24
NGVS-UCD282	-9.86	-9.37	14.71± 0.24	6.3	1291	MMT14	1	0	$u^*gzK + \langle\mu_g\rangle_e + \langle r_h\rangle$	···
NGVS-UCD283	-10.64	-10.15	19.06± 0.18	6.7	···	···	1	0	$u^*gzK + \langle\mu_g\rangle_e + \langle r_h\rangle$	···
NGVS-UCD284	-9.71	-9.28	31.40± 0.55	6.2	···	···	1	0	$u^*gz + \langle\mu_g\rangle_e + \langle r_h\rangle$	···
NGVS-UCD285	-10.67	-10.20	13.09± 0.32	6.7	905	MMT09	1	1	$u^*gzK + \langle\mu_g\rangle_e + \langle r_h\rangle$	M87UCD-34
NGVS-UCD286	-9.98	-9.46	24.80± 0.52	6.4	···	···	1	0	$u^*gz + \langle\mu_g\rangle_e + \langle r_h\rangle$	···

Table 4 *continued*

Table 4 *(continued)*

Name	M_B	M_V	$\langle r_h \rangle$	$\log(M_*/M_{odot})$	v_r	$v_{\rm source}$	Class	Envelope	Method	OtherName
	(mag)	(mag)	(pc)		(km/s)					
(1)	(2)	(3)	(4)	(5)	(6)	(7)	(8)	(9)	(10)	(11)
NGVS-UCD287	-10.27	-9.80	14.13± 0.40	6.5	253	MMT09	1	0	$u^*gzK + \langle\mu_g\rangle_e + \langle r_h\rangle$	···
NGVS-UCD288	-9.90	-9.47	28.29± 1.12	6.4	···	···	1	0	$u^*gz + \langle\mu_g\rangle_e + \langle r_h\rangle$	···
NGVS-UCD289	-9.25	-8.71	17.69± 0.53	6.2	1075	C03,MMT14	1	0	$u^*gz + \langle\mu_g\rangle_e + \langle r_h\rangle$	···
NGVS-UCD290	-10.96	-10.38	11.36± 0.17	6.9	1753	MMT09,AAT12,IMACS16	1	0	$u^*gzK + \langle\mu_g\rangle_e + \langle r_h\rangle$	···
NGVS-UCD291	-9.48	-9.08	16.16± 0.22	6.1	···	···	1	0	$u^*gz + \langle\mu_g\rangle_e + \langle r_h\rangle$	···
NGVS-UCD292	-9.63	-9.14	25.10± 0.44	6.2	···	···	1	1	$u^*gz + \langle\mu_g\rangle_e + \langle r_h\rangle$	···
NGVS-UCD293	-10.01	-9.53	15.62± 0.26	6.4	1675	MMT14	1	0	$u^*gzK + \langle\mu_g\rangle_e + \langle r_h\rangle$	···
NGVS-UCD294	-10.78	-10.24	96.62± 9.09	6.7	452	VCC,MMT09,SDSS,NED	2	0	$(v_r < 3500\mathrm{km/s}) + \langle r_h\rangle$	VCC-1185
NGVS-UCD295	-10.60	-10.12	16.18± 0.14	6.6	1107	MMT14	1	0	$u^*gzK + \langle\mu_g\rangle_e + \langle r_h\rangle$	···
NGVS-UCD296	-10.92	-10.32	17.93± 0.29	6.9	637	MMT14	1	0	$u^*gzK + \langle\mu_g\rangle_e + \langle r_h\rangle$	···
NGVS-UCD297	-10.00	-9.59	25.44± 0.87	6.3	···	···	3	0	$u^*gz + \langle\mu_g\rangle_e + \langle r_h\rangle$	···
NGVS-UCD298	-9.90	-9.37	13.46± 0.34	6.4	1114	MMT14	1	0	$u^*gz + \langle\mu_g\rangle_e + \langle r_h\rangle$	···
NGVS-UCD299	-9.90	-9.49	24.57± 0.41	6.3	···	···	1	0	$u^*gz + \langle\mu_g\rangle_e + \langle r_h\rangle$	···
NGVS-UCD300	-11.47	-10.93	28.59± 1.22	7.1	···	···	3	0	$u^*gz + \langle\mu_g\rangle_e + \langle r_h\rangle$	···
NGVS-UCD301	-10.14	-9.40	13.00± 0.23	6.7	1452	MMT09	1	0	$u^*gzK + \langle\mu_g\rangle_e + \langle r_h\rangle$	···
NGVS-UCD302	-10.31	-9.86	22.69± 0.53	6.5	1014	C03	4	0	$u^*gzK + \langle\mu_g\rangle_e + \langle r_h\rangle$	···
NGVS-UCD303	-13.73	-12.87	88.85± 5.00	8.3	1393	VCC,SDSS,NED	2	0	$(v_r < 3500\mathrm{km/s}) + \langle r_h\rangle$	VCC-1199
NGVS-UCD304	-9.44	-8.98	23.20± 0.47	6.2	···	···	1	0	$u^*gz + \langle\mu_g\rangle_e + \langle r_h\rangle$	···
NGVS-UCD305	-9.84	-9.41	23.28± 0.32	6.3	29510	MMT09	3	0	$u^*gzK + \langle\mu_g\rangle_e + \langle r_h\rangle$	···
NGVS-UCD306	-9.30	-8.83	18.44± 0.34	6.1	···	···	1	0	$u^*gz + \langle\mu_g\rangle_e + \langle r_h\rangle$	···
NGVS-UCD307	-9.69	-9.24	12.57± 0.24	6.3	1748	Ko2017	1	0	$u^*gz + \langle\mu_g\rangle_e + \langle r_h\rangle$	···
NGVS-UCD308	-10.88	-10.37	21.98± 0.16	6.8	1400	AAT12	1	0	$u^*gzK + \langle\mu_g\rangle_e + \langle r_h\rangle$	M87UCD-5
NGVS-UCD309	-9.88	-9.18	11.03± 0.67	6.6	1050	S11	1	0	$u^*gzK + \langle\mu_g\rangle_e + \langle r_h\rangle$	H55210
NGVS-UCD310	-9.73	-9.20	11.13± 0.43	6.3	562	MMT09	1	0	$u^*gz + \langle\mu_g\rangle_e + \langle r_h\rangle$	···
NGVS-UCD311	-10.55	-10.00	17.17± 0.36	6.7	1754	AAT12	1	0	$u^*gzK + \langle\mu_g\rangle_e + \langle r_h\rangle$	M87UCD-20
NGVS-UCD312	-9.86	-9.30	12.02± 0.23	6.4	1314	MMT09,IMACS16	1	0	$u^*gzK + \langle\mu_g\rangle_e + \langle r_h\rangle$	M87UCD-23
NGVS-UCD313	-9.88	-9.38	15.31± 0.30	6.4	1703	MMT09	1	0	$u^*gzK + \langle\mu_g\rangle_e + \langle r_h\rangle$	···
NGVS-UCD314	-10.56	-10.06	25.21± 0.29	6.6	1125	MMT14	1	0	$u^*gzK + \langle\mu_g\rangle_e + \langle r_h\rangle$	···
NGVS-UCD315	-10.28	-9.80	15.74± 0.22	6.5	1568	NED,C03,MMT14	1	0	$u^*gz + \langle\mu_g\rangle_e + \langle r_h\rangle$	···
NGVS-UCD316	-9.40	-8.93	25.07± 0.34	6.1	···	···	1	0	$u^*gz + \langle\mu_g\rangle_e + \langle r_h\rangle$	···
NGVS-UCD317	-10.38	-9.89	11.26± 0.32	6.6	886	VCC,SDSS,NED	2	0	$u^*gzK + \langle\mu_g\rangle_e + \langle r_h\rangle$	VCC-1218
NGVS-UCD318	-10.33	-9.82	13.16± 0.17	6.6	1142	MMT09,AAT12,IMACS16	1	0	$u^*gzK + \langle\mu_g\rangle_e + \langle r_h\rangle$	M87UCD-8
NGVS-UCD319	-10.01	-9.50	15.28± 0.48	6.5	795	C03,MMT14	1	0	$u^*gz + \langle\mu_g\rangle_e + \langle r_h\rangle$	G9992/1226-1
NGVS-UCD320	-10.31	-9.82	12.16± 0.79	6.6	1070	C03,MMT14	1	0	$u^*gzK + \langle\mu_g\rangle_e + \langle r_h\rangle$	···
NGVS-UCD321	-9.99	-9.44	11.31± 0.27	6.5	342	C03,MMT14	1	0	$u^*gz + \langle\mu_g\rangle_e + \langle r_h\rangle$	···
NGVS-UCD322	-10.00	-9.39	13.75± 0.19	6.6	905	MMT09	1	0	$u^*gzK + \langle\mu_g\rangle_e + \langle r_h\rangle$	M87UCD-22
NGVS-UCD323	-11.11	-10.61	35.09± 0.35	6.8	1245	Ko2017	1	0	$u^*gzK + \langle\mu_g\rangle_e + \langle r_h\rangle$	···
NGVS-UCD324	-10.21	-9.80	18.56± 0.27	6.5	816	C03	1	0	$(v_r < 3500\mathrm{km/s}) + \langle r_h\rangle$	···
NGVS-UCD325	-9.26	-8.80	20.42± 0.37	6.2	···	···	1	0	$u^*gz + \langle\mu_g\rangle_e + \langle r_h\rangle$	···
NGVS-UCD326	-9.80	-9.35	27.23± 0.72	6.2	···	···	3	0	$u^*gz + \langle\mu_g\rangle_e + \langle r_h\rangle$	···
NGVS-UCD327	-10.24	-9.78	24.94± 0.33	6.5	···	···	1	0	$u^*gzK + \langle\mu_g\rangle_e + \langle r_h\rangle$	···
NGVS-UCD328	-9.57	-8.75	11.58± 0.16	6.6	402	C03,MMT14	1	0	$u^*gzK + \langle\mu_g\rangle_e + \langle r_h\rangle$	···
NGVS-UCD329	-10.85	-10.38	16.20± 0.40	6.7	788	MMT09,AAT12	2	0	$u^*gzK + \langle\mu_g\rangle_e + \langle r_h\rangle$	VCC-1244
NGVS-UCD330	-10.86	-10.35	19.69± 0.37	6.8	1628	MMT09,AAT12,NED,S11	1	1	$u^*gzK + \langle\mu_g\rangle_e + \langle r_h\rangle$	H36612/1250-1
NGVS-UCD331	-11.07	-10.58	14.82± 0.19	6.9	843	MMT14	1	0	$u^*gzK + \langle\mu_g\rangle_e + \langle r_h\rangle$	···
NGVS-UCD332	-10.59	-10.12	13.70± 0.15	6.6	1495	MMT09,S11	1	0	$u^*gzK + \langle\mu_g\rangle_e + \langle r_h\rangle$	H65115
NGVS-UCD333	-9.41	-8.93	11.14± 0.29	6.1	449	C03,MMT14	1	0	$u^*gz + \langle\mu_g\rangle_e + \langle r_h\rangle$	···
NGVS-UCD334	-9.64	-9.21	24.37± 0.58	6.2	···	···	1	0	$u^*gzK + \langle\mu_g\rangle_e + \langle r_h\rangle$	···

Table 4 *continued*

Table 4 *(continued)*

Name	M_B	M_V	$\langle r_h \rangle$	$\log(M_*/M_{odot})$	v_r	$v_{\rm source}$	Class	Envelope	Method	OtherName
	(mag)	(mag)	(pc)		(km/s)					
(1)	(2)	(3)	(4)	(5)	(6)	(7)	(8)	(9)	(10)	(11)
NGVS-UCD335	-11.02	-10.45	17.61± 0.19	7.0	770	C03,MMT14	1	0	$u^*gzK + \langle\mu_g\rangle_e + \langle r_h\rangle$	···
NGVS-UCD336	-10.70	-10.21	13.42± 0.23	6.6	1156	C03	1	0	$u^*gzK + \langle\mu_g\rangle_e + \langle r_h\rangle$	···
NGVS-UCD337	-9.27	-8.84	17.75± 0.80	6.0	···	···	2	0	$u^*gz + \langle\mu_g\rangle_e + \langle r_h\rangle$	VCC-1246
NGVS-UCD338	-10.17	-9.63	14.47± 0.44	6.6	996	SDSS	1	0	$u^*gzK + \langle\mu_g\rangle_e + \langle r_h\rangle$	···
NGVS-UCD339	-10.52	-10.00	27.99± 0.31	6.7	1487	C03,MMT14	1	0	$u^*gzK + \langle\mu_g\rangle_e + \langle r_h\rangle$	···
NGVS-UCD340	-10.98	-10.55	22.15± 0.12	6.7	1178	AAT12,IMACS16	1	0	$u^*gzK + \langle\mu_g\rangle_e + \langle r_h\rangle$	M87UCD-10
NGVS-UCD341	-10.63	-10.10	15.53± 0.11	6.7	1514	AAT12	1	0	$u^*gzK + \langle\mu_g\rangle_e + \langle r_h\rangle$	M87UCD-6
NGVS-UCD342	-9.83	-9.36	19.18± 0.24	6.3	1834	C03,MMT14	1	0	$u^*gz + \langle\mu_g\rangle_e + \langle r_h\rangle$	···
NGVS-UCD343	-9.82	-9.34	11.93± 0.19	6.3	···	···	1	0	$u^*gz + \langle\mu_g\rangle_e + \langle r_h\rangle$	···
NGVS-UCD344	-9.95	-9.47	12.33± 0.35	6.4	···	···	1	0	$u^*gzK + \langle\mu_g\rangle_e + \langle r_h\rangle$	···
NGVS-UCD345	-11.11	-10.61	12.04± 0.19	6.9	1185	MMT09,S11	1	0	$u^*gzK + \langle\mu_g\rangle_e + \langle r_h\rangle$	H18539
NGVS-UCD346	-9.53	-9.00	25.11± 0.58	6.3	···	···	1	0	$u^*gz + \langle\mu_g\rangle_e + \langle r_h\rangle$	···
NGVS-UCD347	-12.78	-12.16	35.42± 0.97	7.6	1248	VCC,SDSS,NED	2	0	$u^*gzK + \langle\mu_g\rangle_e + \langle r_h\rangle$	VCC-1254
NGVS-UCD348	-10.17	-9.67	11.53± 0.39	6.5	1411	S11	1	0	$u^*gzK + \langle\mu_g\rangle_e + \langle r_h\rangle$	H63998
NGVS-UCD349	-9.77	-9.29	13.94± 0.25	6.3	···	···	1	0	$u^*gz + \langle\mu_g\rangle_e + \langle r_h\rangle$	···
NGVS-UCD350	-11.01	-10.51	12.12± 0.20	6.8	1447	MMT09,S11	1	0	$u^*gzK + \langle\mu_g\rangle_e + \langle r_h\rangle$	H59823
NGVS-UCD351	-9.57	-9.10	14.26± 0.29	6.2	549	MMT14	1	0	$u^*gz + \langle\mu_g\rangle_e + \langle r_h\rangle$	···
NGVS-UCD352	-11.35	-10.79	17.79± 0.19	7.0	1160	AAT12	1	0	$u^*gzK + \langle\mu_g\rangle_e + \langle r_h\rangle$	M87UCD-7
NGVS-UCD353	-10.27	-9.71	14.12± 0.17	6.6	1870	MMT09	1	0	$u^*gzK + \langle\mu_g\rangle_e + \langle r_h\rangle$	M87UCD-28
NGVS-UCD354	-10.67	-10.11	11.10± 0.18	6.8	···	···	1	0	$u^*gzK + \langle\mu_g\rangle_e + \langle r_h\rangle$	···
NGVS-UCD355	-10.37	-9.90	13.41± 0.18	6.6	888	C03,MMT14	1	0	$u^*gzK + \langle\mu_g\rangle_e + \langle r_h\rangle$	···
NGVS-UCD356	···	···	12.34± 0.84	7.7	···	···	4	0	$gzK + \langle\mu_g\rangle_e + \langle r_h\rangle$	···
NGVS-UCD357	-11.76	-11.18	13.55± 0.14	7.2	1227	MMT09,AAT12,NED,S11	1	0	$u^*gzK + \langle\mu_g\rangle_e + \langle r_h\rangle$	VUCD1
NGVS-UCD358	-11.73	-11.15	20.71± 0.51	7.2	···	···	3	0	$u^*gzK + \langle\mu_g\rangle_e + \langle r_h\rangle$	···
NGVS-UCD359	-10.34	-9.89	35.11± 0.82	6.5	···	···	3	0	$u^*gz + \langle\mu_g\rangle_e + \langle r_h\rangle$	···
NGVS-UCD360	-9.79	-9.28	11.67± 0.17	6.4	1324	MMT09	1	0	$u^*gzK + \langle\mu_g\rangle_e + \langle r_h\rangle$	M87UCD-37
NGVS-UCD361	-9.33	-8.84	13.10± 0.30	6.1	···	···	1	0	$u^*gz + \langle\mu_g\rangle_e + \langle r_h\rangle$	···
NGVS-UCD362	-9.38	-8.90	25.03± 0.53	6.1	···	···	1	0	$u^*gz + \langle\mu_g\rangle_e + \langle r_h\rangle$	···
NGVS-UCD363	-9.82	-9.36	29.34± 1.20	6.3	-420	VCC,NED	2	0	$(v_r < 3500\mathrm{km/s}) + \langle r_h\rangle$	VCC-1264
NGVS-UCD364	-10.25	-9.72	12.42± 0.25	6.6	1607	IMACS16	1	0	$u^*gzK + \langle\mu_g\rangle_e + \langle r_h\rangle$	···
NGVS-UCD365	-9.52	-8.99	26.03± 0.49	6.2	···	···	1	0	$u^*gz + \langle\mu_g\rangle_e + \langle r_h\rangle$	···
NGVS-UCD366	-9.83	-9.35	12.11± 0.35	6.3	289	MMT09	1	0	$u^*gz + \langle\mu_g\rangle_e + \langle r_h\rangle$	···
NGVS-UCD367	-10.83	-10.37	17.60± 0.43	6.7	2030	MMT09	1	0	$u^*gzK + \langle\mu_g\rangle_e + \langle r_h\rangle$	M87UCD-26
NGVS-UCD368	-9.95	-9.46	17.35± 0.23	6.4	778	MMT14	1	0	$u^*gz + \langle\mu_g\rangle_e + \langle r_h\rangle$	···
NGVS-UCD369	-9.79	-9.33	12.65± 0.37	6.3	···	···	1	0	$u^*gzK + \langle\mu_g\rangle_e + \langle r_h\rangle$	···
NGVS-UCD370	-9.39	-8.92	24.80± 0.33	6.1	···	···	1	0	$u^*gz + \langle\mu_g\rangle_e + \langle r_h\rangle$	···
NGVS-UCD371	-9.73	-9.23	11.05± 0.41	6.3	···	···	1	0	$u^*gz + \langle\mu_g\rangle_e + \langle r_h\rangle$	···
NGVS-UCD372	-11.32	-10.77	33.65± 0.14	7.1	1070	MMT14,NTT17	1	1	$u^*gzK + \langle\mu_g\rangle_e + \langle r_h\rangle$	···
NGVS-UCD373	-10.31	-9.80	11.75± 0.51	6.6	1520	MMT09	1	0	$u^*gzK + \langle\mu_g\rangle_e + \langle r_h\rangle$	···
NGVS-UCD374	-11.53	-11.03	23.86± 0.20	7.1	1406	MMT09,AAT12	1	1	$u^*gzK + \langle\mu_g\rangle_e + \langle r_h\rangle$	M87UCD-3
NGVS-UCD375	-9.74	-9.17	30.06± 0.51	6.4	···	···	1	0	$u^*gzK + \langle\mu_g\rangle_e + \langle r_h\rangle$	···
NGVS-UCD376	-9.89	-9.40	16.97± 0.22	6.4	1594	Ko2017	1	0	$u^*gz + \langle\mu_g\rangle_e + \langle r_h\rangle$	···
NGVS-UCD377	-9.34	-8.86	18.64± 0.39	6.1	···	···	1	0	$u^*gz + \langle\mu_g\rangle_e + \langle r_h\rangle$	···
NGVS-UCD378	-10.15	-9.71	31.06± 0.56	6.4	···	···	4	0	$u^*gz + \langle\mu_g\rangle_e + \langle r_h\rangle$	···
NGVS-UCD379	-10.87	-10.21	11.88± 0.40	7.0	1279	MMT09,AAT12	1	0	$u^*gzK + \langle\mu_g\rangle_e + \langle r_h\rangle$	M87UCD-4
NGVS-UCD380	-9.46	-9.06	23.05± 0.53	6.2	···	···	1	0	$u^*gz + \langle\mu_g\rangle_e + \langle r_h\rangle$	···
NGVS-UCD381	-11.06	-10.56	20.85± 0.21	6.8	556	MMT09,AAT12	1	1	$u^*gzK + \langle\mu_g\rangle_e + \langle r_h\rangle$	M87UCD-9
NGVS-UCD382	-10.69	-10.20	11.67± 0.27	6.7	1203	IMACS16	1	0	$u^*gzK + \langle\mu_g\rangle_e + \langle r_h\rangle$	···

Table 4 *continued*

Table 4 *(continued)*

Name	M_B	M_V	$\langle r_h \rangle$	$\log(M_*/M_{odot})$	v_r	$v_{\rm source}$	Class	Envelope	Method	OtherName
	(mag)	(mag)	(pc)		(km/s)					
(1)	(2)	(3)	(4)	(5)	(6)	(7)	(8)	(9)	(10)	(11)
NGVS-UCD383	-10.41	-9.91	13.61± 0.30	6.6	1368	S11	1	0	$u^*gzK + \langle\mu_g\rangle_e + \langle r_h\rangle$	S1631/H50032
NGVS-UCD384	-10.50	-10.00	17.45± 0.28	6.6	1129	AAT12,S11,IMACS16	1	0	$u^*gzK + \langle\mu_g\rangle_e + \langle r_h\rangle$	S1629
NGVS-UCD385	-10.92	-10.39	16.48± 0.34	6.8	1406	AAT12,S11	1	0	$u^*gzK + \langle\mu_g\rangle_e + \langle r_h\rangle$	S1617/H44476
NGVS-UCD386	-9.62	-9.00	11.19± 0.28	6.4	1418	MMT09	1	0	$u^*gzK + \langle\mu_g\rangle_e + \langle r_h\rangle$	···
NGVS-UCD387	-10.89	-10.39	11.26± 0.24	6.8	1610	MMT14	1	1	$u^*gzK + \langle\mu_g\rangle_e + \langle r_h\rangle$	···
NGVS-UCD388	-10.79	-10.29	12.27± 0.22	6.7	1026	IMACS16	1	0	$u^*gzK + \langle\mu_g\rangle_e + \langle r_h\rangle$	···
NGVS-UCD389	-10.39	-9.97	20.03± 0.48	6.5	845	AAT12,IMACS16	1	0	$u^*gz + \langle\mu_g\rangle_e + \langle r_h\rangle$	M87UCD-11
NGVS-UCD390	-10.41	-9.85	11.78± 0.19	6.7	1395	MMT14	1	0	$u^*gzK + \langle\mu_g\rangle_e + \langle r_h\rangle$	···
NGVS-UCD391	-10.72	-10.15	22.63± 0.22	6.8	1154	MMT09,IMACS16	1	0	$u^*gzK + \langle\mu_g\rangle_e + \langle r_h\rangle$	M87UCD-38
NGVS-UCD392	-11.11	-10.59	16.14± 0.38	6.9	2408	MMT09,AAT12,NED,S11	1	0	$u^*gzK + \langle\mu_g\rangle_e + \langle r_h\rangle$	VUCD10
NGVS-UCD393	-10.63	-9.99	13.72± 0.54	6.9	1503	MMT09,AAT12	1	1	$u^*gzK + \langle\mu_g\rangle_e + \langle r_h\rangle$	M87UCD-12
NGVS-UCD394	-10.59	-10.14	14.36± 0.21	6.6	858	AAT12,S11,IMACS16	1	0	$u^*gzK + \langle\mu_g\rangle_e + \langle r_h\rangle$	S1504/H49431
NGVS-UCD395	-11.53	-11.01	36.15± 0.34	7.1	1304	MMT09,AAT12,NED,S11,IMACS16	1	1	$u^*gzK + \langle\mu_g\rangle_e + \langle r_h\rangle$	H55930/1297-1
NGVS-UCD396	-9.52	-9.04	16.58± 0.14	6.2	1100	S11	1	0	$u^*gz + \langle\mu_g\rangle_e + \langle r_h\rangle$	S1449/H42852
NGVS-UCD397	-9.32	-8.84	22.09± 0.47	6.1	···	···	1	0	$u^*gz + \langle\mu_g\rangle_e + \langle r_h\rangle$	···
NGVS-UCD398	-10.29	-9.81	36.49± 0.38	6.5	···	···	1	0	$u^*gzK + \langle\mu_g\rangle_e + \langle r_h\rangle$	···
NGVS-UCD399	-10.18	-9.76	13.86± 0.27	6.4	···	···	4	0	$u^*gzK + \langle\mu_g\rangle_e + \langle r_h\rangle$	···
NGVS-UCD400	-10.32	-9.83	16.23± 0.24	6.5	1614	IMACS16	1	0	$u^*gzK + \langle\mu_g\rangle_e + \langle r_h\rangle$	···
NGVS-UCD401	-10.37	-9.90	16.15± 0.79	6.6	···	···	2	0	$u^*gzK + \langle\mu_g\rangle_e + \langle r_h\rangle$	···
NGVS-UCD402	-10.13	-9.67	14.43± 0.39	6.5	1086	S11	1	0	$(v_r < 3500\mathrm{km/s}) + \langle r_h\rangle$	S1301/H40402
NGVS-UCD403	-9.31	-8.89	19.54± 0.50	6.0	···	···	1	0	$u^*gz + \langle\mu_g\rangle_e + \langle r_h\rangle$	···
NGVS-UCD404	-9.68	-9.23	14.55± 0.27	6.2	1211	S11	1	0	$u^*gz + \langle\mu_g\rangle_e + \langle r_h\rangle$	S1201/H44795
NGVS-UCD405	-9.61	-9.13	16.42± 0.33	6.3	···	···	1	0	$u^*gz + \langle\mu_g\rangle_e + \langle r_h\rangle$	···
NGVS-UCD406	-9.29	-8.78	21.52± 0.93	6.1	···	···	3	0	$u^*gz + \langle\mu_g\rangle_e + \langle r_h\rangle$	···
NGVS-UCD407	-10.19	-9.72	22.56± 0.27	6.5	2023	S11	1	0	$u^*gzK + \langle\mu_g\rangle_e + \langle r_h\rangle$	S1044/H38484
NGVS-UCD408	-9.27	-8.69	14.60± 0.49	6.2	···	···	1	0	$u^*gz + \langle\mu_g\rangle_e + \langle r_h\rangle$	···
NGVS-UCD409	-10.57	-10.10	19.77± 0.30	6.6	1503	AAT12,S11	1	0	$u^*gzK + \langle\mu_g\rangle_e + \langle r_h\rangle$	S999/1316-2/H47560
NGVS-UCD410	-9.67	-9.22	30.29± 1.02	6.3	···	···	1	0	$u^*gz + \langle\mu_g\rangle_e + \langle r_h\rangle$	···
NGVS-UCD411	-10.34	-9.86	19.57± 0.36	6.6	1079	S11	1	0	$u^*gzK + \langle\mu_g\rangle_e + \langle r_h\rangle$	S8006/1316-4/H46290
NGVS-UCD412	-11.32	-10.74	17.39± 0.01	7.1	1340	MMT09,AAT12,S11	1	0	$u^*gzK + \langle\mu_g\rangle_e + \langle r_h\rangle$	F6
NGVS-UCD413	-11.14	-10.67	23.17± 0.28	6.8	1280	MMT09,AAT12	1	0	$u^*gzK + \langle\mu_g\rangle_e + \langle r_h\rangle$	M87UCD-2
NGVS-UCD414	-11.05	-10.58	25.05± 0.54	6.8	1328	AAT12,S11,IMACS16	1	0	$u^*gzK + \langle\mu_g\rangle_e + \langle r_h\rangle$	S928/1316-5/H46593
NGVS-UCD415	-9.35	-8.87	11.05± 0.32	6.1	1889	MMT09	1	0	$u^*gz + \langle\mu_g\rangle_e + \langle r_h\rangle$	···
NGVS-UCD416	-11.68	-11.14	11.10± 0.01	7.2	914	MMT09,AAT12,NED,S11,IMACS16	1	1	$u^*gzK + \langle\mu_g\rangle_e + \langle r_h\rangle$	VUCD2
NGVS-UCD417	-10.88	-10.35	12.79± 0.02	6.8	1603	MMT09,AAT12	1	0	$u^*gzK + \langle\mu_g\rangle_e + \langle r_h\rangle$	M87UCD-13
NGVS-UCD418	-10.28	-9.74	17.03± 0.11	6.5	···	···	1	0	$u^*gzK + \langle\mu_g\rangle_e + \langle r_h\rangle$	···
NGVS-UCD419	-9.87	-9.33	11.46± 0.32	6.4	1160	MMT09	1	0	$u^*gzK + \langle\mu_g\rangle_e + \langle r_h\rangle$	VCC-1333
NGVS-UCD420	-10.61	-10.10	11.41± 0.18	6.7	1516	AAT12,S11	1	0	$u^*gz + \langle\mu_g\rangle_e + \langle r_h\rangle$	S5065/1316-6/H45758
NGVS-UCD421	-9.41	-9.01	21.31± 0.45	6.1	···	···	1	0	$u^*gz + \langle\mu_g\rangle_e + \langle r_h\rangle$	···
NGVS-UCD422	-10.73	-10.29	29.51± 0.84	6.7	···	···	1	0	$u^*gz + \langle\mu_g\rangle_e + \langle r_h\rangle$	···
NGVS-UCD423	-11.13	-10.54	13.99± 0.36	7.0	1132	AAT12,S11,IMACS16	1	0	$u^*gzK + \langle\mu_g\rangle_e + \langle r_h\rangle$	S804/H49764
NGVS-UCD424	-9.81	-9.33	13.92± 0.20	6.3	1300	NED,S11	1	0	$u^*gz + \langle\mu_g\rangle_e + \langle r_h\rangle$	H27916
NGVS-UCD425	-10.07	-9.60	11.73± 0.15	6.4	1163	S11	1	0	$u^*gzK + \langle\mu_g\rangle_e + \langle r_h\rangle$	S796/H39097
NGVS-UCD426	-10.31	-9.81	32.76± 0.90	6.6	···	···	3	0	$u^*gz + \langle\mu_g\rangle_e + \langle r_h\rangle$	···
NGVS-UCD427	-9.32	-8.84	16.24± 0.34	6.1	···	···	1	0	$u^*gz + \langle\mu_g\rangle_e + \langle r_h\rangle$	···
NGVS-UCD428	-10.46	-10.02	14.66± 0.53	6.5	···	···	2	0	$u^*gzK + \langle\mu_g\rangle_e + \langle r_h\rangle$	VCC-1320
NGVS-UCD429	-9.71	-9.17	19.95± 0.51	6.4	1020	S11	1	0	$u^*gzK + \langle\mu_g\rangle_e + \langle r_h\rangle$	S731/H32688
NGVS-UCD430	-9.59	-9.18	20.20± 0.28	6.2	1333	NED,S11	1	0	$u^*gz + \langle\mu_g\rangle_e + \langle r_h\rangle$	S682/H38122

Table 4 *continued*

Table 4 *(continued)*

Name	M_B	M_V	$\langle r_h \rangle$	$\log(M_*/M_{odot})$	v_r	$v_{\rm source}$	Class	Envelope	Method	OtherName
	(mag)	(mag)	(pc)		(km/s)					
(1)	(2)	(3)	(4)	(5)	(6)	(7)	(8)	(9)	(10)	(11)
NGVS-UCD431	-11.87	-11.10	20.08± 0.46	7.5	713	MMT09,AAT12,NED,S11,IMACS16,NTT17	1	1	$u^*gzK + \langle\mu_g\rangle_e + \langle r_h\rangle$	VUCD3
NGVS-UCD432	-10.13	-9.71	12.05± 0.39	6.4	···	···	1	0	$u^*gz + \langle\mu_g\rangle_e + \langle r_h\rangle$	···
NGVS-UCD433	-10.83	-10.40	22.96± 0.41	6.7	1651	NED,S11	1	0	$u^*gzK + \langle\mu_g\rangle_e + \langle r_h\rangle$	S477/H34046
NGVS-UCD434	-9.75	-9.27	29.40± 0.49	6.3	···	···	1	0	$u^*gzK + \langle\mu_g\rangle_e + \langle r_h\rangle$	···
NGVS-UCD435	-11.27	-10.81	61.49± 5.36	6.9	1246	VCC,SDSS,NED	2	0	$(v_r < 3500\mathrm{km/s}) + \langle r_h\rangle$	VCC-1333
NGVS-UCD436	-11.15	-10.52	15.05± 0.23	7.1	1857	AAT12,S11,IMACS16	1	0	$u^*gzK + \langle\mu_g\rangle_e + \langle r_h\rangle$	S417/H36395
NGVS-UCD437	-10.23	-9.81	23.06± 0.37	6.4	1215	NED,S11,IMACS16	1	0	$u^*gzK + \langle\mu_g\rangle_e + \langle r_h\rangle$	S376/H52442
NGVS-UCD438	-11.05	-10.62	18.89± 0.28	6.8	1190	AAT12,NED,S11	1	0	$u^*gzK + \langle\mu_g\rangle_e + \langle r_h\rangle$	F12/H62525
NGVS-UCD439	···	···	13.05± 0.74	7.6	95	SDSS	4	0	$(v_r < 3500\mathrm{km/s}) + \langle r_h\rangle$	···
NGVS-UCD440	-9.68	-9.23	11.77± 0.22	6.2	···	···	1	0	$u^*gz + \langle\mu_g\rangle_e + \langle r_h\rangle$	···
NGVS-UCD441	-10.82	-10.36	13.34± 0.25	6.7	705	MMT09,AAT12,S11	1	0	$u^*gzK + \langle\mu_g\rangle_e + \langle r_h\rangle$	H59533
NGVS-UCD442	-9.43	-9.00	27.11± 0.79	6.0	···	···	1	0	$u^*gz + \langle\mu_g\rangle_e + \langle r_h\rangle$	···
NGVS-UCD443	-10.19	-9.75	32.10± 0.69	6.4	1157	NED,S11,IMACS16	1	0	$u^*gzK + \langle\mu_g\rangle_e + \langle r_h\rangle$	S323/H44135
NGVS-UCD444	-11.70	-11.18	18.46± 0.29	7.1	916	MMT09,AAT12,NED,S11	1	1	$u^*gzK + \langle\mu_g\rangle_e + \langle r_h\rangle$	VUCD4
NGVS-UCD445	-10.21	-9.73	14.93± 0.64	6.5	···	···	1	1	$u^*gzK + \langle\mu_g\rangle_e + \langle r_h\rangle$	···
NGVS-UCD446	-10.04	-9.61	11.19± 0.28	6.4	1352	MMT09	1	0	$u^*gzK + \langle\mu_g\rangle_e + \langle r_h\rangle$	···
NGVS-UCD447	-11.04	-10.59	15.87± 0.27	6.8	426	MMT14	1	1	$u^*gzK + \langle\mu_g\rangle_e + \langle r_h\rangle$	···
NGVS-UCD448	-9.52	-9.02	24.11± 0.38	6.2	1818	S11	1	0	$u^*gz + \langle\mu_g\rangle_e + \langle r_h\rangle$	S6004/H30775
NGVS-UCD449	-10.02	-9.44	14.21± 0.50	6.5	1208	MMT09	1	0	$u^*gzK + \langle\mu_g\rangle_e + \langle r_h\rangle$	M87UCD-36
NGVS-UCD450	-9.41	-8.99	15.36± 0.49	6.1	···	···	1	0	$u^*gz + \langle\mu_g\rangle_e + \langle r_h\rangle$	···
NGVS-UCD451	-10.61	-10.15	11.48± 0.17	6.6	1759	MMT09,AAT12,S11,IMACS16	1	0	$u^*gzK + \langle\mu_g\rangle_e + \langle r_h\rangle$	S137/H38656
NGVS-UCD452	-9.28	-8.80	23.13± 0.47	6.0	···	···	1	0	$u^*gz + \langle\mu_g\rangle_e + \langle r_h\rangle$	···
NGVS-UCD453	-11.76	-11.10	20.08± 0.16	7.4	1292	MMT09,AAT12,NED,S11	1	0	$u^*gzK + \langle\mu_g\rangle_e + \langle r_h\rangle$	VUCD5
NGVS-UCD454	-9.55	-9.08	17.03± 0.24	6.2	1087	MMT14	1	0	$u^*gz + \langle\mu_g\rangle_e + \langle r_h\rangle$	···
NGVS-UCD455	-10.70	-10.21	17.67± 0.29	6.7	691	MMT09,AAT12,NED,S11	1	0	$u^*gzK + \langle\mu_g\rangle_e + \langle r_h\rangle$	H27496
NGVS-UCD456	-9.28	-8.84	15.51± 0.39	6.1	···	···	1	0	$u^*gz + \langle\mu_g\rangle_e + \langle r_h\rangle$	···
NGVS-UCD457	-12.59	-12.00	41.72± 2.24	7.6	1788	VCC,SDSS,NED	2	0	$u^*gzK + \langle\mu_g\rangle_e + \langle r_h\rangle$	VCC-1348
NGVS-UCD458	-9.89	-9.41	25.25± 0.33	6.4	1816	MMT09,S11	1	0	$u^*gzK + \langle\mu_g\rangle_e + \langle r_h\rangle$	S41/H35264
NGVS-UCD459	-10.37	-9.95	37.24± 0.55	6.5	···	···	1	0	$u^*gzK + \langle\mu_g\rangle_e + \langle r_h\rangle$	···
NGVS-UCD460	-10.49	-9.97	27.70± 0.37	6.7	1136	AAT12	1	0	$u^*gzK + \langle\mu_g\rangle_e + \langle r_h\rangle$	M87UCD-1
NGVS-UCD461	-10.38	-9.86	11.61± 0.20	6.6	1286	MMT09,AAT12,S11,IMACS16	1	0	$u^*gzK + \langle\mu_g\rangle_e + \langle r_h\rangle$	H24581
NGVS-UCD462	-11.12	-10.65	35.51± 0.28	6.8	1233	MMT14	1	1	$u^*gzK + \langle\mu_g\rangle_e + \langle r_h\rangle$	···
NGVS-UCD463	-9.93	-9.49	29.46± 0.39	6.3	···	···	1	0	$u^*gz + \langle\mu_g\rangle_e + \langle r_h\rangle$	···
NGVS-UCD464	-11.06	-10.58	13.35± 0.14	6.8	1776	MMT09,AAT12	1	0	$u^*gzK + \langle\mu_g\rangle_e + \langle r_h\rangle$	M87UCD-18
NGVS-UCD465	-11.61	-11.12	37.11± 0.32	7.1	14357	NTT17	3	0	$u^*gz + \langle\mu_g\rangle_e + \langle r_h\rangle$	···
NGVS-UCD466	-10.64	-10.20	31.32± 0.35	6.6	1632	MMT09,IMACS16	1	0	$u^*gzK + \langle\mu_g\rangle_e + \langle r_h\rangle$	M87UCD-32
NGVS-UCD467	-10.40	-9.98	33.35± 0.66	6.5	···	···	1	0	$u^*gz + \langle\mu_g\rangle_e + \langle r_h\rangle$	···
NGVS-UCD468	-10.07	-9.62	11.44± 0.14	6.4	984	MMT09	1	0	$u^*gzK + \langle\mu_g\rangle_e + \langle r_h\rangle$	···
NGVS-UCD469	-11.52	-10.99	14.38± 0.31	7.1	2104	MMT09,AAT12,NED,S11	1	1	$u^*gzK + \langle\mu_g\rangle_e + \langle r_h\rangle$	VUCD6
NGVS-UCD470	-9.89	-9.41	16.21± 0.94	6.4	1839	VCC,NED	2	0	$u^*gzK + \langle\mu_g\rangle_e + \langle r_h\rangle$	VCC-1366
NGVS-UCD471	-11.27	-10.78	37.88± 0.46	7.0	1128	MMT09,AAT12	1	0	$(v_r < 3500\mathrm{km/s}) + \langle r_h\rangle$	M87UCD-16
NGVS-UCD472	-9.85	-9.33	12.08± 0.41	6.4	833	MMT14	1	0	$u^*gz + \langle\mu_g\rangle_e + \langle r_h\rangle$	···
NGVS-UCD473	-10.70	-10.10	13.44± 0.49	6.8	956	MMT09,AAT12	1	0	$u^*gzK + \langle\mu_g\rangle_e + \langle r_h\rangle$	M87UCD-17
NGVS-UCD474	-9.61	-9.17	19.36± 0.39	6.2	···	···	1	0	$u^*gz + \langle\mu_g\rangle_e + \langle r_h\rangle$	···
NGVS-UCD475	-10.97	-10.41	19.47± 0.25	6.9	1542	MMT09	1	0	$u^*gzK + \langle\mu_g\rangle_e + \langle r_h\rangle$	···
NGVS-UCD476	-10.62	-10.19	34.05± 1.05	6.6	···	···	1	0	$u^*gz + \langle\mu_g\rangle_e + \langle r_h\rangle$	···
NGVS-UCD477	-10.92	-10.16	19.72± 0.76	7.1	···	···	3	0	$u^*gzK + \langle\mu_g\rangle_e + \langle r_h\rangle$	···
NGVS-UCD478	-10.26	-9.82	11.67± 0.31	6.5	1484	MMT09	1	0	$u^*gz + \langle\mu_g\rangle_e + \langle r_h\rangle$	M87UCD-21

Table 4 *continued*

Table 4 *(continued)*

Name	M_B	M_V	$\langle r_h \rangle$	$\log(M_*/M_{odot})$	v_r	$v_{\rm source}$	Class	Envelope	Method	OtherName
	(mag)	(mag)	(pc)		(km/s)					
(1)	(2)	(3)	(4)	(5)	(6)	(7)	(8)	(9)	(10)	(11)
NGVS-UCD479	-9.90	-9.46	29.37± 0.90	6.4	···	···	3	0	$u^*gz + \langle\mu_g\rangle_e + \langle r_h\rangle$	···
NGVS-UCD480	-10.11	-9.61	19.17± 0.46	6.5	1264	MMT09	1	0	$u^*gzK + \langle\mu_g\rangle_e + \langle r_h\rangle$	M87UCD-25
NGVS-UCD481	-9.68	-9.26	15.74± 0.22	6.2	···	···	1	0	$u^*gz + \langle\mu_g\rangle_e + \langle r_h\rangle$	···
NGVS-UCD482	-9.72	-9.28	19.54± 0.54	6.3	···	···	1	0	$u^*gz + \langle\mu_g\rangle_e + \langle r_h\rangle$	···
NGVS-UCD483	-9.77	-9.27	24.88± 0.34	6.3	···	···	1	0	$u^*gz + \langle\mu_g\rangle_e + \langle r_h\rangle$	···
NGVS-UCD484	-9.53	-9.11	12.58± 0.28	6.2	1320	S11	1	0	$u^*gz + \langle\mu_g\rangle_e + \langle r_h\rangle$	H51655
NGVS-UCD485	-9.99	-9.54	11.55± 0.37	6.4	1033	MMT09	1	0	$u^*gz + \langle\mu_g\rangle_e + \langle r_h\rangle$	···
NGVS-UCD486	-10.14	-9.44	11.23± 0.28	6.7	1270	MMT09	1	0	$u^*gzK + \langle\mu_g\rangle_e + \langle r_h\rangle$	···
NGVS-UCD487	-9.55	-9.12	19.20± 0.36	6.1	···	···	1	0	$u^*gz + \langle\mu_g\rangle_e + \langle r_h\rangle$	···
NGVS-UCD488	-12.24	-11.68	21.91± 0.83	7.5	980	AAT12,SDSS,NED,S11	2	0	$u^*gzK + \langle\mu_g\rangle_e + \langle r_h\rangle$	VUCD7
NGVS-UCD489	-10.31	-9.89	35.40± 0.69	6.5	···	···	1	0	$u^*gzK + \langle\mu_g\rangle_e + \langle r_h\rangle$	···
NGVS-UCD490	-9.71	-9.28	22.66± 0.32	6.2	···	···	1	0	$u^*gz + \langle\mu_g\rangle_e + \langle r_h\rangle$	···
NGVS-UCD491	-10.25	-9.75	26.57± 0.59	6.5	···	···	1	0	$u^*gz + \langle\mu_g\rangle_e + \langle r_h\rangle$	···
NGVS-UCD492	-13.21	-12.34	51.40± 1.26	8.1	13723	SDSS,NED	3	0	$u^*gz + \langle\mu_g\rangle_e + \langle r_h\rangle$	···
NGVS-UCD493	-10.15	-9.69	24.78± 0.43	6.4	···	···	1	0	$u^*gz + \langle\mu_g\rangle_e + \langle r_h\rangle$	···
NGVS-UCD494	-9.70	-9.29	32.21± 0.81	6.2	···	···	1	0	$u^*gz + \langle\mu_g\rangle_e + \langle r_h\rangle$	···
NGVS-UCD495	-10.54	-10.06	18.54± 0.24	6.6	1087	MMT09,AAT12	1	0	$u^*gzK + \langle\mu_g\rangle_e + \langle r_h\rangle$	M87UCD-19
NGVS-UCD496	-11.16	-10.72	37.54± 0.55	6.9	1266	MMT09,AAT12	1	0	$u^*gzK + \langle\mu_g\rangle_e + \langle r_h\rangle$	M87UCD-15
NGVS-UCD497	-10.19	-9.61	11.28± 0.36	6.6	1213	MMT09	1	0	$u^*gzK + \langle\mu_g\rangle_e + \langle r_h\rangle$	···
NGVS-UCD498	-11.21	-10.70	13.14± 0.33	6.9	1649	MMT09,AAT12,NED,S11	1	0	$u^*gzK + \langle\mu_g\rangle_e + \langle r_h\rangle$	VUCD8
NGVS-UCD499	-9.33	-8.86	18.55± 0.47	6.1	···	···	1	0	$u^*gz + \langle\mu_g\rangle_e + \langle r_h\rangle$	···
NGVS-UCD500	-9.46	-9.00	12.44± 0.37	6.2	···	···	2	0	$u^*gz + \langle\mu_g\rangle_e + \langle r_h\rangle$	···
NGVS-UCD501	-9.61	-9.17	25.74± 0.48	6.2	39582	MMT14	3	0	$u^*gz + \langle\mu_g\rangle_e + \langle r_h\rangle$	···
NGVS-UCD502	-11.22	-10.56	12.46± 0.20	7.1	2372	AAT12	1	0	$u^*gzK + \langle\mu_g\rangle_e + \langle r_h\rangle$	···
NGVS-UCD503	-10.21	-9.68	17.40± 0.44	6.6	1833	MMT09	1	0	$u^*gzK + \langle\mu_g\rangle_e + \langle r_h\rangle$	M87UCD-33
NGVS-UCD504	-11.41	-10.85	18.53± 0.44	7.1	1298	MMT09,AAT12,NED,S11	1	1	$u^*gzK + \langle\mu_g\rangle_e + \langle r_h\rangle$	VUCD9
NGVS-UCD505	-10.10	-9.66	28.91± 0.54	6.4	···	···	1	0	$u^*gzK + \langle\mu_g\rangle_e + \langle r_h\rangle$	···
NGVS-UCD506	-10.82	-10.38	43.22± 1.09	6.7	···	···	1	0	$u^*gz + \langle\mu_g\rangle_e + \langle r_h\rangle$	···
NGVS-UCD507	-10.68	-10.15	11.70± 0.25	6.7	1007	MMT09	1	0	$u^*gzK + \langle\mu_g\rangle_e + \langle r_h\rangle$	M87UCD-35
NGVS-UCD508	-9.26	-8.80	26.16± 0.88	6.1	···	···	3	0	$u^*gz + \langle\mu_g\rangle_e + \langle r_h\rangle$	···
NGVS-UCD509	-10.34	-9.87	12.14± 0.30	6.5	1272	MMT09	1	1	$u^*gzK + \langle\mu_g\rangle_e + \langle r_h\rangle$	M87UCD-27
NGVS-UCD510	-9.65	-9.24	19.42± 0.73	6.2	···	···	3	0	$u^*gz + \langle\mu_g\rangle_e + \langle r_h\rangle$	···
NGVS-UCD511	-10.01	-9.60	29.60± 1.67	6.3	···	···	3	0	$u^*gz + \langle\mu_g\rangle_e + \langle r_h\rangle$	···
NGVS-UCD512	-10.02	-9.61	28.42± 1.38	6.4	···	···	3	0	$u^*gz + \langle\mu_g\rangle_e + \langle r_h\rangle$	···
NGVS-UCD513	-9.48	-9.08	18.08± 0.40	6.1	···	···	1	0	$u^*gz + \langle\mu_g\rangle_e + \langle r_h\rangle$	···
NGVS-UCD514	-9.37	-8.92	18.47± 0.29	6.1	···	···	1	0	$u^*gz + \langle\mu_g\rangle_e + \langle r_h\rangle$	···
NGVS-UCD515	-9.44	-8.94	11.19± 0.54	6.2	704	MMT14	1	0	$u^*gz + \langle\mu_g\rangle_e + \langle r_h\rangle$	···
NGVS-UCD516	-9.38	-8.95	18.69± 0.49	6.1	···	···	3	0	$u^*gz + \langle\mu_g\rangle_e + \langle r_h\rangle$	···
NGVS-UCD517	-9.35	-8.89	12.33± 0.43	6.1	···	···	1	0	$u^*gz + \langle\mu_g\rangle_e + \langle r_h\rangle$	···
NGVS-UCD518	-9.73	-9.25	11.35± 0.22	6.3	···	···	1	0	$u^*gz + \langle\mu_g\rangle_e + \langle r_h\rangle$	···
NGVS-UCD519	-9.42	-8.95	26.01± 0.67	6.2	30219	MMT09	3	0	$u^*gz + \langle\mu_g\rangle_e + \langle r_h\rangle$	···
NGVS-UCD520	-12.71	-11.97	36.47± 0.55	7.8	7295	NTT17	3	0	$u^*gzK + \langle\mu_g\rangle_e + \langle r_h\rangle$	···
NGVS-UCD521	-9.36	-8.95	14.24± 0.62	6.1	···	···	1	0	$u^*gz + \langle\mu_g\rangle_e + \langle r_h\rangle$	···
NGVS-UCD522	-9.54	-9.01	17.88± 0.99	6.1	···	···	1	0	$u^*gz + \langle\mu_g\rangle_e + \langle r_h\rangle$	···
NGVS-UCD523	-9.46	-9.00	23.76± 0.62	6.2	···	···	3	0	$u^*gz + \langle\mu_g\rangle_e + \langle r_h\rangle$	···
NGVS-UCD524	-10.72	-10.29	16.86± 0.45	6.6	···	···	3	0	$u^*gzK + \langle\mu_g\rangle_e + \langle r_h\rangle$	···
NGVS-UCD525	-9.48	-9.01	16.80± 0.69	6.2	36365	MMT09	3	0	$u^*gz + \langle\mu_g\rangle_e + \langle r_h\rangle$	···
NGVS-UCD526	-10.16	-9.74	28.73± 0.43	6.4	···	···	1	1	$u^*gzK + \langle\mu_g\rangle_e + \langle r_h\rangle$	···

Table 4 *continued*

Table 4 *(continued)*

Name	M_B	M_V	$\langle r_h \rangle$	$\log(M_*/M_{odot})$	v_r	$v_{\rm source}$	Class	Envelope	Method	OtherName
	(mag)	(mag)	(pc)		(km/s)					
(1)	(2)	(3)	(4)	(5)	(6)	(7)	(8)	(9)	(10)	(11)
NGVS-UCD527	-9.28	-8.74	20.04± 0.45	6.1	···	···	1	0	$u^*gz + \langle\mu_g\rangle_e + \langle r_h\rangle$	···
NGVS-UCD528	-9.37	-8.91	11.44± 0.47	6.1	222826	MMT14	3	0	$u^*gz + \langle\mu_g\rangle_e + \langle r_h\rangle$	···
NGVS-UCD529	-9.31	-8.83	21.18± 0.35	6.1	···	···	3	0	$u^*gz + \langle\mu_g\rangle_e + \langle r_h\rangle$	···
NGVS-UCD530	-9.37	-8.95	21.88± 0.50	6.0	···	···	1	0	$u^*gz + \langle\mu_g\rangle_e + \langle r_h\rangle$	···
NGVS-UCD531	-10.52	-10.09	33.03± 0.81	6.6	···	···	3	0	$u^*gz + \langle\mu_g\rangle_e + \langle r_h\rangle$	···
NGVS-UCD532	-9.78	-9.27	23.91± 0.40	6.4	···	···	3	0	$u^*gz + \langle\mu_g\rangle_e + \langle r_h\rangle$	···
NGVS-UCD533	-10.32	-9.87	12.28± 0.37	6.5	1251	MMT09,NED,S11	1	0	$u^*gzK + \langle\mu_g\rangle_e + \langle r_h\rangle$	F16
NGVS-UCD534	-9.70	-9.20	11.78± 0.20	6.3	···	···	1	0	$u^*gz + \langle\mu_g\rangle_e + \langle r_h\rangle$	···
NGVS-UCD535	-10.94	-10.42	12.26± 0.30	6.8	···	···	1	1	$u^*gzK + \langle\mu_g\rangle_e + \langle r_h\rangle$	···
NGVS-UCD536	-9.57	-9.16	22.35± 1.01	6.1	···	···	1	0	$u^*gz + \langle\mu_g\rangle_e + \langle r_h\rangle$	···
NGVS-UCD537	-10.55	-10.20	62.46± 5.72	6.7	1177	SDSS,NED	2	0	$(v_r < 3500\mathrm{km/s}) + \langle r_h\rangle$	···
NGVS-UCD538	-9.59	-9.11	21.17± 0.63	6.2	···	···	1	0	$u^*gz + \langle\mu_g\rangle_e + \langle r_h\rangle$	···
NGVS-UCD539	-9.42	-8.97	30.52± 0.54	6.1	···	···	1	0	$u^*gz + \langle\mu_g\rangle_e + \langle r_h\rangle$	···
NGVS-UCD540	-9.96	-9.40	16.52± 0.44	6.5	···	···	1	0	$u^*gzK + \langle\mu_g\rangle_e + \langle r_h\rangle$	···
NGVS-UCD541	-9.85	-9.23	11.20± 0.18	6.5	1351	Ko2017	1	0	$u^*gzK + \langle\mu_g\rangle_e + \langle r_h\rangle$	M87UCD-39
NGVS-UCD542	-9.33	-8.92	16.91± 0.28	6.1	···	···	1	0	$u^*gz + \langle\mu_g\rangle_e + \langle r_h\rangle$	···
NGVS-UCD543	-10.68	-10.01	14.35± 0.25	6.9	767	SIMBAD	1	0	$u^*gzK + \langle\mu_g\rangle_e + \langle r_h\rangle$	···
NGVS-UCD544	-9.52	-8.85	11.88± 0.34	6.4	812	MMT14	1	0	$(v_r < 3500\mathrm{km/s}) + \langle r_h\rangle$	···
NGVS-UCD545	···	···	20.73± 0.10	7.5	···	···	5	0	$gzK + \langle\mu_g\rangle_e + r_{h,g}$	···
NGVS-UCD546	-9.66	-9.12	13.84± 0.27	6.4	731	SIMBAD	1	0	$u^*gz + \langle\mu_g\rangle_e + \langle r_h\rangle$	···
NGVS-UCD547	-9.35	-8.90	18.55± 0.56	6.0	···	···	1	0	$u^*gz + \langle\mu_g\rangle_e + \langle r_h\rangle$	···
NGVS-UCD548	-10.51	-9.97	12.64± 0.21	6.7	854	MMT14	1	0	$u^*gz + \langle\mu_g\rangle_e + \langle r_h\rangle$	···
NGVS-UCD549	-10.54	-10.12	44.41± 0.83	6.5	817	SDSS,NED	1	0	$(v_r < 3500\mathrm{km/s}) + \langle r_h\rangle$	···
NGVS-UCD550	-9.53	-9.07	12.77± 0.26	6.2	···	···	1	0	$u^*gz + \langle\mu_g\rangle_e + \langle r_h\rangle$	···
NGVS-UCD551	-9.60	-9.16	28.15± 0.36	6.2	···	···	1	0	$u^*gz + \langle\mu_g\rangle_e + \langle r_h\rangle$	···
NGVS-UCD552	-9.31	-8.85	23.45± 0.67	6.1	···	···	3	0	$u^*gz + \langle\mu_g\rangle_e + \langle r_h\rangle$	···
NGVS-UCD553	-11.79	-11.02	17.54± 0.69	7.5	23801	NTT17	3	0	$u^*gzK + \langle\mu_g\rangle_e + \langle r_h\rangle$	···
NGVS-UCD554	-10.11	-9.67	26.83± 0.58	6.4	···	···	1	0	$u^*gz + \langle\mu_g\rangle_e + \langle r_h\rangle$	···
NGVS-UCD555	-9.64	-9.24	26.48± 0.81	6.2	···	···	3	0	$u^*gz + \langle\mu_g\rangle_e + \langle r_h\rangle$	···
NGVS-UCD556	-9.31	-8.81	25.33± 0.42	6.2	···	···	1	0	$u^*gz + \langle\mu_g\rangle_e + \langle r_h\rangle$	···
NGVS-UCD557	-10.29	-9.82	15.75± 0.32	6.5	···	···	1	0	$u^*gzK + \langle\mu_g\rangle_e + \langle r_h\rangle$	···
NGVS-UCD558	-10.48	-10.05	43.58± 0.55	6.5	···	···	1	0	$u^*gz + \langle\mu_g\rangle_e + \langle r_h\rangle$	···
NGVS-UCD559	-9.26	-8.79	22.71± 0.44	6.1	···	···	1	0	$u^*gz + \langle\mu_g\rangle_e + \langle r_h\rangle$	···
NGVS-UCD560	-11.53	-10.99	11.52± 0.13	7.1	644	MMT14,NTT17	1	0	$u^*gz + \langle\mu_g\rangle_e + \langle r_h\rangle$	···
NGVS-UCD561	-10.87	-10.91	25.22± 0.04	5.9	2018	AAT12	6	0	$(v_r < 3500\mathrm{km/s}) + \langle r_h\rangle$	···
NGVS-UCD562	-9.37	-8.91	23.08± 0.41	6.1	···	···	1	0	$u^*gz + \langle\mu_g\rangle_e + \langle r_h\rangle$	···
NGVS-UCD563	-12.66	-12.78	14.69± 0.66	6.4	1843	SDSS,NED	6	0	$(v_r < 3500\mathrm{km/s}) + \langle r_h\rangle$	···
NGVS-UCD564	-10.98	-11.06	12.53± 0.04	5.8	1919	AAT12	6	0	$(v_r < 3500\mathrm{km/s}) + \langle r_h\rangle$	···
NGVS-UCD565	-10.53	-10.04	12.78± 0.27	6.6	···	···	1	0	$u^*gzK + \langle\mu_g\rangle_e + \langle r_h\rangle$	···
NGVS-UCD566	-9.66	-9.24	14.00± 0.24	6.2	···	···	1	0	$u^*gz + \langle\mu_g\rangle_e + \langle r_h\rangle$	···
NGVS-UCD567	-10.13	-9.66	24.42± 0.49	6.4	···	···	1	0	$u^*gz + \langle\mu_g\rangle_e + \langle r_h\rangle$	···
NGVS-UCD568	-12.19	-12.24	55.08± 0.07	6.5	1844	SDSS,NED	6	0	$(v_r < 3500\mathrm{km/s}) + \langle r_h\rangle$	···
NGVS-UCD569	-11.58	-11.62	17.74± 0.80	6.2	1832	AAT12	6	0	$(v_r < 3500\mathrm{km/s}) + \langle r_h\rangle$	···
NGVS-UCD570	-10.73	-10.83	23.10± 1.03	5.7	1919	AAT12	6	0	$(v_r < 3500\mathrm{km/s}) + \langle r_h\rangle$	···
NGVS-UCD571	-9.62	-9.12	11.90± 0.42	6.3	···	···	1	0	$u^*gz + \langle\mu_g\rangle_e + \langle r_h\rangle$	···
NGVS-UCD572	-9.79	-9.39	29.24± 0.64	6.2	···	···	1	0	$u^*gz + \langle\mu_g\rangle_e + \langle r_h\rangle$	···
NGVS-UCD573	-10.99	-10.45	13.07± 0.26	6.9	···	···	1	0	$u^*gzK + \langle\mu_g\rangle_e + \langle r_h\rangle$	···
NGVS-UCD574	-9.46	-9.04	22.70± 0.36	6.1	···	···	1	0	$u^*gz + \langle\mu_g\rangle_e + \langle r_h\rangle$	···

Table 4 *continued*

Table 4 *(continued)*

Name	M_B	M_V	$\langle r_h \rangle$	$\log(M_*/M_{odot})$	v_r	$v_{\rm source}$	Class	Envelope	Method	OtherName
	(mag)	(mag)	(pc)		(km/s)					
(1)	(2)	(3)	(4)	(5)	(6)	(7)	(8)	(9)	(10)	(11)
NGVS-UCD575	-9.62	-9.16	18.49± 0.30	6.2	···	···	1	0	$u^*gz + \langle\mu_g\rangle_e + \langle r_h\rangle$	···
NGVS-UCD576	···	···	29.11± 0.84	7.1	21993	SDSS,NED	3	0	$gz + \langle\mu_g\rangle_e + r_{h,g}$	···
NGVS-UCD577	···	···	47.86± 0.64	7.2	7769	SDSS,NED	3	0	$gz + \langle\mu_g\rangle_e + r_{h,g}$	···
NGVS-UCD578	-11.53	-10.82	15.43± 0.28	7.3	362	NTT17	1	1	$u^*gzK + \langle\mu_g\rangle_e + \langle r_h\rangle$	···
NGVS-UCD579	-9.36	-8.91	23.25± 0.35	6.1	···	···	1	0	$u^*gz + \langle\mu_g\rangle_e + \langle r_h\rangle$	···
NGVS-UCD580	-11.36	-10.53	23.30± 0.29	7.4	24446	NTT17	3	0	$u^*gzK + \langle\mu_g\rangle_e + \langle r_h\rangle$	···
NGVS-UCD581	-9.71	-9.30	26.38± 0.40	6.2	···	···	1	0	$u^*gz + \langle\mu_g\rangle_e + \langle r_h\rangle$	···
NGVS-UCD582	-10.37	-9.90	19.18± 0.48	6.5	748	VCC,NED	2	0	$u^*gzK + \langle\mu_g\rangle_e + \langle r_h\rangle$	VCC-1606
NGVS-UCD583	-9.37	-8.93	25.07± 0.47	6.1	···	···	1	0	$u^*gz + \langle\mu_g\rangle_e + \langle r_h\rangle$	···
NGVS-UCD584	-9.89	-9.41	13.37± 0.30	6.4	···	···	1	0	$u^*gz + \langle\mu_g\rangle_e + \langle r_h\rangle$	···
NGVS-UCD585	-9.39	-8.96	19.22± 0.89	6.1	···	···	3	0	$u^*gz + \langle\mu_g\rangle_e + \langle r_h\rangle$	···
NGVS-UCD586	-10.05	-9.56	14.50± 0.21	6.4	···	···	1	0	$u^*gz + \langle\mu_g\rangle_e + \langle r_h\rangle$	···
NGVS-UCD587	-10.06	-9.58	21.28± 0.66	6.4	···	···	3	0	$u^*gz + \langle\mu_g\rangle_e + \langle r_h\rangle$	···
NGVS-UCD588	-11.61	-11.05	24.10± 0.20	7.1	389	NTT17	1	0	$u^*gzK + \langle\mu_g\rangle_e + \langle r_h\rangle$	···
NGVS-UCD589	-10.50	-10.03	25.68± 0.40	6.5	···	···	3	0	$u^*gz + \langle\mu_g\rangle_e + \langle r_h\rangle$	···
NGVS-UCD590	-10.66	-10.08	21.63± 0.18	6.7	···	···	1	0	$u^*gzK + \langle\mu_g\rangle_e + \langle r_h\rangle$	···
NGVS-UCD591	-11.03	-10.61	46.99± 0.80	6.7	···	···	3	0	$u^*gz + \langle\mu_g\rangle_e + \langle r_h\rangle$	···
NGVS-UCD592	-9.27	-8.86	23.72± 0.80	6.1	···	···	3	0	$u^*gz + \langle\mu_g\rangle_e + \langle r_h\rangle$	···
NGVS-UCD593	-9.85	-9.37	14.07± 0.35	6.4	···	···	1	0	$u^*gzK + \langle\mu_g\rangle_e + \langle r_h\rangle$	···
NGVS-UCD594	-10.48	-10.05	42.60± 0.80	6.5	···	···	4	0	$u^*gzK + \langle\mu_g\rangle_e + \langle r_h\rangle$	···
NGVS-UCD595	-10.35	-9.89	19.54± 0.63	6.5	801	VCC,NED	2	0	$u^*gzK + \langle\mu_g\rangle_e + \langle r_h\rangle$	VCC-1637
NGVS-UCD596	-9.40	-8.92	21.25± 0.84	6.1	···	···	3	0	$u^*gz + \langle\mu_g\rangle_e + \langle r_h\rangle$	···
NGVS-UCD597	-10.15	-9.70	13.43± 0.66	6.4	179	VCC,SDSS,NED	2	0	$u^*gz + \langle\mu_g\rangle_e + \langle r_h\rangle$	VCC-1642
NGVS-UCD598	-10.29	-9.87	30.05± 0.69	6.4	···	···	1	0	$u^*gz + \langle\mu_g\rangle_e + \langle r_h\rangle$	···
NGVS-UCD599	-9.95	-9.50	22.24± 0.44	6.3	···	···	1	0	$u^*gzK + \langle\mu_g\rangle_e + \langle r_h\rangle$	···
NGVS-UCD600	-9.56	-9.08	11.85± 0.52	6.2	···	···	1	0	$u^*gz + \langle\mu_g\rangle_e + \langle r_h\rangle$	···
NGVS-UCD601	-9.69	-9.25	26.62± 1.43	6.2	···	···	3	0	$u^*gz + \langle\mu_g\rangle_e + \langle r_h\rangle$	···
NGVS-UCD602	-10.13	-9.70	28.48± 0.41	6.4	···	···	1	0	$u^*gz + \langle\mu_g\rangle_e + \langle r_h\rangle$	···
NGVS-UCD603	-9.76	-9.28	24.42± 0.55	6.3	···	···	1	0	$u^*gz + \langle\mu_g\rangle_e + \langle r_h\rangle$	···
NGVS-UCD604	-9.27	-8.78	23.89± 0.33	6.2	···	···	1	0	$u^*gz + \langle\mu_g\rangle_e + \langle r_h\rangle$	···
NGVS-UCD605	-9.57	-9.13	22.93± 0.49	6.1	···	···	1	0	$u^*gz + \langle\mu_g\rangle_e + \langle r_h\rangle$	···
NGVS-UCD606	-9.36	-8.94	21.17± 0.60	6.1	···	···	1	0	$u^*gz + \langle\mu_g\rangle_e + \langle r_h\rangle$	···
NGVS-UCD607	-10.82	-10.37	42.00± 0.44	6.7	···	···	3	0	$u^*gz + \langle\mu_g\rangle_e + \langle r_h\rangle$	···
NGVS-UCD608	-9.43	-8.90	25.38± 0.49	6.2	···	···	1	0	$u^*gz + \langle\mu_g\rangle_e + \langle r_h\rangle$	···
NGVS-UCD609	-9.40	-8.87	14.52± 0.29	6.3	···	···	1	0	$u^*gz + \langle\mu_g\rangle_e + \langle r_h\rangle$	···
NGVS-UCD610	···	···	30.98± 1.34	7.2	20314	NED	3	0	$gz + \langle\mu_g\rangle_e + r_{h,g}$	···
NGVS-UCD611	-9.62	-9.21	24.46± 0.40	6.1	···	···	1	0	$u^*gz + \langle\mu_g\rangle_e + \langle r_h\rangle$	···
NGVS-UCD612	-11.06	-10.49	23.31± 0.60	6.9	···	···	3	0	$u^*gz + \langle\mu_g\rangle_e + \langle r_h\rangle$	···
NGVS-UCD613	-11.78	-11.03	28.43± 0.65	7.5	20589	NTT17	3	0	$u^*gzK + \langle\mu_g\rangle_e + \langle r_h\rangle$	···
NGVS-UCD614	-9.70	-9.29	21.11± 0.31	6.2	···	···	1	0	$u^*gz + \langle\mu_g\rangle_e + \langle r_h\rangle$	···
NGVS-UCD615	-9.52	-9.00	21.12± 0.45	6.2	···	···	1	0	$u^*gz + \langle\mu_g\rangle_e + \langle r_h\rangle$	···
NGVS-UCD616	-10.24	-9.77	12.69± 0.52	6.5	···	···	2	0	$u^*gz + \langle\mu_g\rangle_e + \langle r_h\rangle$	VCC-1672
NGVS-UCD617	-9.80	-9.35	22.94± 0.59	6.2	···	···	1	0	$u^*gz + \langle\mu_g\rangle_e + \langle r_h\rangle$	···
NGVS-UCD618	-9.31	-8.86	22.37± 0.48	6.1	···	···	1	0	$u^*gz + \langle\mu_g\rangle_e + \langle r_h\rangle$	···
NGVS-UCD619	-9.62	-9.16	25.34± 0.84	6.2	···	···	1	0	$u^*gz + \langle\mu_g\rangle_e + \langle r_h\rangle$	···
NGVS-UCD620	-9.51	-9.07	26.36± 0.86	6.2	···	···	3	0	$u^*gz + \langle\mu_g\rangle_e + \langle r_h\rangle$	···
NGVS-UCD621	-10.09	-9.58	20.46± 0.23	6.5	···	···	1	0	$u^*gz + \langle\mu_g\rangle_e + \langle r_h\rangle$	···
NGVS-UCD622	···	···	27.45± 0.78	7.0	23356	SDSS,NED	3	0	$gz + \langle\mu_g\rangle_e + r_{h,g}$	···

Table 4 *continued*

Table 4 *(continued)*

Name	M_B	M_V	$\langle r_h \rangle$	$\log(M_*/M_{odot})$	v_r	$v_{\rm source}$	Class	Envelope	Method	OtherName
	(mag)	(mag)	(pc)		(km/s)					
(1)	(2)	(3)	(4)	(5)	(6)	(7)	(8)	(9)	(10)	(11)
NGVS-UCD623	-9.58	-9.14	17.65± 0.66	6.2	···	···	1	0	$u^*gz + \langle\mu_g\rangle_e + \langle r_h\rangle$	···
NGVS-UCD624	-9.40	-9.00	15.77± 0.26	6.1	···	···	1	0	$u^*gz + \langle\mu_g\rangle_e + \langle r_h\rangle$	···
NGVS-UCD625	-10.12	-9.69	32.58± 0.82	6.3	···	···	1	0	$u^*gz + \langle\mu_g\rangle_e + \langle r_h\rangle$	···
NGVS-UCD626	···	···	35.54± 1.02	6.5	1699	NED	6	0	$(v_r < 3500\mathrm{km/s}) + \langle r_h\rangle$	···
NGVS-UCD627	-11.46	-11.00	41.60± 1.70	7.0	···	···	3	0	$u^*gz + \langle\mu_g\rangle_e + \langle r_h\rangle$	···
NGVS-UCD628	-9.49	-9.02	20.36± 0.45	6.2	···	···	1	0	$u^*gz + \langle\mu_g\rangle_e + \langle r_h\rangle$	···
NGVS-UCD629	-10.16	-9.74	24.93± 0.33	6.5	···	···	1	0	$u^*gz + \langle\mu_g\rangle_e + \langle r_h\rangle$	···
NGVS-UCD630	-9.26	-8.75	16.24± 0.50	6.2	···	···	1	0	$u^*gz + \langle\mu_g\rangle_e + \langle r_h\rangle$	···
NGVS-UCD631	-12.06	-11.19	13.05± 1.72	7.6	2	SDSS,NTT17	5	0	$u^*gzK + \langle\mu_g\rangle_e + r_{h,g}$	···
NGVS-UCD632	-9.84	-9.38	24.42± 0.24	6.3	···	···	1	0	$u^*gz + \langle\mu_g\rangle_e + \langle r_h\rangle$	···
NGVS-UCD633	-11.38	-10.84	24.70± 0.82	7.1	5513	NTT17	3	0	$u^*gz + \langle\mu_g\rangle_e + \langle r_h\rangle$	···
NGVS-UCD634	-9.49	-9.02	20.94± 0.35	6.2	···	···	1	0	$u^*gz + \langle\mu_g\rangle_e + \langle r_h\rangle$	···
NGVS-UCD635	-9.93	-9.49	29.53± 0.52	6.3	···	···	1	0	$u^*gz + \langle\mu_g\rangle_e + \langle r_h\rangle$	···
NGVS-UCD636	-9.67	-9.22	26.84± 0.41	6.2	···	···	1	0	$u^*gz + \langle\mu_g\rangle_e + \langle r_h\rangle$	···
NGVS-UCD637	-9.36	-8.92	16.91± 0.31	6.1	···	···	4	0	$u^*gz + \langle\mu_g\rangle_e + \langle r_h\rangle$	···
NGVS-UCD638	-9.62	-9.15	21.58± 0.27	6.2	···	···	1	0	$u^*gz + \langle\mu_g\rangle_e + \langle r_h\rangle$	···
NGVS-UCD639	-9.51	-9.07	28.36± 1.47	6.2	···	···	1	0	$u^*gz + \langle\mu_g\rangle_e + \langle r_h\rangle$	···
NGVS-UCD640	-10.09	-9.63	21.12± 0.29	6.4	···	···	1	0	$u^*gz + \langle\mu_g\rangle_e + \langle r_h\rangle$	···
NGVS-UCD641	-9.47	-8.99	20.91± 0.46	6.1	···	···	1	0	$u^*gz + \langle\mu_g\rangle_e + \langle r_h\rangle$	···
NGVS-UCD642	-10.66	-10.13	12.47± 0.25	6.7	689	AAT12	1	0	$u^*gzK + \langle\mu_g\rangle_e + \langle r_h\rangle$	···
NGVS-UCD643	-9.51	-9.08	24.07± 0.43	6.1	···	···	1	0	$u^*gz + \langle\mu_g\rangle_e + \langle r_h\rangle$	···
NGVS-UCD644	-10.29	-9.89	29.52± 0.50	6.4	···	···	1	0	$u^*gz + \langle\mu_g\rangle_e + \langle r_h\rangle$	···
NGVS-UCD645	-9.74	-9.32	15.85± 0.37	6.2	···	···	1	0	$u^*gz + \langle\mu_g\rangle_e + \langle r_h\rangle$	···
NGVS-UCD646	-9.30	-8.79	20.39± 0.41	6.2	···	···	1	0	$u^*gz + \langle\mu_g\rangle_e + \langle r_h\rangle$	···
NGVS-UCD647	-12.98	-12.66	52.34± 0.99	6.7	1139	VCC,SDSS,NED	6	0	$(v_r < 3500\mathrm{km/s}) + \langle r_h\rangle$	VCC-1744
NGVS-UCD648	-9.76	-9.28	24.53± 0.45	6.3	···	···	1	0	$u^*gzK + \langle\mu_g\rangle_e + \langle r_h\rangle$	···
NGVS-UCD649	-11.41	-10.72	25.45± 0.66	7.2	18284	NTT17	3	0	$u^*gz + \langle\mu_g\rangle_e + \langle r_h\rangle$	···
NGVS-UCD650	-11.44	-10.99	55.66± 1.10	6.9	···	···	1	0	$u^*gz + \langle\mu_g\rangle_e + \langle r_h\rangle$	···
NGVS-UCD651	-9.65	-9.23	26.39± 0.54	6.2	···	···	1	0	$u^*gz + \langle\mu_g\rangle_e + \langle r_h\rangle$	···
NGVS-UCD652	-9.83	-9.41	17.45± 1.30	6.3	···	···	4	0	$u^*gz + \langle\mu_g\rangle_e + \langle r_h\rangle$	···
NGVS-UCD653	-10.49	-10.05	23.34± 0.62	6.6	···	···	3	0	$u^*gzK + \langle\mu_g\rangle_e + \langle r_h\rangle$	···
NGVS-UCD654	-10.96	-10.52	39.27± 1.02	6.7	···	···	1	0	$u^*gz + \langle\mu_g\rangle_e + \langle r_h\rangle$	···
NGVS-UCD655	-10.20	-9.80	29.50± 0.29	6.4	···	···	1	0	$u^*gzK + \langle\mu_g\rangle_e + \langle r_h\rangle$	···
NGVS-UCD656	-9.95	-9.50	18.91± 0.39	6.3	···	···	1	0	$u^*gzK + \langle\mu_g\rangle_e + \langle r_h\rangle$	···
NGVS-UCD657	-9.72	-9.31	13.86± 0.27	6.2	···	···	1	0	$u^*gz + \langle\mu_g\rangle_e + \langle r_h\rangle$	···
NGVS-UCD658	···	···	39.78± 0.61	7.2	20304	SDSS,NED	3	0	$gz + \langle\mu_g\rangle_e + r_{h,g}$	···
NGVS-UCD659	-9.31	-8.82	13.96± 0.80	6.1	···	···	1	0	$u^*gz + \langle\mu_g\rangle_e + \langle r_h\rangle$	···
NGVS-UCD660	-9.30	-8.86	19.74± 0.34	6.1	···	···	1	0	$u^*gz + \langle\mu_g\rangle_e + \langle r_h\rangle$	···
NGVS-UCD661	-10.44	-9.95	11.26± 0.32	6.6	···	···	1	0	$u^*gzK + \langle\mu_g\rangle_e + \langle r_h\rangle$	···
NGVS-UCD662	-9.88	-9.39	30.24± 0.94	6.4	···	···	1	0	$u^*gzK + \langle\mu_g\rangle_e + \langle r_h\rangle$	···
NGVS-UCD663	···	···	13.09± 1.38	7.3	···	···	5	0	$gzK + \langle\mu_g\rangle_e + r_{h,g}$	···
NGVS-UCD664	-9.63	-8.96	13.47± 0.48	6.5	···	···	1	0	$u^*gzK + \langle\mu_g\rangle_e + \langle r_h\rangle$	···
NGVS-UCD665	-9.52	-9.10	14.62± 0.23	6.2	···	···	1	0	$u^*gz + \langle\mu_g\rangle_e + \langle r_h\rangle$	···
NGVS-UCD666	-11.36	-10.96	33.58± 0.62	6.8	30220	NTT17	3	0	$u^*gz + \langle\mu_g\rangle_e + \langle r_h\rangle$	···
NGVS-UCD667	-9.32	-8.85	21.10± 0.57	6.1	···	···	1	0	$u^*gz + \langle\mu_g\rangle_e + \langle r_h\rangle$	···
NGVS-UCD668	-9.32	-8.84	20.44± 0.60	6.0	···	···	1	0	$u^*gz + \langle\mu_g\rangle_e + \langle r_h\rangle$	···
NGVS-UCD669	-9.32	-8.88	23.19± 0.74	6.1	44750	MMT09	3	0	$u^*gz + \langle\mu_g\rangle_e + \langle r_h\rangle$	···
NGVS-UCD670	-9.49	-9.03	22.38± 0.64	6.1	···	···	1	0	$u^*gz + \langle\mu_g\rangle_e + \langle r_h\rangle$	···

Table 4 *continued*

Table 4 *(continued)*

Name	M_B	M_V	$\langle r_h \rangle$	$\log(M_*/M_{odot})$	v_r	$v_{\rm source}$	Class	Envelope	Method	OtherName
	(mag)	(mag)	(pc)		(km/s)					
(1)	(2)	(3)	(4)	(5)	(6)	(7)	(8)	(9)	(10)	(11)
NGVS-UCD671	-12.18	-11.36	33.41± 0.71	7.7	21638	SDSS,NED	3	0	$u^*gzK + \langle\mu_g\rangle_e + r_{h,g}$	···
NGVS-UCD672	···	···	47.63± 0.79	7.5	21053	SDSS,NED	3	0	$gz + \langle\mu_g\rangle_e + r_{h,g}$	···
NGVS-UCD673	-9.63	-9.23	23.31± 0.29	6.1	···	···	1	0	$u^*gzK + \langle\mu_g\rangle_e + \langle r_h\rangle$	···
NGVS-UCD674	-9.52	-9.04	22.36± 0.44	6.2	···	···	1	0	$u^*gz + \langle\mu_g\rangle_e + \langle r_h\rangle$	···
NGVS-UCD675	-11.82	-11.09	25.31± 0.33	7.4	13742	NTT17	3	0	$u^*gzK + \langle\mu_g\rangle_e + \langle r_h\rangle$	···
NGVS-UCD676	···	···	39.56± 0.44	7.3	21158	SDSS,NED	3	0	$gz + \langle\mu_g\rangle_e + r_{h,g}$	···
NGVS-UCD677	-9.41	-8.98	18.66± 0.37	6.1	···	···	1	0	$u^*gz + \langle\mu_g\rangle_e + \langle r_h\rangle$	···
NGVS-UCD678	-9.42	-8.98	24.34± 0.49	6.1	42993	SDSS	3	0	$u^*gz + \langle\mu_g\rangle_e + \langle r_h\rangle$	···
NGVS-UCD679	-10.28	-9.84	32.34± 0.51	6.5	···	···	1	0	$u^*gz + \langle\mu_g\rangle_e + \langle r_h\rangle$	···
NGVS-UCD680	-9.90	-9.48	18.51± 0.41	6.3	···	···	1	0	$u^*gz + \langle\mu_g\rangle_e + \langle r_h\rangle$	···
NGVS-UCD681	-9.29	-8.81	21.45± 0.57	6.0	···	···	1	0	$u^*gz + \langle\mu_g\rangle_e + \langle r_h\rangle$	···
NGVS-UCD682	-12.34	-11.74	81.92± 0.63	7.5	1977	VCC,SDSS,NED	2	0	$(v_r < 3500\mathrm{km/s}) + \langle r_h\rangle$	VCC-1826
NGVS-UCD683	-9.33	-8.89	18.28± 0.49	6.0	···	···	1	0	$u^*gz + \langle\mu_g\rangle_e + \langle r_h\rangle$	···
NGVS-UCD684	-9.40	-8.91	16.35± 0.37	6.1	···	···	1	0	$u^*gzK + \langle\mu_g\rangle_e + \langle r_h\rangle$	···
NGVS-UCD685	···	···	90.30± 1.47	7.9	21160	NED	3	0	$gz + \langle\mu_g\rangle_e + r_{h,g}$	···
NGVS-UCD686	-13.37	-12.64	33.19± 0.10	8.0	···	···	4	0	$u^*gzK + \langle\mu_g\rangle_e + r_{h,g}$	···
NGVS-UCD687	-9.99	-9.57	26.43± 0.68	6.3	···	···	1	0	$u^*gzK + \langle\mu_g\rangle_e + \langle r_h\rangle$	···
NGVS-UCD688	-10.44	-9.75	13.68± 0.58	6.8	···	···	1	0	$u^*gzK + \langle\mu_g\rangle_e + \langle r_h\rangle$	···
NGVS-UCD689	-9.56	-9.13	18.54± 0.35	6.2	···	···	1	0	$u^*gz + \langle\mu_g\rangle_e + \langle r_h\rangle$	···
NGVS-UCD690	-9.68	-9.20	18.40± 0.42	6.3	···	···	1	0	$u^*gz + \langle\mu_g\rangle_e + \langle r_h\rangle$	···
NGVS-UCD691	-9.93	-9.50	18.98± 0.40	6.3	26272	SDSS	3	0	$u^*gz + \langle\mu_g\rangle_e + \langle r_h\rangle$	···
NGVS-UCD692	-13.00	-12.13	50.23± 0.53	8.0	20997	SDSS,NED	3	0	$u^*gz + \langle\mu_g\rangle_e + r_{h,g}$	···
NGVS-UCD693	-9.40	-8.91	18.92± 0.44	6.1	···	···	1	0	$u^*gz + \langle\mu_g\rangle_e + \langle r_h\rangle$	···
NGVS-UCD694	-9.47	-9.05	17.67± 0.44	6.1	···	···	1	0	$u^*gz + \langle\mu_g\rangle_e + \langle r_h\rangle$	···
NGVS-UCD695	-9.37	-8.95	15.58± 0.29	6.1	···	···	1	0	$u^*gz + \langle\mu_g\rangle_e + \langle r_h\rangle$	···
NGVS-UCD696	-9.48	-8.91	15.11± 0.60	6.4	···	···	1	0	$u^*gzK + \langle\mu_g\rangle_e + \langle r_h\rangle$	···
NGVS-UCD697	-9.85	-9.40	12.33± 0.52	6.3	···	···	1	0	$u^*gzK + \langle\mu_g\rangle_e + \langle r_h\rangle$	···
NGVS-UCD698	-9.61	-9.15	16.91± 0.35	6.3	···	···	1	0	$u^*gz + \langle\mu_g\rangle_e + \langle r_h\rangle$	···
NGVS-UCD699	-9.82	-9.37	30.28± 0.52	6.3	···	···	1	0	$u^*gz + \langle\mu_g\rangle_e + \langle r_h\rangle$	···
NGVS-UCD700	-9.67	-9.24	22.06± 0.33	6.2	···	···	1	0	$u^*gz + \langle\mu_g\rangle_e + \langle r_h\rangle$	···
NGVS-UCD701	-9.56	-9.15	25.90± 0.82	6.1	···	···	1	0	$u^*gz + \langle\mu_g\rangle_e + \langle r_h\rangle$	···
NGVS-UCD702	-9.69	-9.21	26.24± 0.54	6.3	···	···	1	0	$u^*gz + \langle\mu_g\rangle_e + \langle r_h\rangle$	···
NGVS-UCD703	-9.97	-9.52	29.87± 0.66	6.3	···	···	1	0	$u^*gzK + \langle\mu_g\rangle_e + \langle r_h\rangle$	···
NGVS-UCD704	-9.52	-9.03	24.78± 0.43	6.2	···	···	1	0	$u^*gzK + \langle\mu_g\rangle_e + \langle r_h\rangle$	···
NGVS-UCD705	-9.47	-8.95	16.09± 0.32	6.3	···	···	1	0	$u^*gzK + \langle\mu_g\rangle_e + \langle r_h\rangle$	···
NGVS-UCD706	-9.56	-9.09	19.00± 0.27	6.2	···	···	1	0	$u^*gz + \langle\mu_g\rangle_e + \langle r_h\rangle$	···
NGVS-UCD707	···	···	47.84± 2.53	7.4	21008	SDSS,NED	3	0	$gz + \langle\mu_g\rangle_e + r_{h,g}$	···
NGVS-UCD708	-10.50	-9.96	34.57± 0.46	6.7	···	···	1	0	$u^*gz + \langle\mu_g\rangle_e + \langle r_h\rangle$	···
NGVS-UCD709	-10.21	-9.72	20.78± 0.22	6.4	···	···	1	0	$u^*gzK + \langle\mu_g\rangle_e + \langle r_h\rangle$	···
NGVS-UCD710	···	···	12.66± 0.45	7.1	95	NTT17	5	0	$gzK + \langle\mu_g\rangle_e + r_{h,g}$	···
NGVS-UCD711	-10.52	-10.05	23.96± 0.51	6.5	···	···	1	0	$u^*gzK + \langle\mu_g\rangle_e + \langle r_h\rangle$	···
NGVS-UCD712	···	···	33.67± 0.23	7.2	20610	NTT17	3	0	$gz + \langle\mu_g\rangle_e + r_{h,g}$	···
NGVS-UCD713	···	···	13.32± 0.82	6.9	78	SDSS	5	0	$(v_r < 3500\mathrm{km/s}) + \langle r_h\rangle$	···
NGVS-UCD714	···	···	13.02± 0.49	7.7	-50	SDSS	5	0	$(v_r < 3500\mathrm{km/s}) + \langle r_h\rangle$	···
NGVS-UCD715	-9.42	-9.01	22.62± 0.74	6.1	···	···	3	0	$u^*gz + \langle\mu_g\rangle_e + \langle r_h\rangle$	···
NGVS-UCD716	-9.79	-9.10	11.36± 0.25	6.6	···	···	1	0	$u^*gzK + \langle\mu_g\rangle_e + \langle r_h\rangle$	···
NGVS-UCD717	-9.64	-9.12	25.55± 0.40	6.3	···	···	1	0	$u^*gz + \langle\mu_g\rangle_e + \langle r_h\rangle$	···
NGVS-UCD718	-9.31	-8.85	19.00± 0.55	6.0	···	···	1	0	$u^*gz + \langle\mu_g\rangle_e + \langle r_h\rangle$	···

Table 4 *continued*

Table 4 *(continued)*

Name	M_B	M_V	$\langle r_h \rangle$	$\log(M_*/M_{odot})$	v_r	$v_{\rm source}$	Class	Envelope	Method	OtherName
	(mag)	(mag)	(pc)		(km/s)					
(1)	(2)	(3)	(4)	(5)	(6)	(7)	(8)	(9)	(10)	(11)
NGVS-UCD719	-12.70	-11.91	36.40± 0.21	7.9	711	SDSS,NED,NTT17	1	1	$u^*gzK + \langle\mu_g\rangle_e + \langle r_h\rangle$	M59cO
NGVS-UCD720	-9.41	-8.96	24.58± 0.41	6.1	···	···	1	0	$u^*gz + \langle\mu_g\rangle_e + \langle r_h\rangle$	···
NGVS-UCD721	···	···	26.17± 0.08	7.6	···	···	4	0	$gz + \langle\mu_g\rangle_e + r_{h,g}$	···
NGVS-UCD722	-9.88	-9.36	12.43± 0.24	6.4	···	···	1	0	$u^*gz + \langle\mu_g\rangle_e + \langle r_h\rangle$	···
NGVS-UCD723	-9.93	-9.44	13.80± 0.22	6.4	···	···	1	0	$u^*gzK + \langle\mu_g\rangle_e + \langle r_h\rangle$	···
NGVS-UCD724	-9.36	-8.87	19.86± 0.36	6.1	···	···	1	0	$u^*gz + \langle\mu_g\rangle_e + \langle r_h\rangle$	···
NGVS-UCD725	-13.94	-13.16	25.01± 0.27	8.4	441	AAT12	1	1	$u^*gzK + \langle\mu_g\rangle_e + \langle r_h\rangle$	M59-UCD3
NGVS-UCD726	-11.22	-10.76	53.56± 1.54	6.8	···	···	3	0	$u^*gz + \langle\mu_g\rangle_e + \langle r_h\rangle$	···
NGVS-UCD727	-9.40	-8.88	11.38± 0.49	6.2	···	···	1	0	$u^*gz + \langle\mu_g\rangle_e + \langle r_h\rangle$	···
NGVS-UCD728	-9.60	-9.13	27.24± 0.86	6.2	···	···	1	0	$u^*gz + \langle\mu_g\rangle_e + \langle r_h\rangle$	···
NGVS-UCD729	-10.03	-9.60	21.32± 0.16	6.4	···	···	1	0	$u^*gzK + \langle\mu_g\rangle_e + \langle r_h\rangle$	···
NGVS-UCD730	-10.88	-10.32	12.74± 0.20	6.8	1493	AAT12	1	0	$u^*gzK + \langle\mu_g\rangle_e + \langle r_h\rangle$	···
NGVS-UCD731	-9.72	-9.25	13.37± 0.17	6.3	···	···	1	0	$u^*gz + \langle\mu_g\rangle_e + \langle r_h\rangle$	···
NGVS-UCD732	-9.43	-8.88	12.08± 0.50	6.3	···	···	1	0	$u^*gz + \langle\mu_g\rangle_e + \langle r_h\rangle$	···
NGVS-UCD733	-9.25	-8.84	19.11± 0.75	6.0	···	···	3	0	$u^*gz + \langle\mu_g\rangle_e + \langle r_h\rangle$	···
NGVS-UCD734	-9.40	-8.94	24.20± 0.62	6.1	···	···	1	0	$u^*gz + \langle\mu_g\rangle_e + \langle r_h\rangle$	···
NGVS-UCD735	-11.04	-10.56	14.72± 0.42	6.8	1241	AAT12	1	1	$u^*gzK + \langle\mu_g\rangle_e + \langle r_h\rangle$	···
NGVS-UCD736	-11.77	-11.06	14.96± 0.47	7.4	537	AAT12	1	0	$u^*gzK + \langle\mu_g\rangle_e + \langle r_h\rangle$	···
NGVS-UCD737	-9.40	-8.93	20.25± 0.34	6.1	···	···	1	0	$u^*gz + \langle\mu_g\rangle_e + \langle r_h\rangle$	···
NGVS-UCD738	···	···	37.09± 0.12	7.7	···	···	5	0	$gzK + \langle\mu_g\rangle_e + r_{h,g}$	···
NGVS-UCD739	-9.80	-9.30	12.75± 0.17	6.3	···	···	1	0	$u^*gzK + \langle\mu_g\rangle_e + \langle r_h\rangle$	···
NGVS-UCD740	-10.73	-10.32	39.18± 0.88	6.7	···	···	3	0	$u^*gz + \langle\mu_g\rangle_e + \langle r_h\rangle$	···
NGVS-UCD741	-10.62	-10.19	37.48± 0.29	6.6	547	SIMBAD	1	1	$u^*gzK + \langle\mu_g\rangle_e + \langle r_h\rangle$	···
NGVS-UCD742	···	···	37.22± 0.52	7.2	25296	NTT17	3	0	$gzK + \langle\mu_g\rangle_e + r_{h,g}$	···
NGVS-UCD743	-11.60	-11.19	30.14± 0.44	7.0	47708	NTT17	3	0	$u^*gz + \langle\mu_g\rangle_e + \langle r_h\rangle$	···
NGVS-UCD744	-9.49	-8.95	18.58± 0.48	6.2	···	···	1	0	$u^*gzK + \langle\mu_g\rangle_e + \langle r_h\rangle$	···
NGVS-UCD745	-10.01	-9.55	25.33± 0.65	6.4	···	···	1	0	$u^*gz + \langle\mu_g\rangle_e + \langle r_h\rangle$	···
NGVS-UCD746	-10.16	-9.69	11.83± 0.24	6.4	1300	SIMBAD	1	0	$u^*gz + \langle\mu_g\rangle_e + \langle r_h\rangle$	···
NGVS-UCD747	-10.06	-9.60	25.11± 0.29	6.4	···	···	1	0	$u^*gzK + \langle\mu_g\rangle_e + \langle r_h\rangle$	···
NGVS-UCD748	-10.01	-9.49	16.96± 0.30	6.4	974	SIMBAD	1	0	$u^*gz + \langle\mu_g\rangle_e + \langle r_h\rangle$	···
NGVS-UCD749	-9.44	-8.98	26.83± 0.81	6.2	···	···	1	0	$u^*gz + \langle\mu_g\rangle_e + \langle r_h\rangle$	···
NGVS-UCD750	-9.26	-8.79	22.06± 0.72	6.1	···	···	1	0	$u^*gz + \langle\mu_g\rangle_e + \langle r_h\rangle$	···
NGVS-UCD751	-9.82	-9.38	22.71± 0.25	6.3	···	···	1	0	$u^*gz + \langle\mu_g\rangle_e + \langle r_h\rangle$	···
NGVS-UCD752	-10.53	-9.87	14.86± 0.54	6.8	93	AAT12	1	0	$u^*gzK + \langle\mu_g\rangle_e + \langle r_h\rangle$	···
NGVS-UCD753	-13.26	-12.41	19.58± 0.37	8.1	1307	AAT12	1	1	$u^*gzK + \langle\mu_g\rangle_e + \langle r_h\rangle$	M60-UCD1
NGVS-UCD754	-9.96	-9.46	29.81± 0.60	6.4	1005	SIMBAD	1	0	$u^*gz + \langle\mu_g\rangle_e + \langle r_h\rangle$	NGC4649-D68
NGVS-UCD755	-9.55	-9.06	25.26± 0.71	6.2	···	···	1	0	$u^*gz + \langle\mu_g\rangle_e + \langle r_h\rangle$	···
NGVS-UCD756	-10.05	-9.59	17.23± 0.39	6.4	···	···	1	0	$u^*gz + \langle\mu_g\rangle_e + \langle r_h\rangle$	···
NGVS-UCD757	-10.63	-10.19	38.86± 0.78	6.6	···	···	1	0	$u^*gz + \langle\mu_g\rangle_e + \langle r_h\rangle$	···
NGVS-UCD758	-9.88	-9.42	26.17± 0.48	6.3	···	···	1	0	$u^*gz + \langle\mu_g\rangle_e + \langle r_h\rangle$	···
NGVS-UCD759	-9.66	-9.21	23.44± 0.34	6.2	1027	SIMBAD	1	0	$u^*gz + \langle\mu_g\rangle_e + \langle r_h\rangle$	···
NGVS-UCD760	-9.84	-9.41	28.42± 0.74	6.3	···	···	3	0	$u^*gz + \langle\mu_g\rangle_e + \langle r_h\rangle$	···
NGVS-UCD761	-11.95	-11.27	16.66± 0.36	7.4	849	NTT17	1	0	$u^*gzK + \langle\mu_g\rangle_e + \langle r_h\rangle$	···
NGVS-UCD762	-10.55	-10.04	17.90± 0.28	6.6	1208	SIMBAD	1	0	$u^*gzK + \langle\mu_g\rangle_e + \langle r_h\rangle$	···
NGVS-UCD763	-9.66	-9.22	27.41± 0.53	6.2	···	···	1	0	$u^*gz + \langle\mu_g\rangle_e + \langle r_h\rangle$	···
NGVS-UCD764	-9.90	-9.38	24.13± 0.32	6.4	···	···	1	0	$u^*gz + \langle\mu_g\rangle_e + \langle r_h\rangle$	···
NGVS-UCD765	-9.72	-9.32	14.03± 0.24	6.2	···	···	3	0	$u^*gz + \langle\mu_g\rangle_e + \langle r_h\rangle$	···
NGVS-UCD766	-11.33	-10.80	11.65± 0.35	7.0	1430	AAT12	1	1	$u^*gzK + \langle\mu_g\rangle_e + \langle r_h\rangle$	···

Table 4 *continued*

Table 4 *(continued)*

Name	M_B	M_V	$\langle r_h \rangle$	$\log(M_*/M_{odot})$	v_r	$v_{\rm source}$	Class	Envelope	Method	OtherName
	(mag)	(mag)	(pc)		(km/s)					
(1)	(2)	(3)	(4)	(5)	(6)	(7)	(8)	(9)	(10)	(11)
NGVS-UCD767	-10.89	-10.40	13.69± 0.29	6.8	···	···	1	0	$u^*gz + \langle\mu_g\rangle_e + \langle r_h\rangle$	···
NGVS-UCD768	-9.86	-9.30	15.57± 0.39	6.5	···	···	1	0	$u^*gz + \langle\mu_g\rangle_e + \langle r_h\rangle$	···
NGVS-UCD769	-11.52	-10.77	57.99± 0.56	7.4	1262	AAT12	1	1	$(v_r < 3500\mathrm{km/s}) + \langle r_h\rangle$	···
NGVS-UCD770	-10.33	-9.92	34.48± 1.02	6.4	···	···	1	0	$u^*gz + \langle\mu_g\rangle_e + \langle r_h\rangle$	···
NGVS-UCD771	-10.83	-10.31	20.44± 0.23	6.8	···	···	1	0	$u^*gzK + \langle\mu_g\rangle_e + \langle r_h\rangle$	···
NGVS-UCD772	-10.67	-10.16	13.37± 0.25	6.7	···	···	1	1	$u^*gzK + \langle\mu_g\rangle_e + \langle r_h\rangle$	···
NGVS-UCD773	-9.34	-8.92	21.45± 0.32	6.1	···	···	1	0	$u^*gz + \langle\mu_g\rangle_e + \langle r_h\rangle$	···
NGVS-UCD774	-9.63	-9.10	11.83± 0.31	6.3	···	···	1	0	$u^*gzK + \langle\mu_g\rangle_e + \langle r_h\rangle$	···
NGVS-UCD775	-9.47	-9.06	23.16± 0.45	6.1	···	···	1	0	$u^*gz + \langle\mu_g\rangle_e + \langle r_h\rangle$	···
NGVS-UCD776	-9.83	-9.32	30.00± 0.37	6.4	···	···	1	0	$u^*gzK + \langle\mu_g\rangle_e + \langle r_h\rangle$	···
NGVS-UCD777	-9.94	-9.40	25.10± 0.35	6.4	···	···	1	0	$u^*gzK + \langle\mu_g\rangle_e + \langle r_h\rangle$	···
NGVS-UCD778	-9.85	-9.42	32.14± 0.60	6.3	···	···	1	0	$u^*gz + \langle\mu_g\rangle_e + \langle r_h\rangle$	···
NGVS-UCD779	-9.49	-9.06	18.91± 0.43	6.2	···	···	1	0	$u^*gz + \langle\mu_g\rangle_e + \langle r_h\rangle$	···
NGVS-UCD780	-10.89	-10.44	36.90± 0.70	6.8	···	···	1	1	$u^*gz + \langle\mu_g\rangle_e + \langle r_h\rangle$	···
NGVS-UCD781	-11.35	-10.68	12.29± 0.20	7.2	879	NTT17	1	0	$u^*gzK + \langle\mu_g\rangle_e + \langle r_h\rangle$	···
NGVS-UCD782	-9.66	-9.20	26.93± 0.54	6.2	···	···	1	0	$u^*gz + \langle\mu_g\rangle_e + \langle r_h\rangle$	···
NGVS-UCD783	-10.50	-9.99	13.16± 0.41	6.6	···	···	1	0	$u^*gzK + \langle\mu_g\rangle_e + \langle r_h\rangle$	···
NGVS-UCD784	-10.81	-10.22	12.31± 0.40	6.9	···	···	1	0	$u^*gzK + \langle\mu_g\rangle_e + \langle r_h\rangle$	···
NGVS-UCD785	-9.85	-9.39	32.47± 0.72	6.3	···	···	1	0	$u^*gz + \langle\mu_g\rangle_e + \langle r_h\rangle$	···
NGVS-UCD786	-9.88	-9.30	14.43± 0.48	6.5	···	···	1	0	$u^*gzK + \langle\mu_g\rangle_e + \langle r_h\rangle$	···
NGVS-UCD787	-11.08	-10.64	40.81± 1.04	6.8	···	···	3	0	$u^*gz + \langle\mu_g\rangle_e + \langle r_h\rangle$	···
NGVS-UCD788	-9.99	-9.52	16.21± 0.24	6.4	···	···	1	0	$u^*gzK + \langle\mu_g\rangle_e + \langle r_h\rangle$	···
NGVS-UCD789	-10.10	-9.62	20.30± 0.23	6.4	···	···	1	0	$u^*gzK + \langle\mu_g\rangle_e + \langle r_h\rangle$	···
NGVS-UCD790	-9.46	-9.03	24.90± 0.68	6.0	···	···	1	0	$u^*gz + \langle\mu_g\rangle_e + \langle r_h\rangle$	···
NGVS-UCD791	···	···	17.63± 0.61	7.4	82	NTT17	5	0	$gz + \langle\mu_g\rangle_e + r_{h,g}$	···
NGVS-UCD792	-9.43	-8.97	17.00± 0.50	6.1	···	···	1	0	$u^*gz + \langle\mu_g\rangle_e + \langle r_h\rangle$	···
NGVS-UCD793	-9.27	-8.86	19.24± 0.43	6.1	···	···	1	0	$u^*gz + \langle\mu_g\rangle_e + \langle r_h\rangle$	···
NGVS-UCD794	-9.31	-8.78	24.56± 0.65	6.1	···	···	1	0	$u^*gz + \langle\mu_g\rangle_e + \langle r_h\rangle$	···
NGVS-UCD795	-9.37	-8.87	21.42± 0.25	6.1	···	···	1	0	$u^*gz + \langle\mu_g\rangle_e + \langle r_h\rangle$	···
NGVS-UCD796	-10.22	-9.75	14.72± 0.50	6.4	···	···	1	0	$u^*gz + \langle\mu_g\rangle_e + \langle r_h\rangle$	···
NGVS-UCD797	-9.68	-9.24	17.12± 0.21	6.2	···	···	1	0	$u^*gzK + \langle\mu_g\rangle_e + \langle r_h\rangle$	···
NGVS-UCD798	-9.93	-9.49	25.55± 0.41	6.4	···	···	1	0	$u^*gzK + \langle\mu_g\rangle_e + \langle r_h\rangle$	···
NGVS-UCD799	···	···	54.90± 2.07	7.6	15976	SDSS,NED	3	0	$gzK + \langle\mu_g\rangle_e + r_{h,g}$	···
NGVS-UCD800	-9.75	-9.35	20.50± 0.74	6.2	···	···	1	0	$u^*gz + \langle\mu_g\rangle_e + \langle r_h\rangle$	···
NGVS-UCD801	-9.61	-9.18	16.43± 0.56	6.2	···	···	1	0	$u^*gz + \langle\mu_g\rangle_e + \langle r_h\rangle$	···
NGVS-UCD802	-9.53	-9.07	12.18± 0.37	6.2	···	···	1	0	$u^*gz + \langle\mu_g\rangle_e + \langle r_h\rangle$	···
NGVS-UCD803	-10.51	-10.06	35.03± 1.11	6.6	···	···	1	1	$u^*gzK + \langle\mu_g\rangle_e + \langle r_h\rangle$	···
NGVS-UCD804	-9.26	-8.82	15.51± 0.30	6.1	···	···	1	0	$u^*gz + \langle\mu_g\rangle_e + \langle r_h\rangle$	···
NGVS-UCD805	-9.75	-9.17	11.49± 0.43	6.3	···	···	1	0	$u^*gz + \langle\mu_g\rangle_e + \langle r_h\rangle$	···
NGVS-UCD806	-9.46	-9.04	24.26± 0.59	6.2	···	···	1	0	$u^*gz + \langle\mu_g\rangle_e + \langle r_h\rangle$	···
NGVS-UCD807	-9.90	-9.46	12.11± 0.24	6.3	···	···	1	0	$u^*gz + \langle\mu_g\rangle_e + \langle r_h\rangle$	···
NGVS-UCD808	-9.95	-9.46	20.00± 0.35	6.3	···	···	1	0	$u^*gz + \langle\mu_g\rangle_e + \langle r_h\rangle$	···
NGVS-UCD809	-10.24	-9.79	31.17± 0.98	6.4	···	···	3	0	$u^*gz + \langle\mu_g\rangle_e + \langle r_h\rangle$	···
NGVS-UCD810	-10.77	-10.33	27.45± 0.01	6.7	···	···	3	0	$u^*gzK + \langle\mu_g\rangle_e + \langle r_h\rangle$	···
NGVS-UCD811	-9.81	-9.31	19.48± 0.34	6.3	···	···	1	0	$u^*gzK + \langle\mu_g\rangle_e + \langle r_h\rangle$	···
NGVS-UCD812	-9.83	-9.38	24.21± 0.43	6.2	···	···	1	0	$u^*gz + \langle\mu_g\rangle_e + \langle r_h\rangle$	···
NGVS-UCD813	-11.40	-10.59	26.15± 0.66	7.3	25702	NTT17	3	0	$u^*gzK + \langle\mu_g\rangle_e + \langle r_h\rangle$	···
NGVS-UCD814	-9.34	-8.89	17.56± 0.37	6.1	···	···	1	0	$u^*gz + \langle\mu_g\rangle_e + \langle r_h\rangle$	···

Table 4 *continued*

Table 4 *(continued)*

Name	M_B	M_V	$\langle r_h \rangle$	$\log(M_*/M_{odot})$	v_r	$v_{\rm source}$	Class	Envelope	Method	OtherName
	(mag)	(mag)	(pc)		(km/s)					
(1)	(2)	(3)	(4)	(5)	(6)	(7)	(8)	(9)	(10)	(11)
NGVS-UCD815	-9.95	-9.55	16.35± 0.29	6.3	···	···	1	0	$u^*gz + \langle\mu_g\rangle_e + \langle r_h\rangle$	···
NGVS-UCD816	-10.10	-9.68	27.75± 0.72	6.4	···	···	3	0	$u^*gz + \langle\mu_g\rangle_e + \langle r_h\rangle$	···
NGVS-UCD817	-9.56	-8.75	12.42± 0.44	6.6	···	···	1	0	$u^*gzK + \langle\mu_g\rangle_e + \langle r_h\rangle$	···
NGVS-UCD818	-9.60	-9.16	24.55± 0.67	6.1	···	···	1	0	$u^*gz + \langle\mu_g\rangle_e + \langle r_h\rangle$	···
NGVS-UCD819	-10.96	-10.47	12.48± 0.28	6.8	···	···	1	0	$u^*gzK + \langle\mu_g\rangle_e + \langle r_h\rangle$	···
NGVS-UCD820	-9.30	-8.82	23.83± 0.37	6.1	···	···	1	0	$u^*gz + \langle\mu_g\rangle_e + \langle r_h\rangle$	···
NGVS-UCD821	-9.58	-9.59	30.57± 1.13	5.3	220	SIMBAD	1	0	$(v_r < 3500\mathrm{km/s}) + \langle r_h\rangle$	···
NGVS-UCD822	-9.37	-8.72	11.44± 0.24	6.4	1194	SIMBAD	1	0	$(v_r < 3500\mathrm{km/s}) + \langle r_h\rangle$	···
NGVS-UCD823	-9.26	-8.61	12.13± 0.28	6.4	2140	SIMBAD	1	0	$(v_r < 3500\mathrm{km/s}) + \langle r_h\rangle$	···
NGVS-UCD824	-10.06	-9.67	16.08± 0.07	6.3	2365	SIMBAD	6	0	$(v_r < 3500\mathrm{km/s}) + \langle r_h\rangle$	VCC-980
NGVS-UCD825	-9.50	-8.78	19.77± 0.74	6.6	777	SIMBAD	1	0	$(v_r < 3500\mathrm{km/s}) + \langle r_h\rangle$	···
NGVS-UCD826	-9.32	-8.62	11.57± 0.32	6.4	867	SIMBAD	1	0	$(v_r < 3500\mathrm{km/s}) + \langle r_h\rangle$	···
NGVS-UCD827	-10.29	-9.63	19.86± 0.57	6.8	971	SIMBAD	1	0	$(v_r < 3500\mathrm{km/s}) + \langle r_h\rangle$	···
NGVS-UCD828	-10.06	-9.45	31.50± 0.75	6.6	952	SIMBAD	1	0	$(v_r < 3500\mathrm{km/s}) + \langle r_h\rangle$	···

NOTE– (1) UCD name; (2-3) Absolute B and V band magnitude, calculated using the transformation equation $B = u^* - 0.8116(u^* - g) + 0.1313$, $V = g - 0.2906(u^* - g) + 0.0885$ (Lupton 2005) and a distance modulus of 31.1 mag (Mei et al. 2007; Blakeslee et al. 2009); (4) Weighted mean half-light radius in the g and i bands, $\langle r_h \rangle = r_{h,g}$ if an i-band measurement is not available; (5) Stellar mass; (6) Heliocentric radial velocity (or weighted mean value if multiple measurements are available); (7) The source of our adopted v_r measurement, SDSS: Abolfathi et al. (2018); NED: NASA/IPAC Extragalactic Database; SIMBAD: SIMBAD Astronomical Database (Wenger et al. 2000); VCC: Binggeli et al. (1985); NTT17: NTT 2017 program; AAT12: AAT 2012 program; MMT09: MMT 2009 program; Toloba2018: Toloba et al. (2018); Ko2017: Ko et al. (2017); MMT14: MMT 2014 program; Keck: Keck program; C03: Côté et al. (2003); IMACS16: Megallan/IMACS 2016 program; S11: Strader et al. (2011); (8) Class parameter: 1=probable UCD, 2=dwarf nucleus, 3=background galaxy, 4=blended object, 5=star, 6=star-forming region; (9) Envelope: 0=lacks obvious envelope, 1=has obvious envelope; (10) Selection method; (11) Altenative names, if available.